STUDY ON NAIL HEAD-GROUND INTERACTION USING NUMERICAL MODELLING

GEO REPORT No. 251

S.P.Y. Cheung & C.H.W. Chan

GEOTECHNICAL ENGINEERING OFFICE
CIVIL ENGINEERING AND DEVELOPMENT DEPARTMENT
THE GOVERNMENT OF THE HONG KONG
SPECIAL ADMINISTRATIVE REGION

STUDY ON NAIL HEAD-GROUND INTERACTION USING NUMERICAL MODELLING

GEO REPORT No. 251

S.P.Y. Cheung & C.H.W. Chan

This report is largely based on GEO Special Project Report No. SPR 5/2008 produced in July 2008

First published, July 2010

Prepared by:

Geotechnical Engineering Office,
Civil Engineering and Development Department,
Civil Engineering and Development Building,
101 Princess Margaret Road,
Homantin, Kowloon,
Hong Kong.

PREFACE

In keeping with our policy of releasing information which may be of general interest to the geotechnical profession and the public, we make available selected internal reports in a series of publications termed the GEO Report series. The GEO Reports can be downloaded from the website of the Civil Engineering and Development Department (http://www.cedd.gov.hk) on the Internet. Printed copies are also available for some GEO Reports. For printed copies, a charge is made to cover the cost of printing.

The Geotechnical Engineering Office also produces documents specifically for publication. These include guidance documents and results of comprehensive reviews. These publications and the printed GEO Reports may be obtained from the Government's Information Services Department. Information on how to purchase these documents is given on the second last page of this report.

R.K.S. Chan
Head, Geotechnical Engineering Office
July 2010

Table of Contents
Table of Contents
Table of Contents

FOREWORD

This study forms a part of a series of studies to optimize the design methodology, improve construction techniques and enhance quality assurance of soil nailing works.

This report presents the results of a numerical modelling study on the effect of soil nails in stabilizing a slope. The nail-ground interaction; including the deformation and the mobilization of stresses in various elements of a soil nailed slope has been investigated.

The study was carried out by Mr S.P.Y. Cheung and Mr C.H.W. Chan of the Standards and Testing Division. Many other colleagues provided constructive comments on a draft of this report. Their contributions are gratefully acknowledged.

W K Pun
Chief Geotechnical Engineer/Standards & Testing

ABSTRACT

A study using numerical modelling has been carried out to investigate the nail-ground interaction in a soil nailed slope. The effects of soil nails in stabilizing a slope have been examined by restraining the deformation of the soil nail heads. No soil nail elements were put in the model, which avoid the presence of a continuous steel 'plate' and the soil could theoretically move downward between the steel bars. This numerical model is different from other two-dimensional analysis assuming steel bars in plane strain conditions but it gives an upper bound solution of the confinement effect of the soil nail heads.

The results of the study have revealed that the confinement effect behind the soil nail heads increases the mean effective stress and the forces acting behind the soil nail head are not directly proportional to its size. In particular, the relative displacement between the soil mass and the soil nail head in gentle slope is found to be mainly in parallel direction to the slope surface. In light of this, a soil nail head with a steeper face intercepting the relative displacement would be more effective in mobilising axial force in the soil nail and new details have been developed.

CONTENTS

1. INTRODUCTION

Since the early 1990s, soil nailing has been commonly used as a structural support to enhance stability of existing and newly formed slopes. It is particularly well suited to the residual soil profiles in Hong Kong and the robustness of soil nailed slopes is discussed in Ho et al (2003). Design guidelines for slopes stabilised with steel soil nails are given in Geoguide 7: Guide to Soil Nail Design and Construction (GEO, 2008). In general, the external stability of a soil nailed slope is considered by limit equilibrium analysis based on the method of slices, such as Morgenstern & Price method, using an assumed distribution of forces in soil nails to achieve the design factor of safety. The assumed forces in soil nails are then used in the checking of internal stability against possible modes of failures, including:

(a) structural failures of steel bar,

(b) pull-out failure of soil nails from the passive zone, and

(c) bearing capacity and structural failures of soil nail heads.

The performance of soil nailed slopes that are designed using the current design approach is generally satisfactory, as manifested in the observations that no major failures involving soil nailed slopes were reported. The limit equilibrium method of analysis does not account for the nail-ground interaction in a soil nailed slope, in particular the deformation of soil mass and the associated mobilisation of stresses and forces in the structural elements that contribute to the enhancement in slope stability. Consideration of nail-ground interaction becomes important when further optimization of the soil nailing design is warranted; new structural material for the soil nail is proposed; or unconventional layout of soil nailing is required.

The GEO has been undertaking a series of studies to optimize the design methodology, improve construction techniques and enhance quality assurance of soil nailing works. Numerical modelling has been conducted as part of the series of the study to investigate the nail-ground interaction; including the deformation and the mobilization of stresses in various elements of a soil nailed slope. Past numerical modelling (Shiu & Chang, 2005; 2006) were carried out using the finite difference program based on Fast Lagrangian Analysis of Continua (FLAC) (Itasca, 2005). These FLAC models simulated soil nails as either cable or bar elements in two-dimensional analyses with a plane strain condition. This, in effect, made the soil nail element as a continuous plate in the out-of-plane direction and soil could not pass beyond the soil nails. A 3-D numerical analysis may be carried out to make the model more realistic. Such analysis is complicated and time consuming, and will be explored in a separate study.

A simplified model that can overcome the limitation of having a 'plate' in the 2-D model was adopted in the analyses to study the interaction between soil nail head and the ground. Further details are given in the next section.

It is not the intention of this study to provide a quantification of design parameters based on limited number of numerical modelling, since such a scope requires extensive parametric studies and verifications.

2. NUMERICAL STUDY OF INTERACTION OF SOIL NAIL HEADS AND GROUND

2.1 General

The stability of an unreinforced slope relies on the mobilisation of shear strength in the soil mass. When the slope becomes unstable, as a result of deterioration and changes in environmental factors, the deformation would accelerate and may even result in complete detachment. This could happen rapidly, as in most landslide cases in Hong Kong. The deformation zone can be conveniently used to divide the soil mass into two distinct regions, the active and passive zones.

Soil nails commonly used in Hong Kong can be regarded as passive elements, as no prestressing force is applied to the soil nails. Therefore, the mobilisation of forces in the soil nails are the reaction to the deformation of the soil mass and it could be attributed to two nail-ground interactions, including:

(a) the effect of restraining the outward movement of the soil mass by the soil nail heads, which are structurally connected to the steel bars bonded to the soil in the passive zone, and

(b) the relative movement between the soil nail elements and the soil mass in the active zone, which induces stresses in the soil nails through friction and bearing.

In this study, numerical modelling has been carried out to investigate the interaction between soil nail heads and the ground; and examine the failure mechanism of soil near nail heads. The interaction of the ground and nail heads were studied by restraining the movement of the soils at the position of the nail heads. No soil nail elements were put in the model. As a continuous plate did not present, the soil could theoretically move downward. While overcoming the limitation of a continuous 'plate', this inevitably means that the interaction between the ground and the soil nail elements is not considered. Hence, this study does not aim to give a full picture of nail-ground interaction in a soil-nailed system, but the interaction of the nail-head only.

The models essentially assumed that the soil nail head did not move. In reality, the soil nail head would move down together with the ground but its movement would be restricted by the soil nail elements. The model therefore gives an upper bound solution of the confinement effect of the soil nail heads.

In these investigations, numerical analyses of unreinforced slopes were first conducted for setting baselines for comparing the effect of soil nails on reinforced slopes.

The modelling conducted in this study focused on existing slopes stabilised by steel soil nails. Discussions and observations given in this section may not be applicable to the behaviour of soil nails in newly formed cut slopes, as installation of soil nails and excavation are progressed in stages.

2.2 Numerical Models

Figure 1 shows the basic geometry of the modelled slope, which is 10 m high and standing at an angle of 55°. Various models were derived from this basic geometry for simulating the stability of the soil nailed slopes, including slopes with different rows of soil nails and of different sizes of the soil nail heads, and slope formed to a gentler gradient.

Numerical modelling conducted in this study were carried out using the finite element code developed by PLAXIS BV, which is developed for two-dimensional analysis of deformations and stability in geotechnical engineering. The latest edition of V8 has been used in the numerical modelling.

A plane strain condition was assumed. The mechanical behaviour of the soil is modelled as linear-elastic, perfectly-plastic, Mohr-Coulomb (MC) model. The computation of using MC model is relatively fast and provides a good approximate for a first-order solution. As it is not an attempt in this study to quantify design parameters or to calibrate deformation against actual displacement, the assumed MC model is adequate to demonstrate the deformation and the corresponding mobilisation of stresses and strains in the soil mass and the structural elements.

The parameters for the MC model were unit weight, γ = 18 kN/m^3, apparent cohesion, c' = 20 kPa and shearing angle, ϕ' = 30°. The high apparent cohesion was mainly used in the initial stage of the numerical modelling, such that an unreinforced slope remained stable prior to any changes in the environmental setting. This simulated the presence of soil suction in the slope. Poisson's ratio, *v*, was assumed to be 0.35 and the initial tangent stiffness, E was taken as 20 MPa. In the numerical models adopted for this study, the angle of dilatancy had been taken as zero to avoid over-predicting its effect on soil strengths and the shear strain. In addition, groundwater table was explicitly not modelled in the simulations. This assumption would not affect the study of the soil-nail interaction, but could greatly simplify the modelling and allow a faster computation in each numerical analysis. The effect of pore water changes was simulated in the analyses by reducing the apparent cohesion of the soil mass.

The vertical boundaries of the models were fixed in the horizontal direction, whereas the bottom boundary was fixed in both directions. These boundary conditions are also illustrated in Figure 1.

In the numerical models, 15-node triangular elements with 12 Gaussian stress points were used. The high-order elements provided a more versatile simulation of stresses and strains in the mesh elements and are particularly useful in solving problems with highly variable strain fields, such as the concentration of stress and strain around the soil nail heads investigated in this study.

2.3 Study of Behaviour of Unreinforced Slopes

The behaviour of unreinforced slopes was modelled as baselines for comparing the effect of soil nails on the reinforced slopes. The unreinforced slope was simulated with a high apparent cohesion initially, so as to make it stable prior to any changes in environmental

loading. Deformation of the unreinforced slopes and instability was then effected by either:

(a) gradually reducing the apparent cohesion of the soil mass, or

(b) applying incrementally a surcharge at the slope crest.

These changes in the numerical models were applied in steps until non-convergence of the numerical solutions. The displacement vectors and development of plastic zones were examined to confirm that a distinct failure mechanism was indeed being developed, and the non-convergence was not due to other numerical instability, such as boundary effect, high contrast in material stiffness or occurrence of instability in zones not related to the slope failure itself.

2.4 Study of Behaviour of Reinforced Slopes

Numerical models were set up to study the behaviour of reinforced slopes in different settings. These configurations are intended for investigating:

(a) the confinement effect of soil nail heads,

(b) the mobilization of soil nail forces due to soil nail heads with different size of soil nail heads, and

(c) the distribution and mobilization of soil nail forces due to soil nail heads in different rows of soil nail supporting the slope, including steep and gentle slope.

As in the modelling of unreinforced slopes, deformation and instability of the slopes were introduced by either reducing the apparent cohesion or applying a vertical load on the slope crest.

Figure 2 shows the numerical model for the slope with two rows of soil nails. In this model, the apparent cohesion was reduced incrementally until the development of a failure mechanism and non-convergence of the solution. Since full fixity was assumed in the nodes of soil nail head, the head could be considered as a rigid block as no deflection was allowed between the nodes of the soil nail head.

3. RESULTS AND DISCUSSIONS

3.1 Unreinforced Slopes

Typical outputs for the numerical modelling carried out for this study are given in the Appendices A, B and C. The results include contour plots for the mean effective stress, shear strain, total displacement vectors and plastic zones before failure occurs.

Figure 3 shows the development of plastic zones for the 55° slope when the apparent cohesion of the soil was reduced from 20 kPa to 12.7 kPa. It was at this step that further

reduction in apparent cohesion could not give a converged numerical solution. The development of failure plane was obvious. It was first initiated at the slope toe and progressed upward. Figure 4 shows the development of shear strain along the failure zone and the maximum shear strain achieved was about 3.29 %. The displacement vectors in Figure 5(d) indicate that the soil mass in the upper part of the slope was largely moving downward and parallel to the slope surface, whereas the soil mass near the toe was moving outward from the slope. Two sections (A-A and B-B) across the displacement vector field are drawn in Figure 6. The displacement across the failure plane can be very distinct as given in Section B-B; or in a more gradual manner as given in Section A-A. It can be inferred from these sections that soil nails installing across the failure plane will be subject to different displacement patterns.

The reduction of apparent cohesion can somewhat be considered as representing the loss of soil suction in a soil slope, which is one of the common causes of rainfall-induced landslides in Hong Kong. However, it should be noted that the reduction of soil suction in rainfall-induced infiltration would not be uniform and such modelling does not replicate exactly the stress path experienced in the soil for a rain-induced failure. Figure 7 shows the stress path of a soil element near the slope toe when the apparent cohesion was gradually reduced.

Figure 8 shows the development of plastic zones when a vertical load was applied incrementally at the slope crest. It can be seen that the initiation of the failure plane also started at the toe and was similar to the slope failure simulated by strength reduction, despite the fact that the load was applied on the slope crest. No local failure was evident in the mid-slope. The displacement vector plot in Figure 9 also depicts that the soil mass in the upper part of the slope was moving downward and parallel to the slope surface. This was particularly the case as the vertical stress at the crest had a greater and direct influence on the soil movement. This was exemplified in the development of shear strain in Figure 10. Strain concentration is initiated from the slope toe.

Numerical analyses of the unreinforced slope were repeated for a gentle slope. Figure 11 shows the configuration of the gentle slope with a gradient of 35°. The properties of the soil and the boundary conditions in the model remained unchanged as in the model of 55° slope. Figure 12 shows the displacement vectors of the unreinforced slope subject to reduction in apparent cohesion. The observations on deformation and mobilization of stress and strain were similar to that for a steep slope. Obviously, a greater reduction in apparent cohesion could be achieved before the slope failed.

3.2 Confinement Effect of the Soil Nail Head

Figure 13 shows the changes of mean effective stress behind the soil nail heads, as the apparent cohesion was gradually reduced. The increase in mean effective stress could be attributed to the compression of the soil, as the soil mass moved down but was prevented from moving outward by the soil nail heads. At the position of the soil nail heads, a build up of concentrated stress beneath the soil nail head could be observed. Figure 13(h) shows the mean effective stress of the unreinforced slope after the apparent cohesion was reduced to 12.7 kPa. The confinement effect of the soil nail heads had resulted in a higher mean effective stress in the soil mass in the vicinity of the soil nail heads. This, in turn, increased

the maximum shear stress and the number of soil elements reaching the plastic yield points was smaller than that in the unreinforced slopes. Figure 14 depicts the relative shear stress in the reinforced slope with two rows of soil nails and unreinforced slope when the apparent cohesion of the soil was both reduced to 13 kPa. The relative shear stress is defined in the PLAXIS manual as:

$$\tau_{relative} = \frac{\tau_{mobilised}}{\tau_{maximum}} \quad \text{.....(1)}$$

where $\tau_{maximum} = c' + \sigma_n \tan \phi'$

When $\tau_{relative}$ equals to unity, the stress state of the soil element is at the MC failure envelope and the shear stress is fully mobilized. Along the failure plane in the reinforced slope, the extent of the fully mobilized zone was smaller and more soil elements were within the elastic state.

3.3 Mobilisation of Nail Forces in Different Size of Nail Heads

Two numerical models with different sizes of soil nail head had been assembled to study the mobilisation of the forces in the soil nails. These included soil nail heads with size of 400 mm x 400 mm square and 800 mm x 800 mm square. As the numerical model assumed a plane strain condition, the soil nail head was in effect a beam. The same strength parameters and constitutive model of the soil were used. The reinforced slopes became unstable when the apparent cohesion was reduced to 5.2 kPa and 4.9 kPa for the 400 mm and 800 mm square soil nail heads respectively. For the unreinforced slope of the same configuration, the apparent cohesion could only be reduced to 12.7 kPa for a converged solution.

Figure 15 shows the mean effective stress in the reinforced slopes with soil nail heads of 400 mm and 800 mm in size and the apparent cohesion was reduced to 5.2 kPa in both cases. The reinforced slope with the 800 mm soil nail heads appeared to have a slightly greater extent in term of increase in mean effective stress, but the difference between the two cases was small. Table 1 summarizes the forces acting on the soil nail heads. It should be noted that these forces are generally less than the maximum tensile forces along soil nails.

The forces acting on the soil nail heads were resolved to the normal and shear stress on the nodes of the soil nail heads. It was noted that the magnitude of the total forces acting on the soil nail head was larger for larger nail head size. However, it is apparent that the increase in the forces was not directly proportion to the sizes of the soil nail heads. There was a diminishing return as the size increased. This observation is consistent with Shiu & Chang (2005).

The numerical analyses of the reinforced slopes with different size of soil nail heads were also repeated for the 35° slope. Figure 16 shows the mean effective stress in an unreinforced slope and provides a basis for comparison. Figure 17 shows the mean effective stress in the reinforced slopes with soil nail heads of 400 mm and 800 mm in sizes. In both models, the apparent cohesion could be reduced to 2.4 kPa. Unlike the cases for the steep slope, the increases in mean effective stress beneath the soil nail heads were not noticeable. The force acting on the nail heads was much smaller when compared with that derived from

the 55° slope (see Table 1). Also, it is noted that the forces on the soil nail heads were dominated by the shear force, which implied that the tensile forces in the soil nails could not be mobilised. This could be attributed to the observation that the majority of the soil mass was in fact moving downward and parallel to the slope surface. The confinement effect of the soil nail heads was not significant in these models. This highlights the need to modify the typical details of soil nail heads, that are developed for steep slopes, when they are applied on gentle slope, e.g. in natural terrain.

4. CONCLUSIONS

The interaction between soil nail heads and the ground in a soil-nailed slope has been examined by means of numerical simulation and the following observations are found:

(a) With the presence of soil nails, the confinement effect behind the soil nail heads increases the mean effective stress. This, in turn, increases the mobilised shear strength and reduce the displacement of the soil mass.

(b) The forces mobilised in the soil nails are not directly proportional to the size of the soil nail heads and there is a diminishing return as the size of the nail head increased.

(c) The typical details of soil nail head developed for steep slope may not be applicable to soil nails installed in a gentle slope. The relative displacement between the soil mass and the soil nail head is mainly parallel to the slope surface and shear force is the major component mobilised in the soil nail due to soil-ground interaction. A soil nail head with a steeper face intercepting the relative displacement would be more effective in mobilising axial force in the soil nail. In light of this finding, new details of soil nail head for gentle slope have been developed and is given in GEO (2008).

5. REFERENCES

Geotechnical Engineering Office (2008). Geoguide 7: Guide to Soil Nail Design and Construction. Geotechnical Engineering Office, Hong Kong, 97 p.

Ho, K.K.S., Sun, H.W. & Hui, T.H.H. (2003). Enhancing the Reliability and Robustness of Engineered Slopes. GEO Report No. 139. Geotechnical Engineering Office, Hong Kong, 63 p.

Itasca (2005). Fast Lagrangian Analysis of Continus (FLAC) Manual, Version 5.0. Itasca Consulting Group, Inc., Minnesota.

Morgenstern, N.R. & Price, V.E. (1965). The analysis of the stability of general slip surfaces. Géotechnique, vol. 15, no. 1, pp 79-93.

Plaxis (2006). Plaxis 2D - Version 8 Manual. Plaxis BV, Netherlands.

Shiu, Y.K. & Chang, G.W.K. (2005). Soil Nail Head Review. GEO Report No. 175. Geotechnical Engineering Office, Hong Kong, 106 p.

Shiu, Y.K. & Chang, G.W.K. (2006). Effects of Inclination, Length Pattern and Bending Stiffness of Soil Nails on Behaviour of Nailed Structures. GEO Report No. 197. Geotechnical Engineering Office, Hong Kong, 116 p.

LIST OF TABLES

Table 1 - Mobilised Forces in Soil Nail in Reinforced Slope with Two Rows of Soil Nails

Nail Head Size (mm)	Row	Slope Angle = 55°			Slope Angle = 35°		
		Resultant Force (kN)	Force Normal to Soil Nail Head (kN)	Force along Soil Nail Head (kN)	Resultant Force (kN)	Force Normal to Soil Nail Head (kN)	Force along Soil Nail Head (kN)
400	Middle	50.1	44.6	22.7	5.5	2.9	4.65
	Lower	70.8	63.5	31.2	9.0	6.6	6.1
800	Middle	49.3	41.5	26.7	4.8	0.7	4.72
	Lower	92.6	80.1	46.3	3.3	0.4	3.3

Table 2 - Mobilised Forces in Soil Nail in Reinforced Slope with Three Rows of Soil Nails

Nail Head Size (mm)	Row	Slope Angle = 55°			
		Resultant Force (kN)	Force Normal to Soil Nail Head (kN)	Force along Soil Nail Head (kN)	Orientation to Horizontal Plane
400	Upper	22.8	19.2	12.4	22.1°
	Middle	44.1	39.4	19.8	28.3°
	Lower	68.6	61.6	30.1	30.0°
800	Upper	21.4	17.5	12.3	19.9°
	Middle	48.0	40.3	26.1	22.1°
	Lower	88.8	77.4	43.4	25.7°

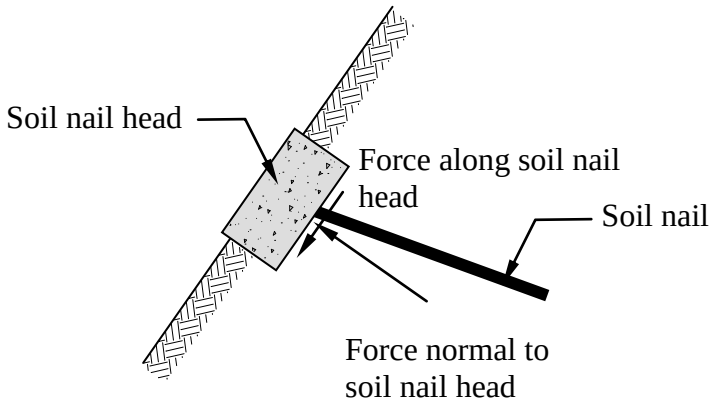

Diagrammatic Illustration of Various Force Components Acting on Soil Nail Head

LIST OF FIGURES

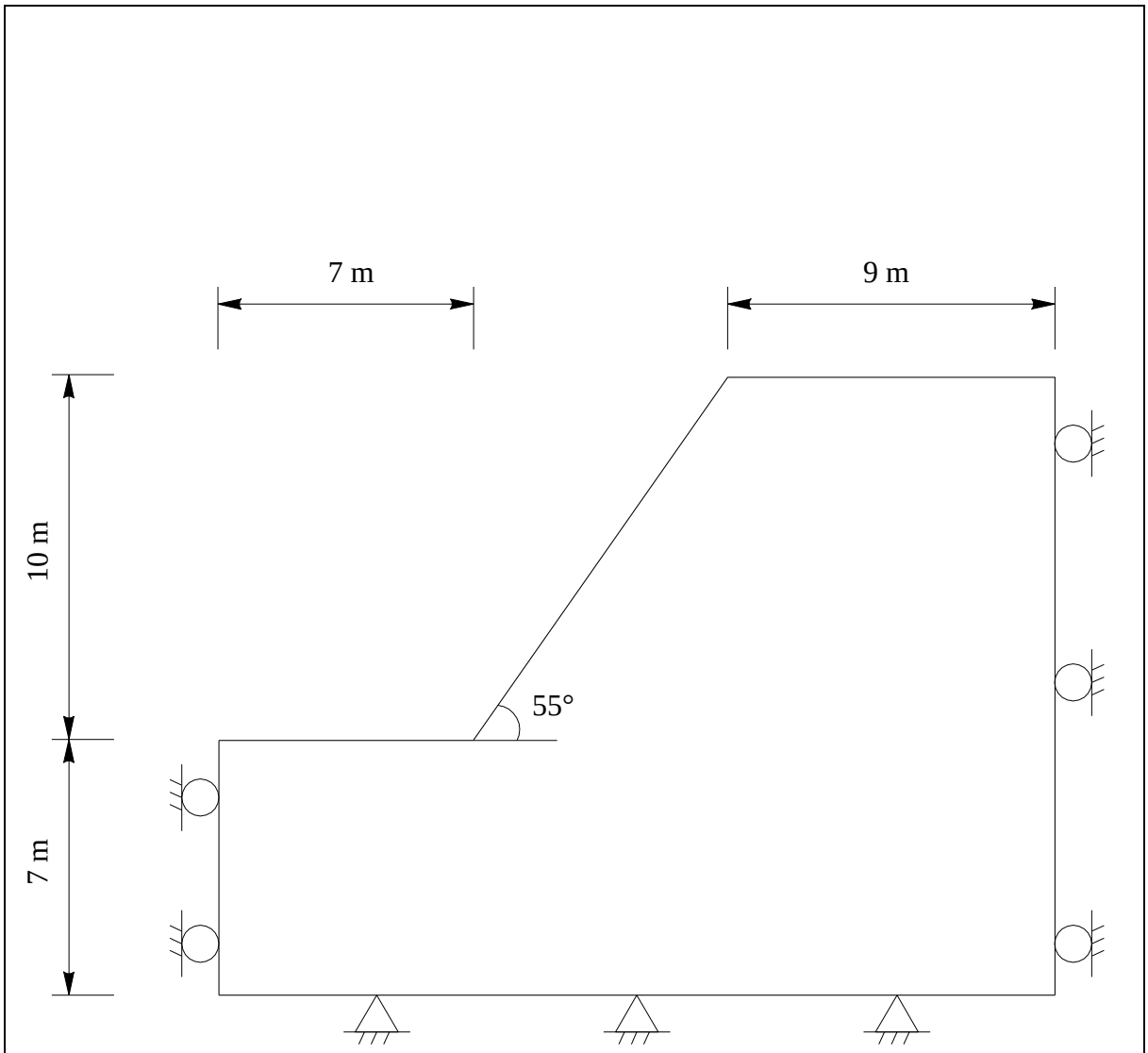

c' = 20 kPa (initial)
ϕ' = 30°
ψ = 0°
γ = 18 kN/m^3
E = 20 MPa
ν = 0.35

Figure 1 - Geometry of the Modelled Unreinforced Slope

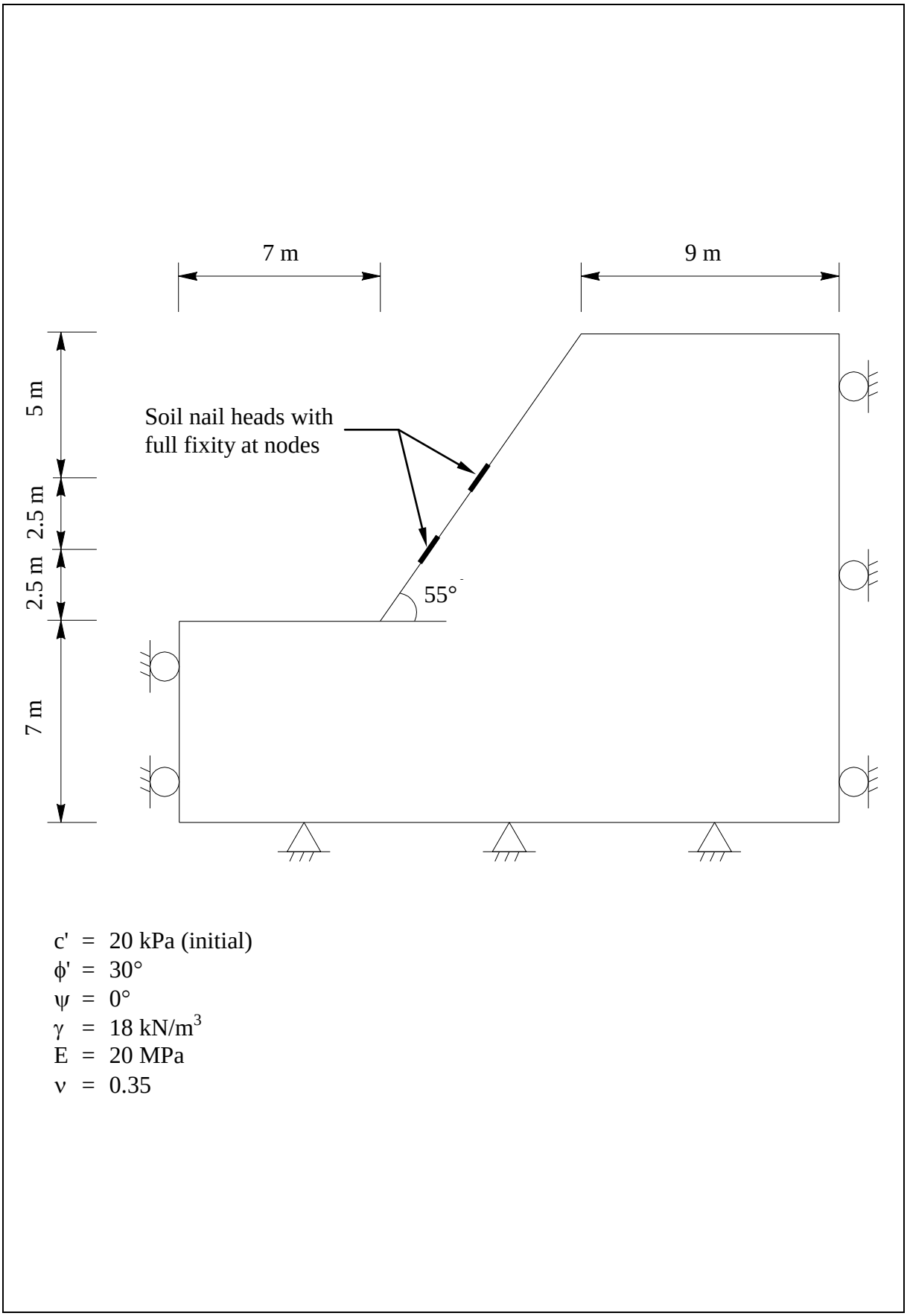

c' = 20 kPa (initial)
ϕ' = 30°
ψ = 0°
γ = 18 kN/m^3
E = 20 MPa
ν = 0.35

Figure 2 - Geometry of the Modelled Reinforced Slope

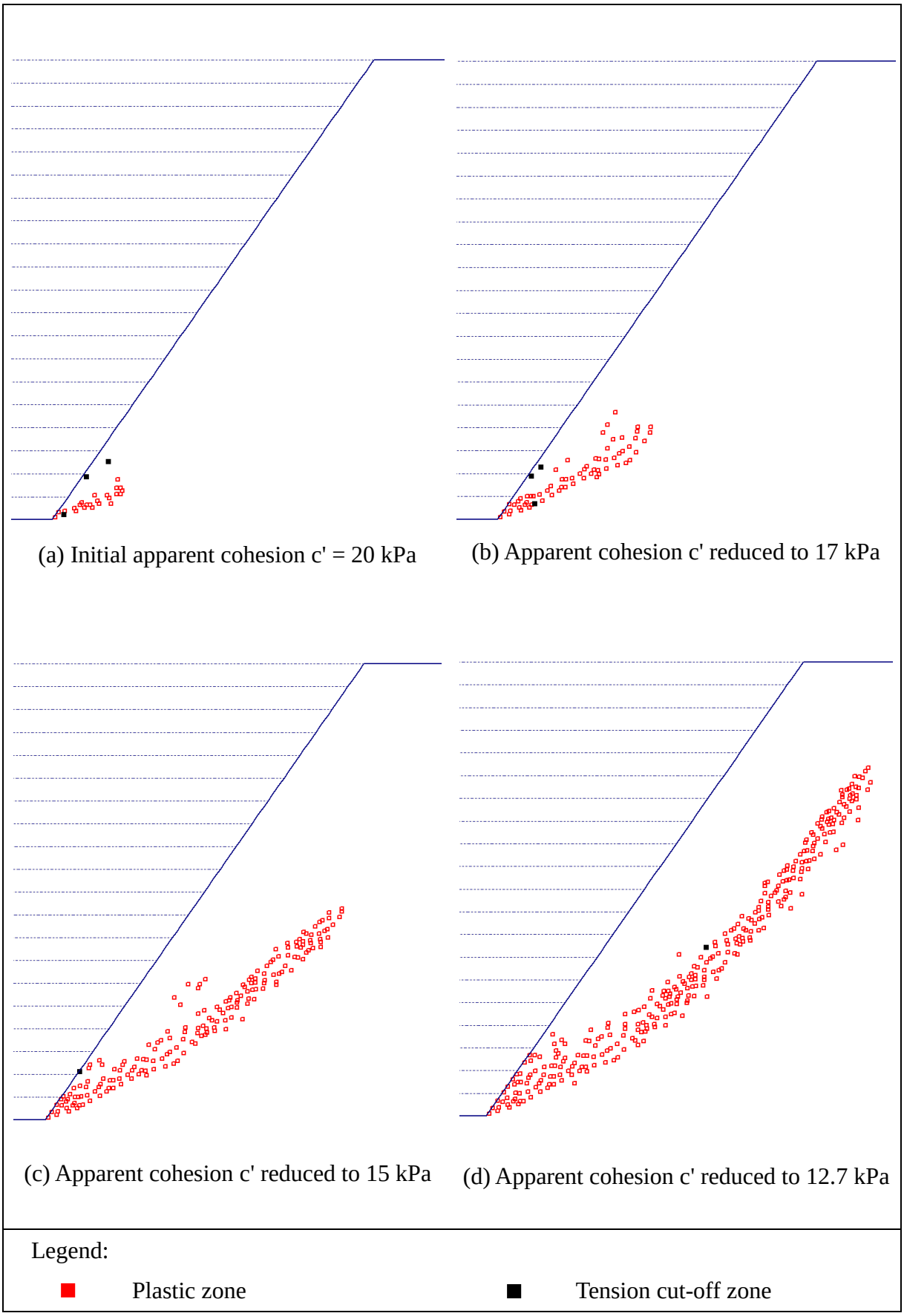

Figure 3 - Development of Plastic Zones for Unreinforced Slope

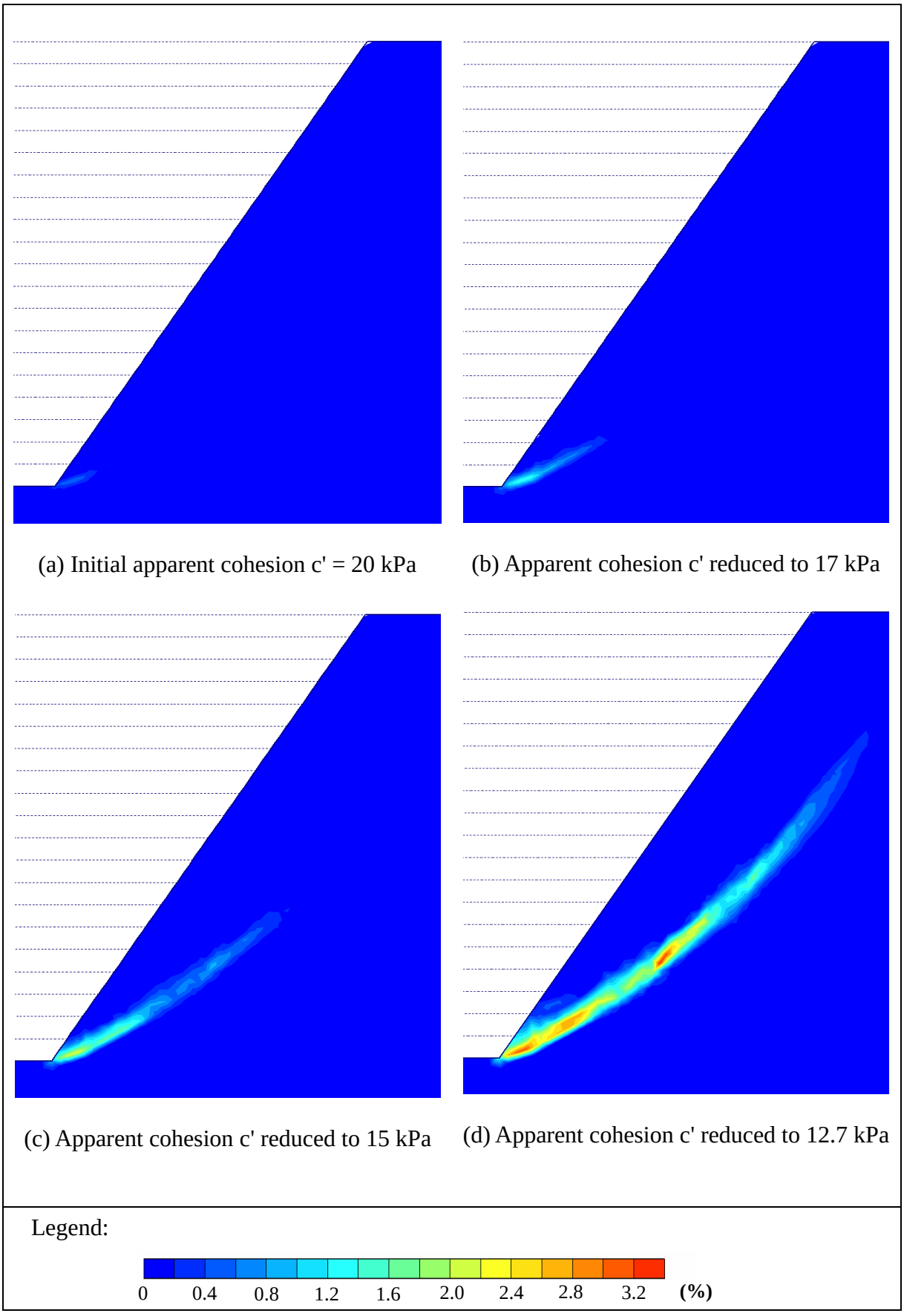

Figure 4 - Development of Shear Strain along the Failure Plane for Unreinforced Slope

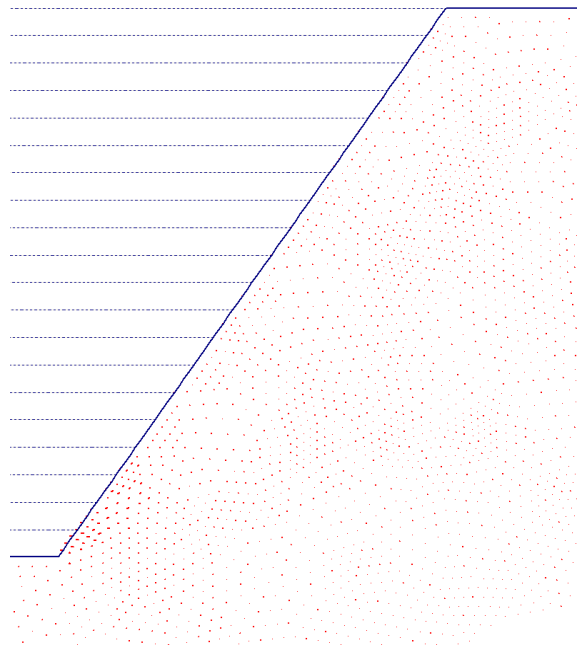

(a) Initial apparent cohesion c' = 20 kPa

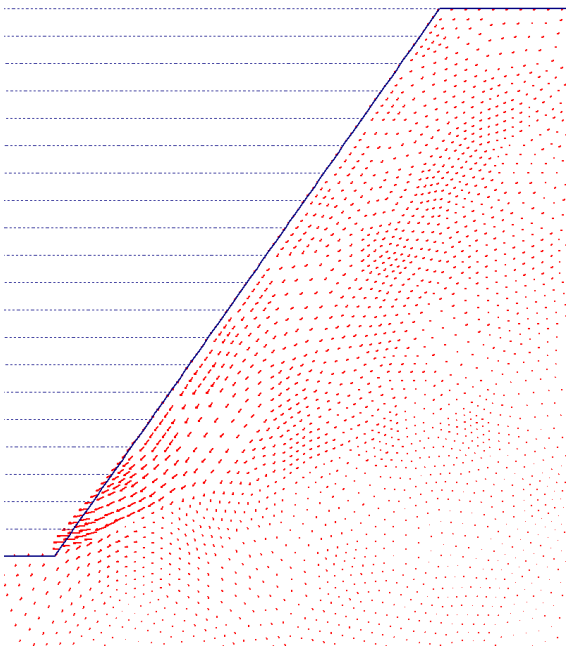

(b) Apparent cohesion c' reduced to 17 kPa

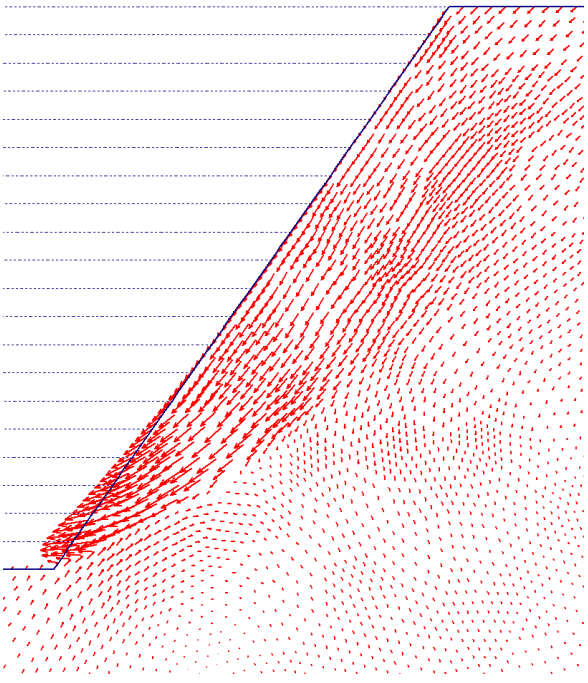

(c) Apparent cohesion c' reduced to 15 kPa

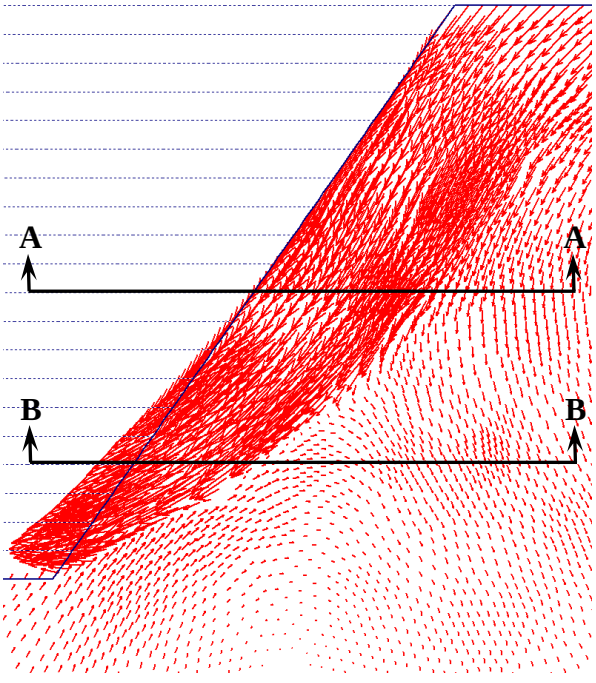

(d) Apparent cohesion c' reduced to 12.7 kPa

Note: See the cross sections in Figure 6.

Figure 5 - Displacement Vectors for Unreinforced Slope

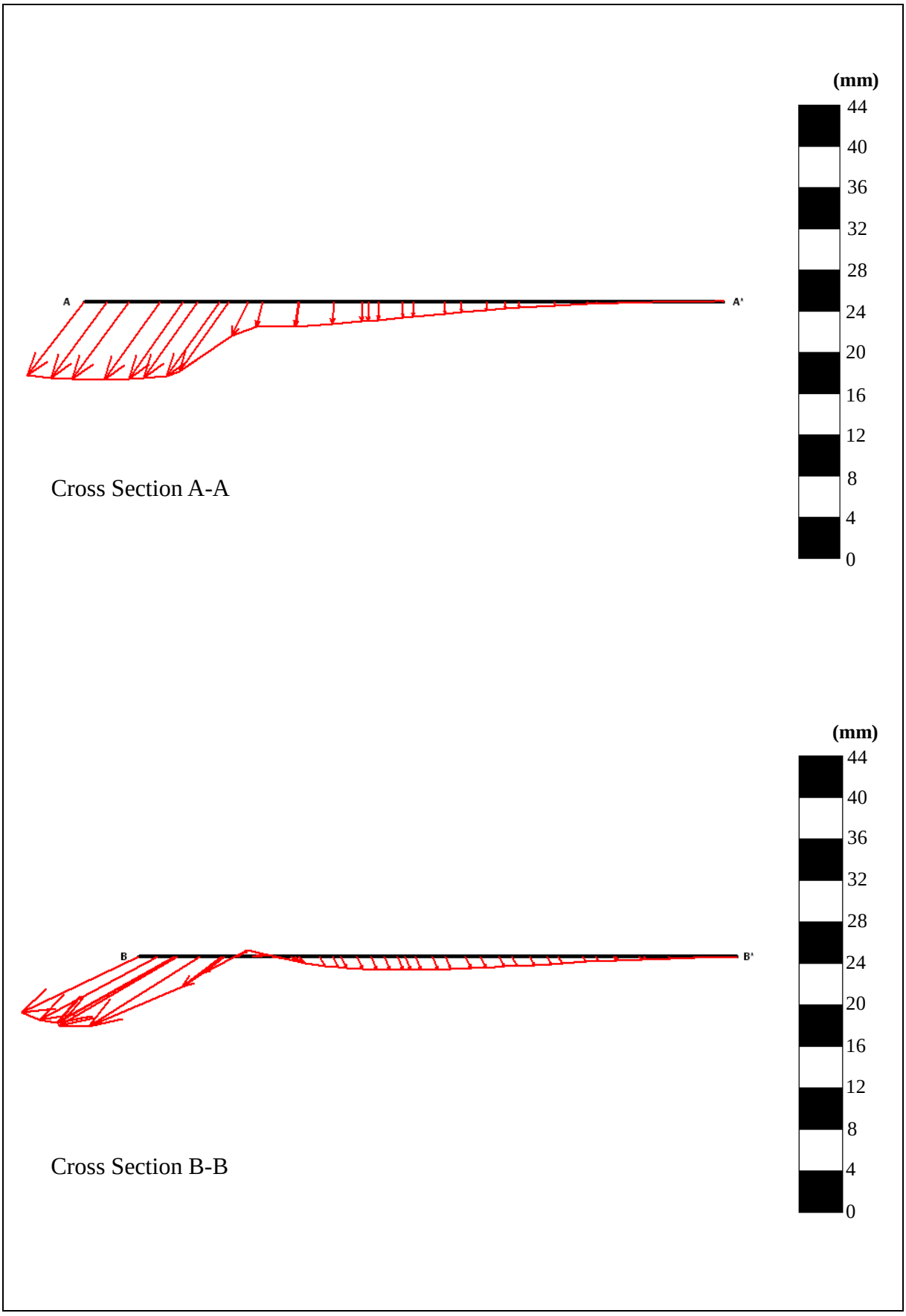

Figure 6 - Sections Cutting across the Displacement Vectors for Unreinforced Slope

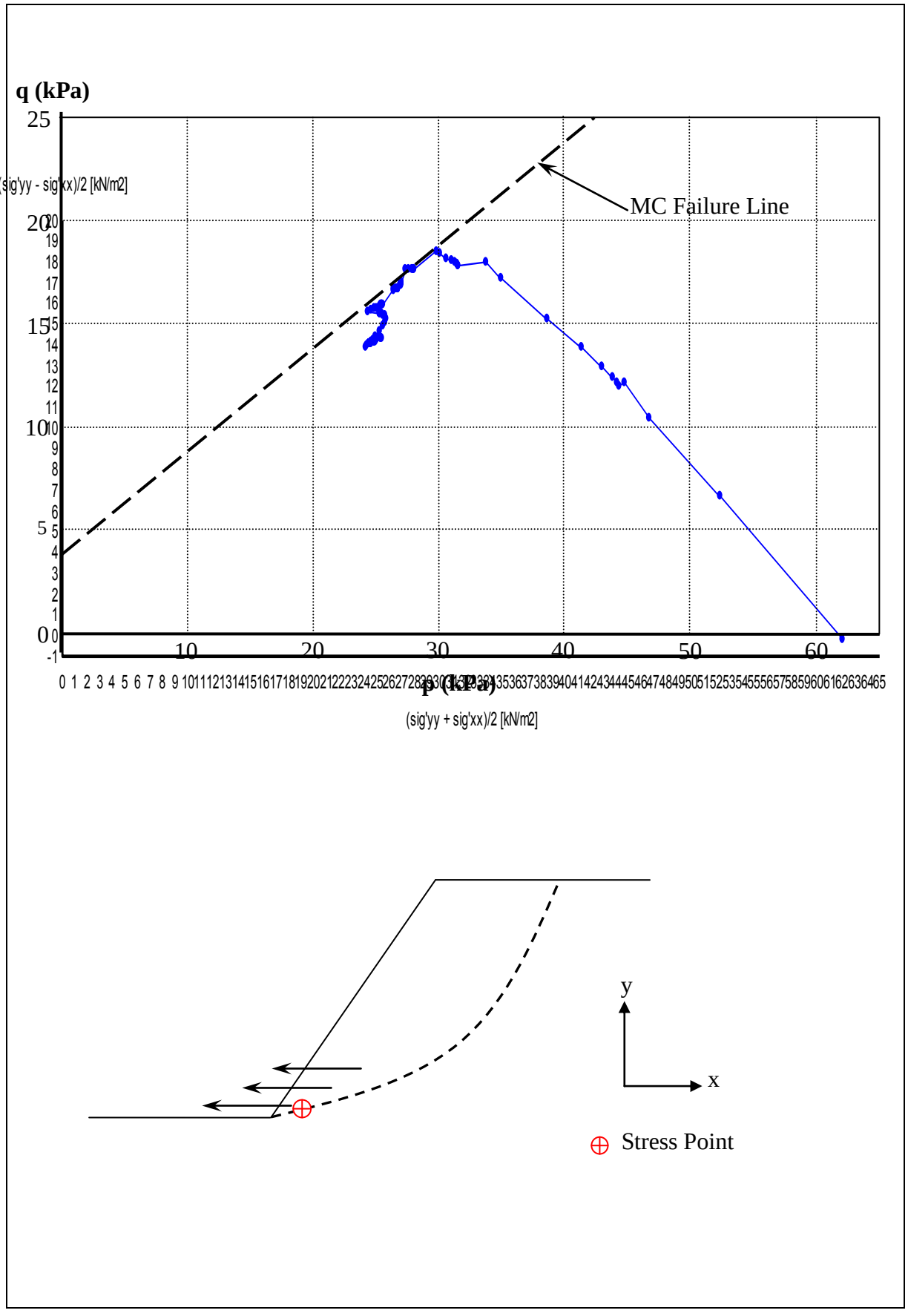

Figure 7 - Stress State of a Soil Element Near Slope Toe for Unreinforced Slope

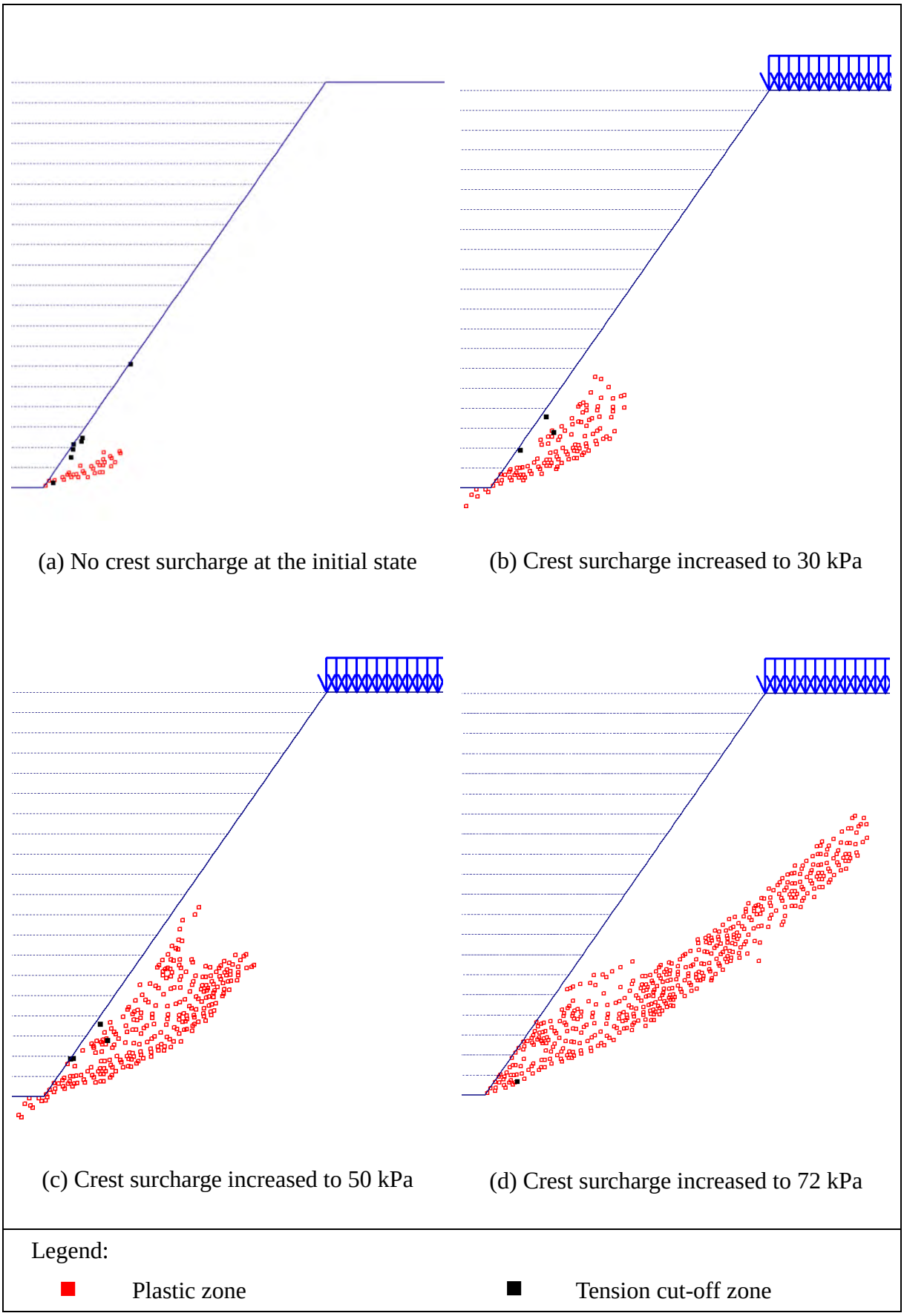

Figure 8 - Development of Plastic Zones for Unreinforced Slope Subject to Crest Surcharge

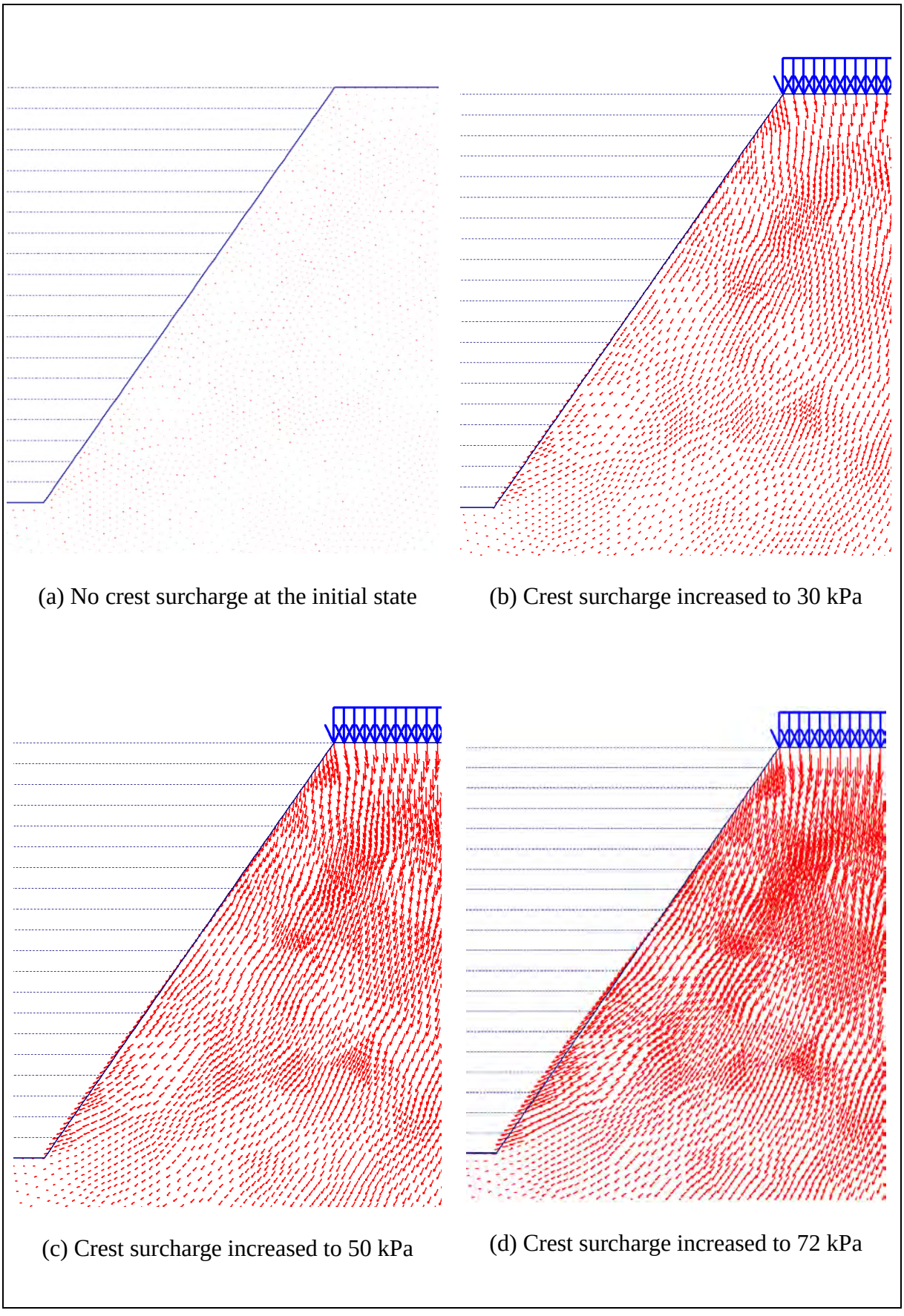

(a) No crest surcharge at the initial state

(b) Crest surcharge increased to 30 kPa

(c) Crest surcharge increased to 50 kPa

(d) Crest surcharge increased to 72 kPa

Figure 9 - Displacement Vectors for Unreinforced Slope Subject to Crest Surcharge

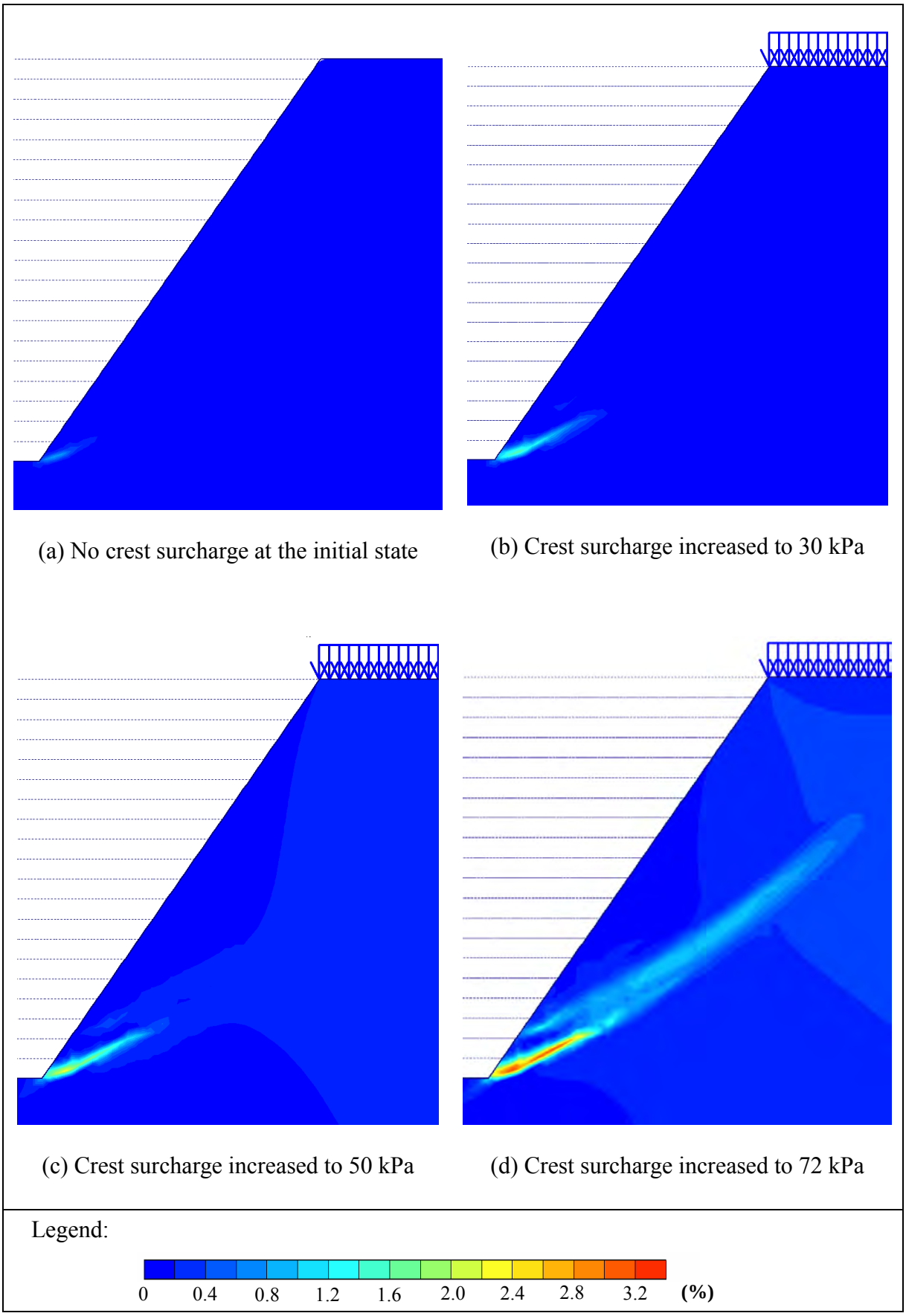

Figure 10 - Development of Shear Strain for Unreinforced Slope Subject to Crest Surcharge

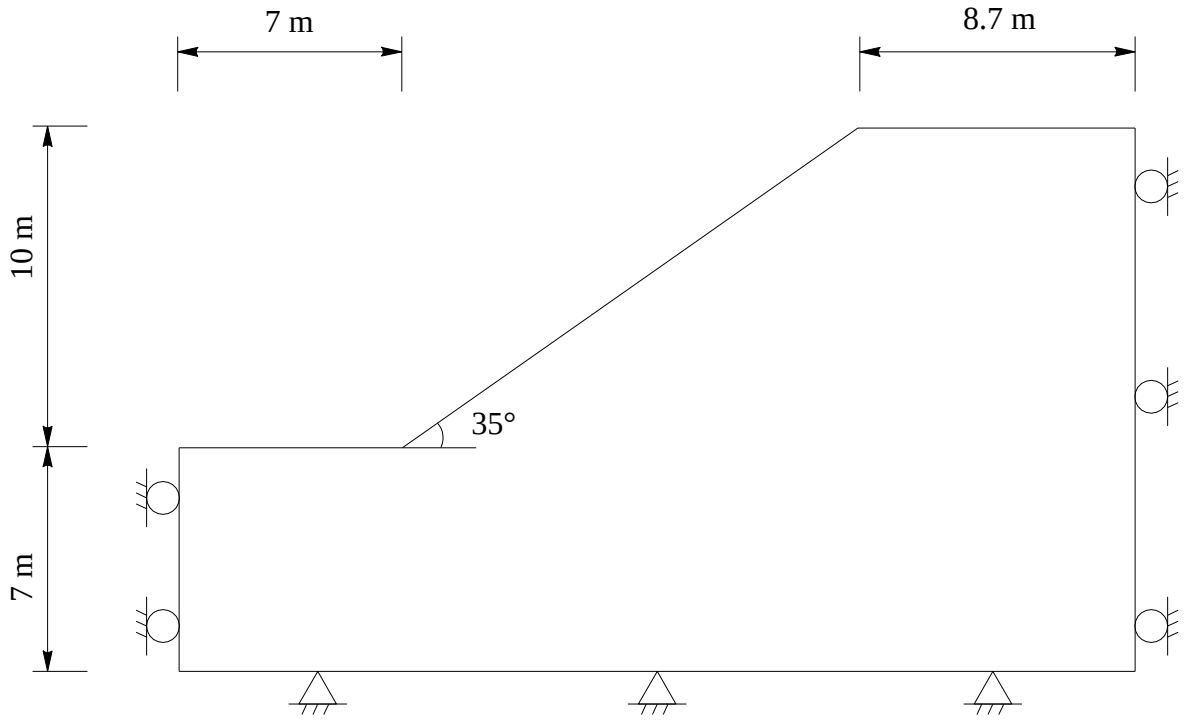

c' = 20 kPa (initial)
ϕ' = 30°
ψ = 0°
γ = 18 kN/m^3
E = 20 MPa
ν = 0.35

Figure 11 - Geometry of the Modelled Unreinforced Slope with Gentle Gradient

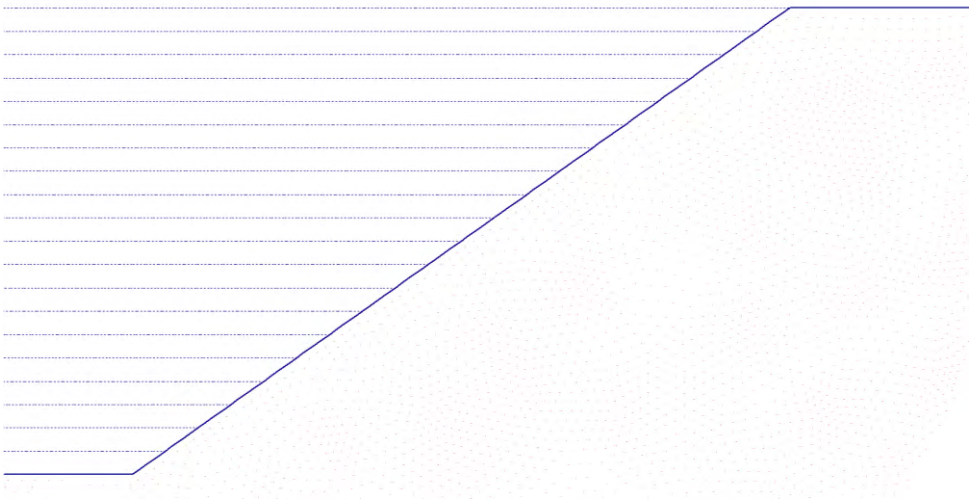

(a) Initial apparent cohesion c' = 20 kPa

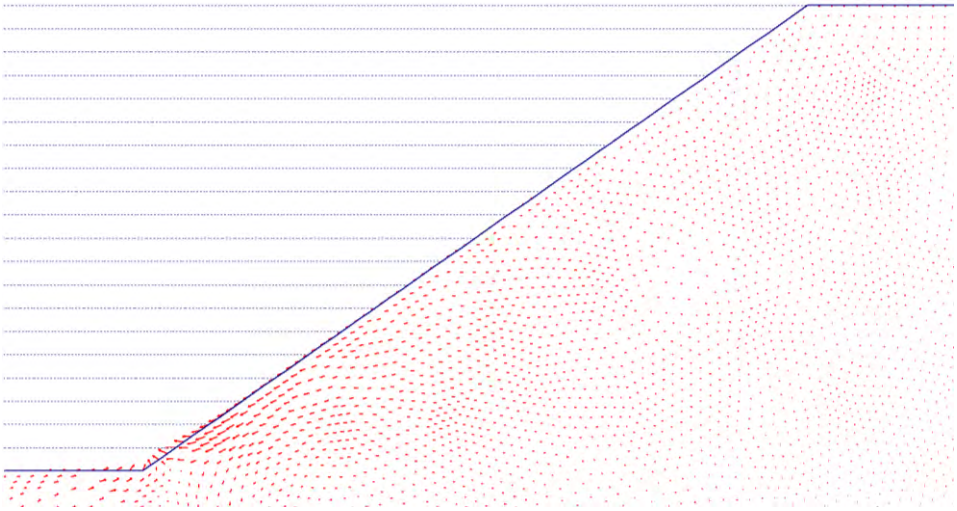

(b) Apparent cohesion c' reduced to 7 kPa

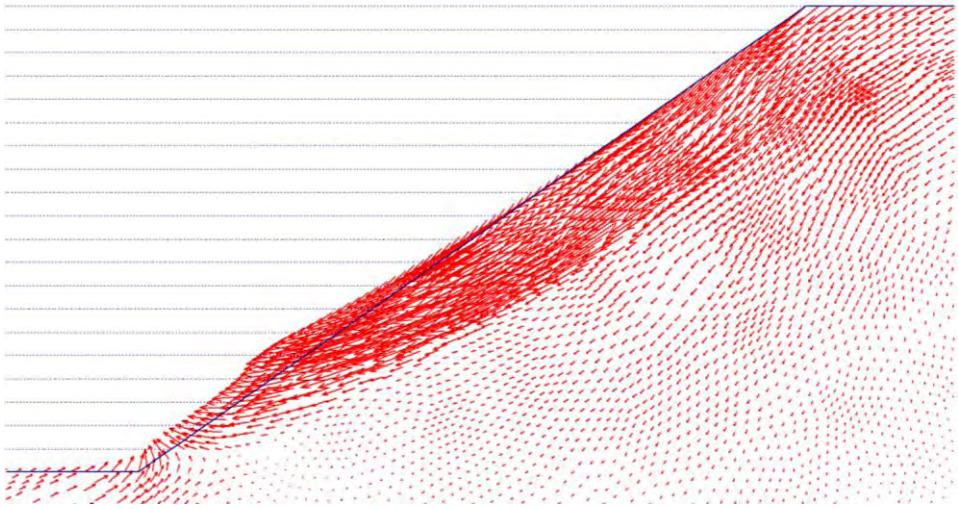

(c) Cohesive strength c' reduced to 2.6 kPa

Figure 12 - Displacement Vectors for Unreinforced Slope of 35° Gradient

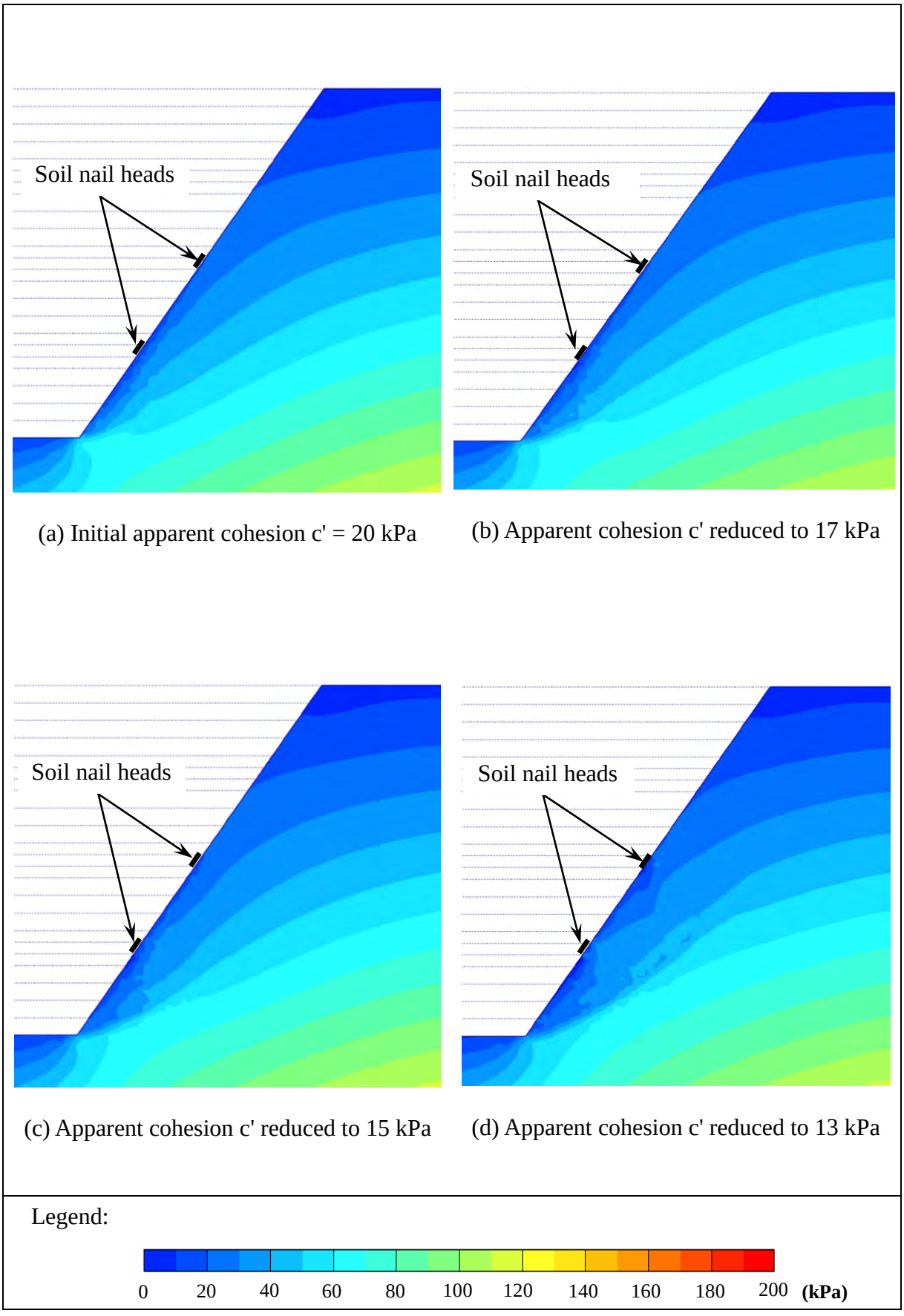

(a) Initial apparent cohesion c' = 20 kPa

(b) Apparent cohesion c' reduced to 17 kPa

(c) Apparent cohesion c' reduced to 15 kPa

(d) Apparent cohesion c' reduced to 13 kPa

Figure 13 - Change of Mean Effective Stress for Reinforced Slope (Sheet 1 of 2)

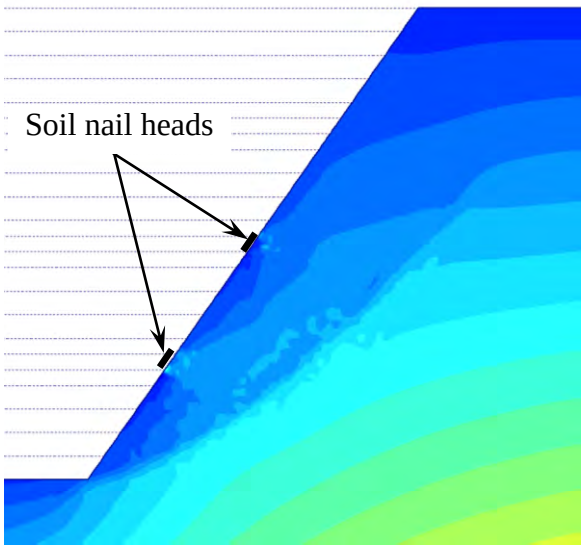

(e) Apparent cohesion c' reduced to 10 kPa

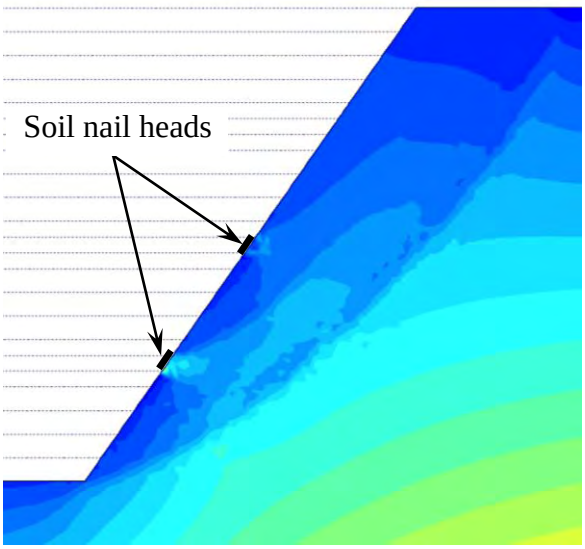

(f) Apparent cohesion c' reduced to 7 kPa

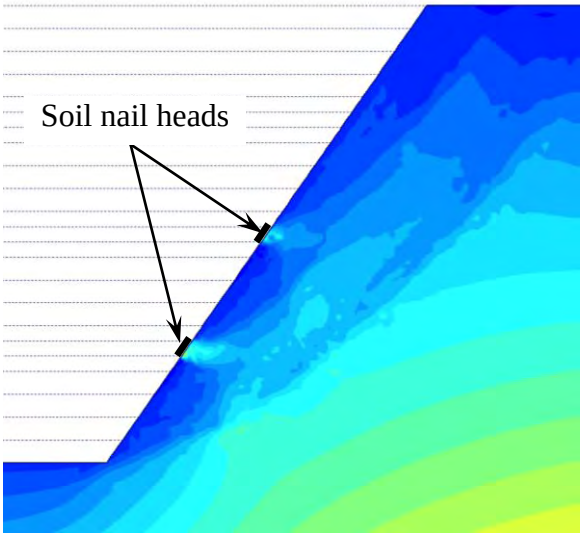

(g) Apparent cohesion c' reduced to 5.2 kPa

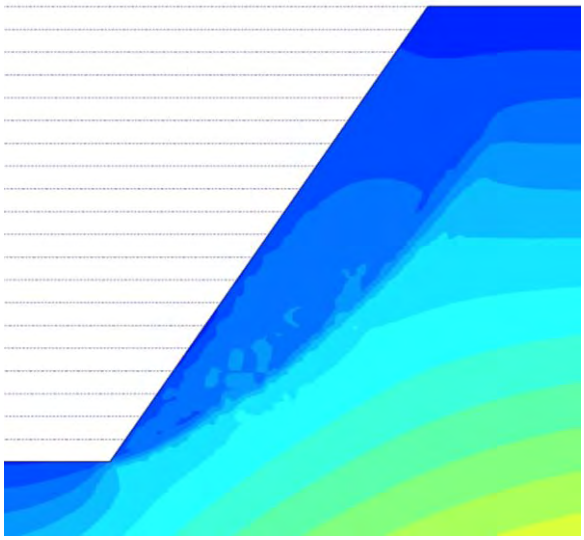

(h) Apparent cohesion c' reduced to 12.7 kPa for unreinforced slope

Legend:

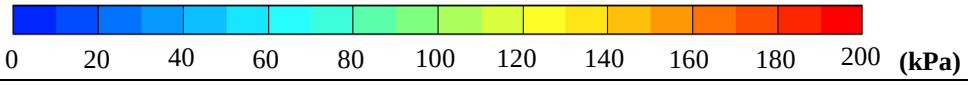

Figure 13 - Change of Mean Effective Stress for Reinforced Slope (Sheet 2 of 2)

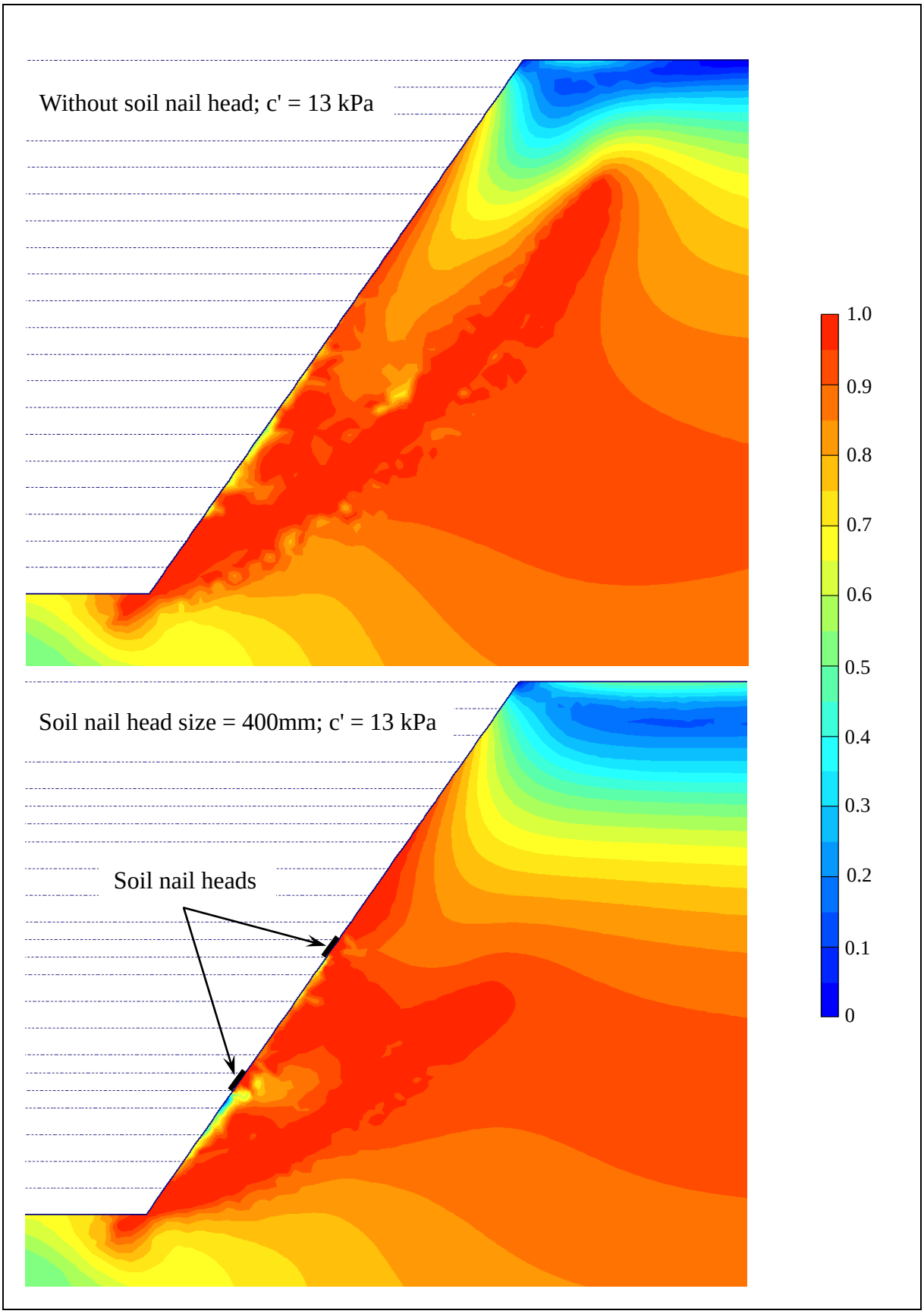

Figure 14 - Comparison of Relative Shear Stress for Unreinforced Slope and Reinforced Slope

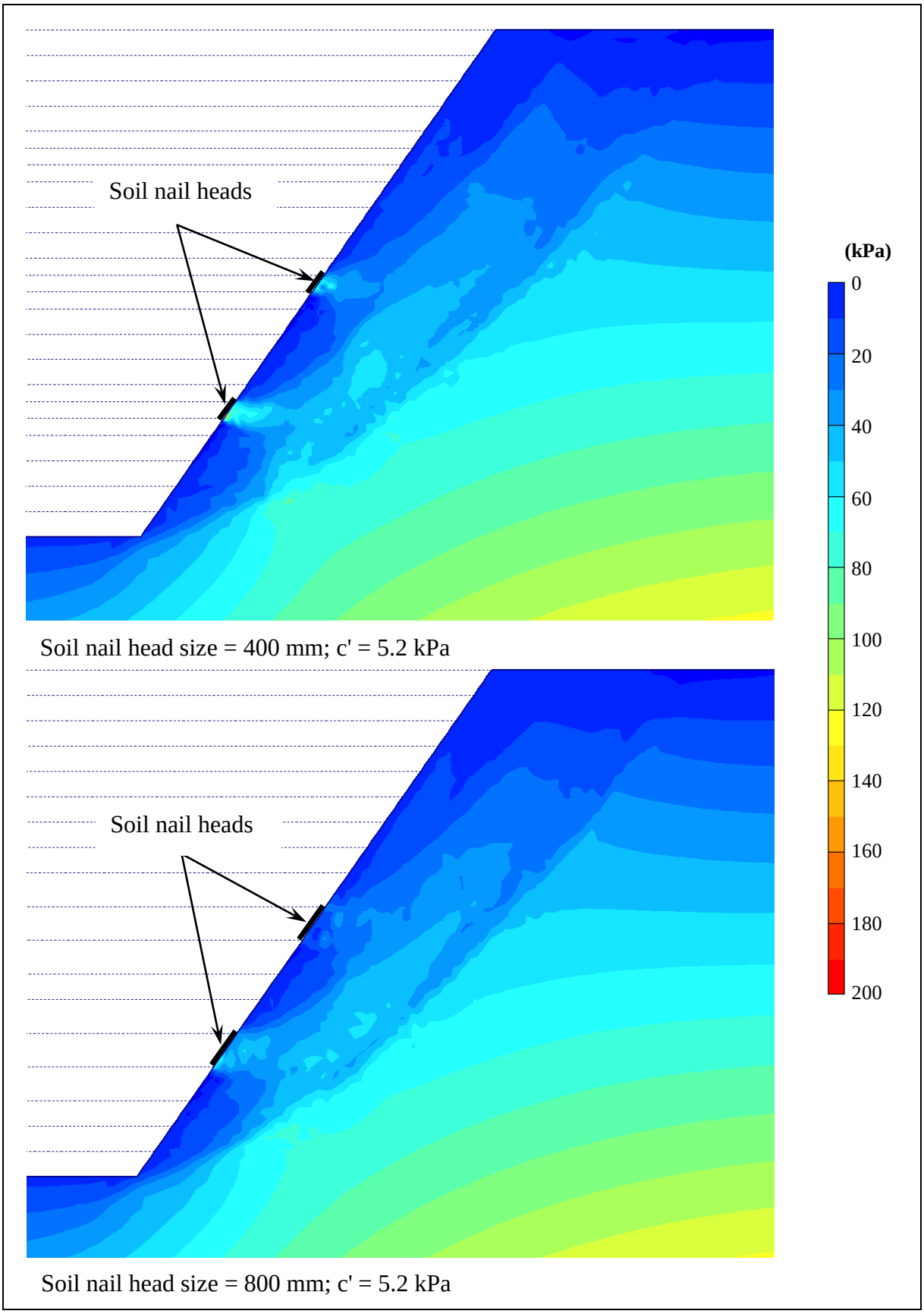

Figure 15 - Comparison of Mean Effective Stress for Reinforced Slopes with Different Nail Head Sizes

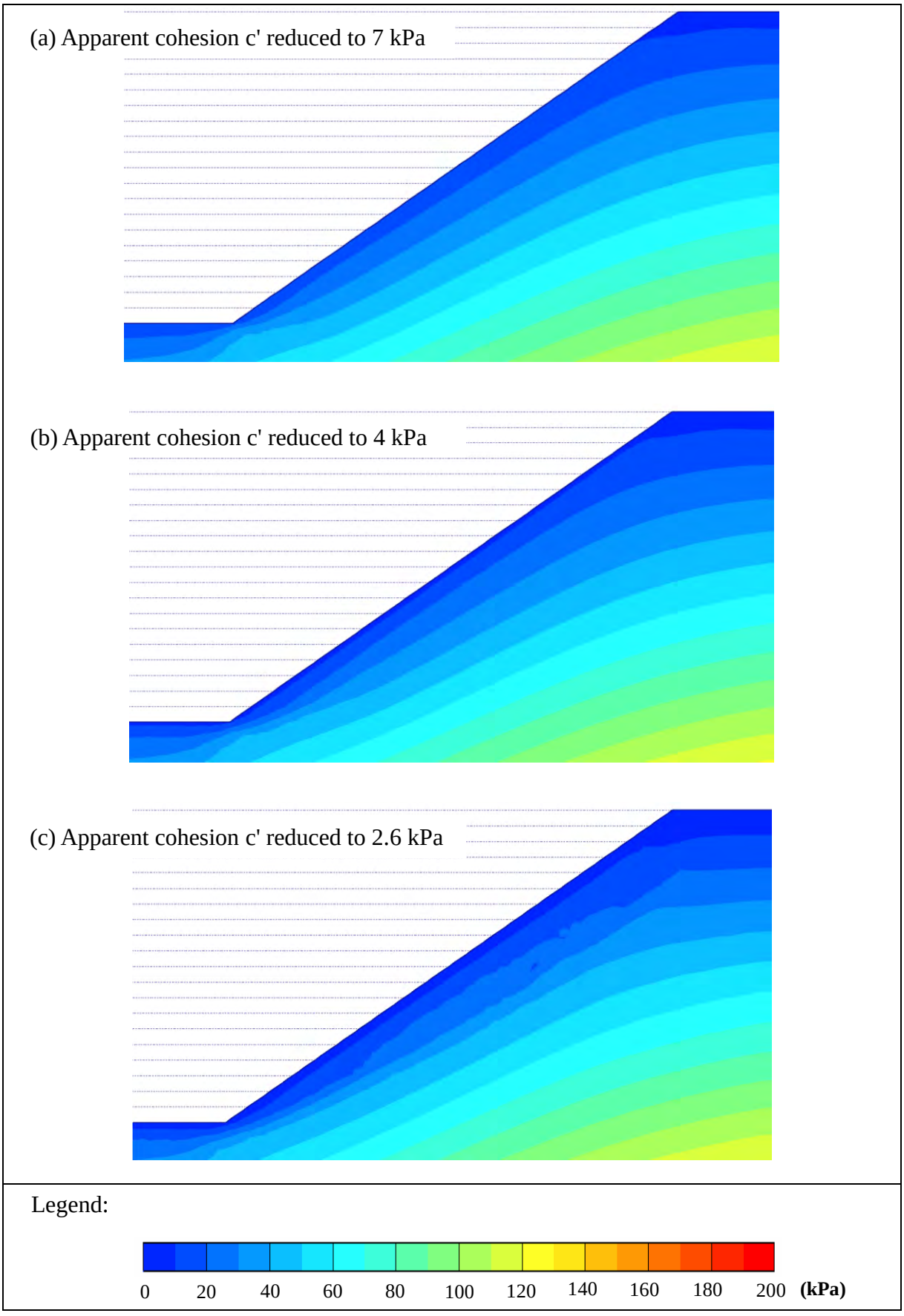

Figure 16 - Mean Effective Stress for Unreinforced Slopes with Gentle Gradient

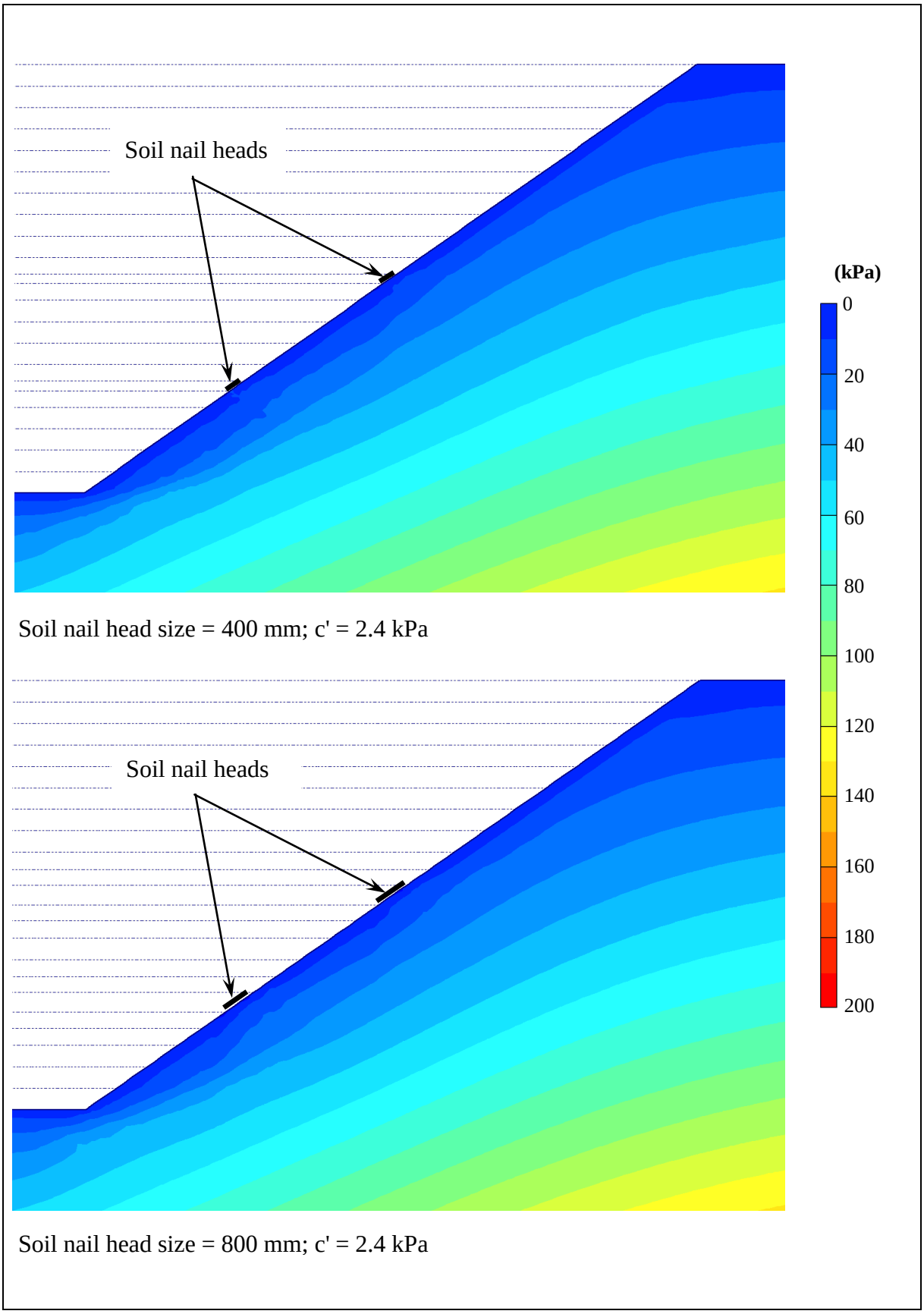

Figure 17 - Comparison of Mean Effective Stress for Reinforced Slopes with Gentle Gradient and Different Nail Head Sizes

Table of Contents
Table of Contents
Table of Contents

APPENDIX A

OUTPUT FROM NUMERICAL MODELLING FOR UNREINFORCED SLOPES

LIST OF FIGURES

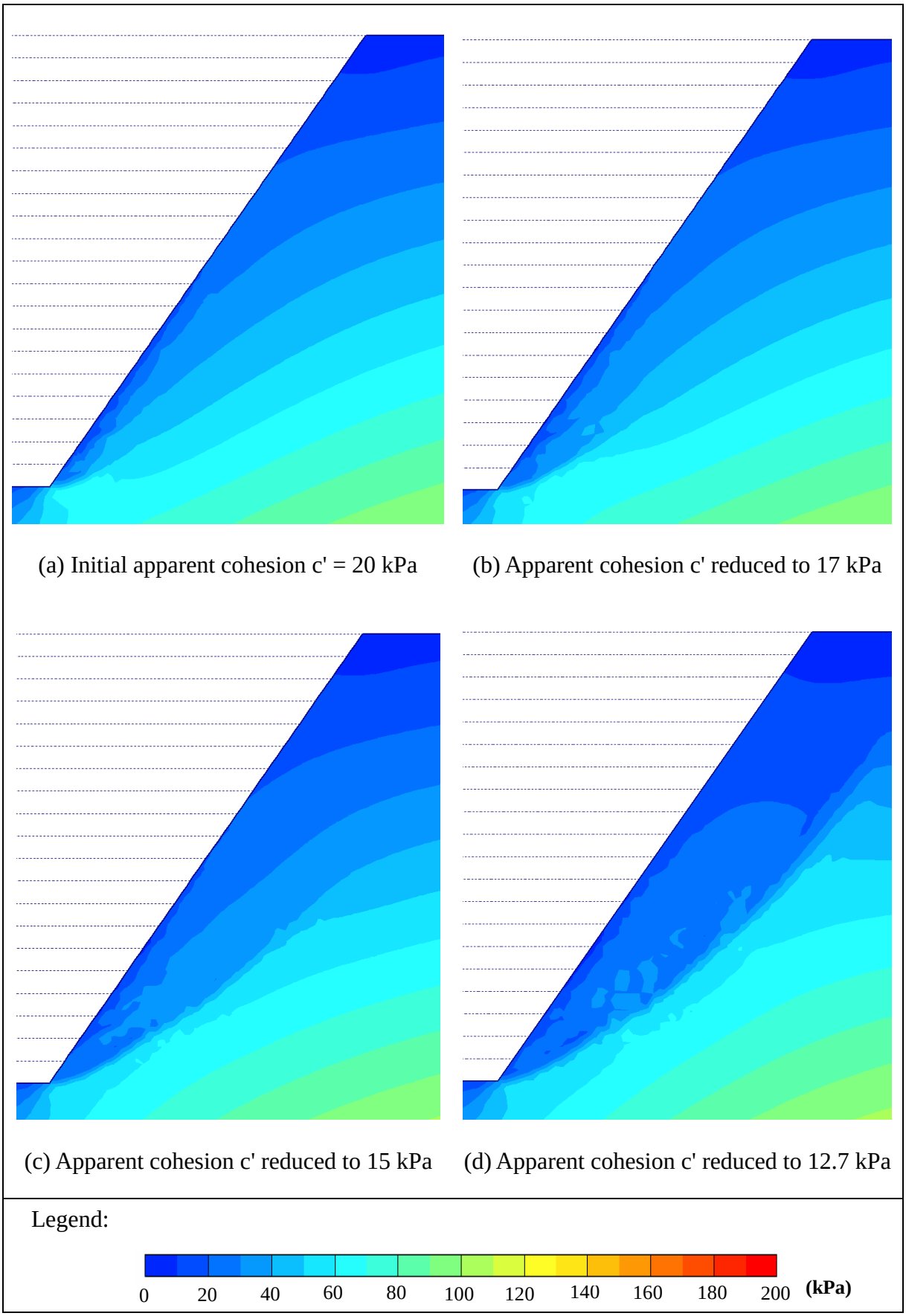

Figure A1 - Development of Mean Effective Stress

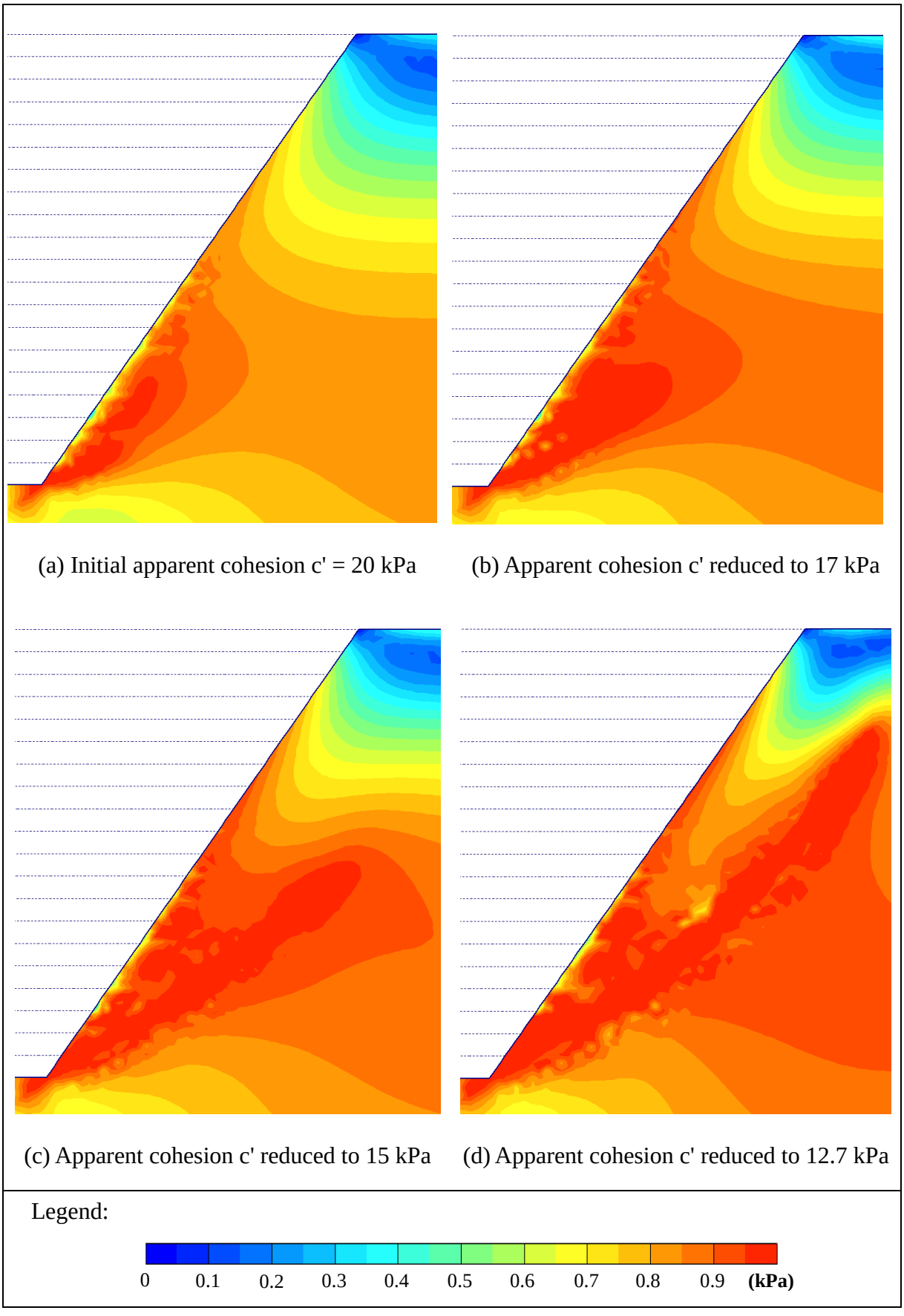

Figure A2 - Development of Relative Shear Stress

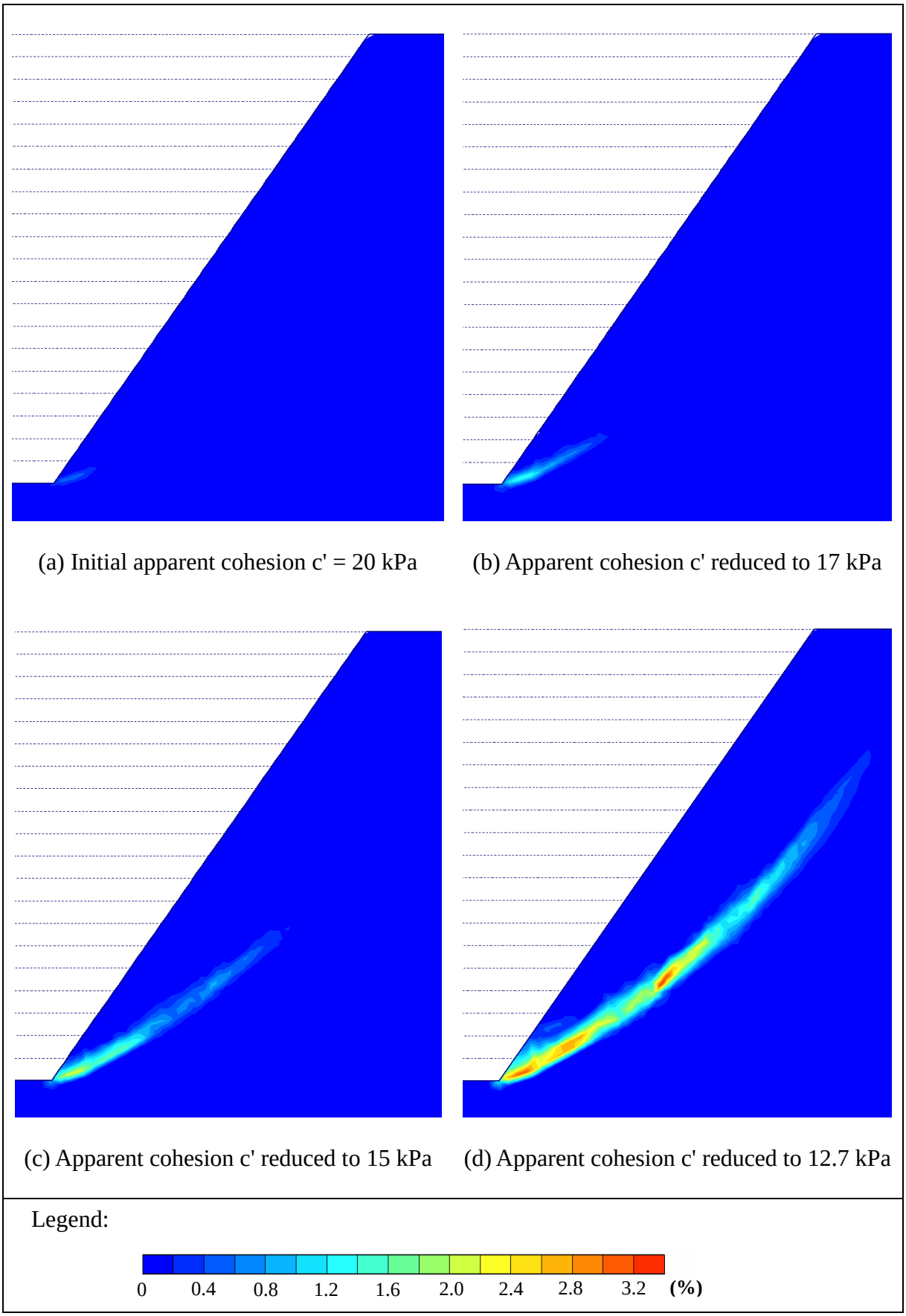

Figure A3 - Development of Shear Strain

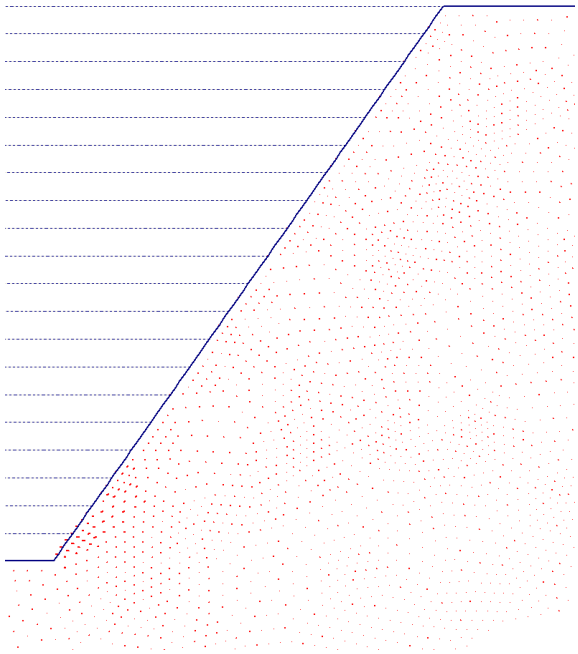

(a) Initial apparent cohesion c' = 20 kPa

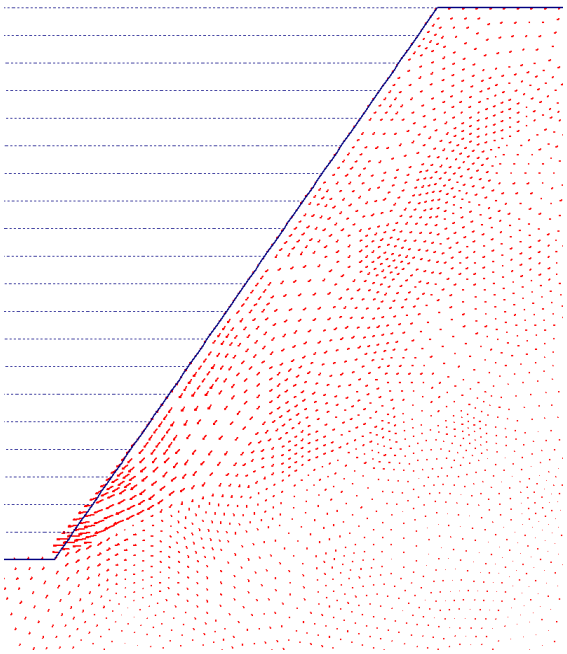

(b) Apparent cohesion c' reduced to 17 kPa

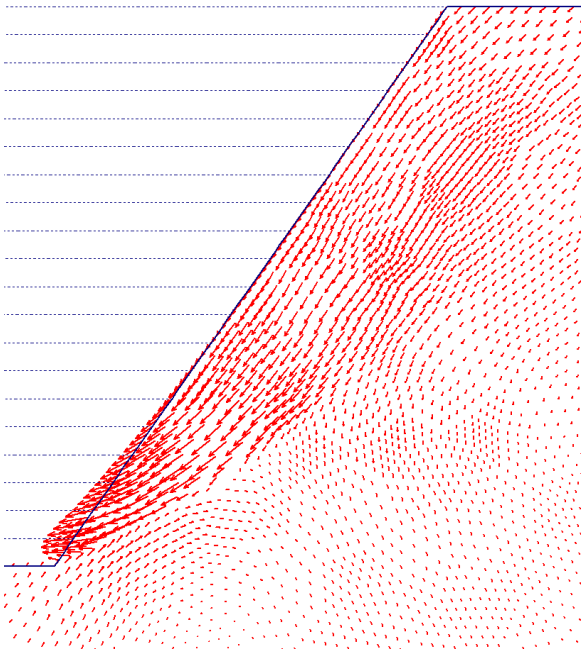

(c) Apparent cohesion c' reduced to 15 kPa

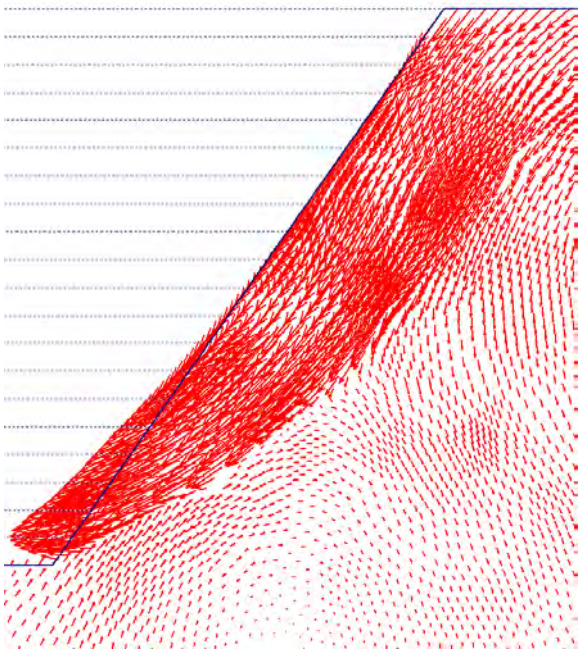

(d) Apparent cohesion c' reduced to 12.7 kPa

Figure A4 - Displacement Vectors

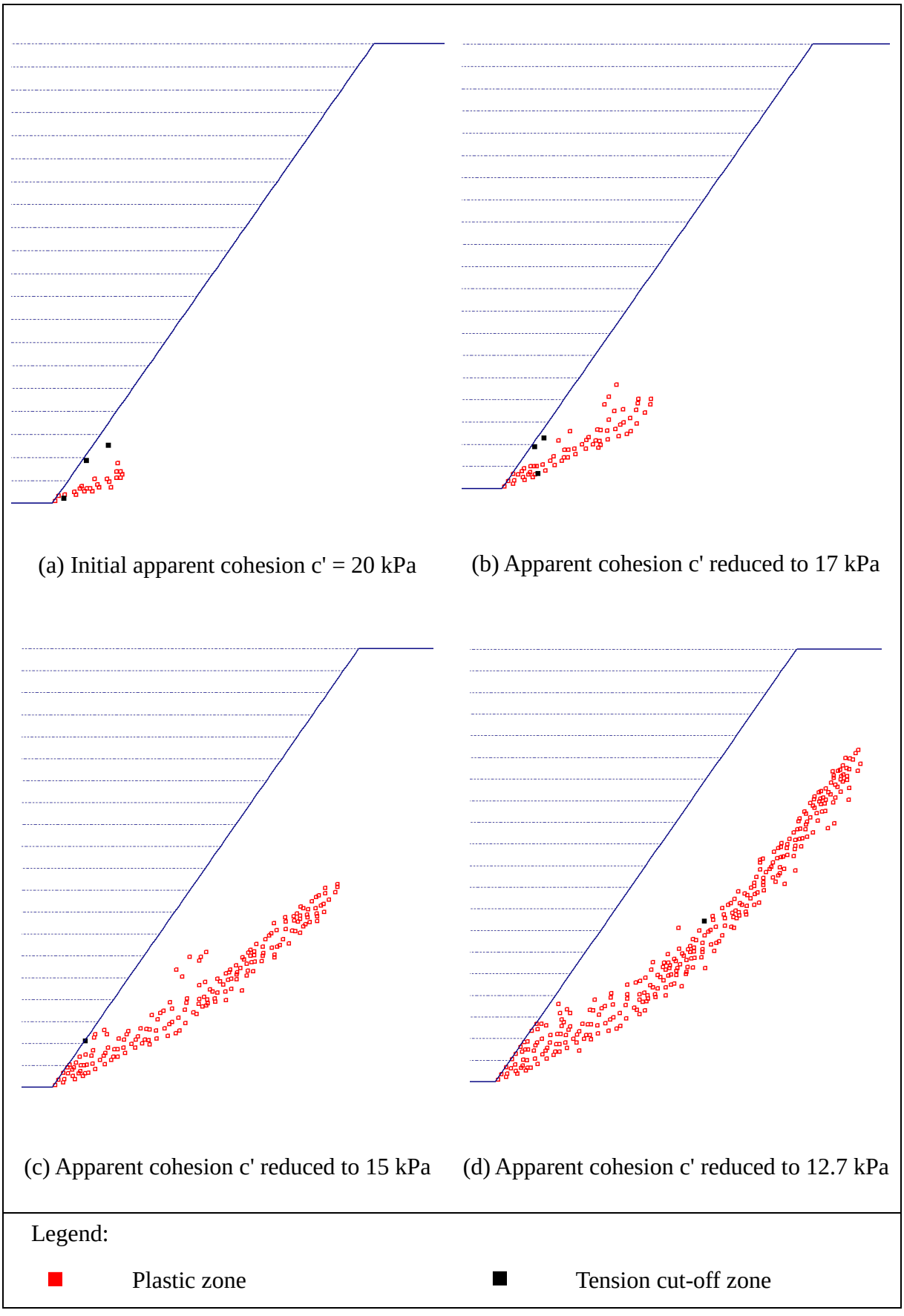

Figure A5 - Development of Plastic Zones

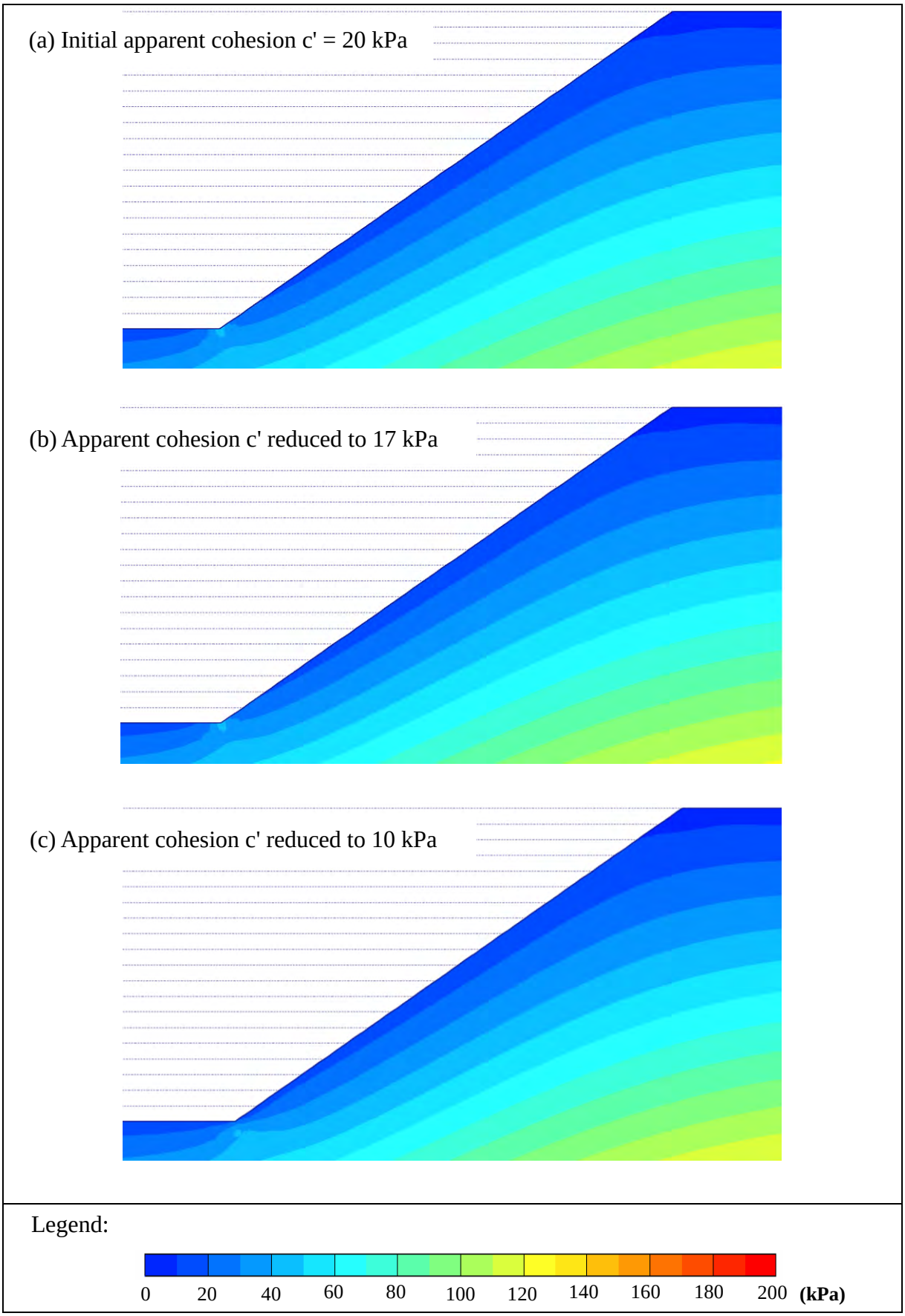

Figure A6 - Development of Mean Effective Stress - 35° Slope (Sheet 1 of 2)

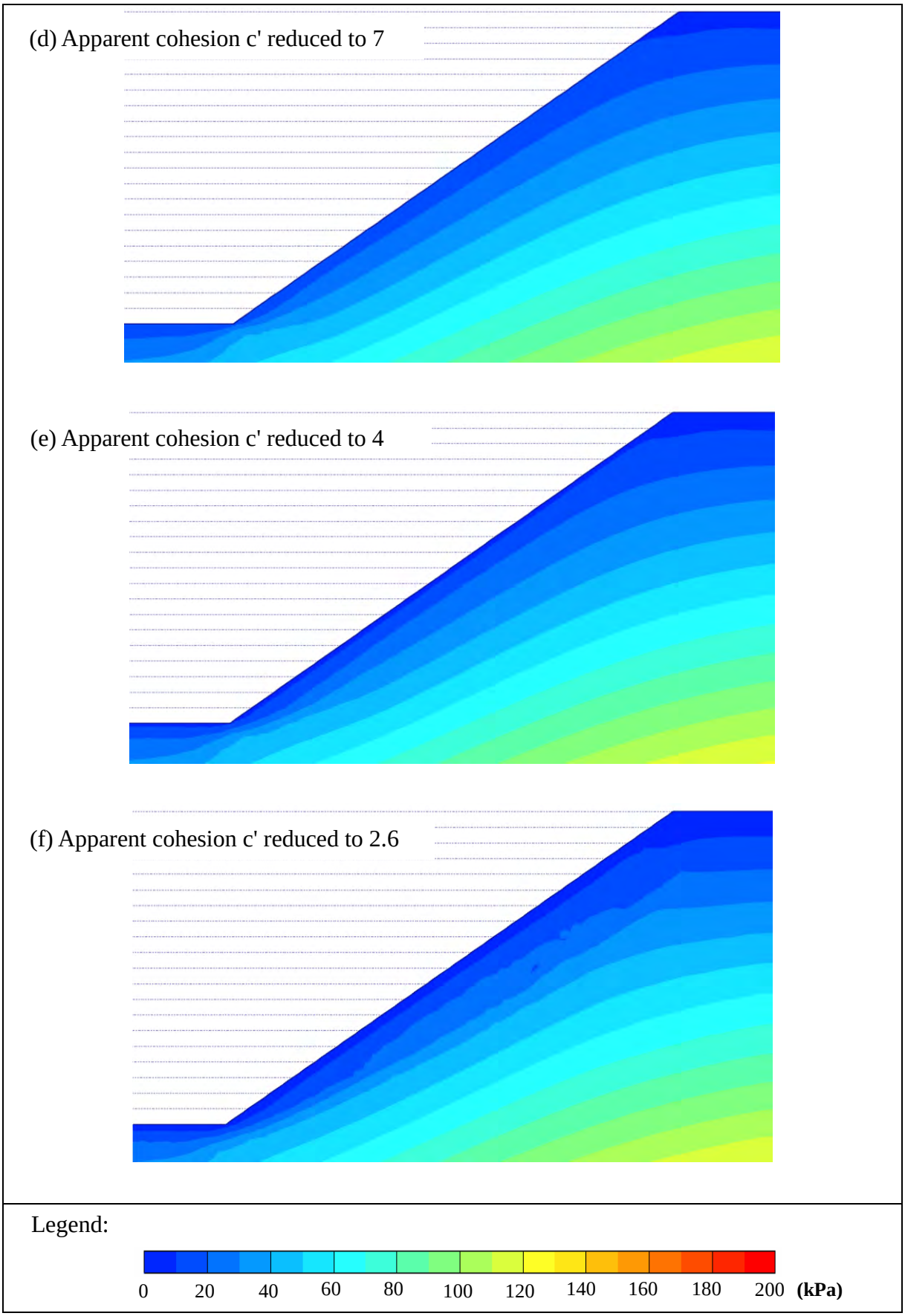

Figure A6 - Development of Mean Effective Stress - 35° Slope (Sheet 2 of 2)

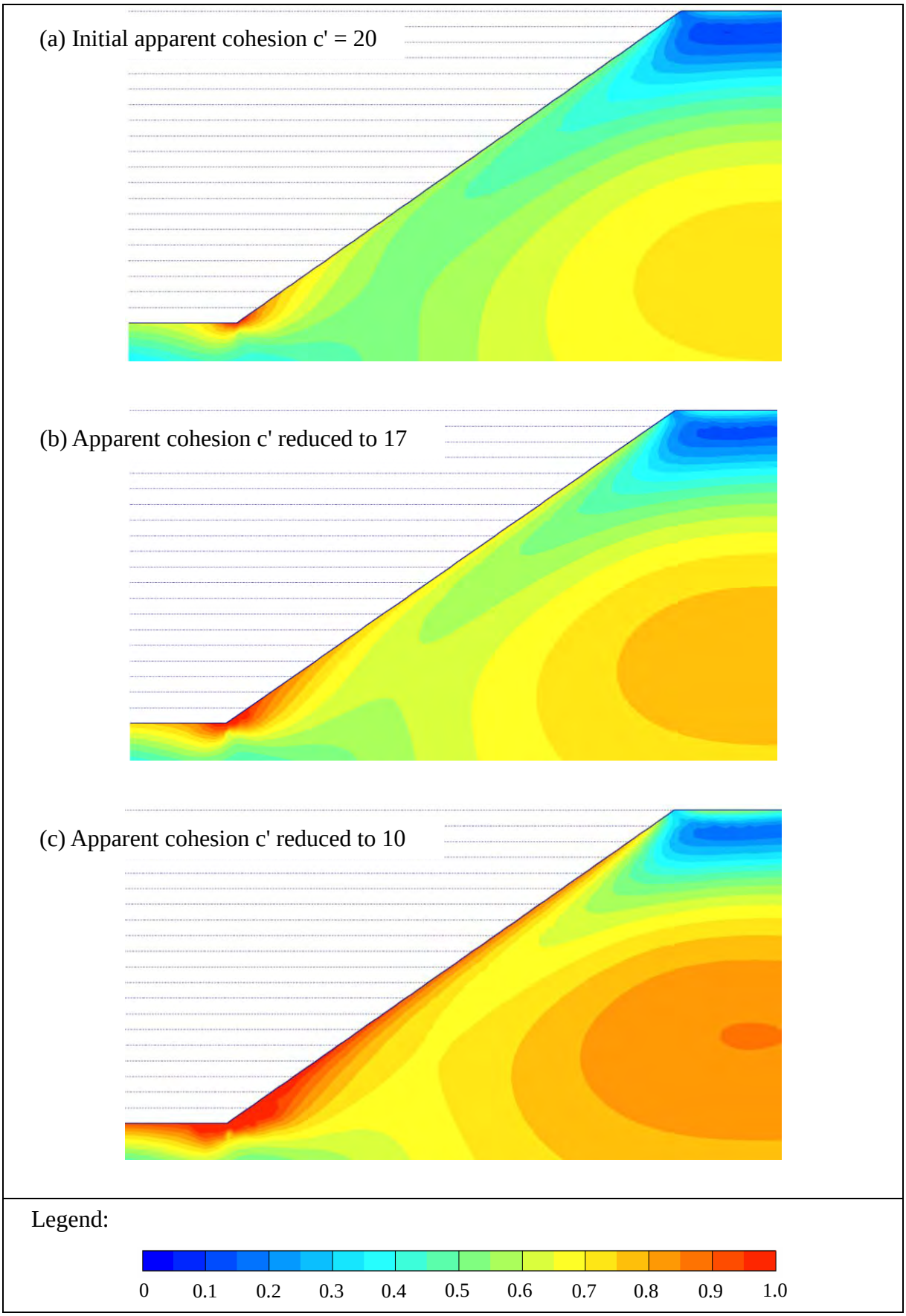

Figure A7 - Development of Relative Shear Stress - 35° Slope (Sheet 1 of 2)

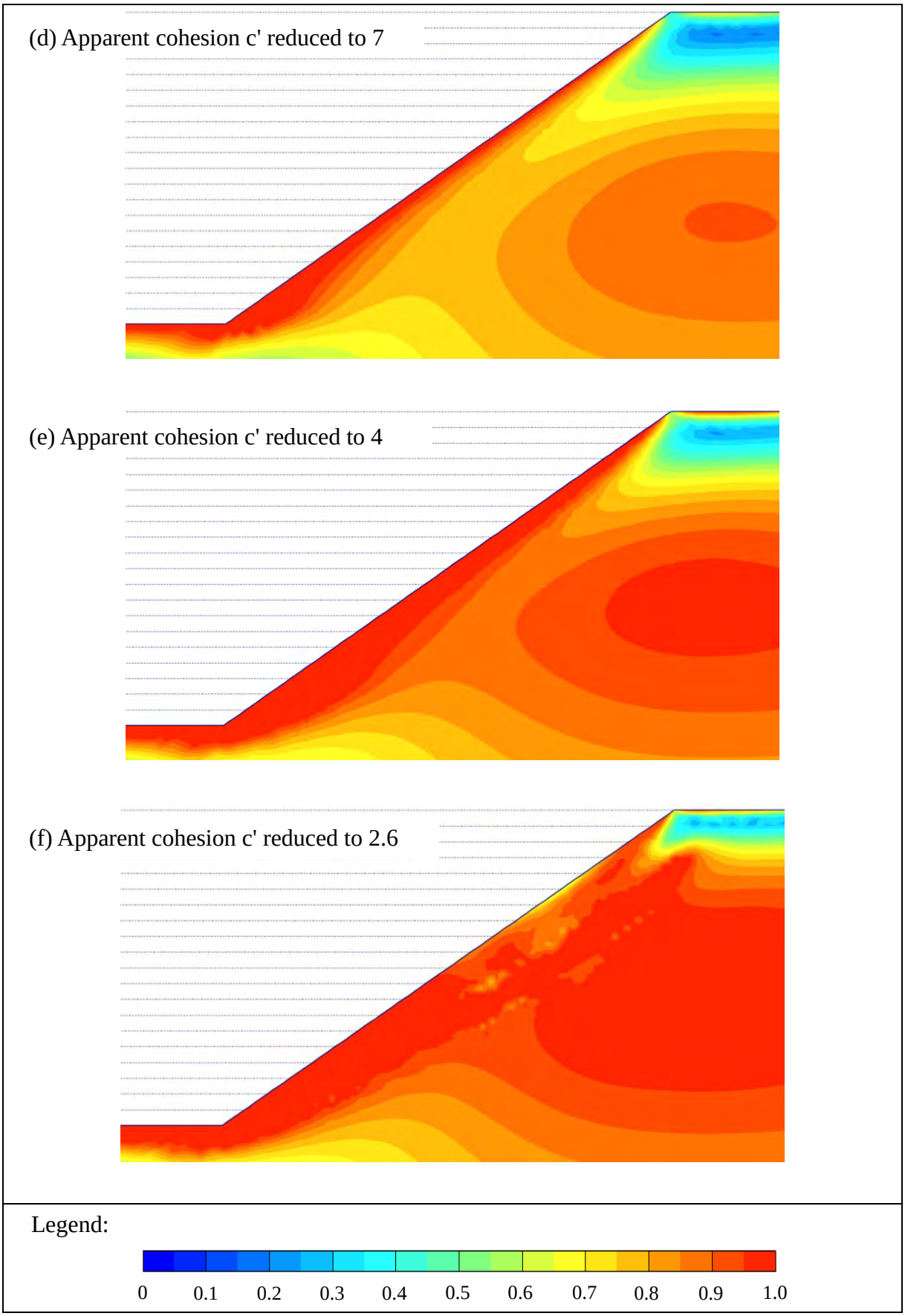

Figure A7 - Development of Relative Shear Stress - 35° Slope (Sheet 2 of 2)

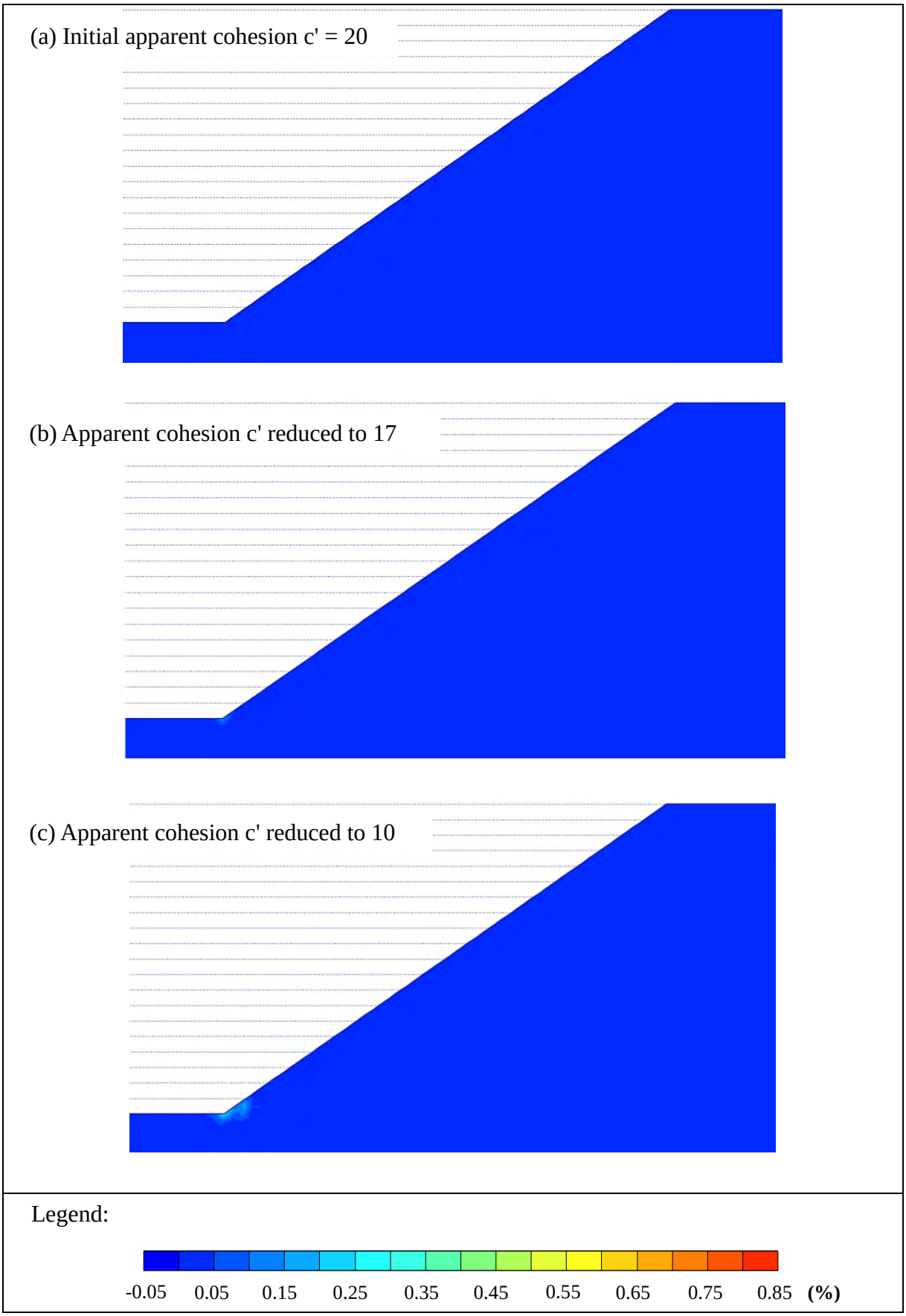

Figure A8 - Development of Shear Strain - 35° Slope (Sheet 1 of 2)

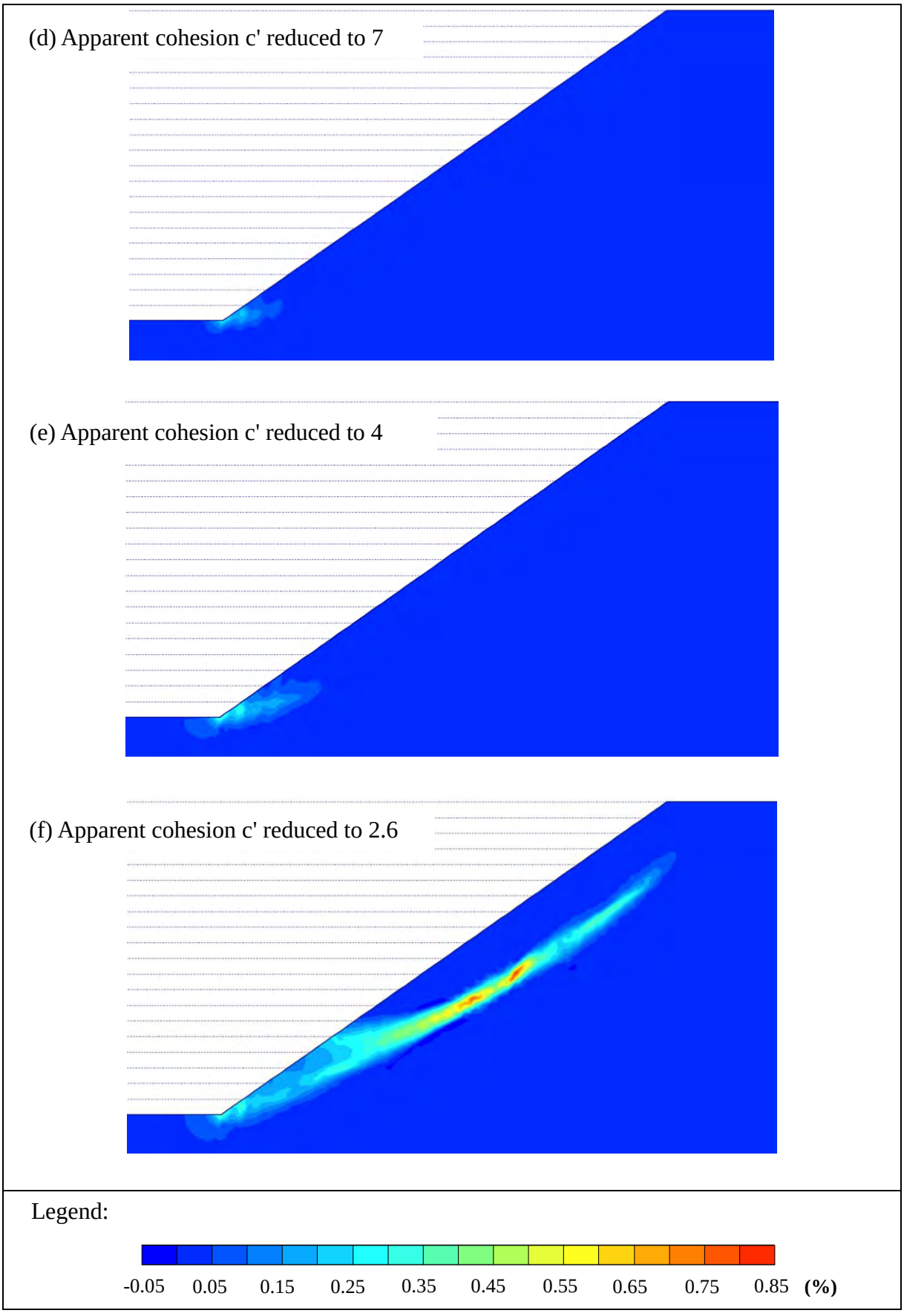

Figure A8 - Development of Shear Strain - 35° Slope (Sheet 2 of 2)

(a) Initial apparent cohesion c' = 20 kPa

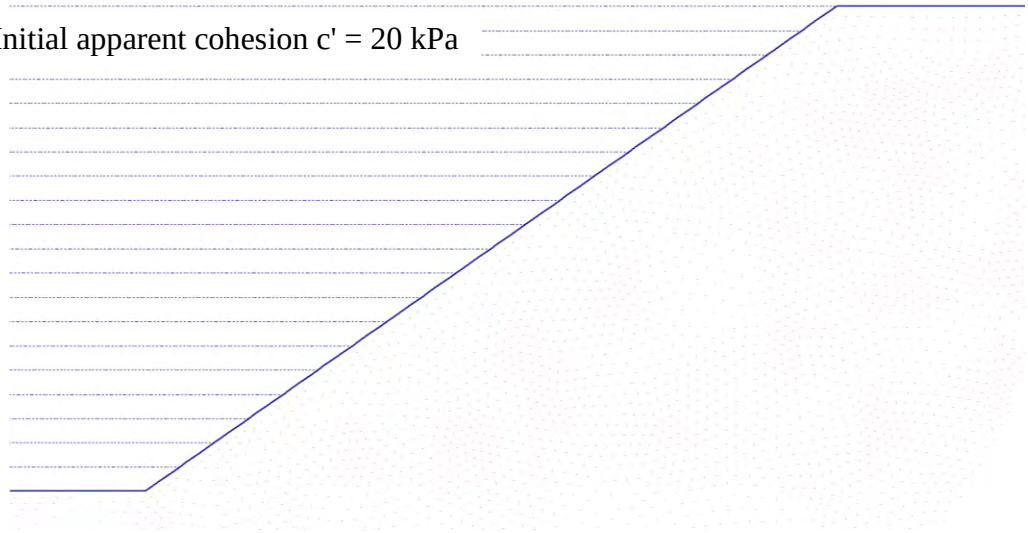

(b) Apparent cohesion c' reduced to 17 kPa

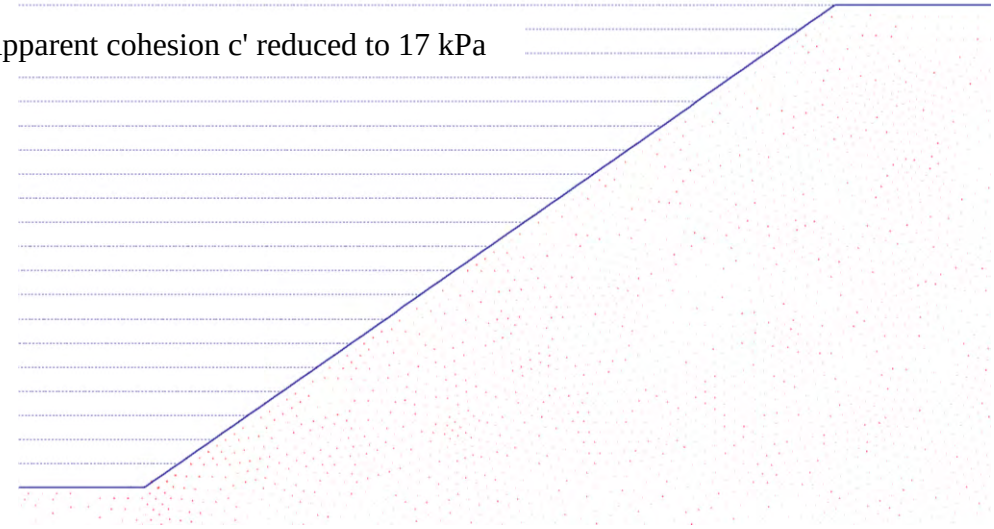

(c) Apparent cohesion c' reduced to 10 kPa

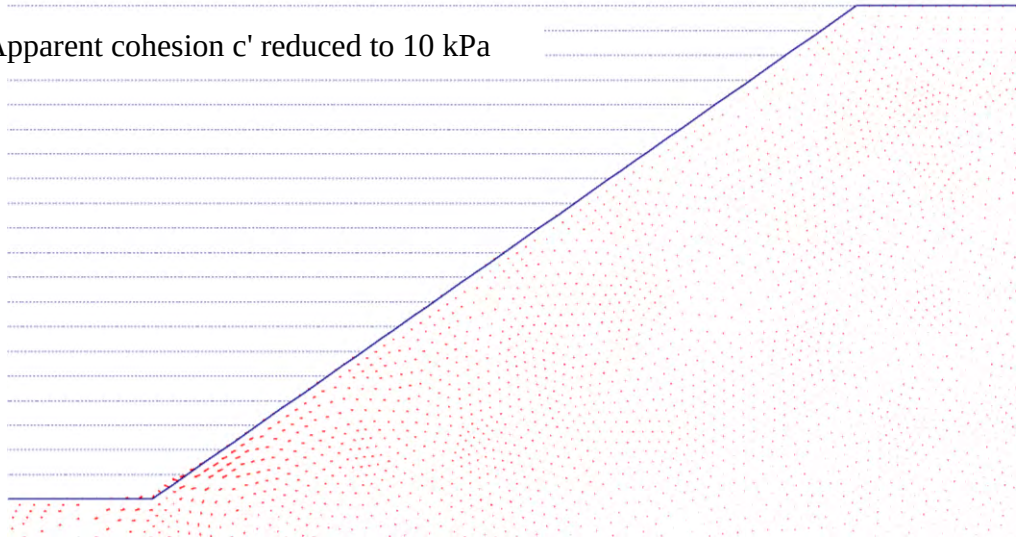

Figure A9 - Displacement Vectors - 35° Slope (Sheet 1 of 2)

(d) Apparent cohesion c' reduced to 7 kPa

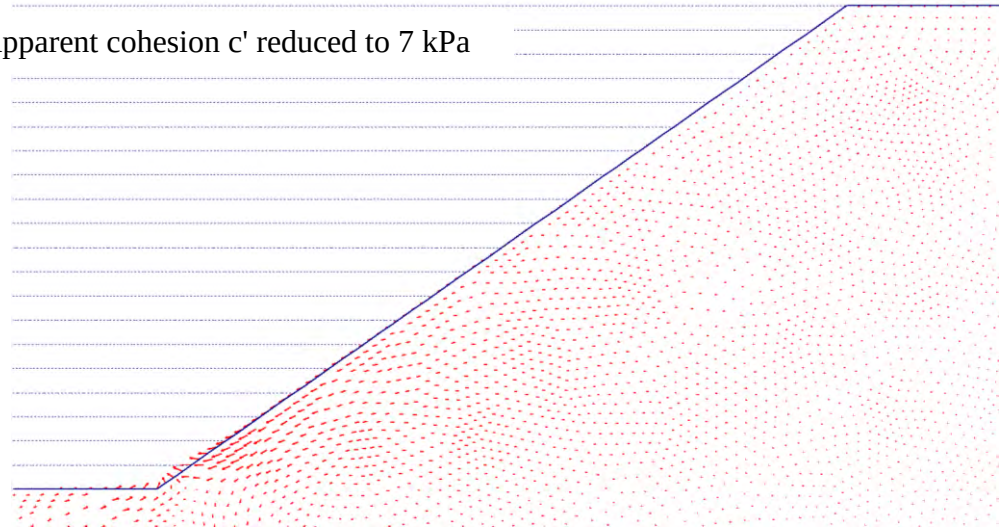

(e) Apparent cohesion c' reduced to 4 kPa

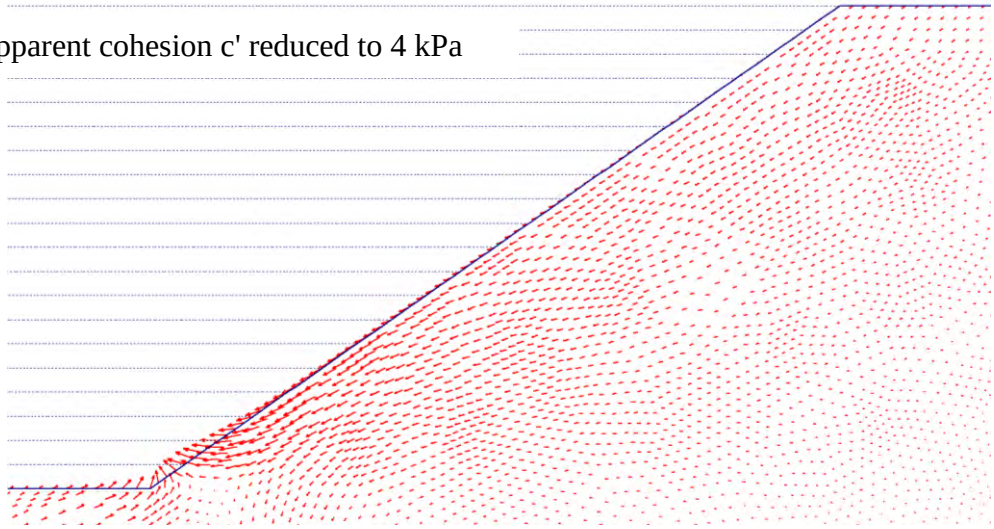

(f) Apparent cohesion c' reduced to 2.6 kPa

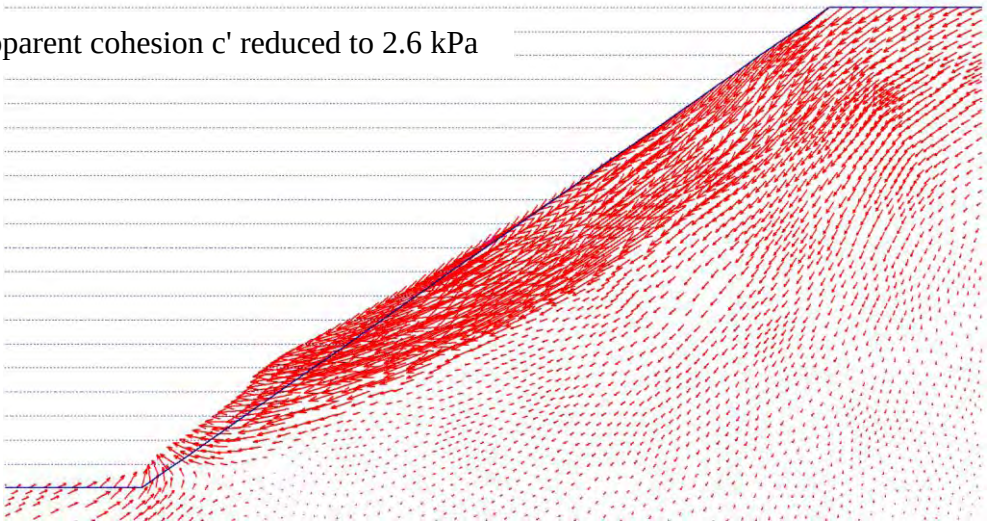

Figure A9 - Displacement Vectors - 35° Slope (Sheet 2 of 2)

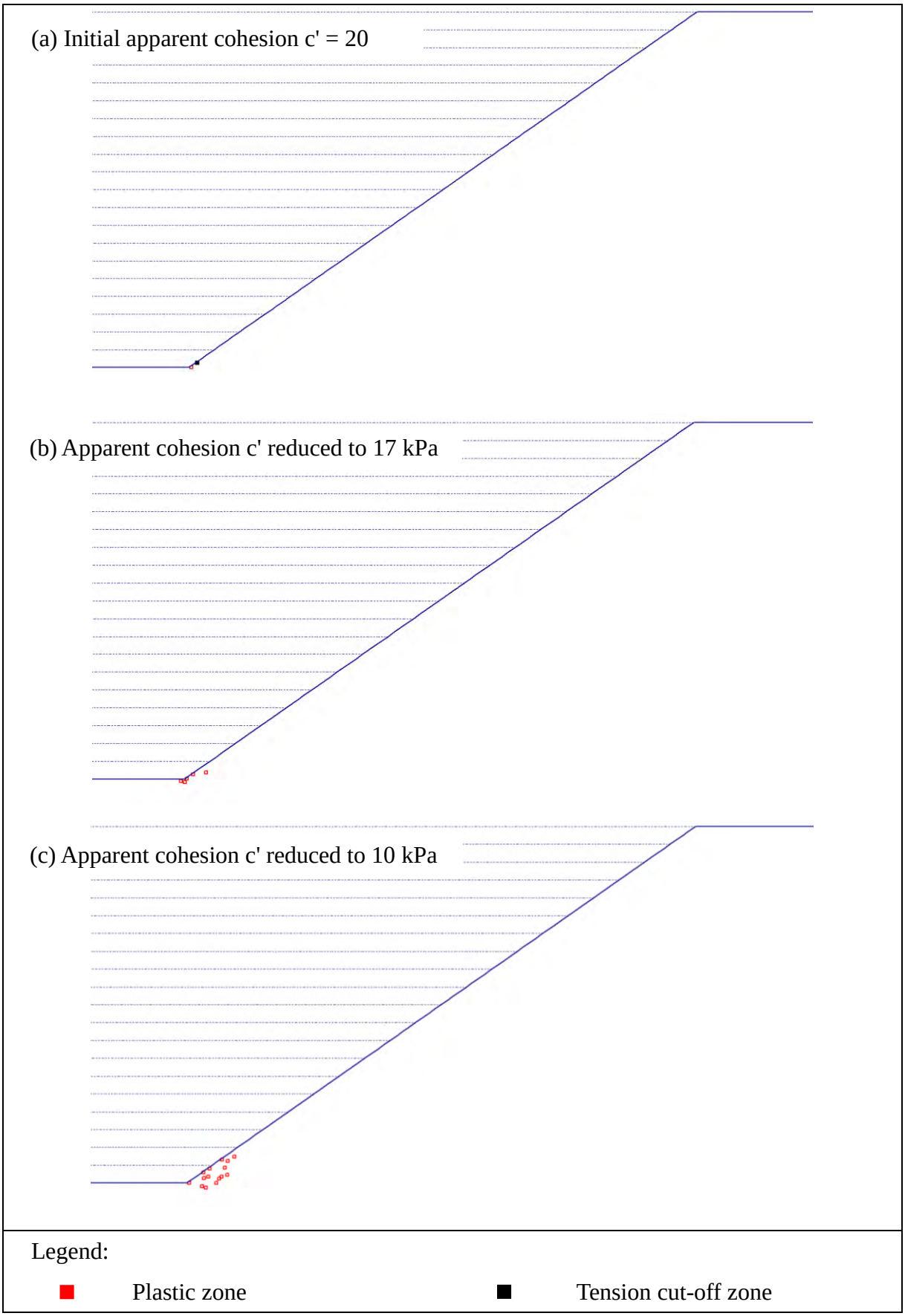

Figure A10 - Development of Plastic Zones - 35° Slope (Sheet 1 of 2)

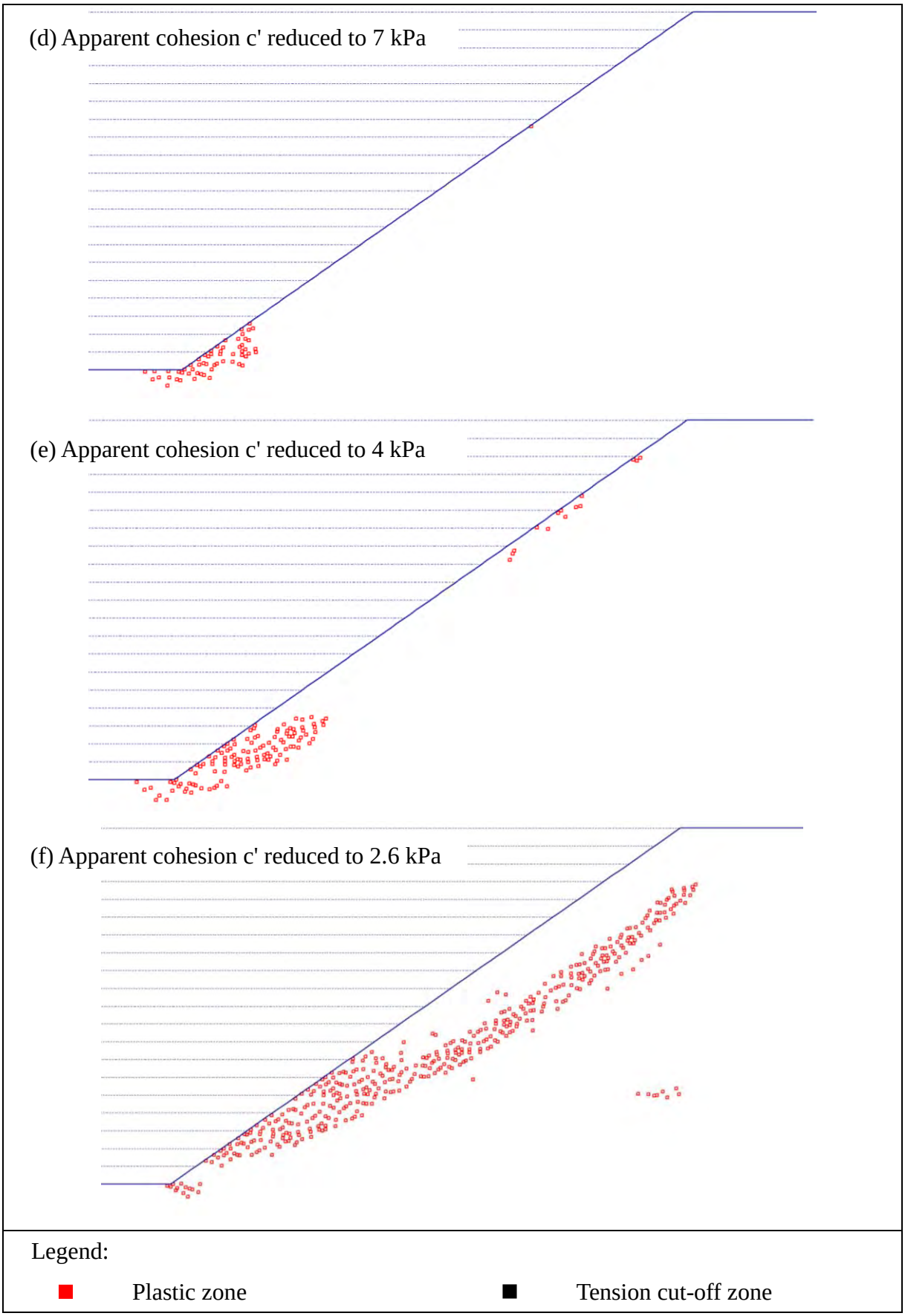

Figure A10 - Development of Plastic Zones - 35° Slope (Sheet 2 of 2)

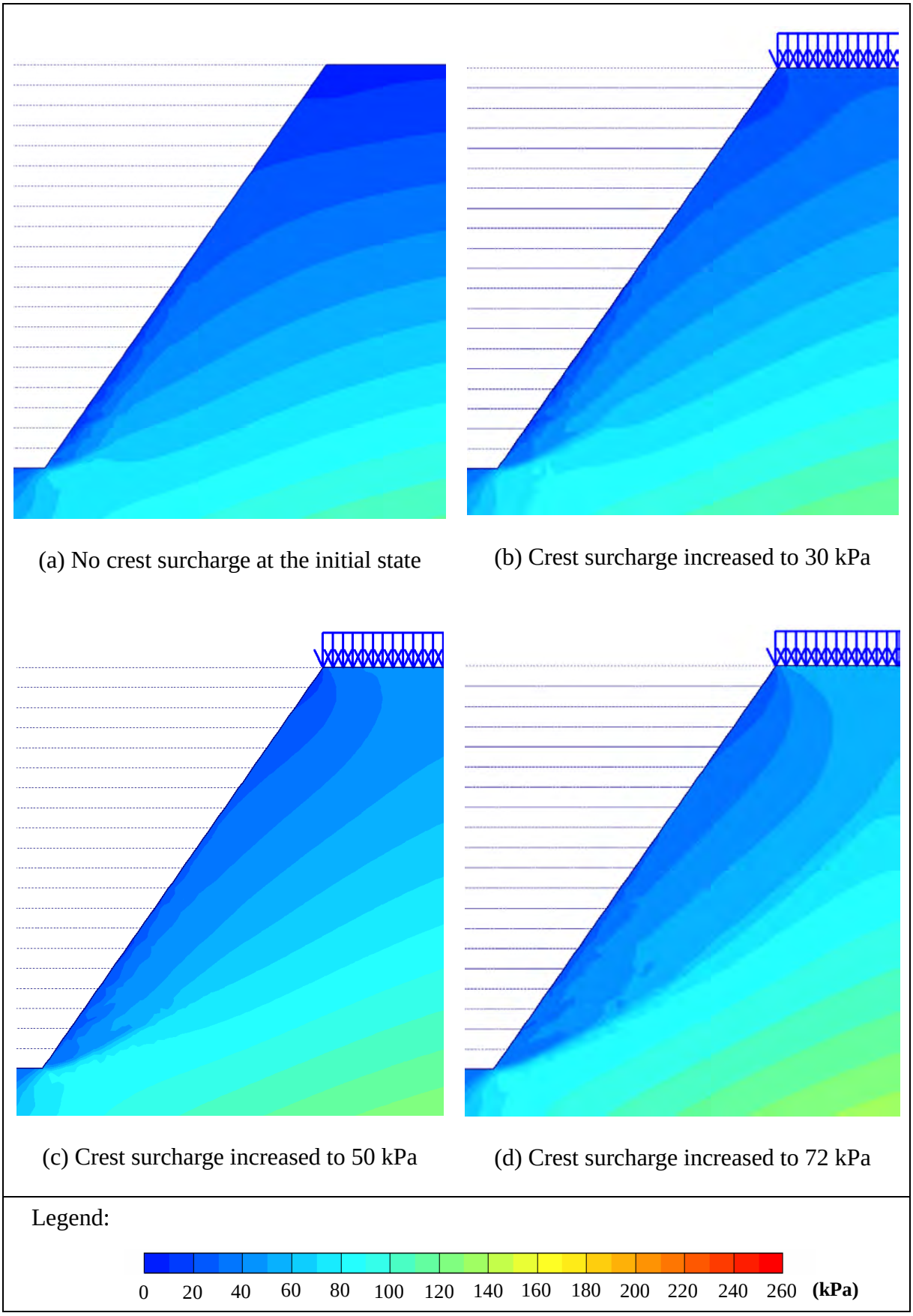

Figure A11 - Development of Mean Effective Stress - with Crest Surcharge

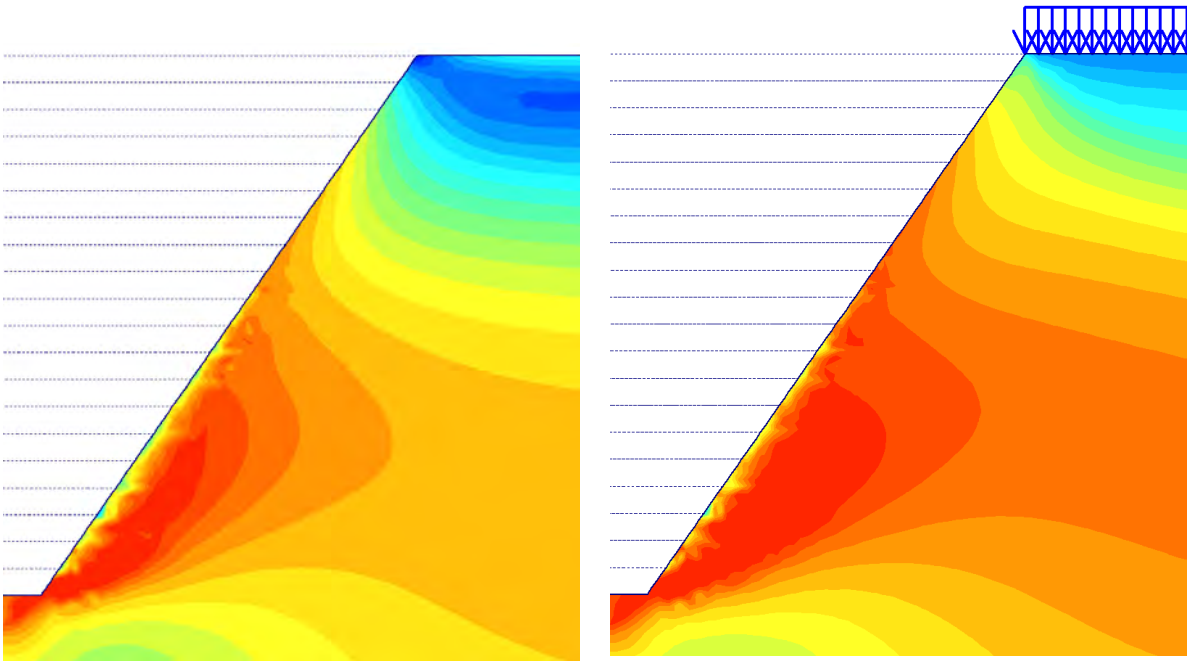

(a) No crest surcharge at the initial state

(b) Crest surcharge increased to 30 kPa

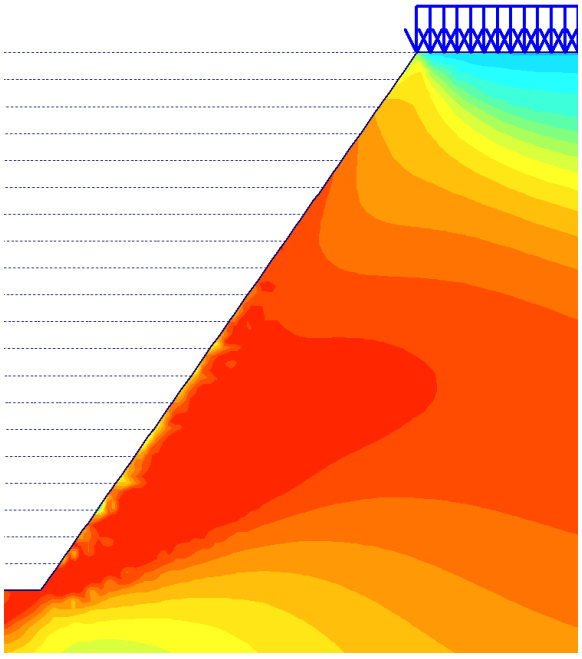

(c) Crest surcharge increased to 50 kPa

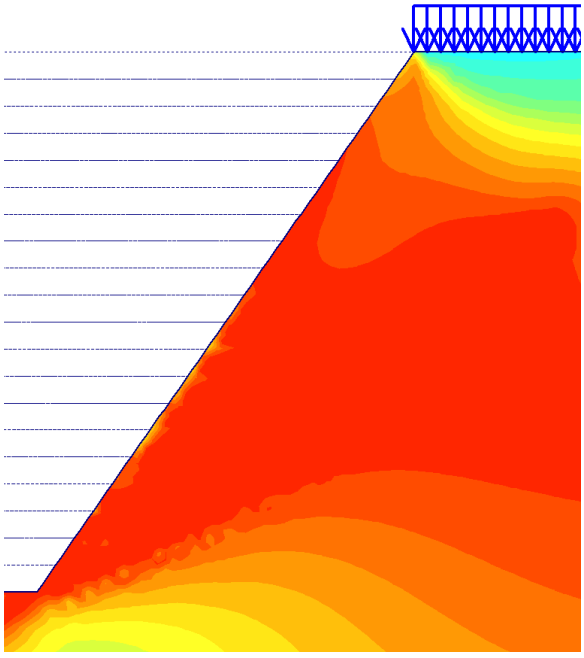

(d) Crest surcharge increased to 72 kPa

Legend:

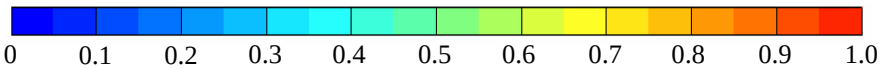

Figure A12 - Development of Relative Shear Stress - with Crest Surcharge

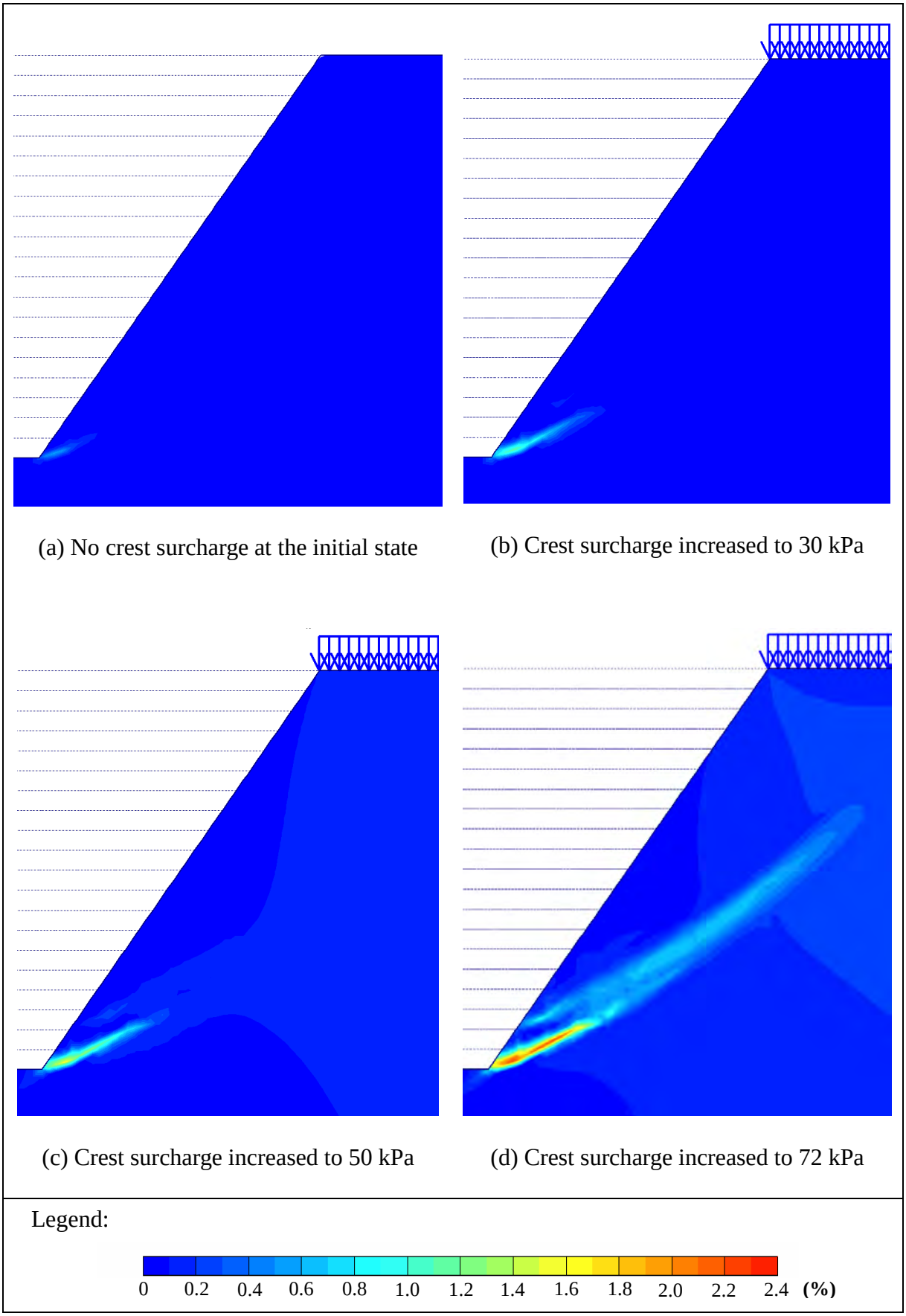

Figure A13 - Development of Shear Strain - with Crest Surcharge

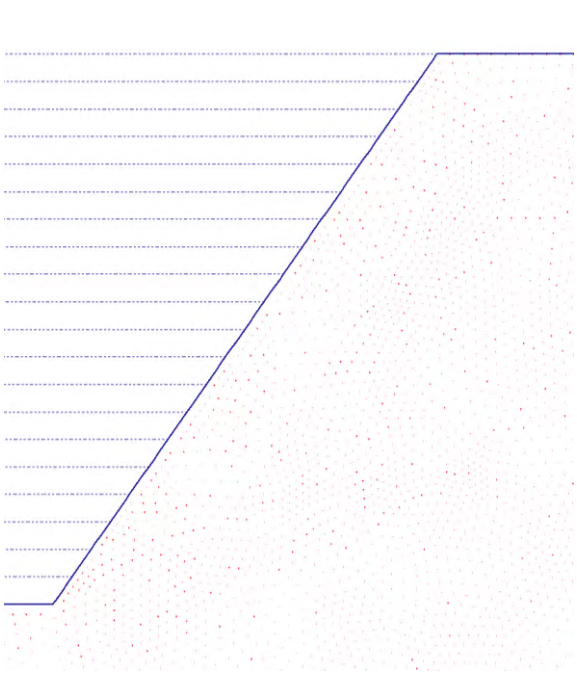

(a) No crest surcharge at the initial state

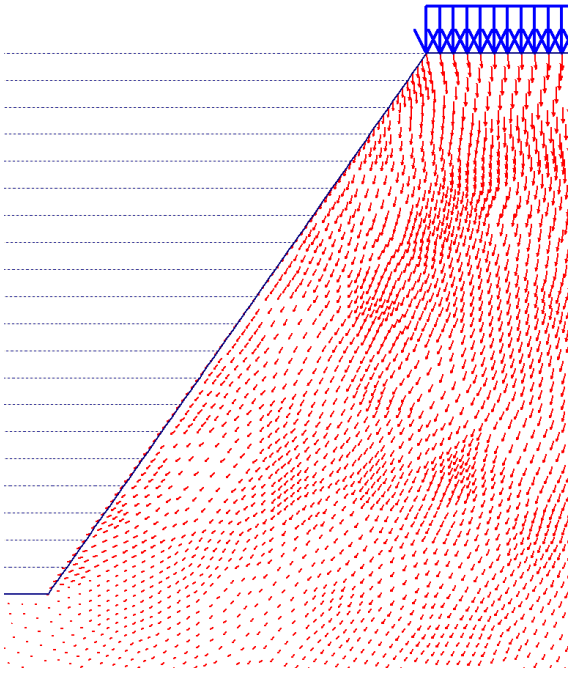

(b) Crest surcharge increased to 30 kPa

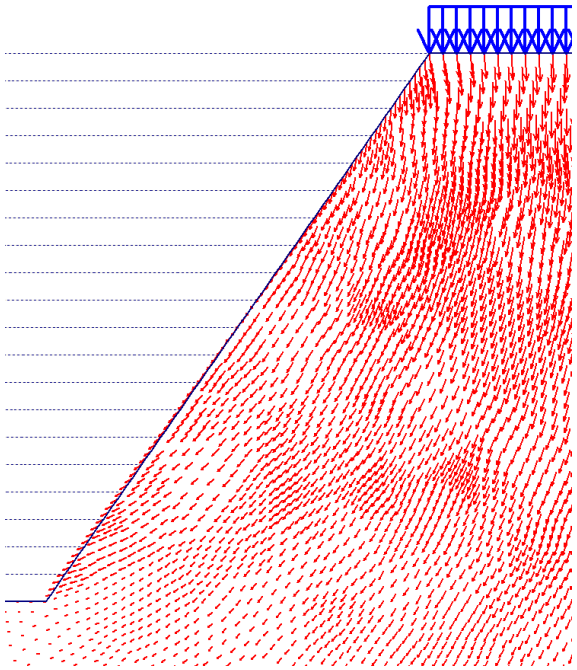

(c) Crest surcharge increased to 50 kPa

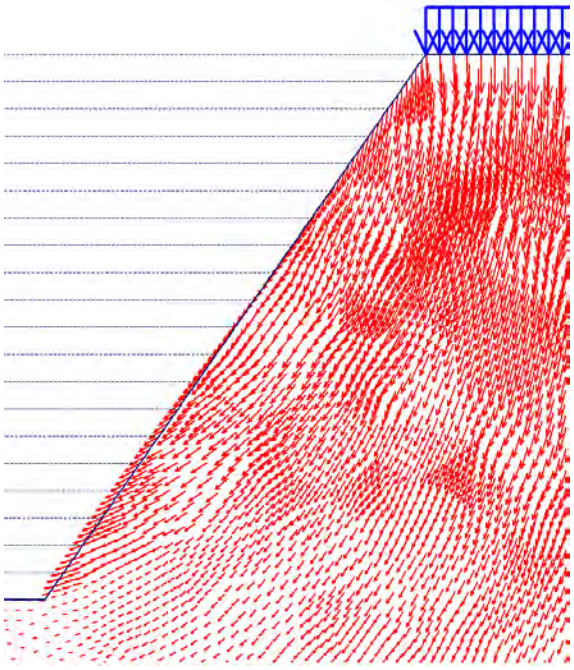

(d) Crest surcharge increased to 72 kPa

Figure A14 - Displacement Vectors - with Crest Surcharge

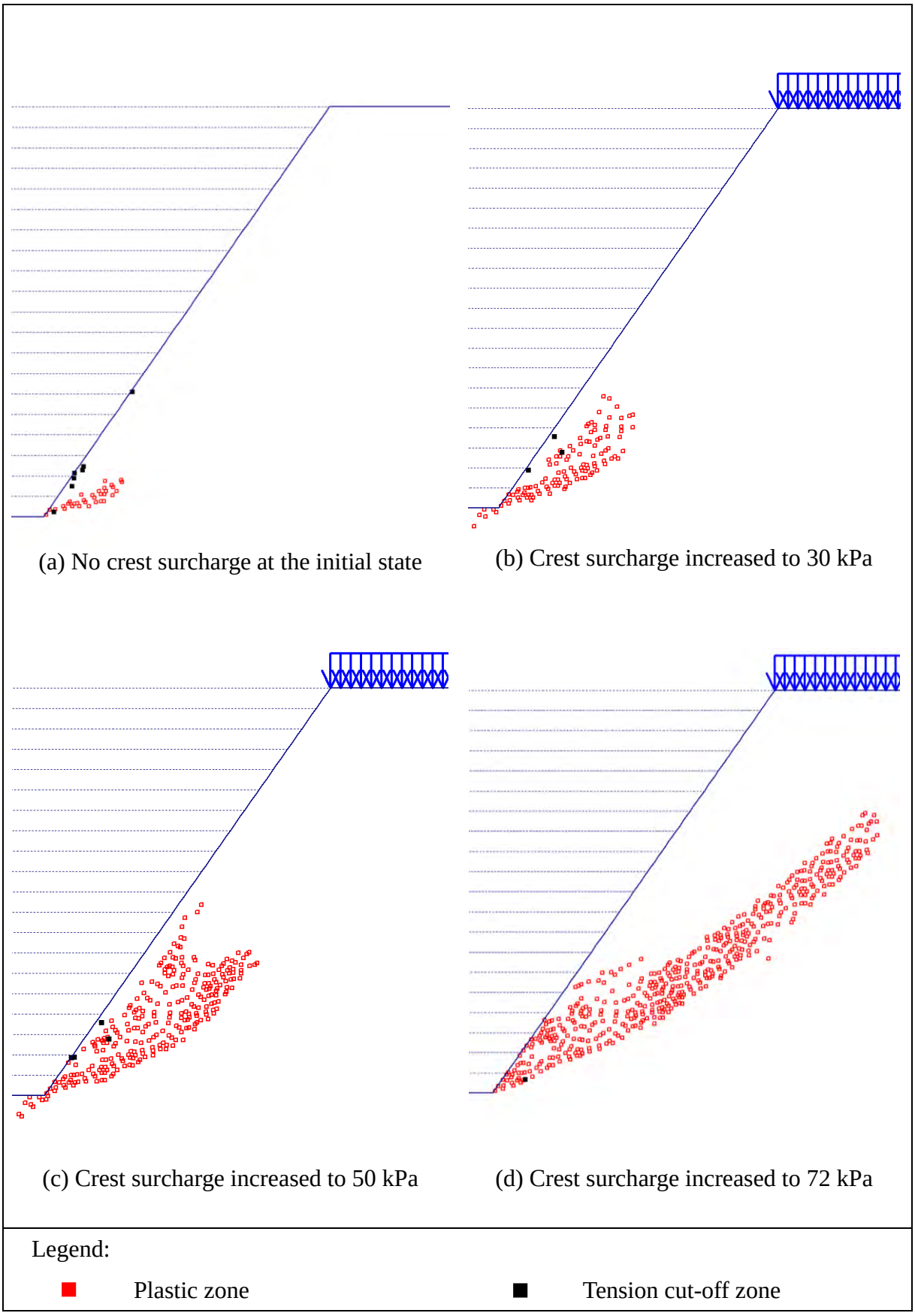

Figure A15 - Development of Plastic Zones - with Crest Surcharge

Table of Contents
Table of Contents
Table of Contents

APPENDIX B

OUTPUT FROM NUMERICAL MODELLING FOR REINFORCED SLOPES WITH TWO ROWS OF SOIL NAILS

LIST OF FIGURES

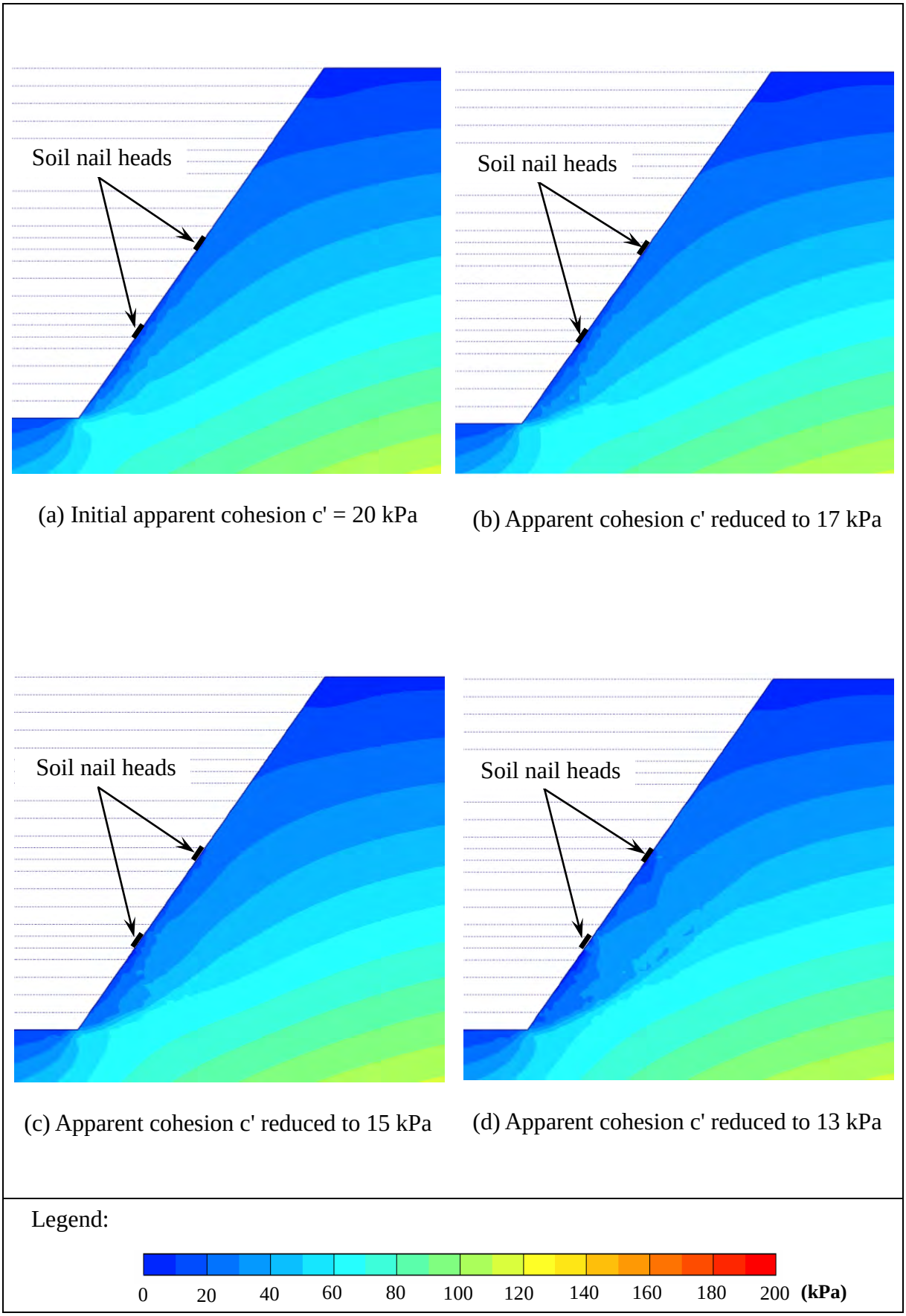

Figure B1 - Development of Mean Effective Stress - Nail Head Size = 400 mm (Sheet 1 of 2)

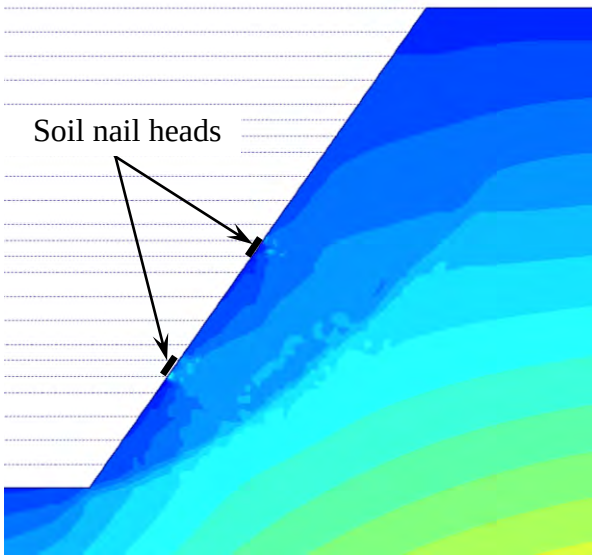

(e) Apparent cohesion c' reduced to 10 kPa

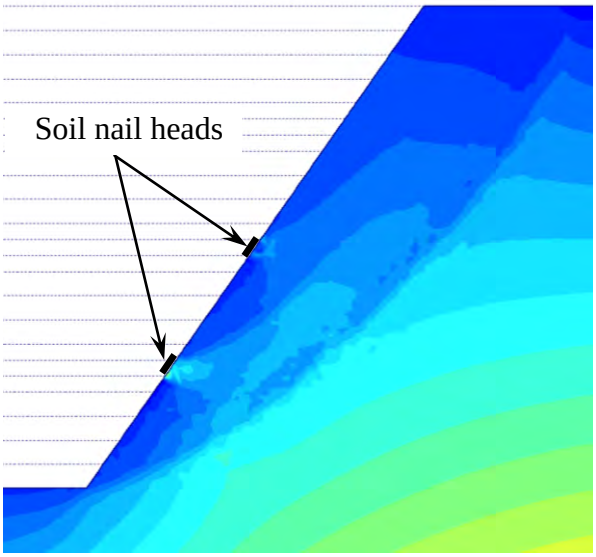

(f) Apparent cohesion c' reduced to 7 kPa

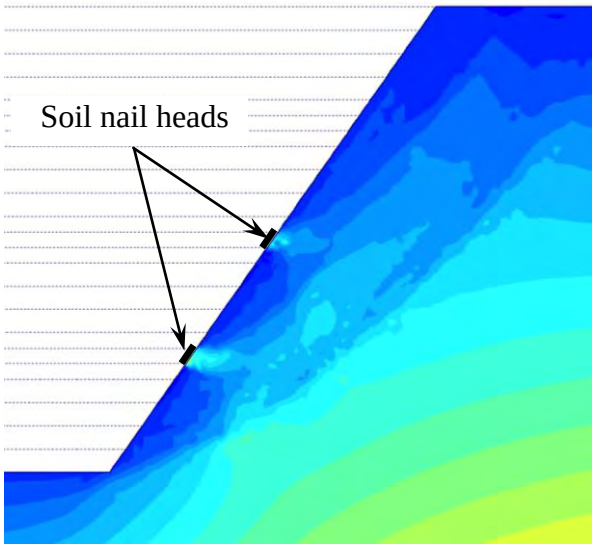

(g) Apparent cohesion c' reduced to 5.2 kPa

Legend:

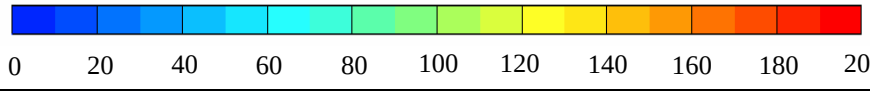

Figure B1 - Development of Mean Effective Stress - Nail Head Size = 400 mm (Sheet 2 of 2)

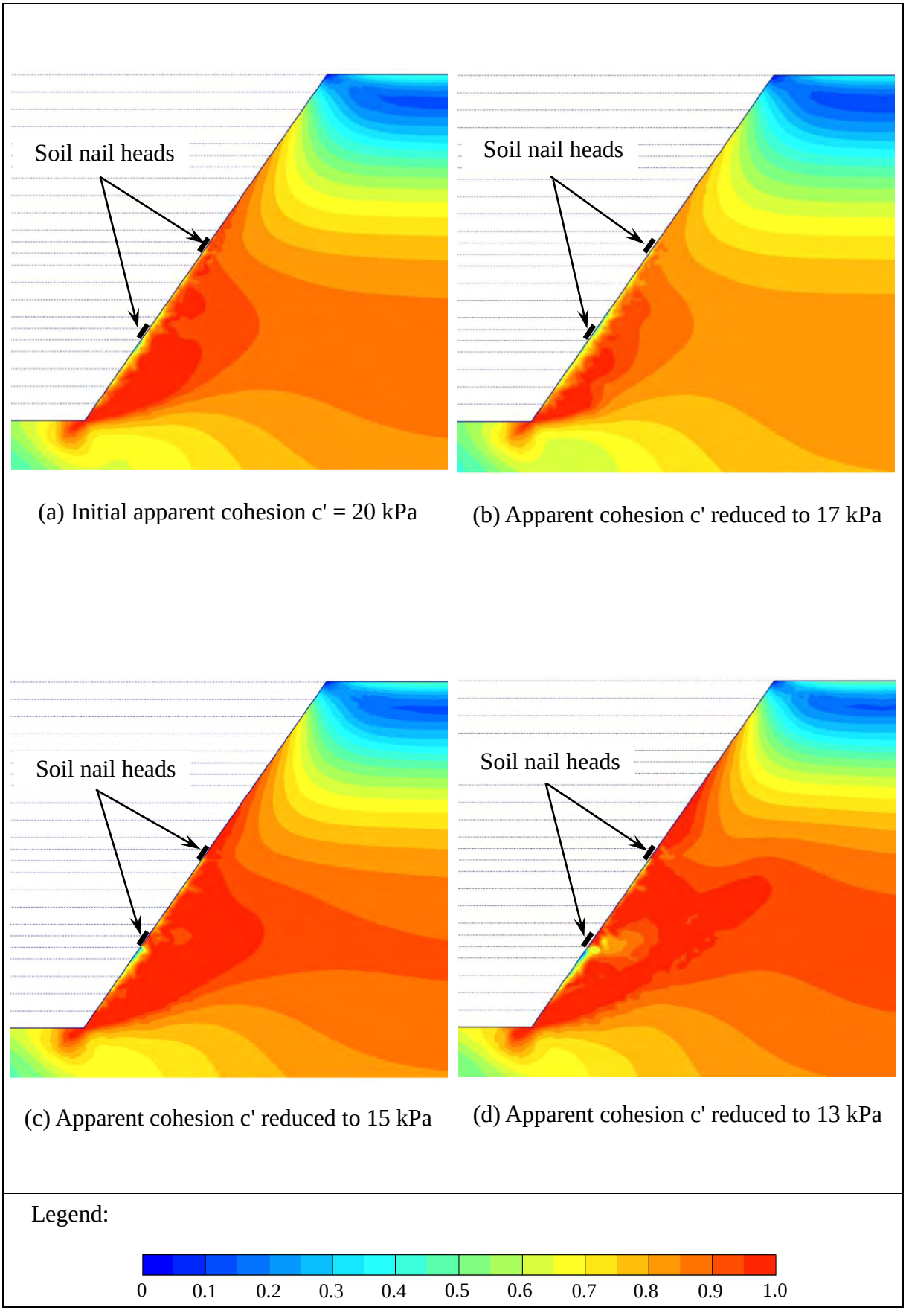

(a) Initial apparent cohesion c' = 20 kPa

(b) Apparent cohesion c' reduced to 17 kPa

(c) Apparent cohesion c' reduced to 15 kPa

(d) Apparent cohesion c' reduced to 13 kPa

Figure B2 - Development of Relative Shear Stress - Nail Head Size = 400 mm (Sheet 1 of 2)

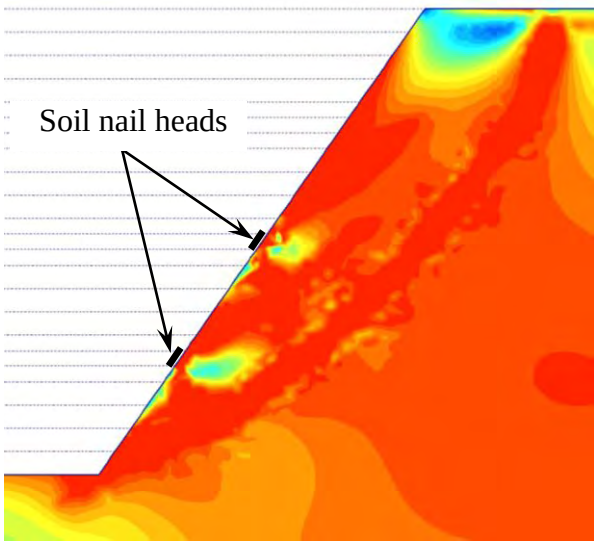

(e) Apparent cohesion c' reduced to 10 kPa

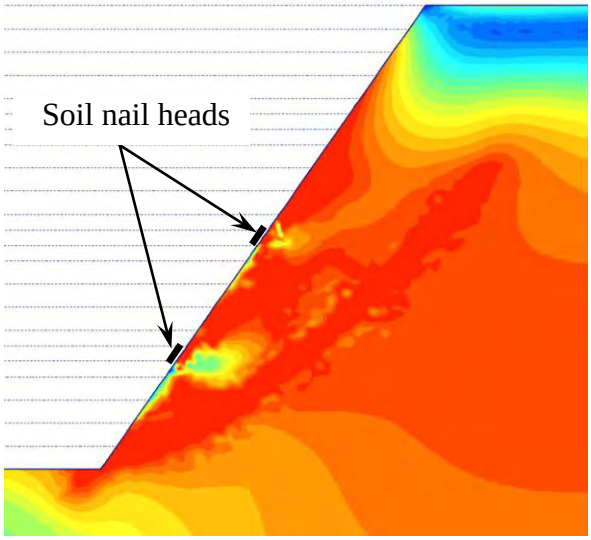

(f) Apparent cohesion c' reduced to 7 kPa

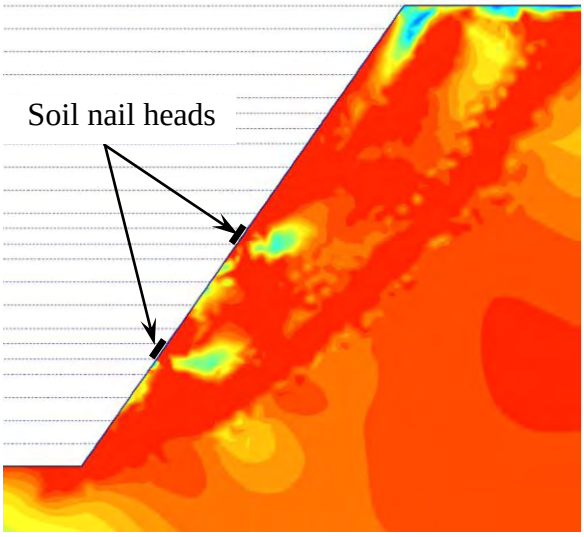

(g) Apparent cohesion c' reduced to 5.2 kPa

Legend:

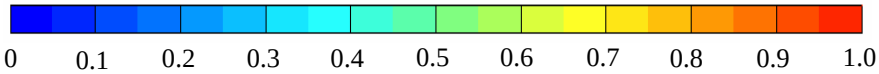

Figure B2 - Development of Relative Shear Stress - Nail Head Size = 400 mm (Sheet 2 of 2)

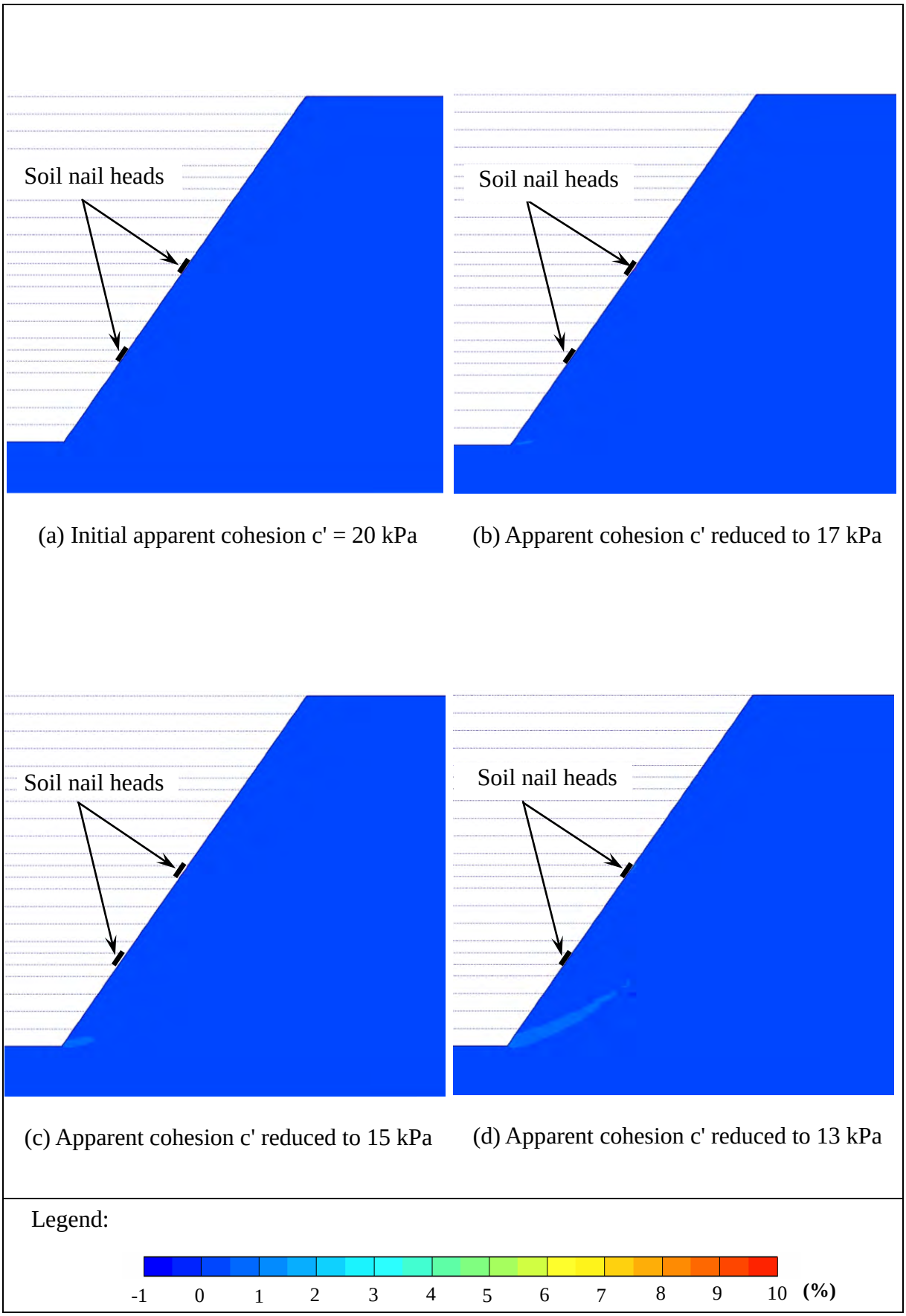

Figure B3 - Development of Shear Strain - Nail Head Size = 400 mm (Sheet 1 of 2)

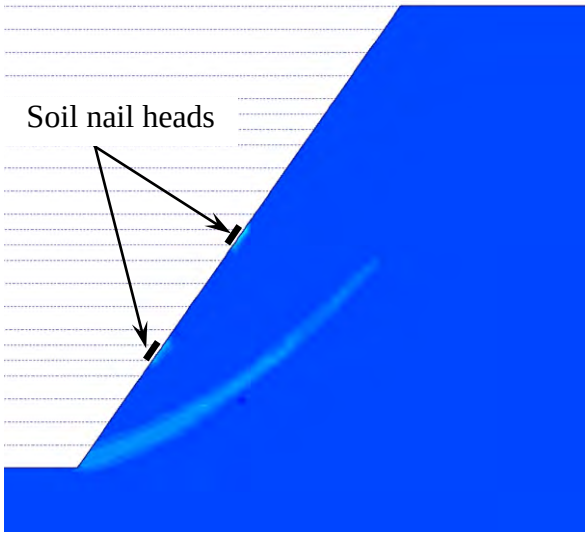

(e) Apparent cohesion c' reduced to 10 kPa

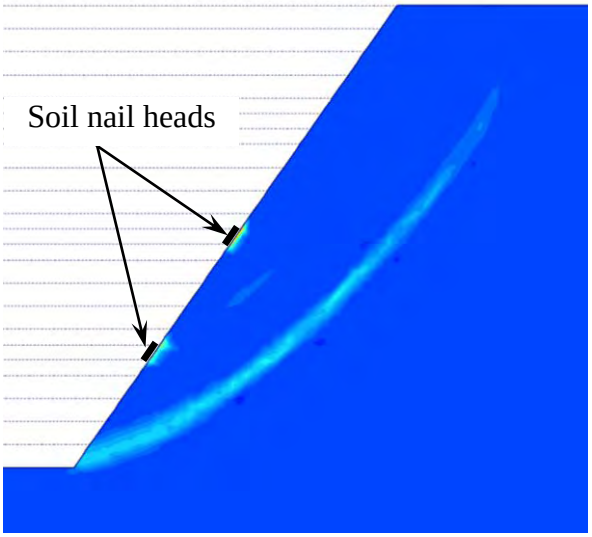

(f) Apparent cohesion c' reduced to 7 kPa

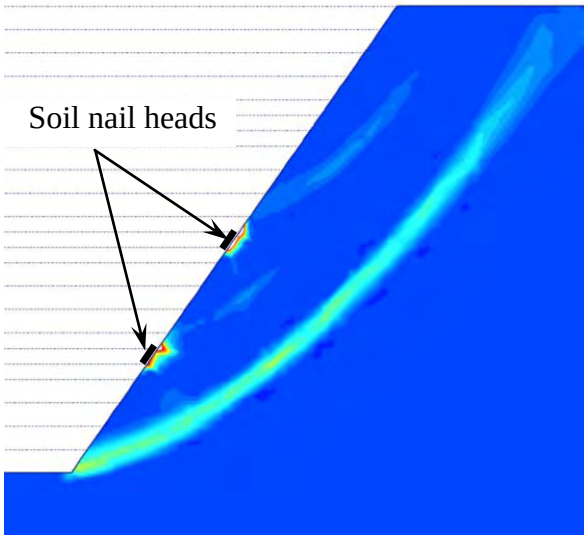

(g) Apparent cohesion c' reduced to 5.2 kPa

Legend:

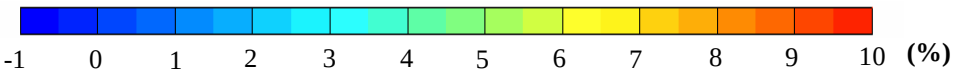

Figure B3 - Development of Shear Strain - Nail Head Size = 400 mm (Sheet 2 of 2)

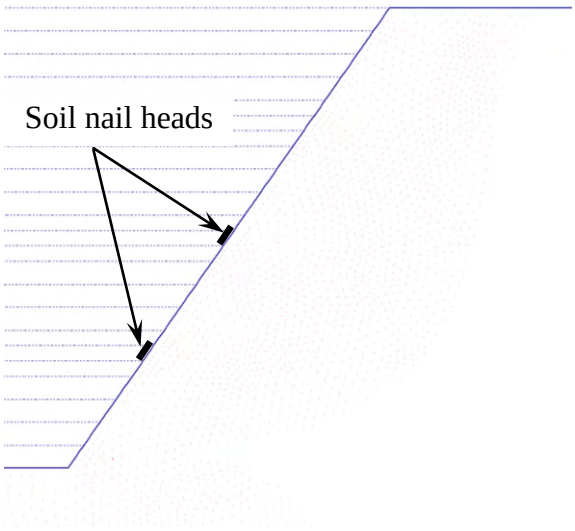

(a) Initial apparent cohesion c' = 20 kPa

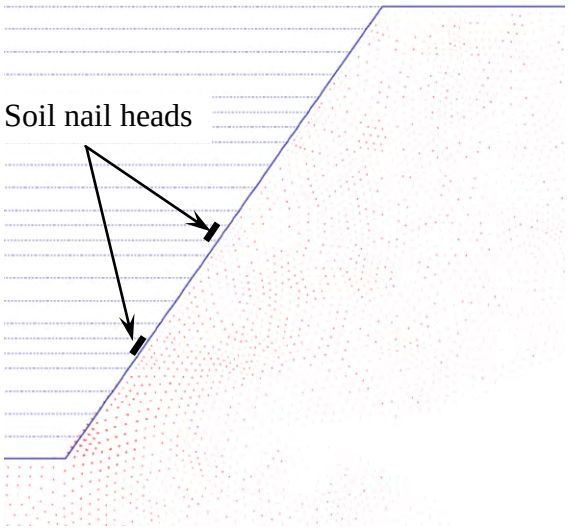

(b) Apparent cohesion c' reduced to 17 kPa

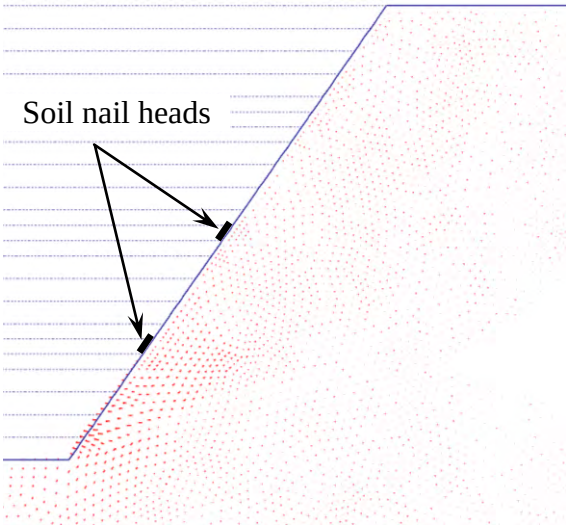

(c) Apparent cohesion c' reduced to 15 kPa

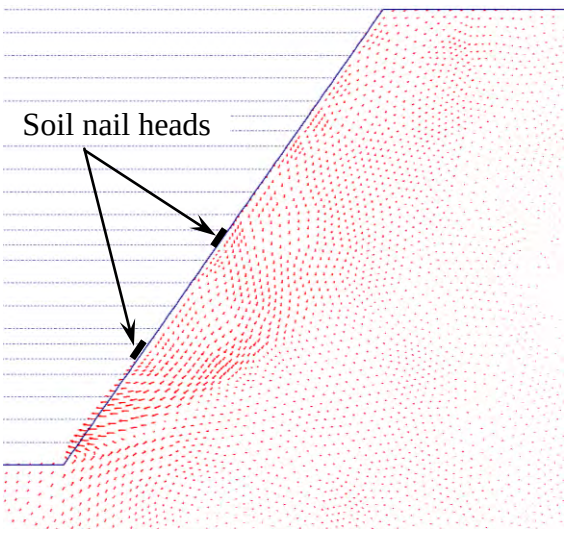

(d) Apparent cohesion c' reduced to 13 kPa

Figure B4 - Displacement Vectors - Nail Head Size = 400 mm (Sheet 1 of 2)

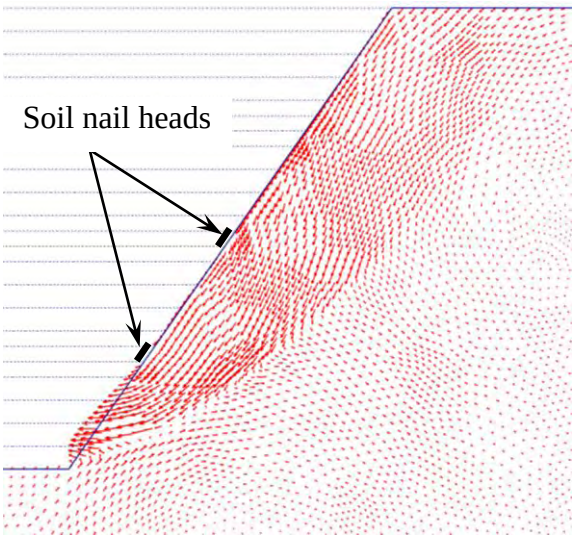

(e) Apparent cohesion c' reduced to 10 kPa

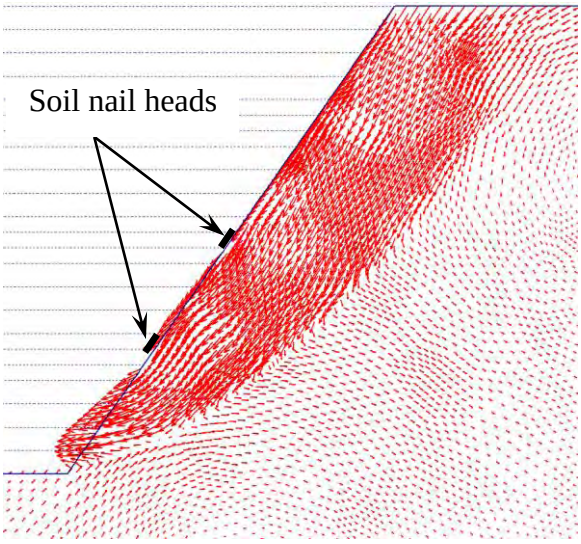

(f) Apparent cohesion c' reduced to 7 kPa

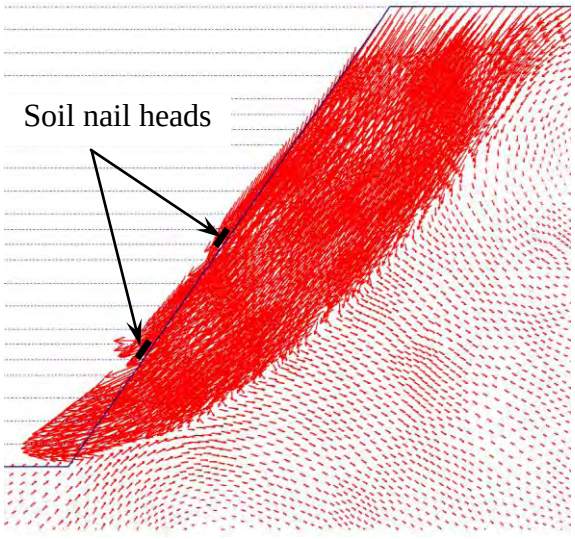

(g) Apparent cohesion c' reduced to 5.2 kPa

Figure B4 - Displacement Vectors - Nail Head Size = 400 mm (Sheet 2 of 2)

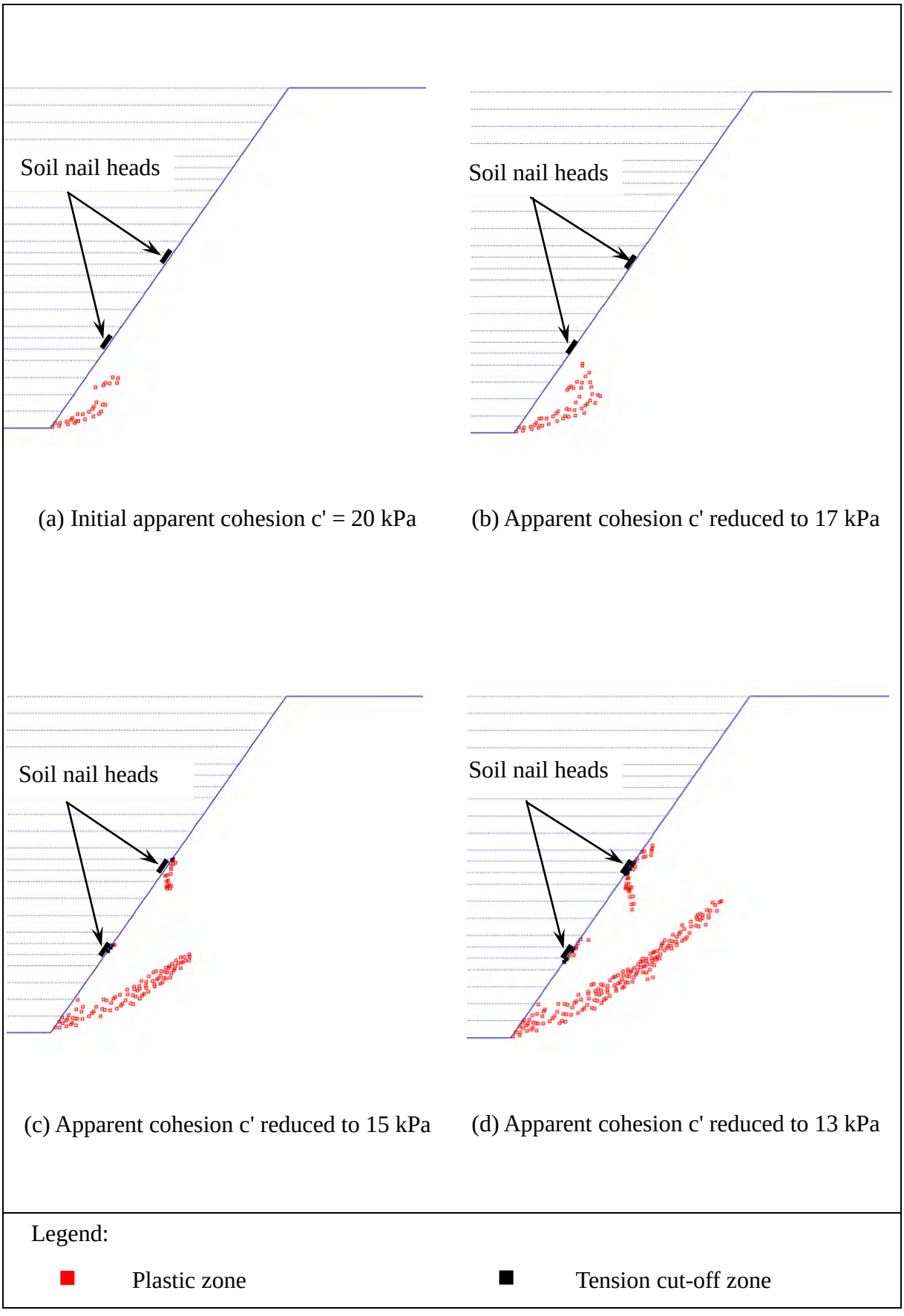

Figure B5 - Development of Plastic Zones - Nail Head Size = 400 mm (Sheet 1 of 2)

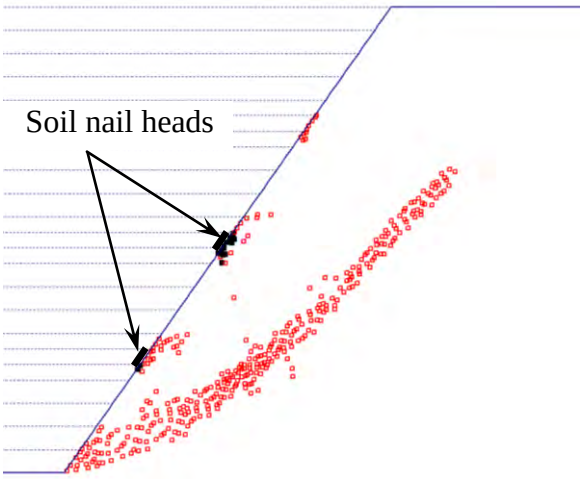

(e) Apparent cohesion c' reduced to 10 kPa

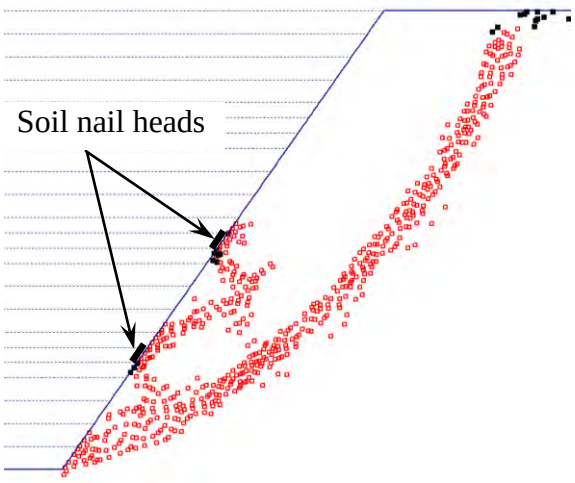

(f) Apparent cohesion c' reduced to 7 kPa

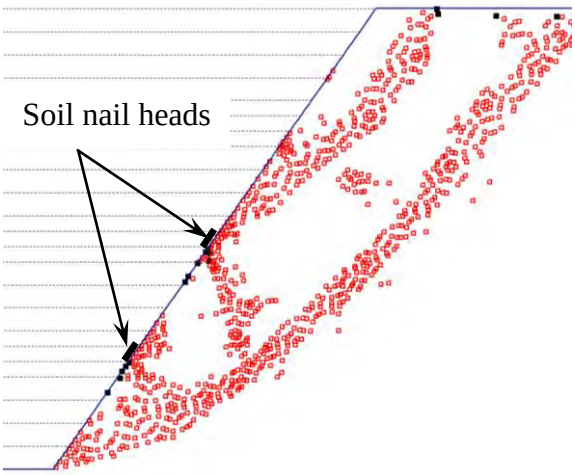

(g) Apparent cohesion c' reduced to 5.2 kPa

Legend:

■ Plastic zone ■ Tension cut-off zone

Figure B5 - Development of Plastic Zones - Nail Head Size = 400 mm (Sheet 2 of 2)

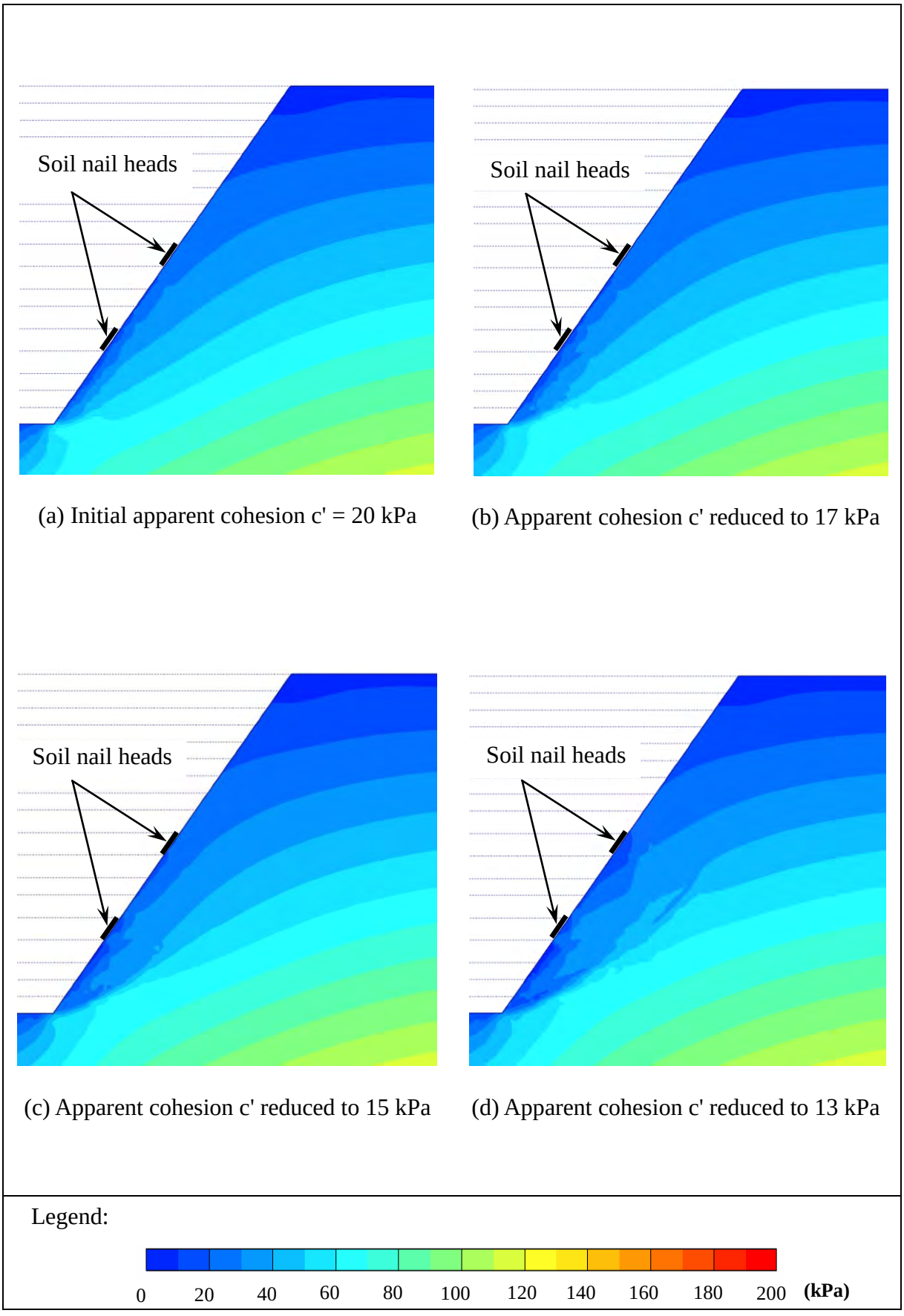

(a) Initial apparent cohesion c' = 20 kPa

(b) Apparent cohesion c' reduced to 17 kPa

(c) Apparent cohesion c' reduced to 15 kPa

(d) Apparent cohesion c' reduced to 13 kPa

Figure B6 - Development of Mean Effective Stress - Nail Head Size = 800 mm (Sheet 1 of 2)

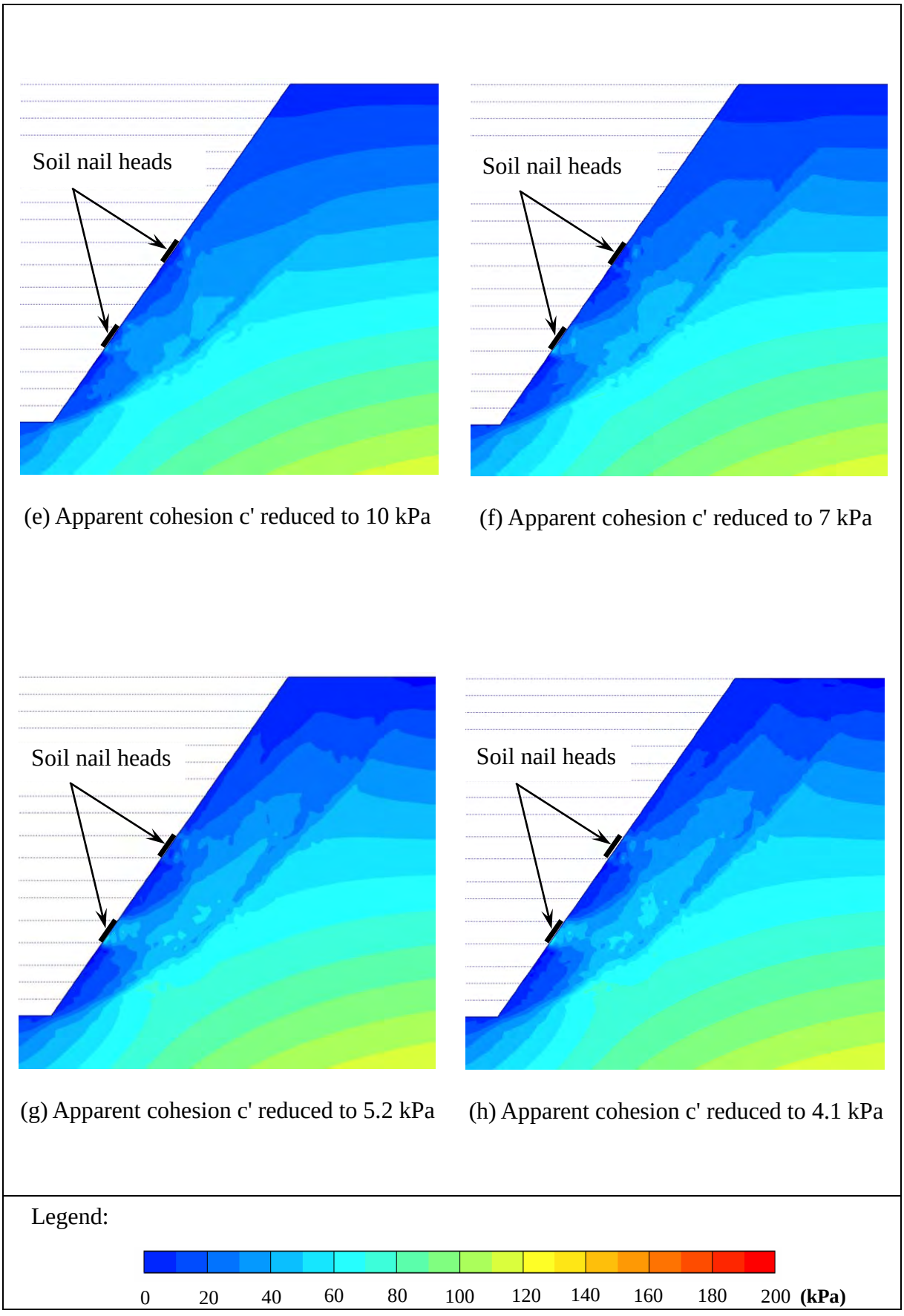

Figure B6 - Development of Mean Effective Stress - Nail Head Size = 800 mm (Sheet 2 of 2)

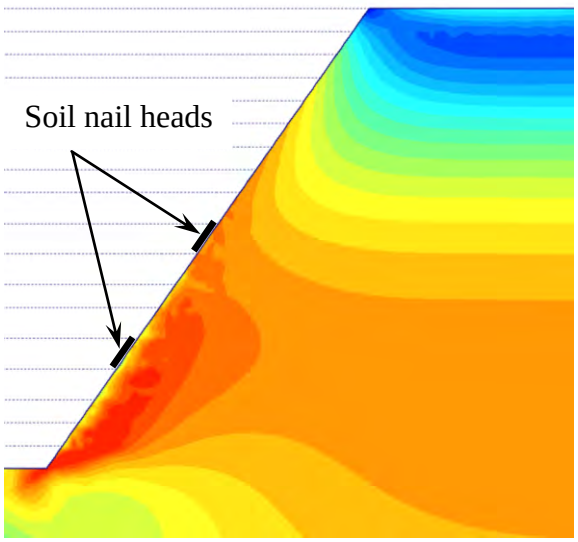

(a) Initial apparent cohesion c' = 20 kPa

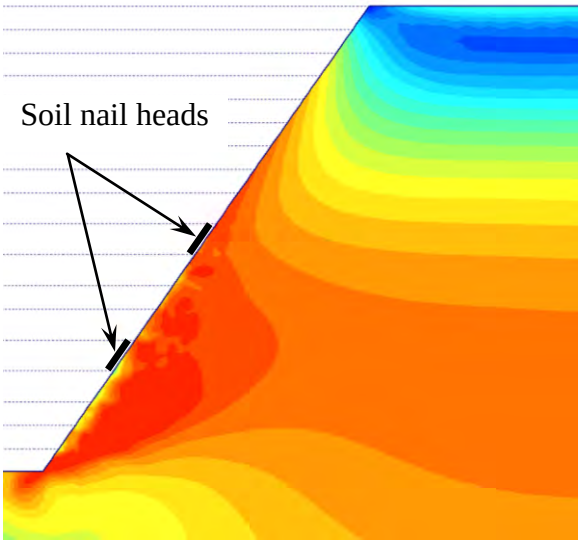

(b) Apparent cohesion c' reduced to 17 kPa

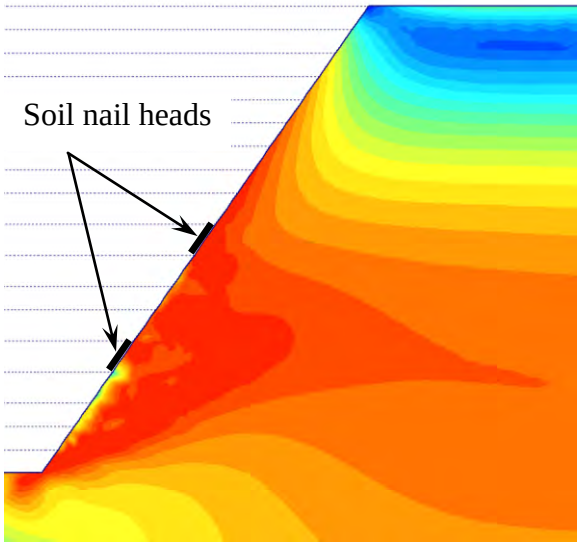

(c) Apparent cohesion c' reduced to 15 kPa

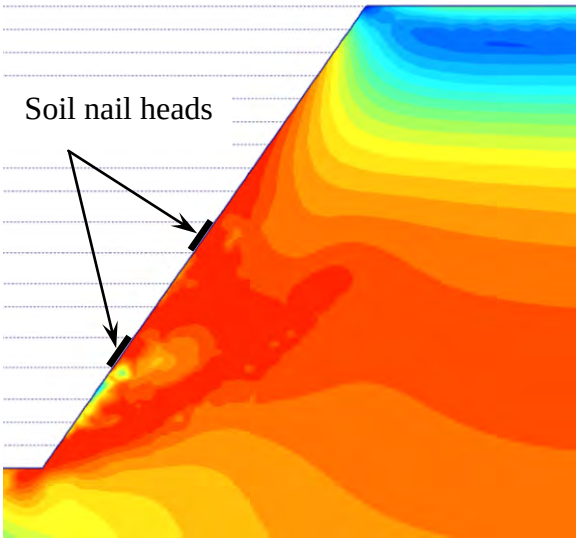

(d) Apparent cohesion c' reduced to 13 kPa

Legend:

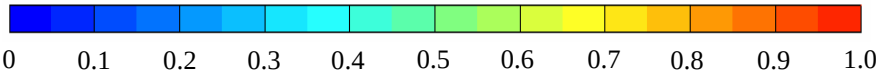

Figure B7 - Development of Relative Shear Stress - Nail Head Size = 800 mm (Sheet 1 of 2)

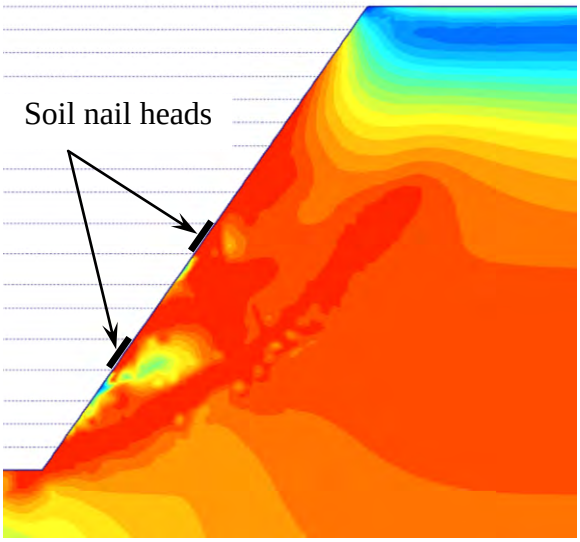

(e) Apparent cohesion c' reduced to 10 kPa

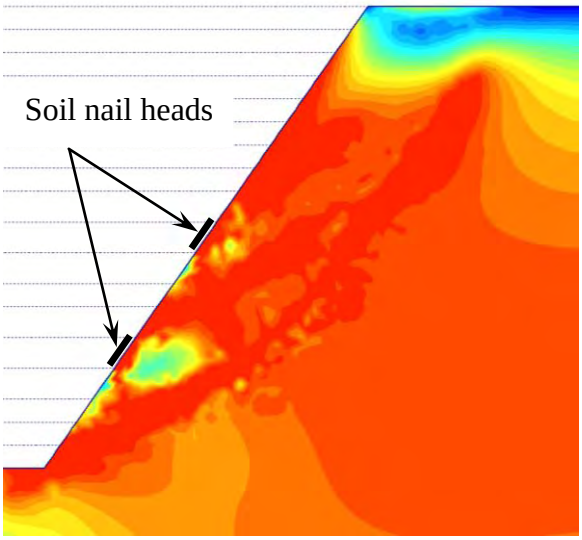

(f) Apparent cohesion c' reduced to 7 kPa

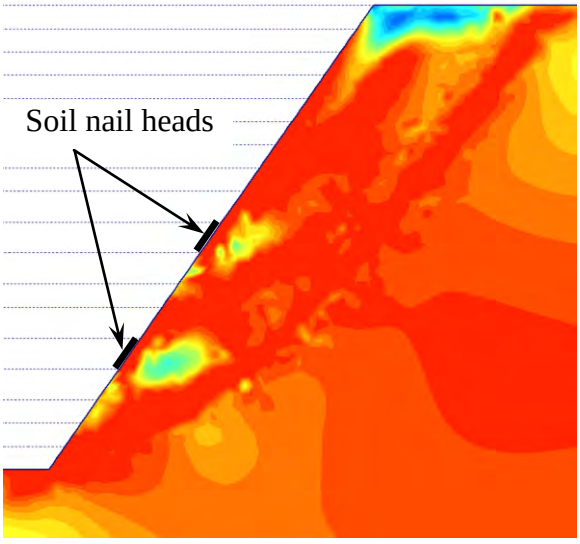

(g) Apparent cohesion c' reduced to 5.2 kPa

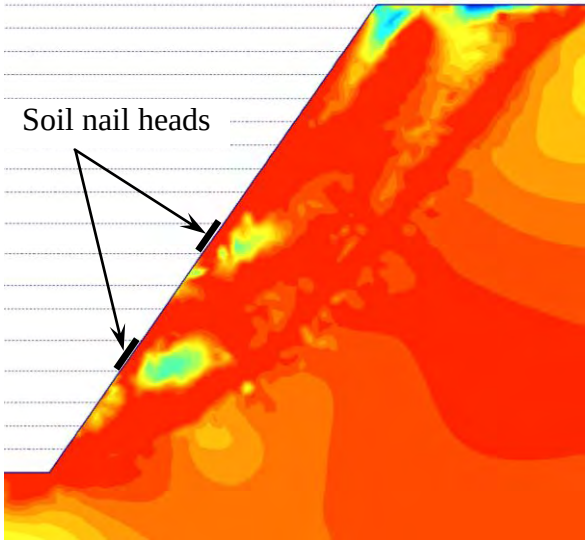

(h) Apparent cohesion c' reduced to 4.1 kPa

Legend:

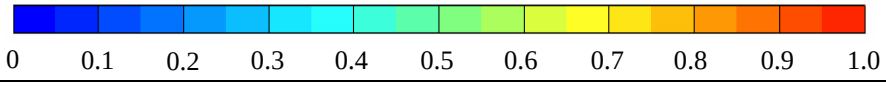

Figure B7 - Development of Relative Shear Stress - Nail Head Size = 800 mm (Sheet 2 of 2)

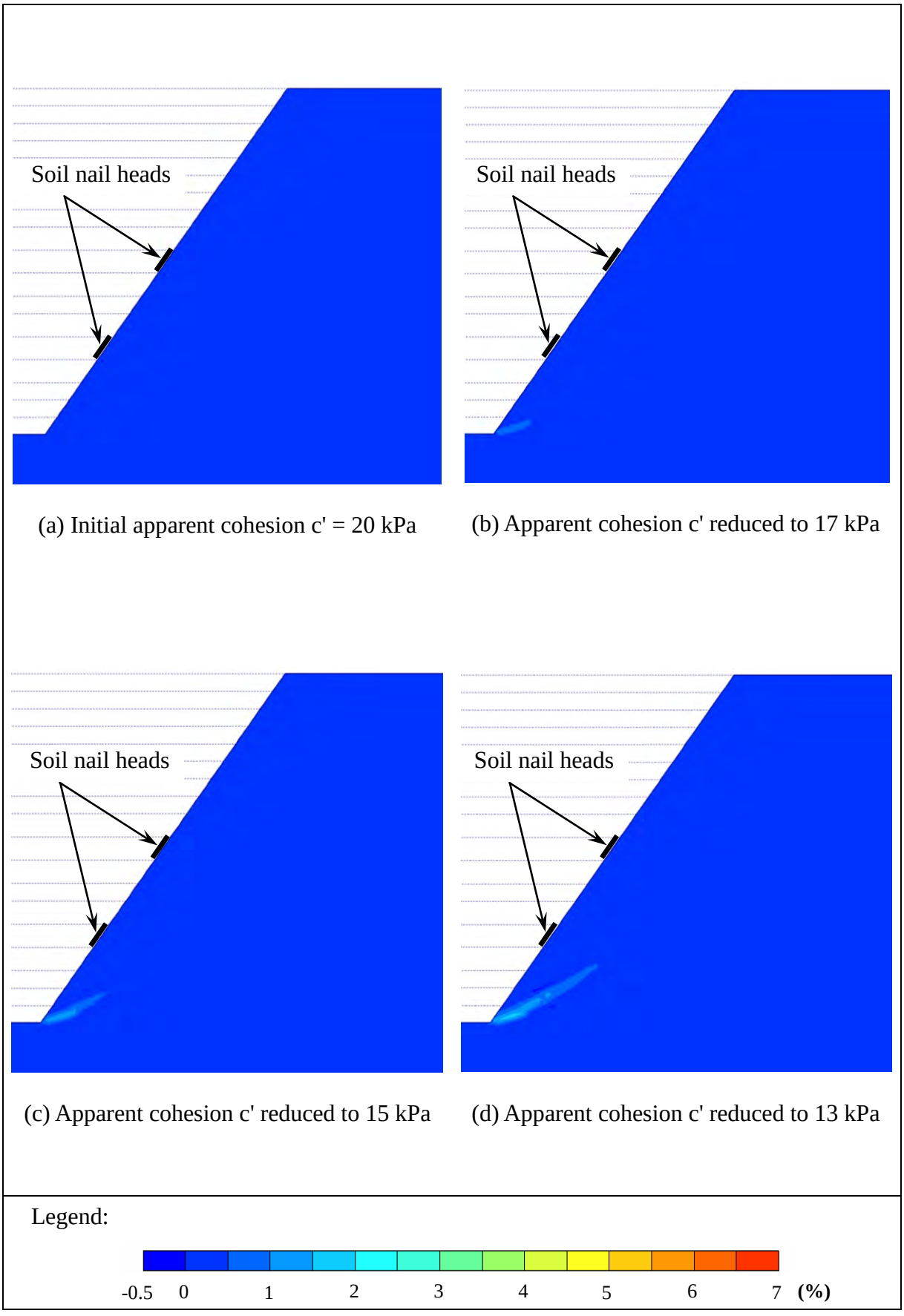

Figure B8 - Development of Shear Strain - Nail Head Size = 800 mm (Sheet 1 of 2)

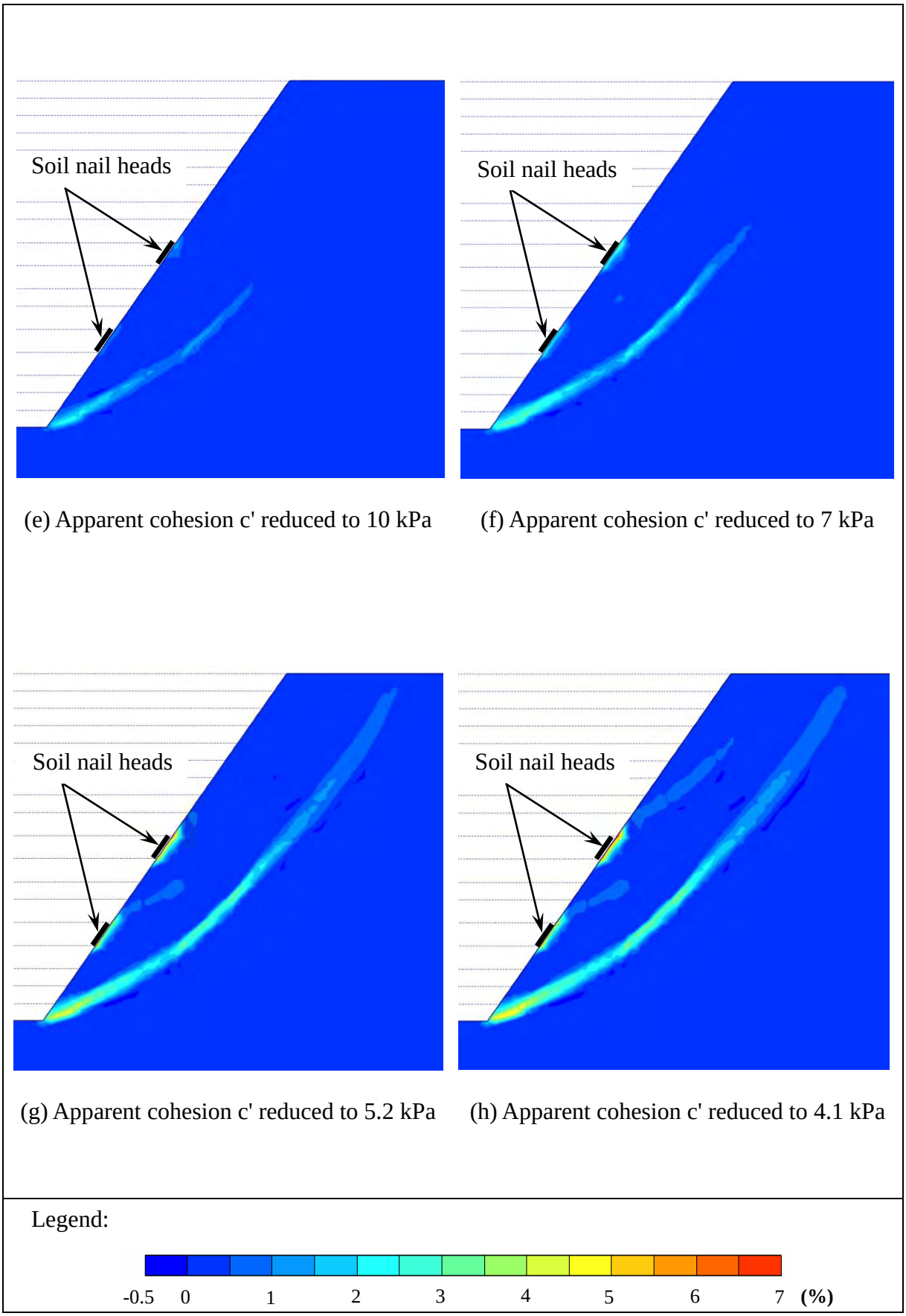

Figure B8 - Development of Shear Strain - Nail Head Size = 800 mm (Sheet 2 of 2)

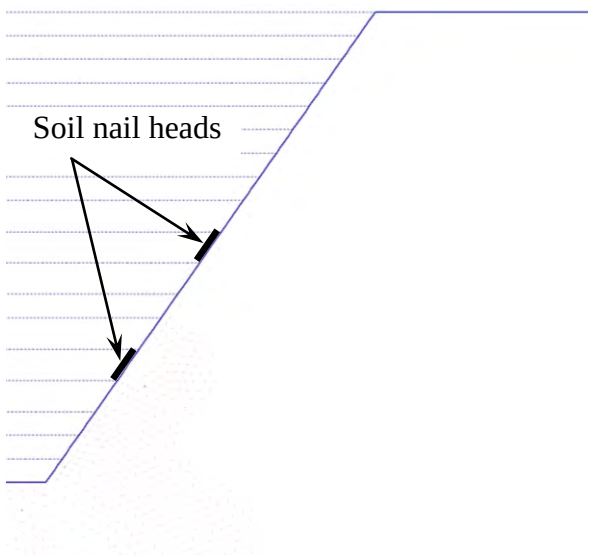

(a) Initial apparent cohesion c' = 20 kPa

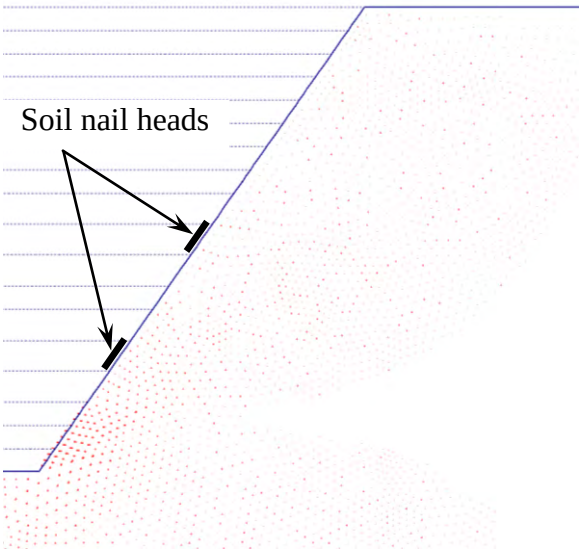

(b) Apparent cohesion c' reduced to 17 kPa

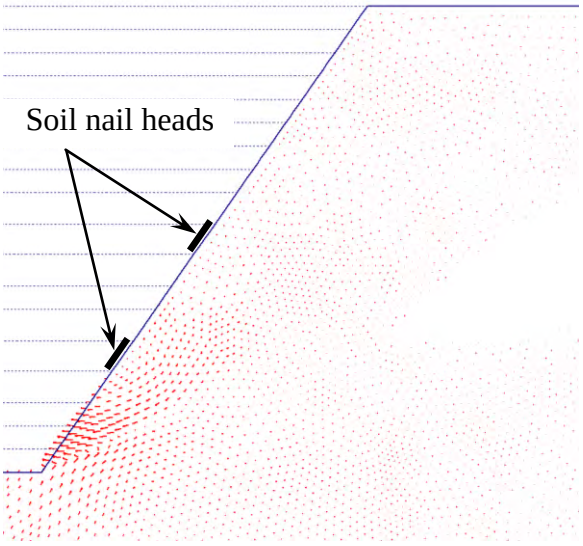

(c) Apparent cohesion c' reduced to 15 kPa

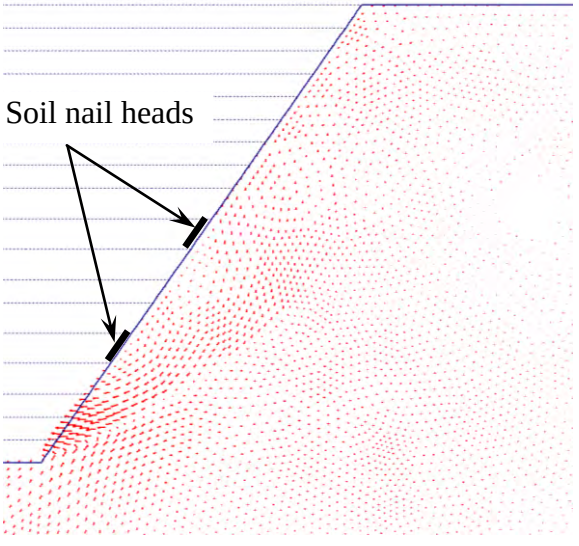

(d) Apparent cohesion c' reduced to 13 kPa

Figure B9 - Displacement Vectors - Nail Head Size = 800 mm (Sheet 1 of 2)

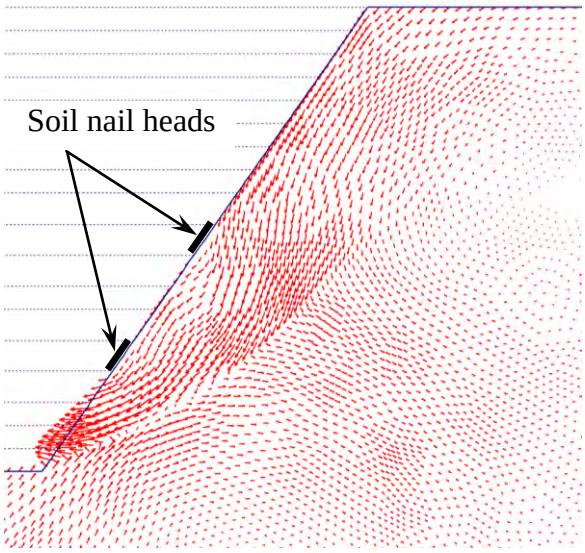

(e) Apparent cohesion c' reduced to 10 kPa

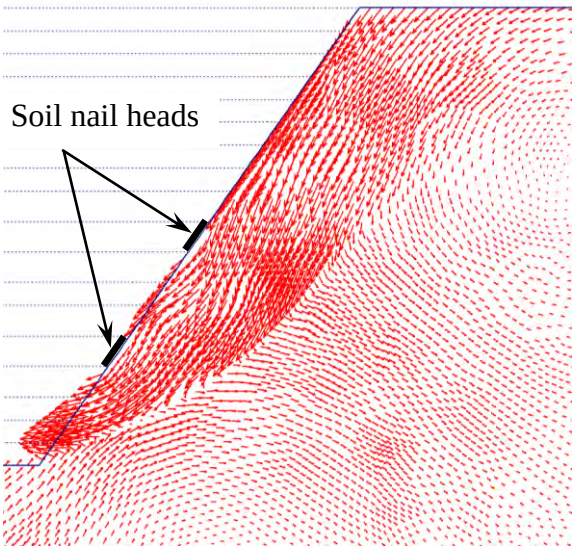

(f) Apparent cohesion c' reduced to 7 kPa

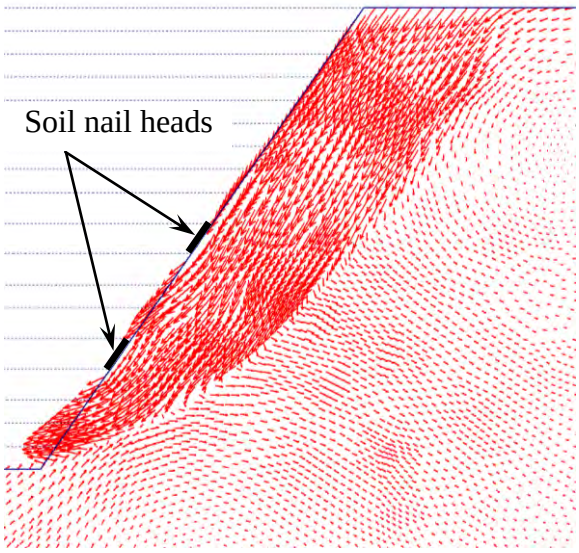

(g) Apparent cohesion c' reduced to 5.2 kPa

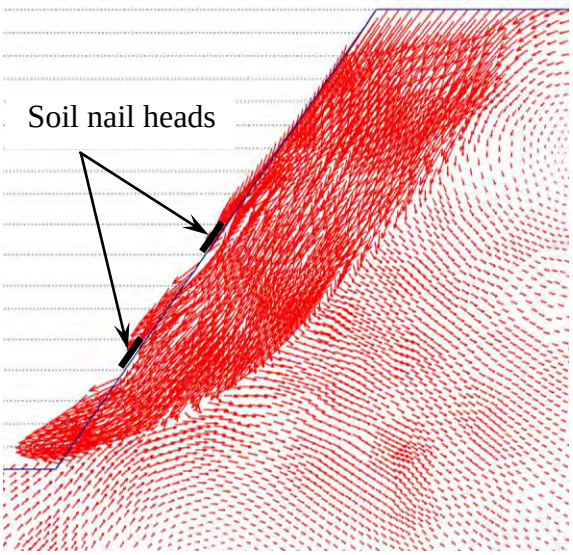

(h) Apparent cohesion c' reduced to 4.1 kPa

Figure B9 - Displacement Vectors - Nail Head Size = 800 mm (Sheet 2 of 2)

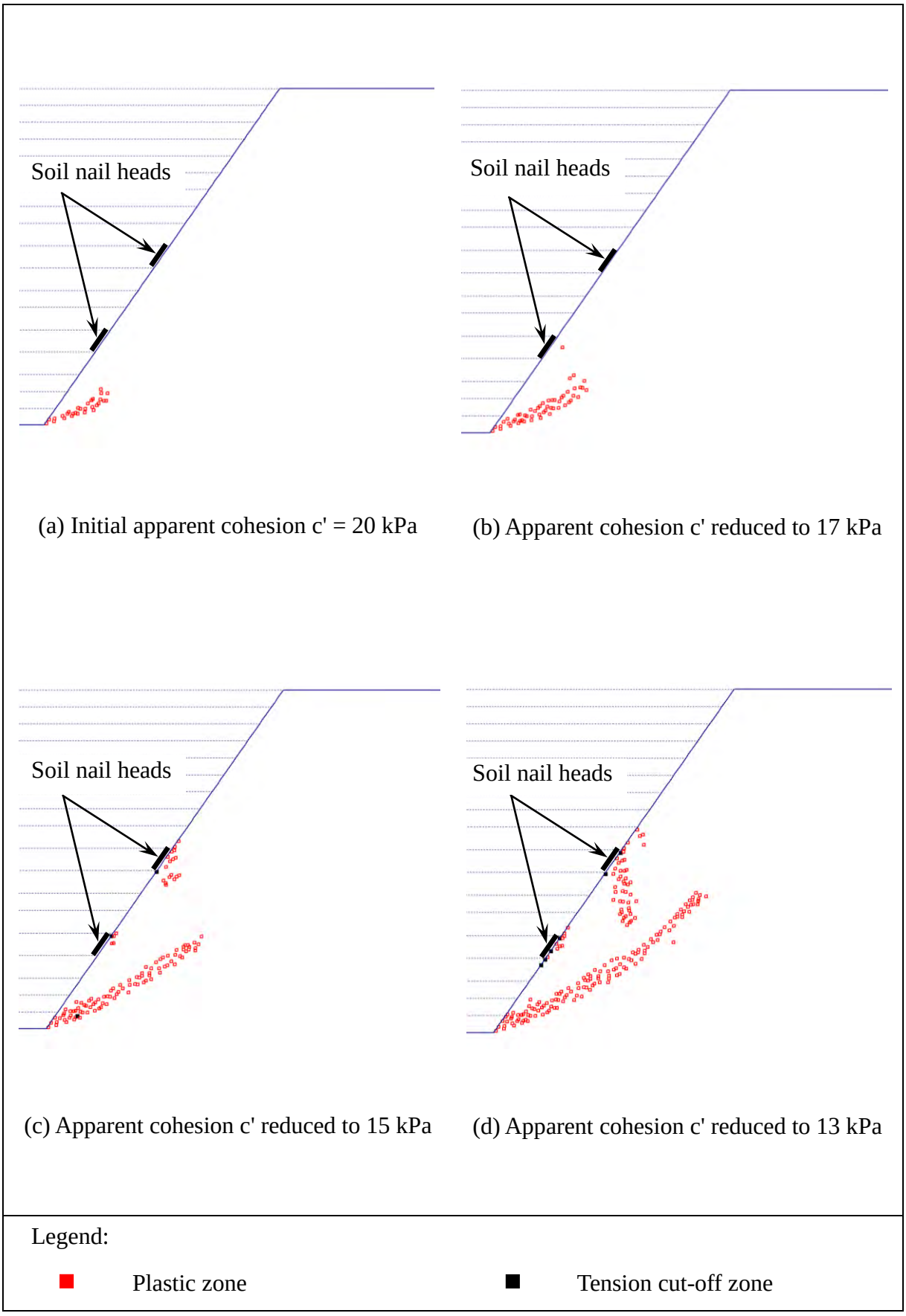

Figure B10 - Development of Plastic Zones - Nail Head Size = 800 mm (Sheet 1 of 2)

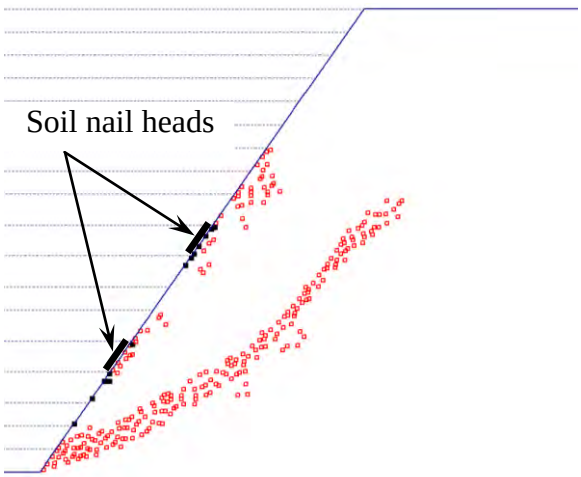

(e) Apparent cohesion c' reduced to 10 kPa

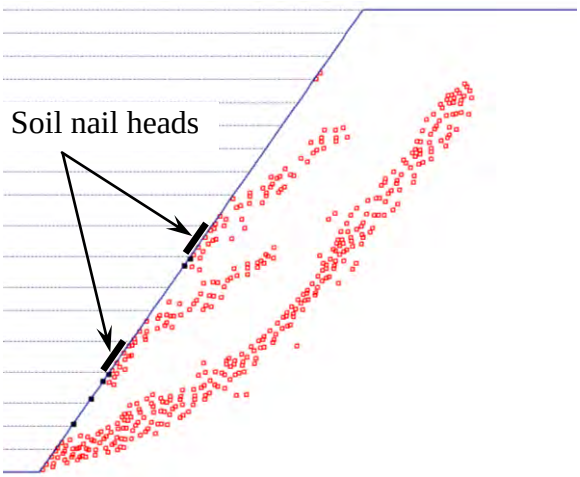

(f) Apparent cohesion c' reduced to 7 kPa

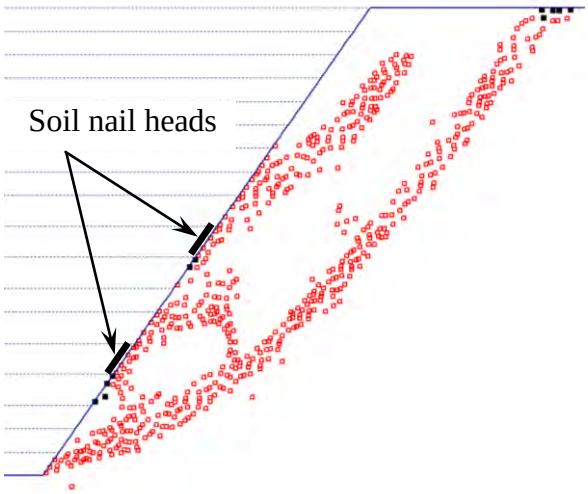

(g) Apparent cohesion c' reduced to 5.2 kPa

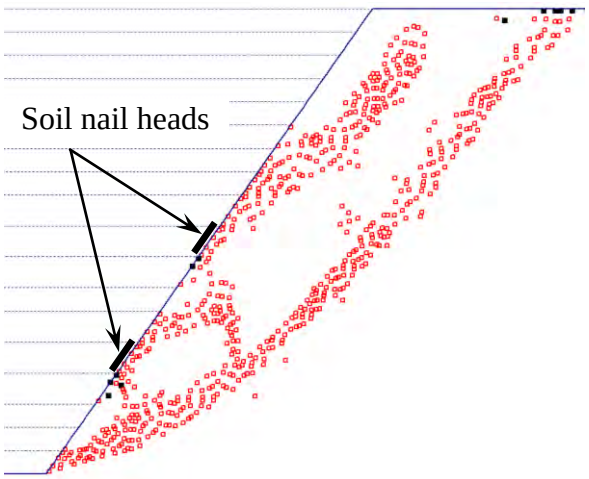

(h) Apparent cohesion c' reduced to 4.1 kPa

Legend:

Plastic zone

Tension cut-off zone

Figure B10 - Development of Plastic Zones - Nail Head Size = 800 mm (Sheet 2 of 2)

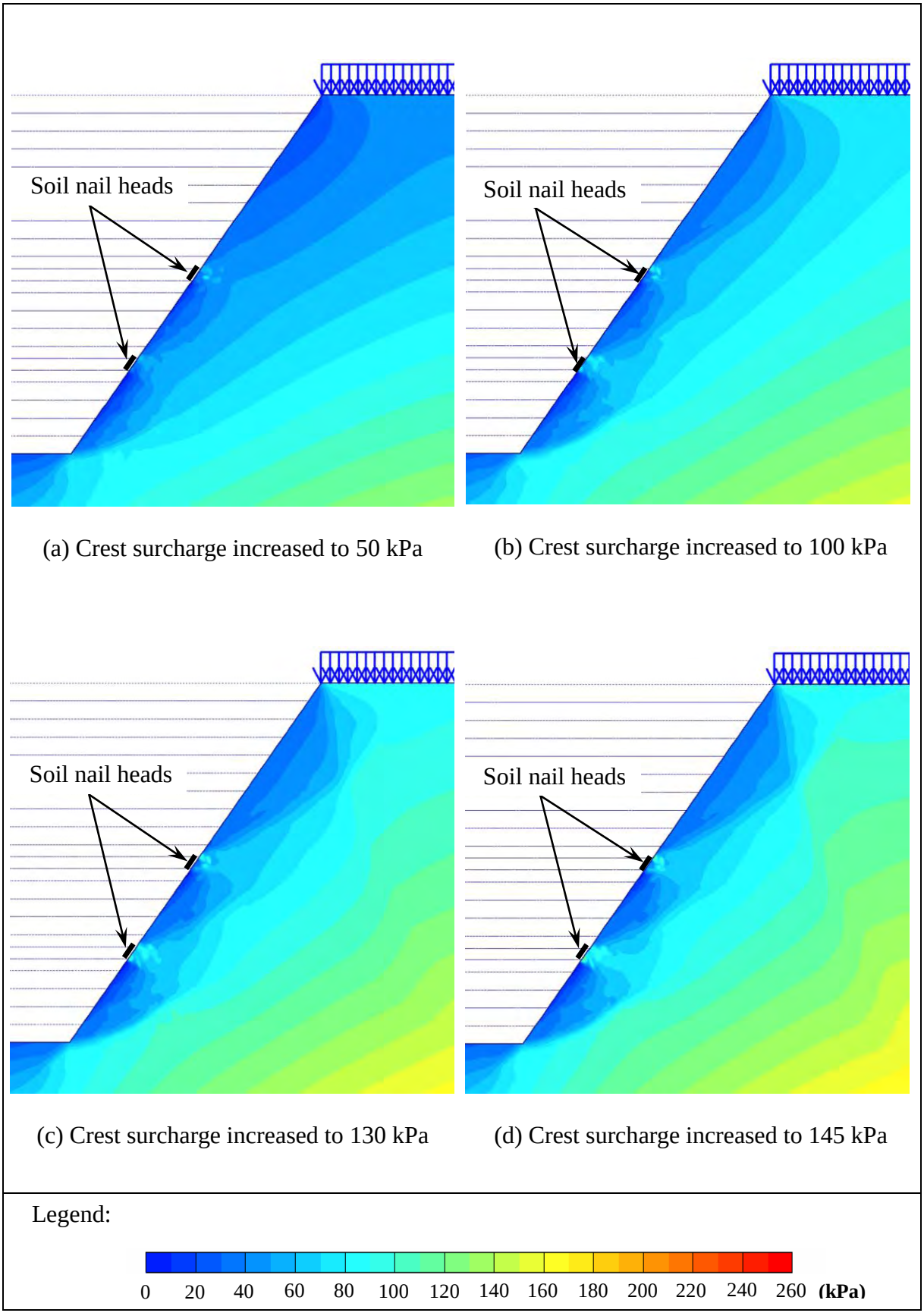

Figure B11 - Development of Mean Effective Stress - with Crest Surcharge; Nail Head Size = 400 mm

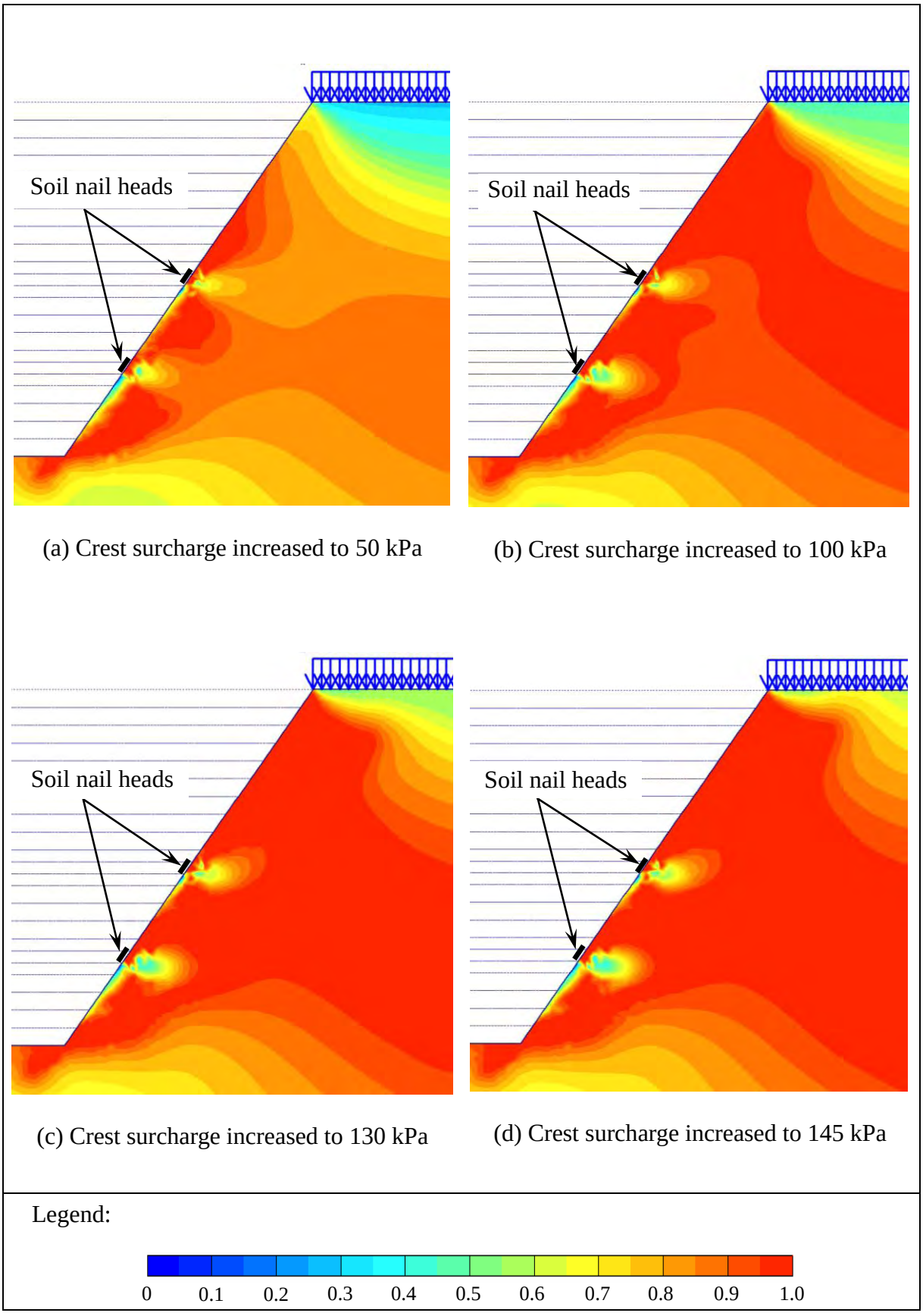

(a) Crest surcharge increased to 50 kPa

(b) Crest surcharge increased to 100 kPa

(c) Crest surcharge increased to 130 kPa

(d) Crest surcharge increased to 145 kPa

Figure B12 - Development of Relative Shear Stress - with Crest Surcharge; Nail Head Size = 400 mm

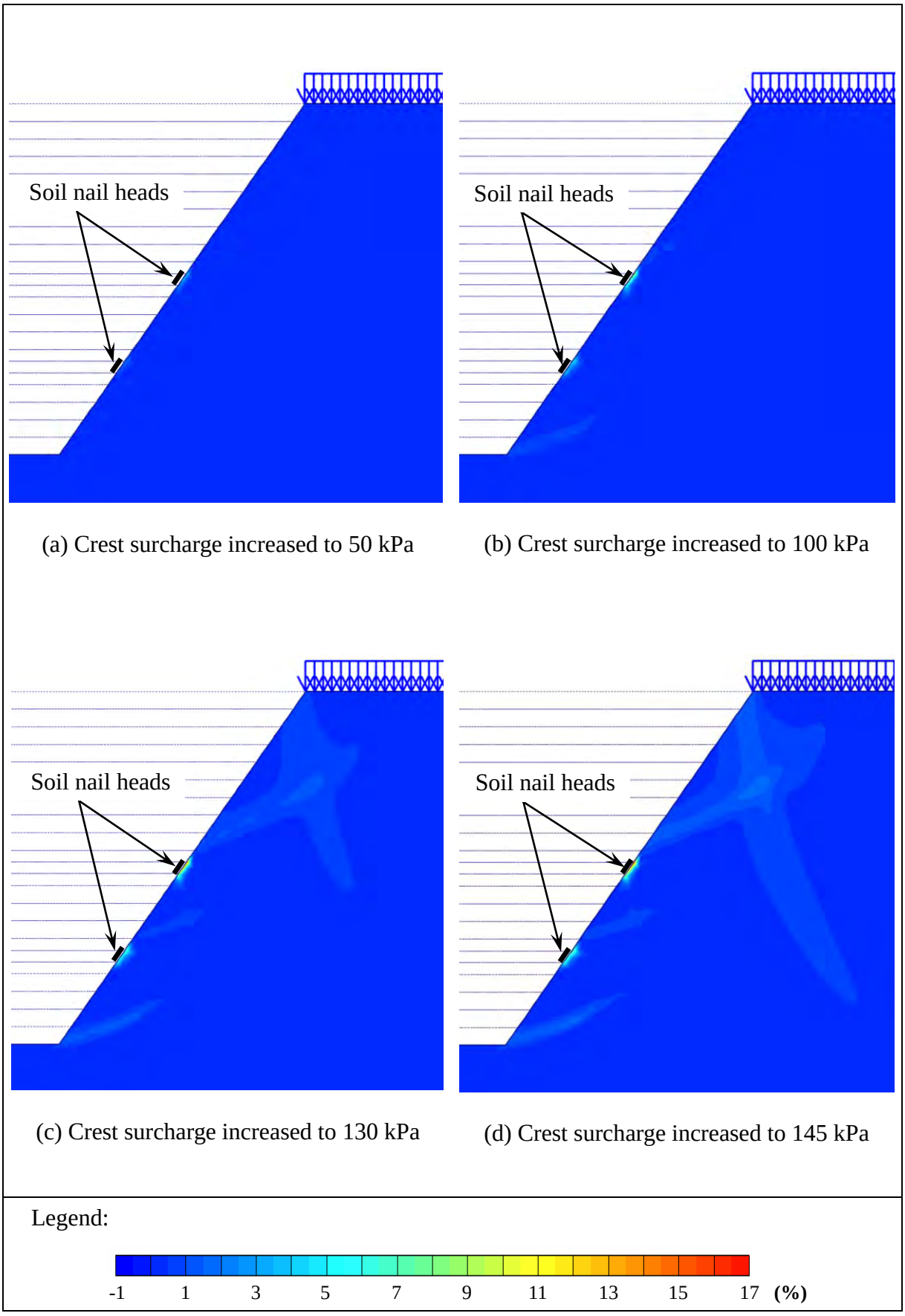

Figure B13 - Development of Shear Strain - with Crest Surcharge; Nail Head Size = 400 mm

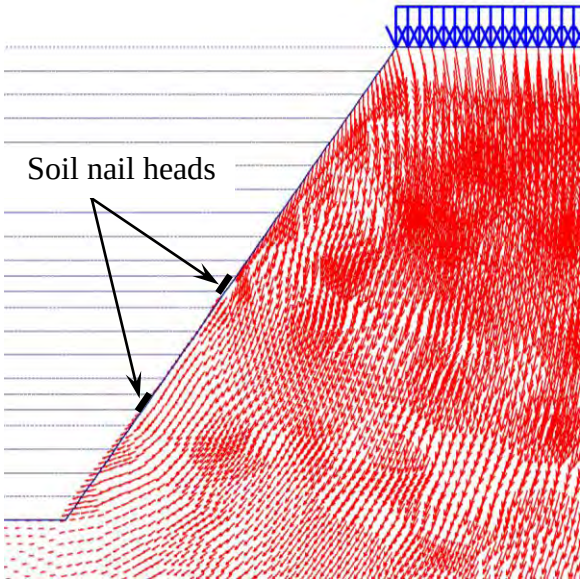

(a) Crest surcharge increased to 50 kPa

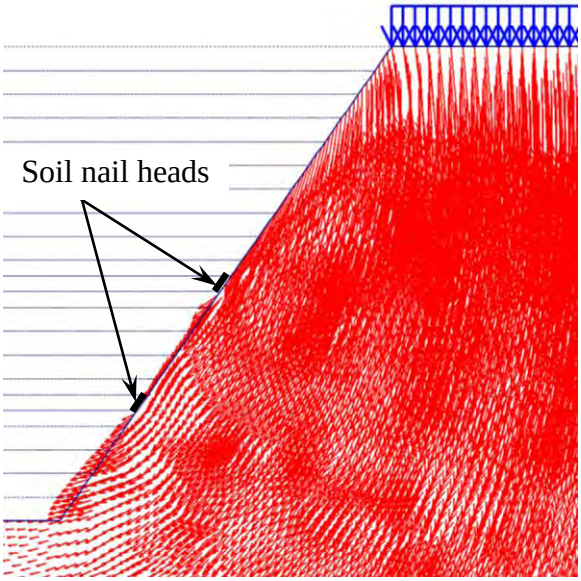

(b) Crest surcharge increased to 100 kPa

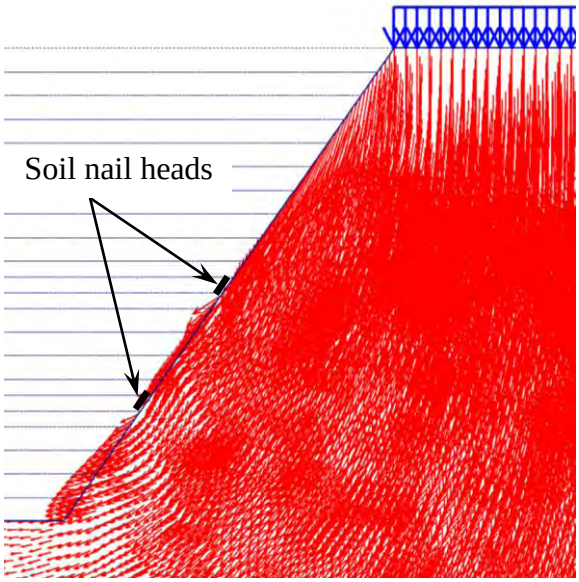

(c) Crest surcharge increased to 130 kPa

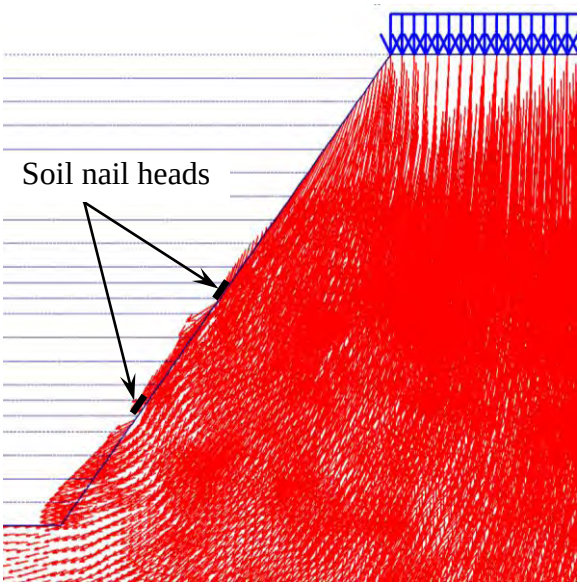

(d) Crest surcharge increased to 145 kPa

Figure B14 - Displacement Vectors - with Crest Surcharge; Nail Head Size = 400 mm

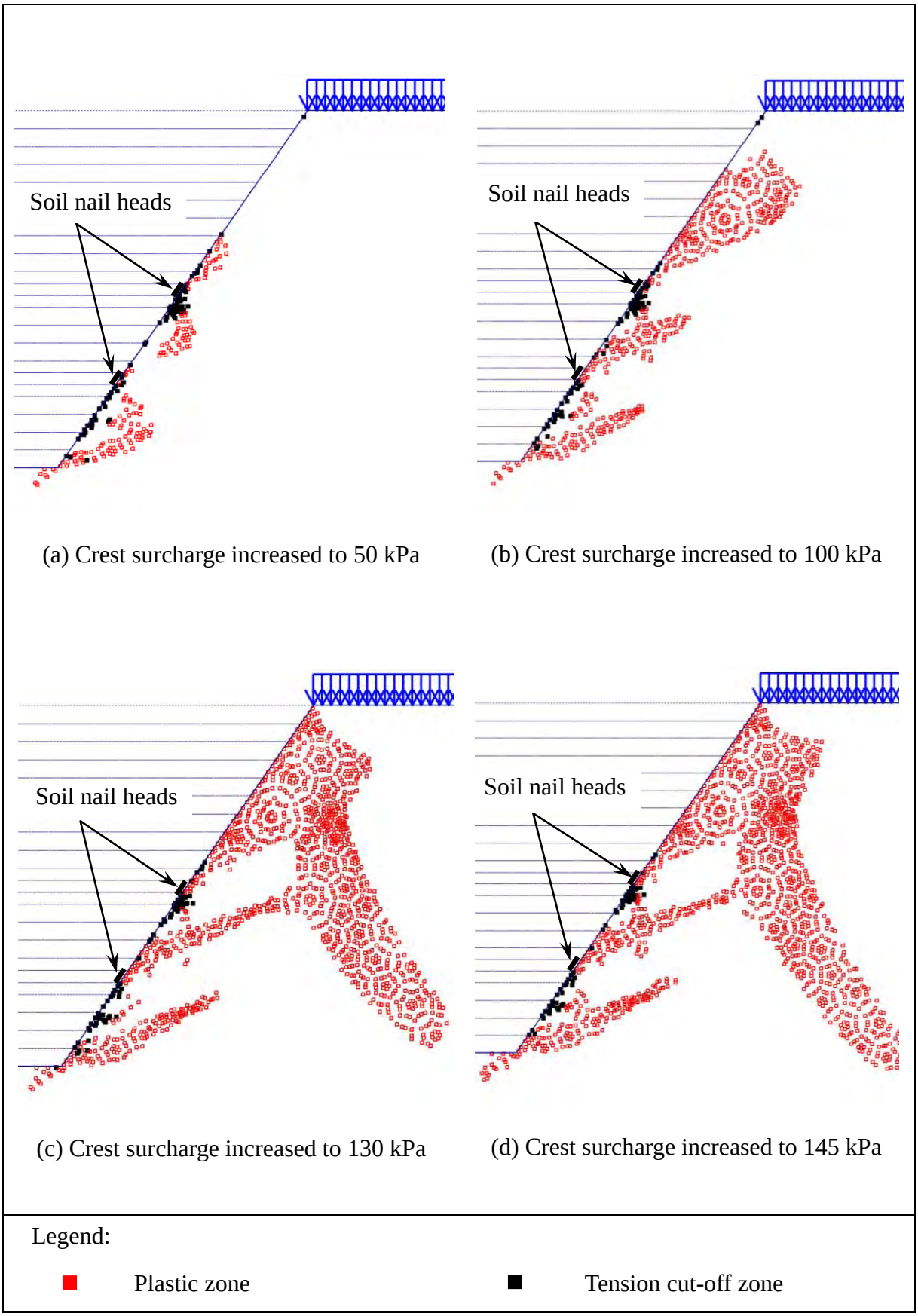

Figure B15 - Development of Plastic Zones - with Crest Surcharge; Nail Head Size = 400 mm

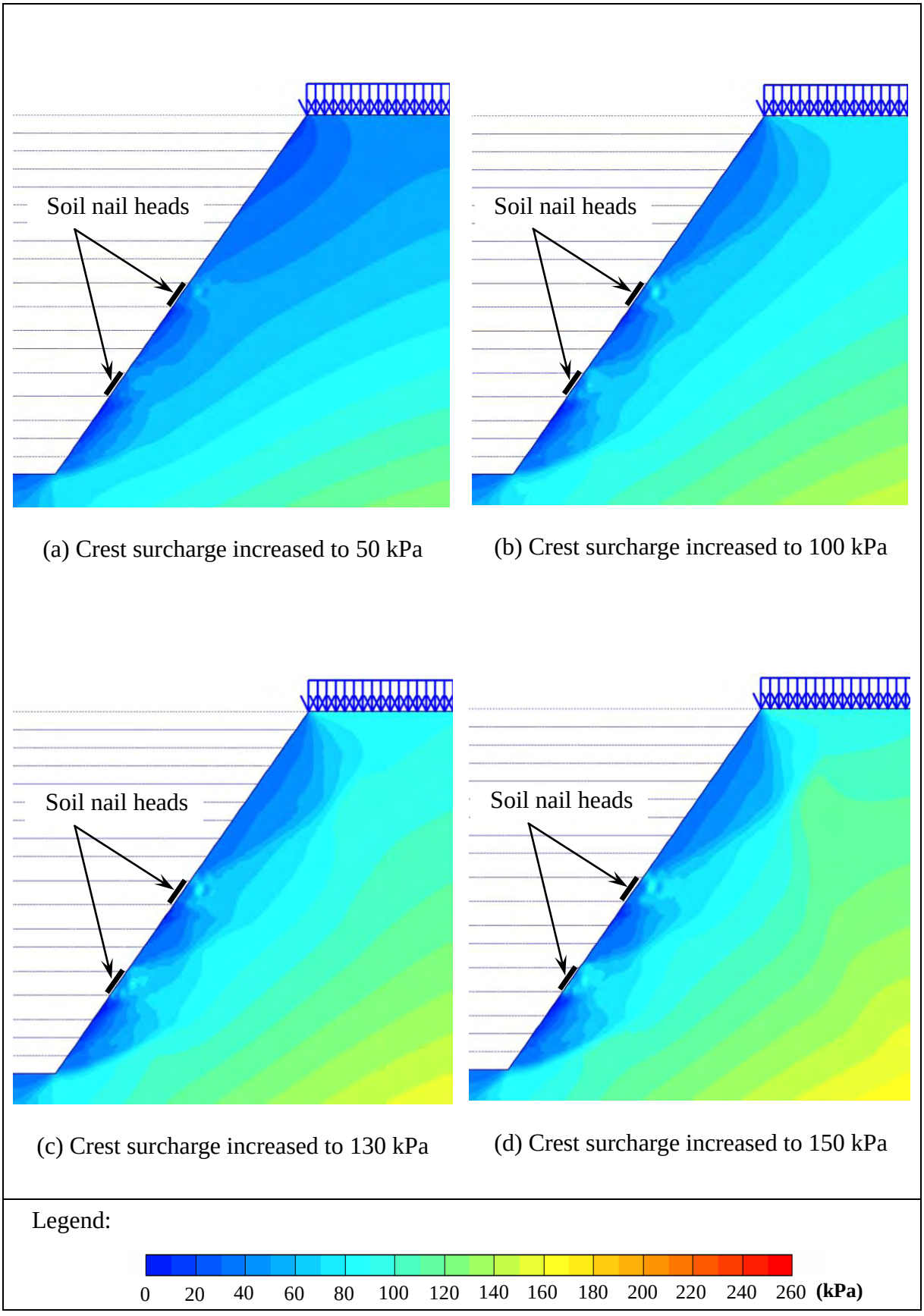

(a) Crest surcharge increased to 50 kPa

(b) Crest surcharge increased to 100 kPa

(c) Crest surcharge increased to 130 kPa

(d) Crest surcharge increased to 150 kPa

Figure B16 - Development of Mean Effective Stress - with Crest Surcharge; Nail Head Size = 800 mm

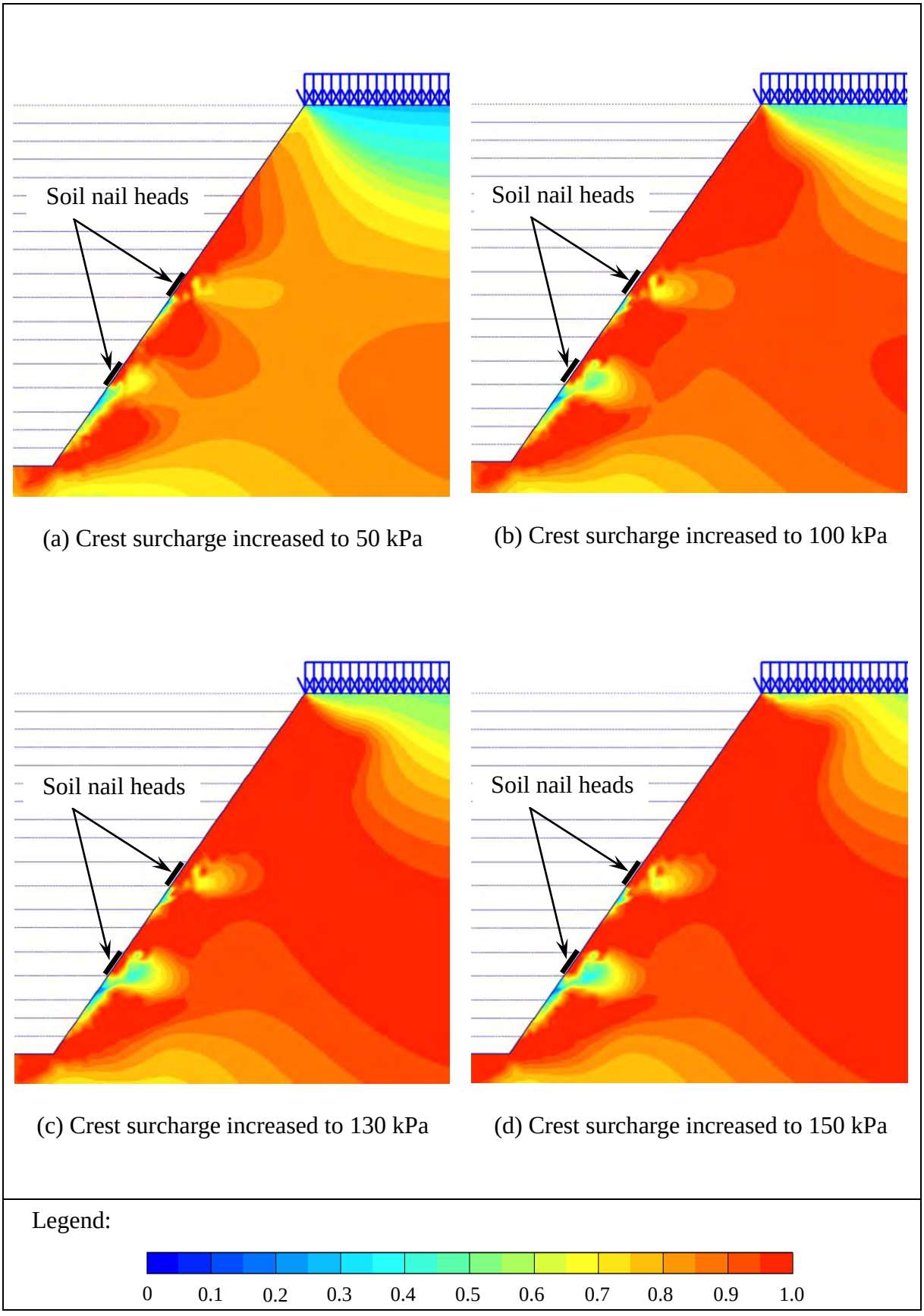

(a) Crest surcharge increased to 50 kPa

(b) Crest surcharge increased to 100 kPa

(c) Crest surcharge increased to 130 kPa

(d) Crest surcharge increased to 150 kPa

Figure B17 - Development of Relative Shear Stress - with Crest Surcharge; Nail Head Size = 800 mm

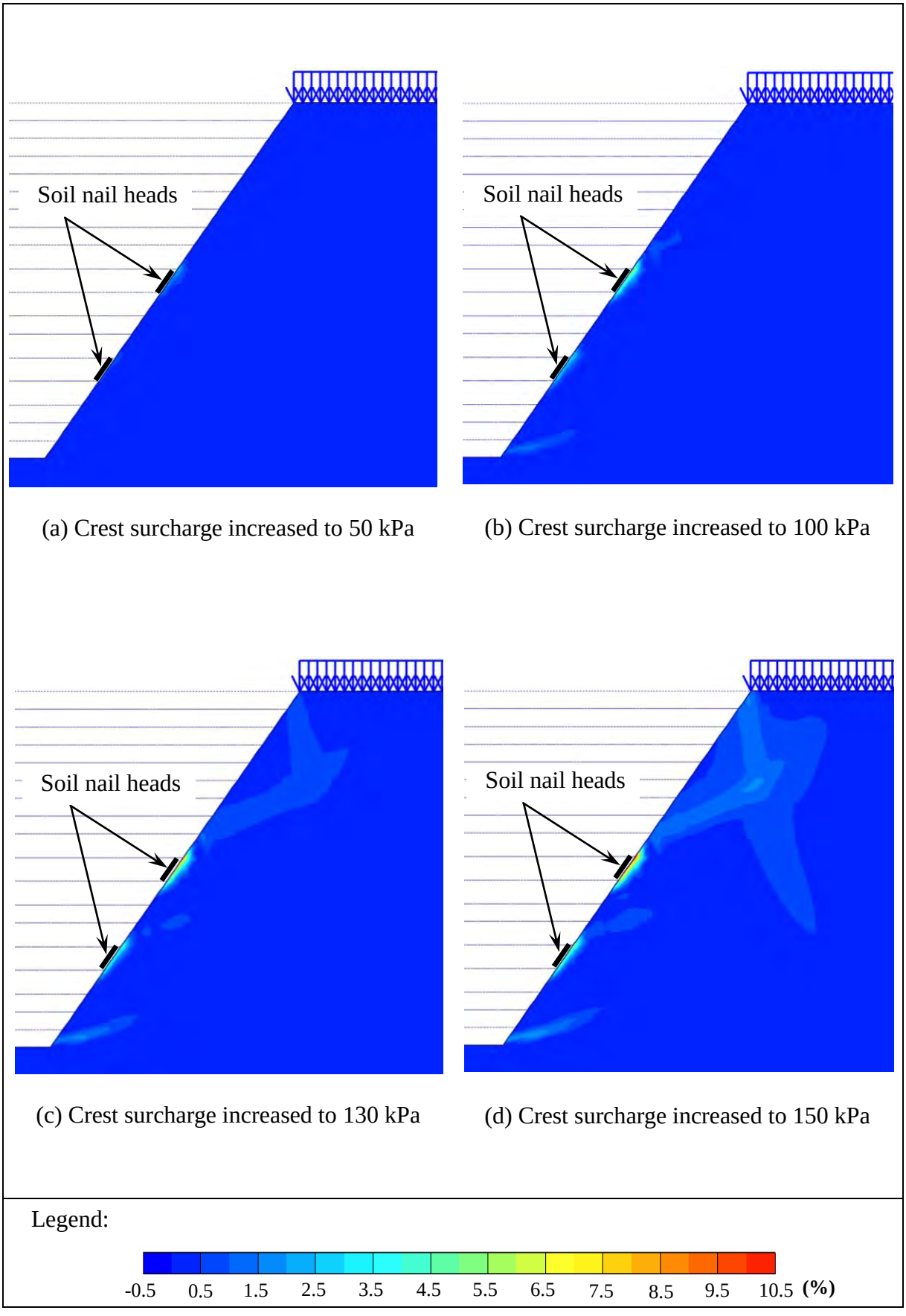

(a) Crest surcharge increased to 50 kPa

(b) Crest surcharge increased to 100 kPa

(c) Crest surcharge increased to 130 kPa

(d) Crest surcharge increased to 150 kPa

Figure B18 - Development of Shear Strain - with Crest Surcharge; Nail Head Size = 800 mm

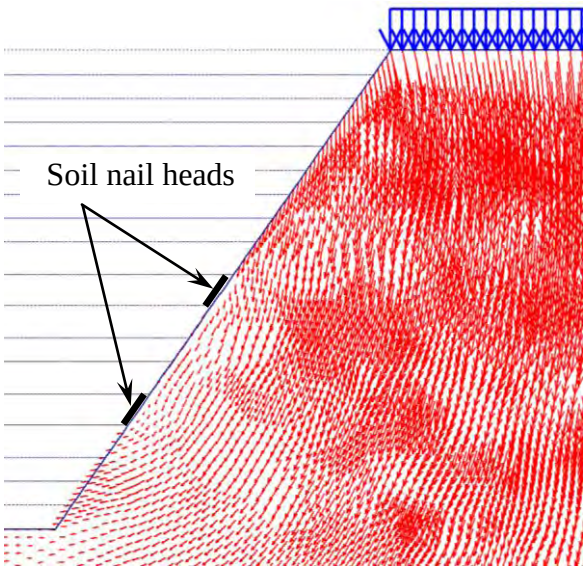

(a) Crest surcharge increased to 50 kPa

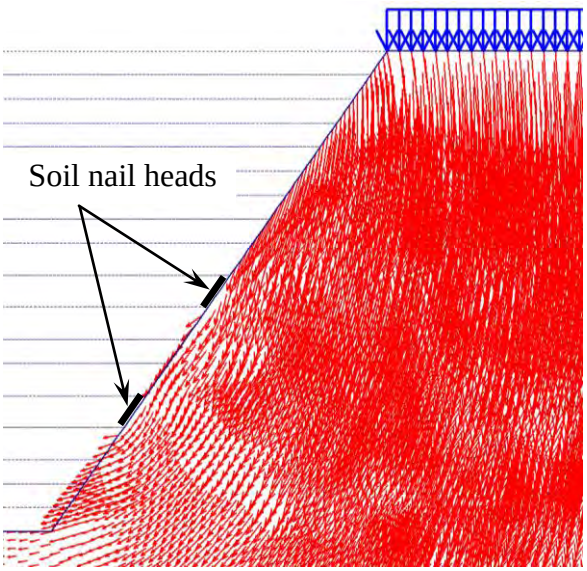

(b) Crest surcharge increased to 100 kPa

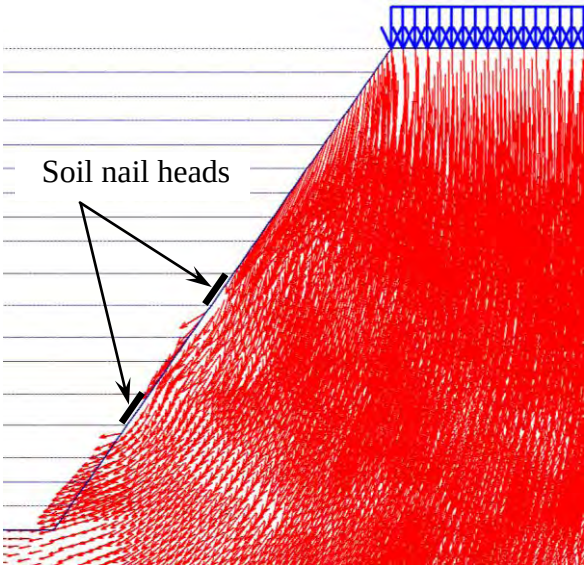

(c) Crest surcharge increased to 130 kPa

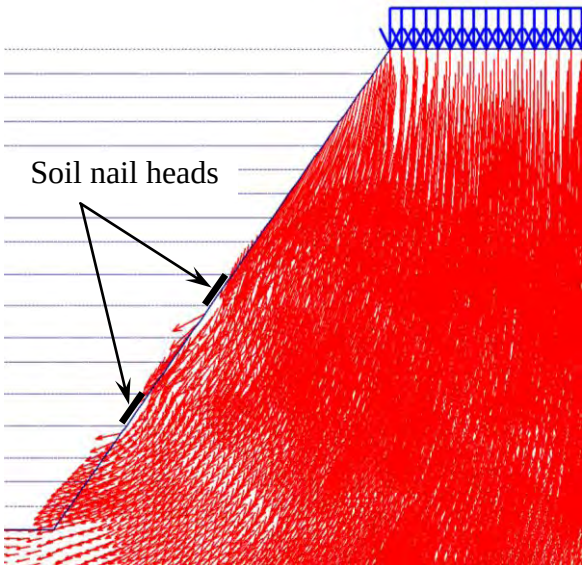

(d) Crest surcharge increased to 150 kPa

Figure B19 - Displacement Vectors - with Crest Surcharge; Nail Head Size = 800 mm

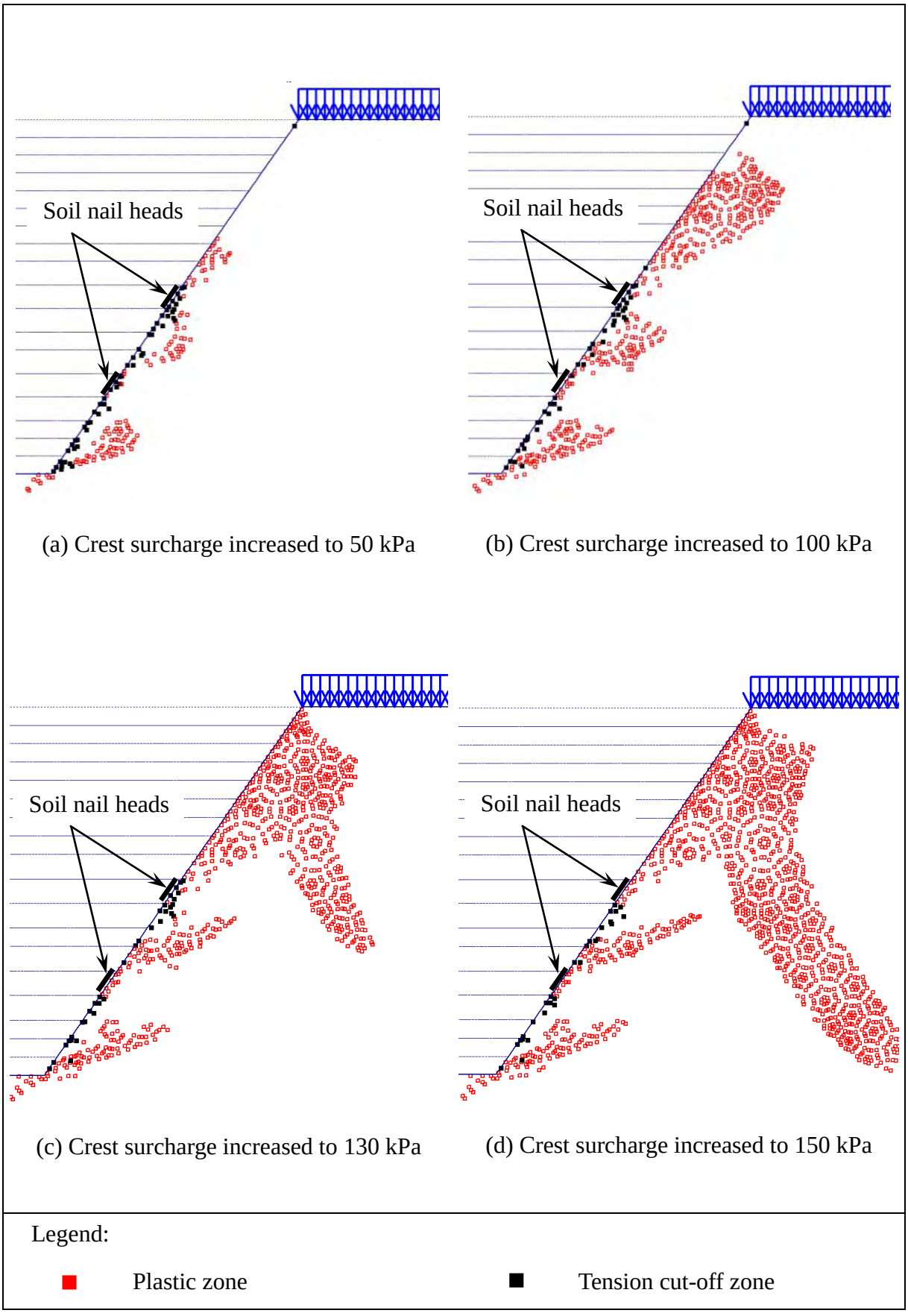

Figure B20 - Development of Plastic Zones - with Crest Surcharge; Nail Head Size = 800 mm

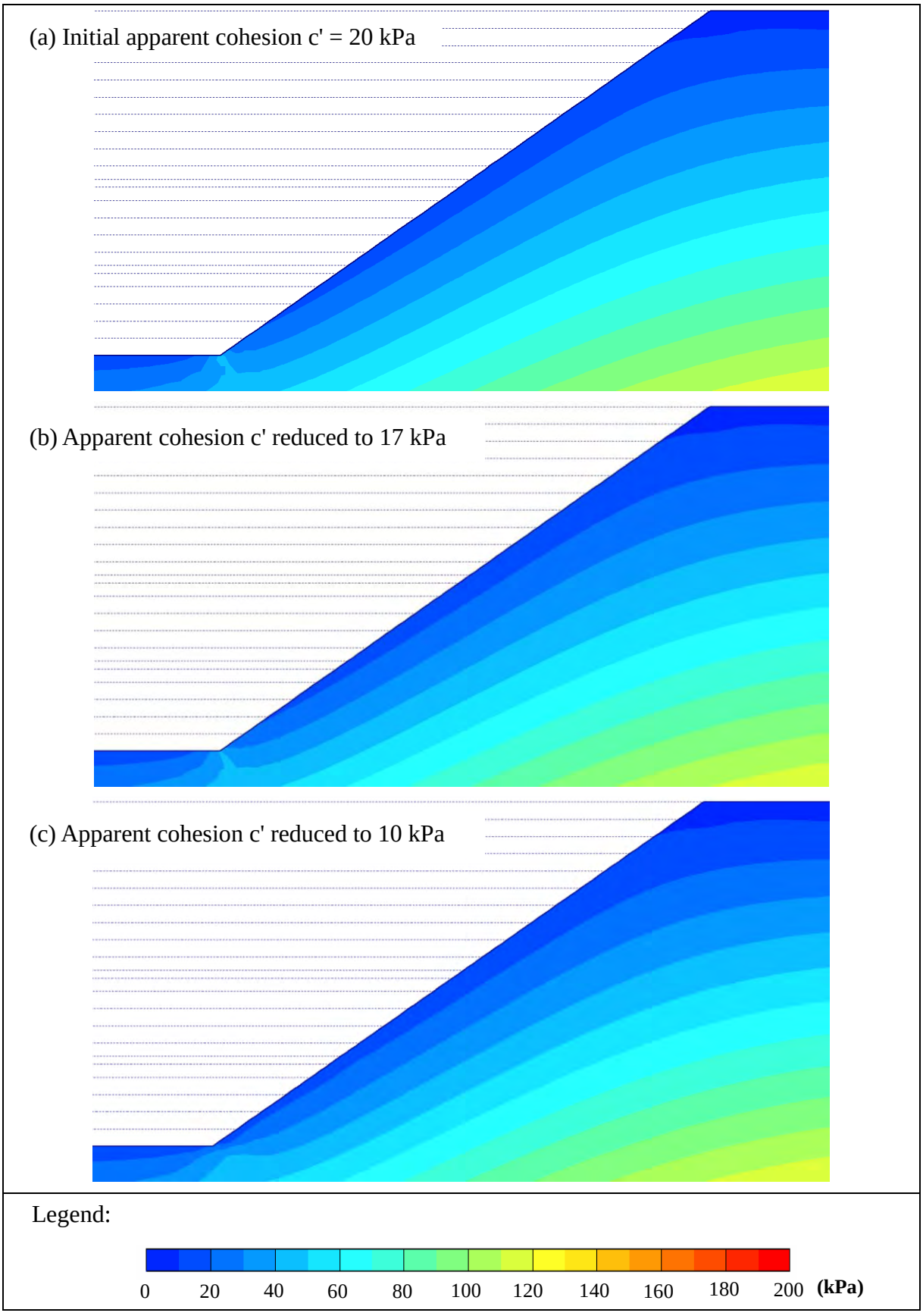

Figure B21 - Development of Mean Effective Stress - 35° Slopes; Nail Head Size = 400 mm (Sheet 1 of 2)

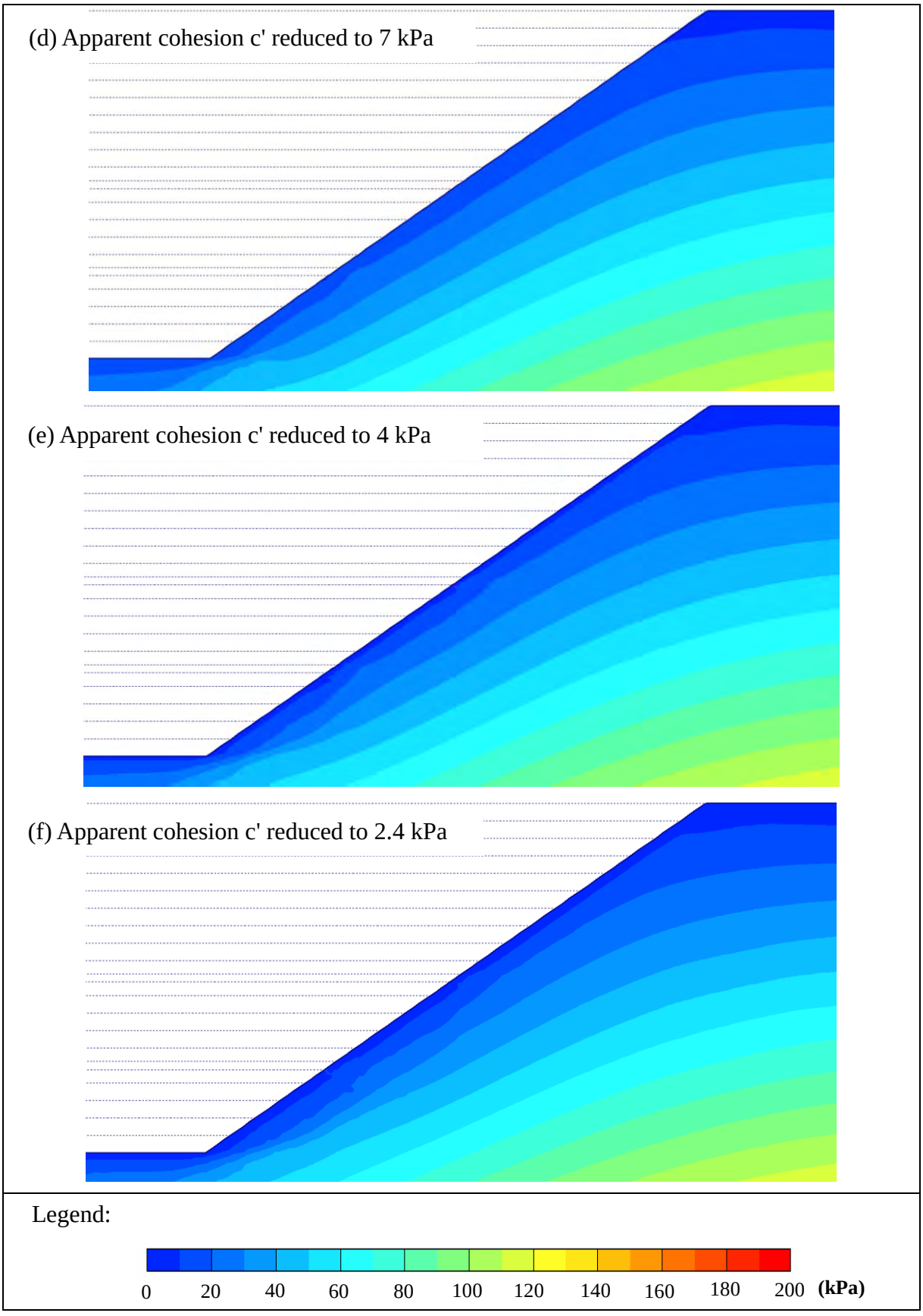

Figure B21 - Development of Mean Effective Stress - 35° Slopes; Nail Head Size = 400 mm (Sheet 2 of 2)

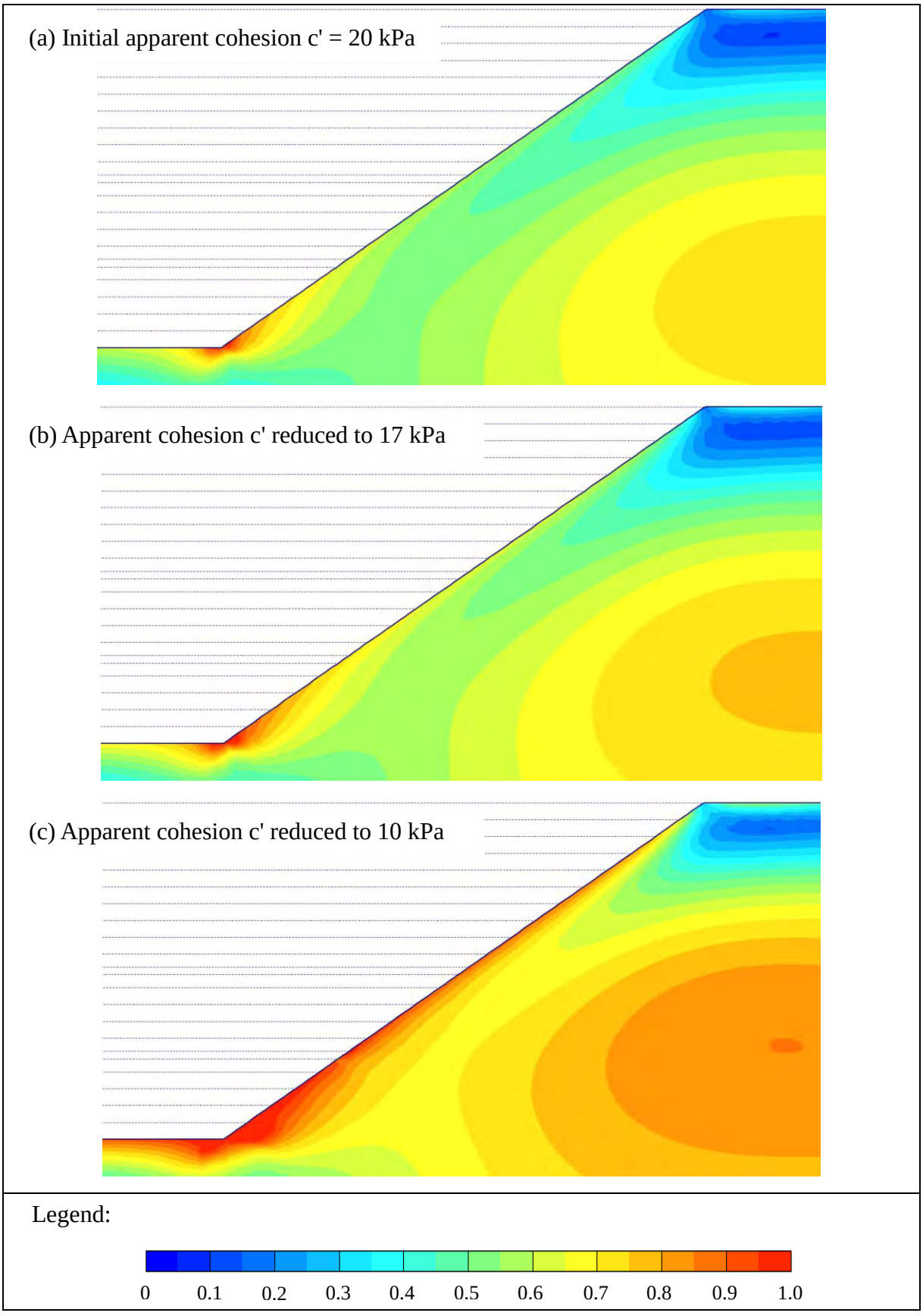

Figure B22 - Development of Relative Shear Stress - 35° Slopes; Nail Head Size = 400 mm
(Sheet 1 of 2)

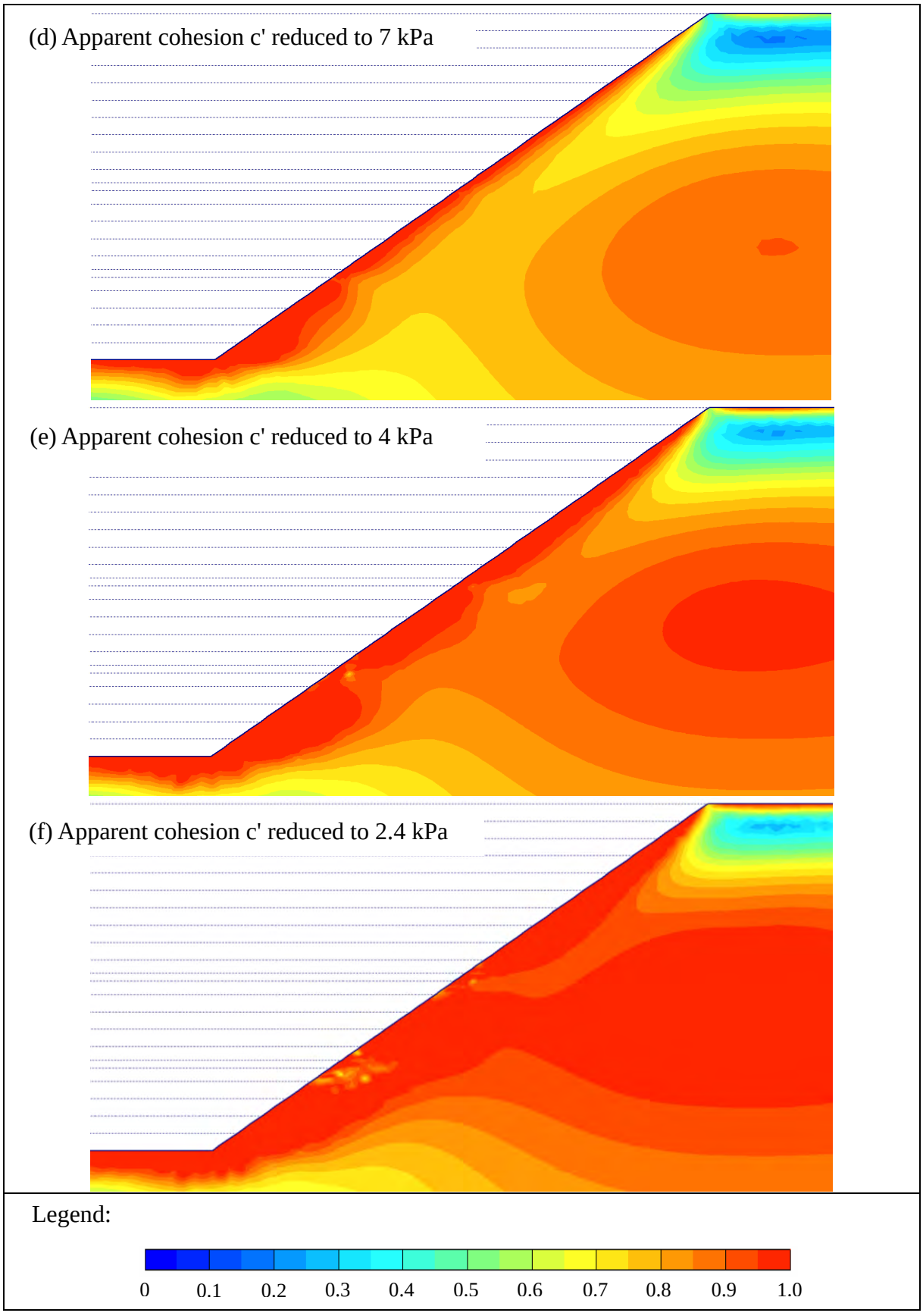

Figure B22 - Development of Relative Shear Stress - 35° Slopes; Nail Head Size = 400 mm (Sheet 2 of 2)

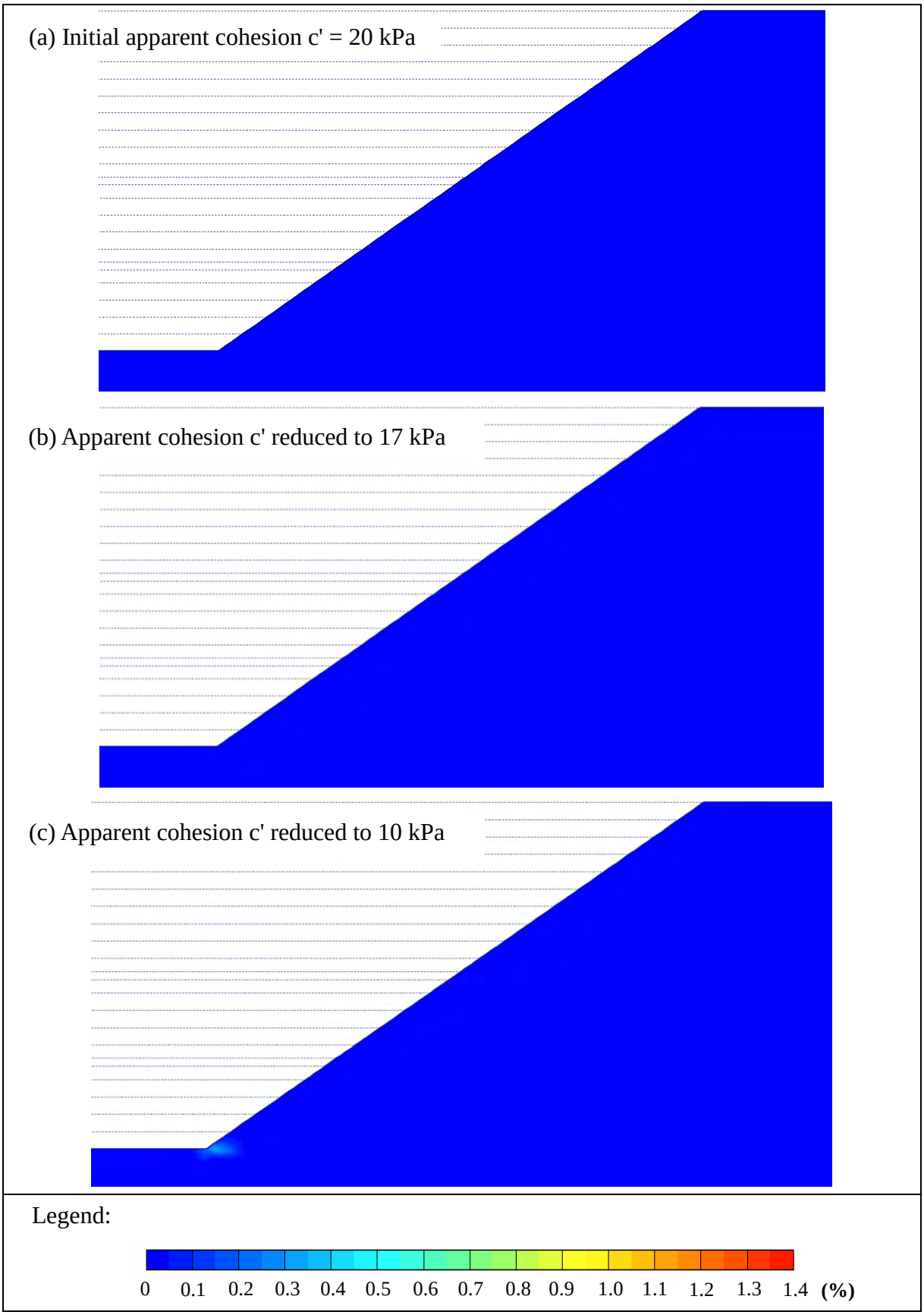

Figure B23 - Development of Shear Strain - 35° Slopes; Nail Head Size = 400 mm
(Sheet 1 of 2)

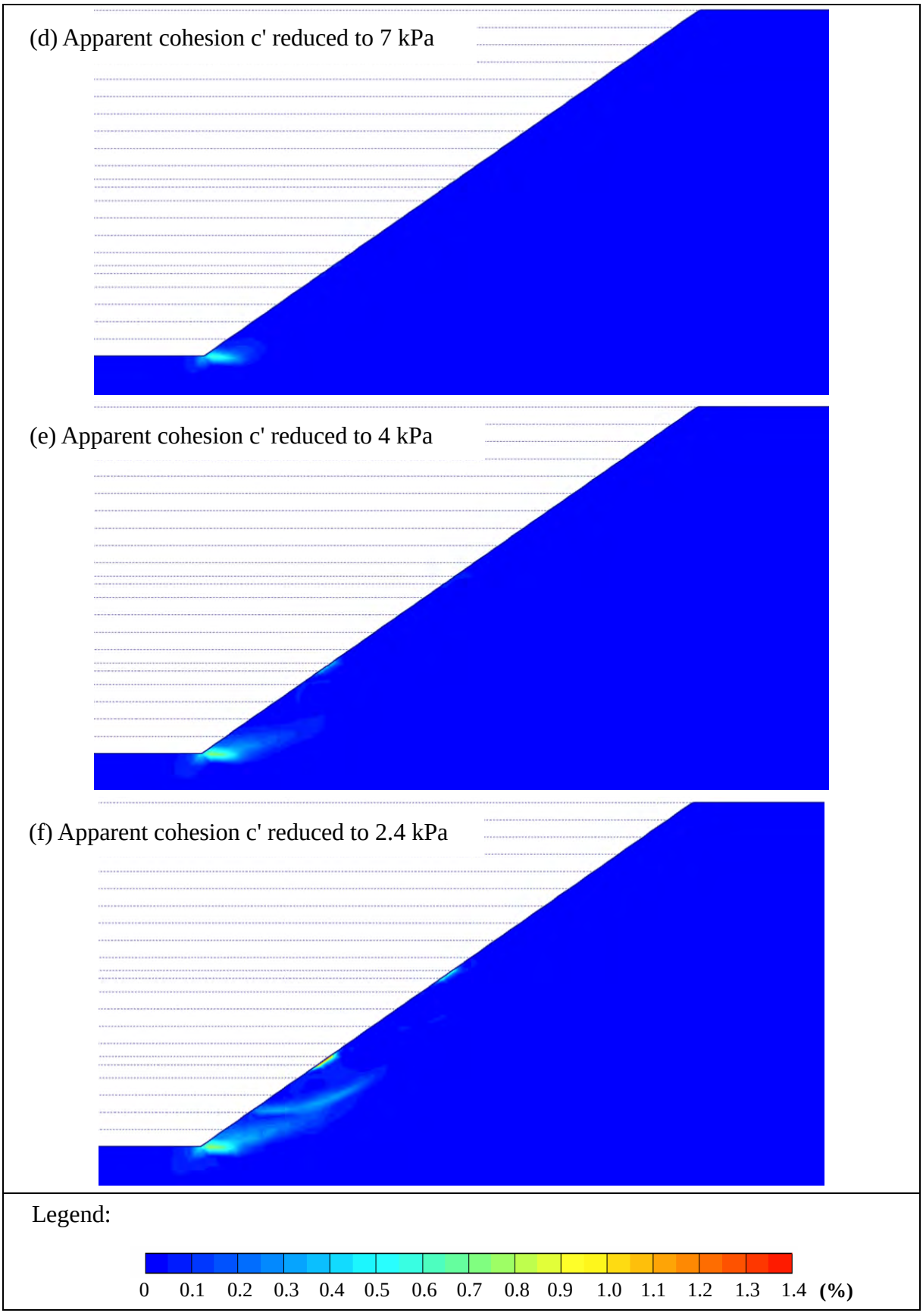

Figure B23 - Development of Shear Strain - 35° Slopes; Nail Head Size = 400 mm
(Sheet 2 of 2)

(a) Initial apparent cohesion c' = 20 kPa

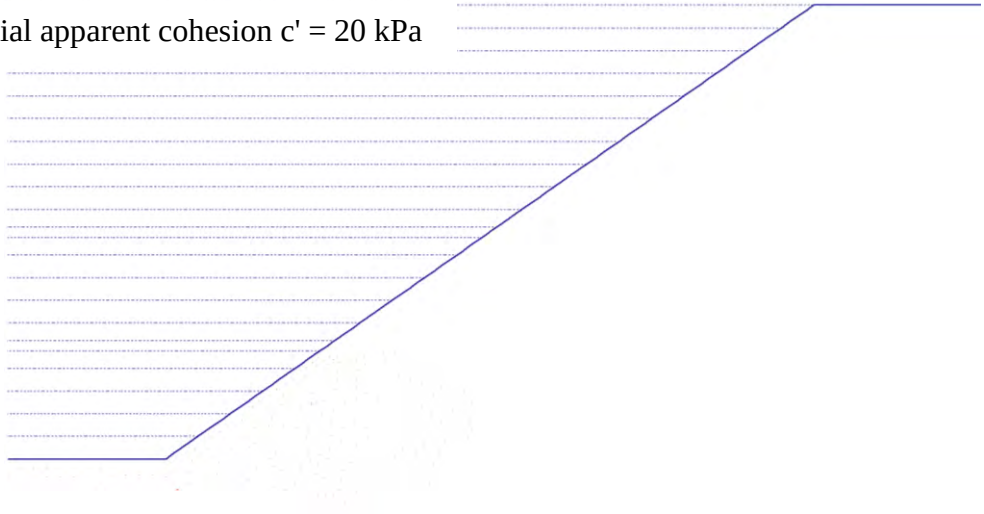

(b) Apparent cohesion c' reduced to 17 kPa

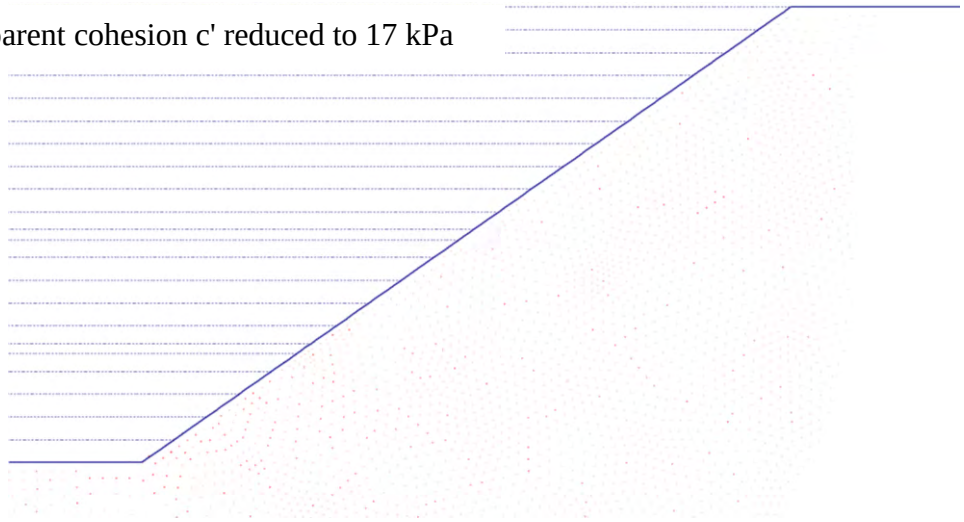

(c) Apparent cohesion c' reduced to 10 kPa

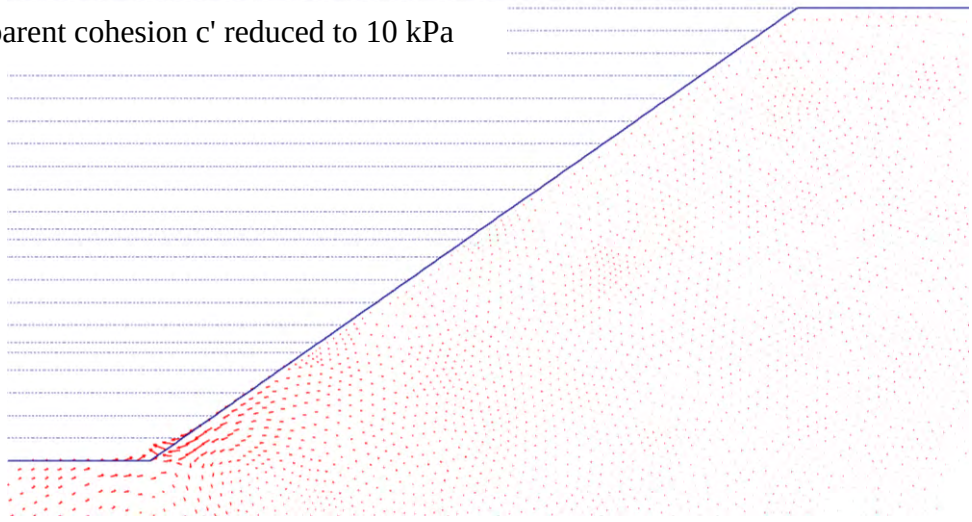

Figure B24 - Displacement Vectors - 35° Slopes; Nail Head Size = 400 mm (Sheet 1 of 2)

(d) Apparent cohesion c' reduced to 7 kPa

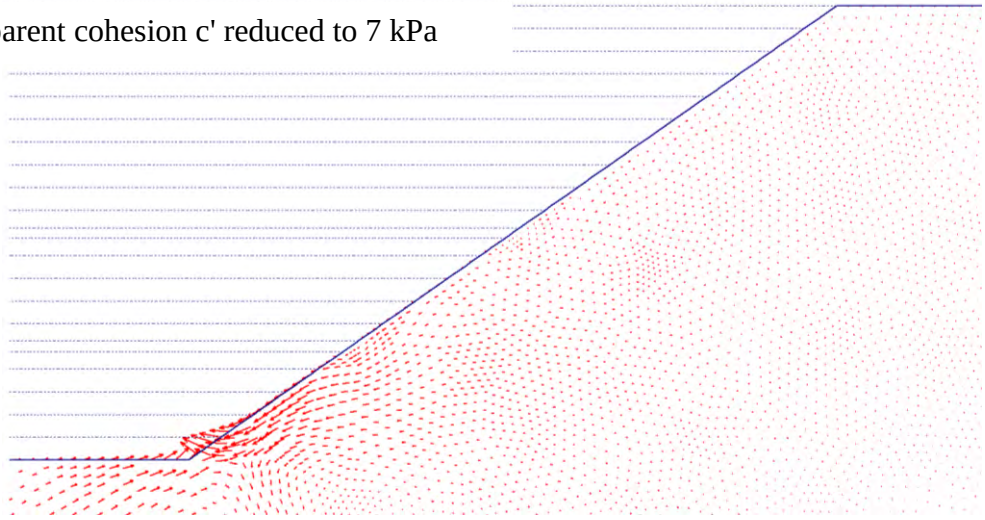

(e) Apparent cohesion c' reduced to 4 kPa

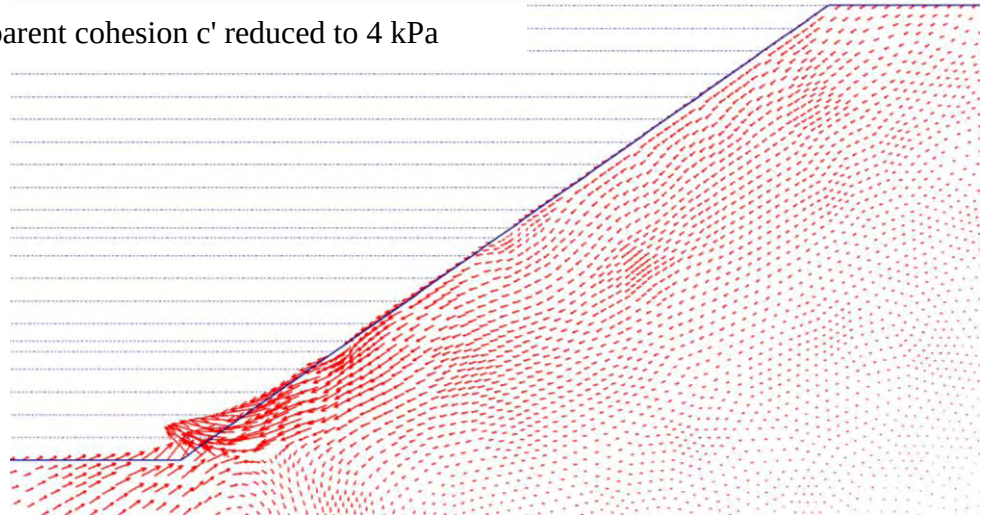

(f) Apparent cohesion c' reduced to 2.4 kPa

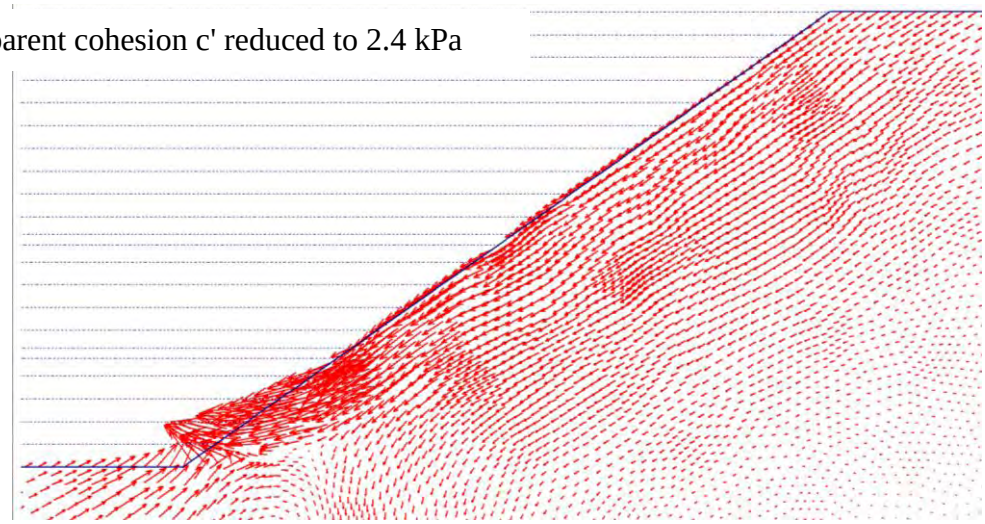

Figure B24 - Displacement Vectors - 35° Slopes; Nail Head Size = 400 mm (Sheet 2 of 2)

(a) Initial apparent cohesion c' = 20 kPa

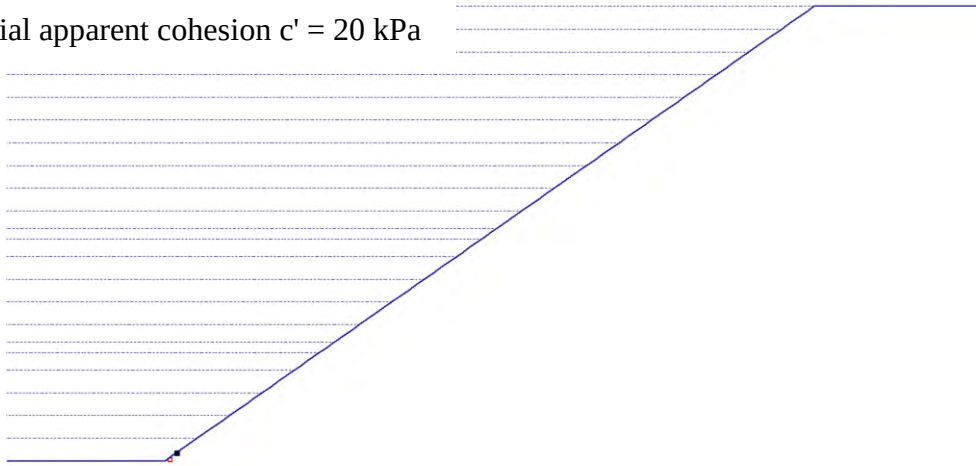

(b) Apparent cohesion c' reduced to 17 kPa

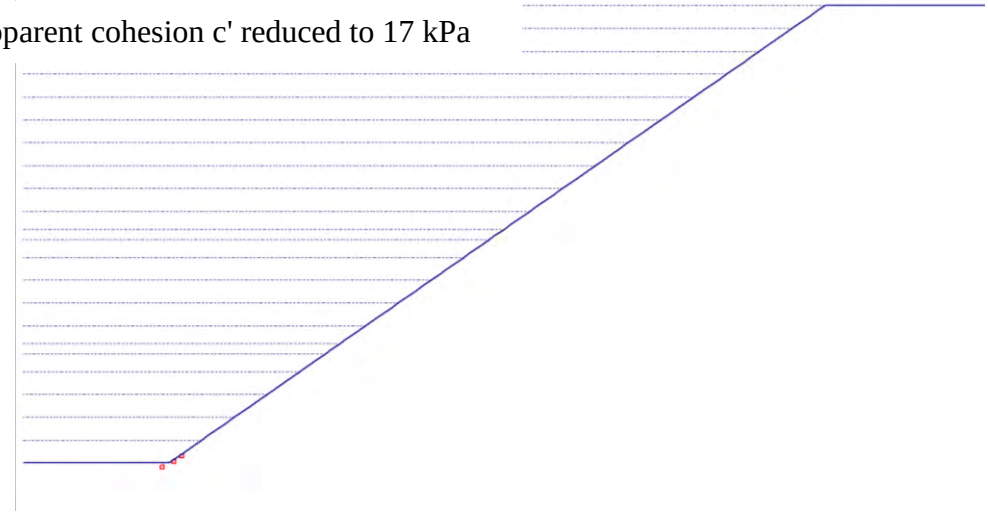

(c) Apparent cohesion c' reduced to 10 kPa

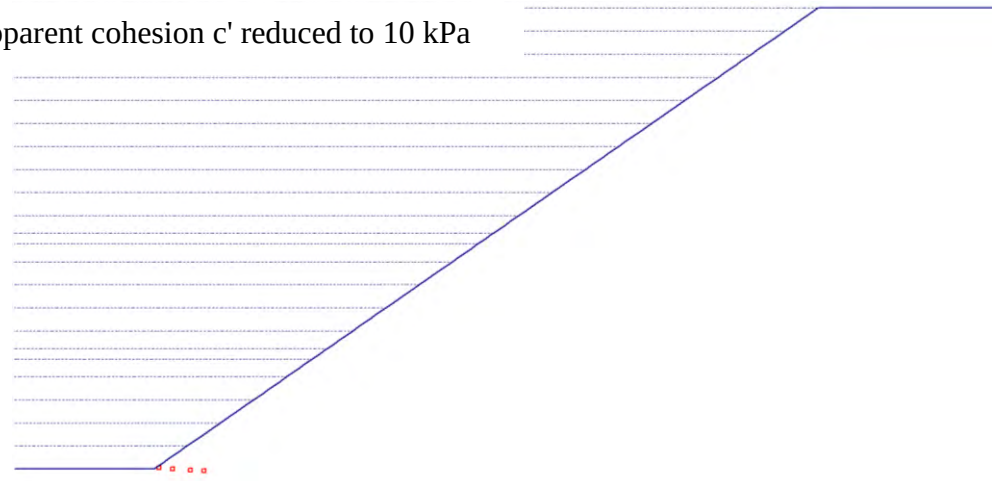

Legend:

■ Plastic zone ■ Tension cut-off zone

Figure B25 - Development of Plastic Zones - 35° Slopes; Nail Head Size = 400 mm
(Sheet 1 of 2)

(d) Apparent cohesion c' reduced to 7 kPa

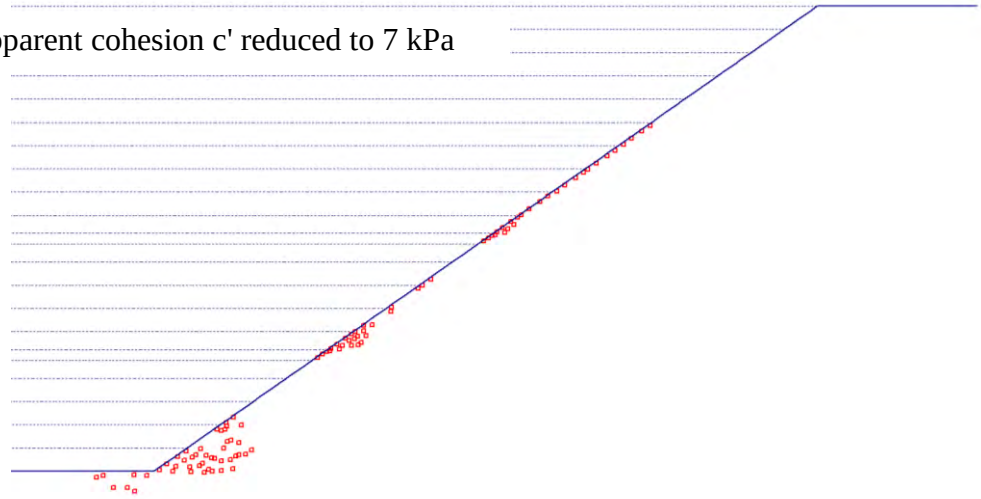

(e) Apparent cohesion c' reduced to 4 kPa

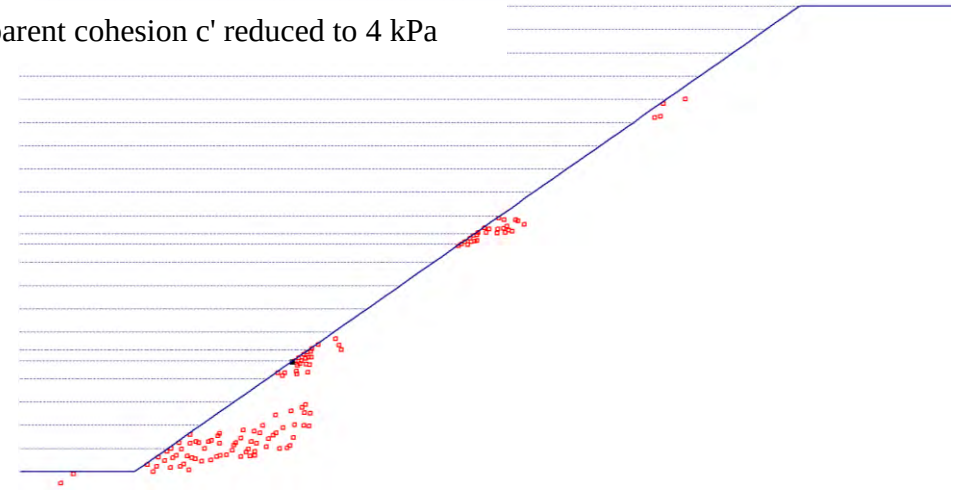

(f) Apparent cohesion c' reduced to 2.4 kPa

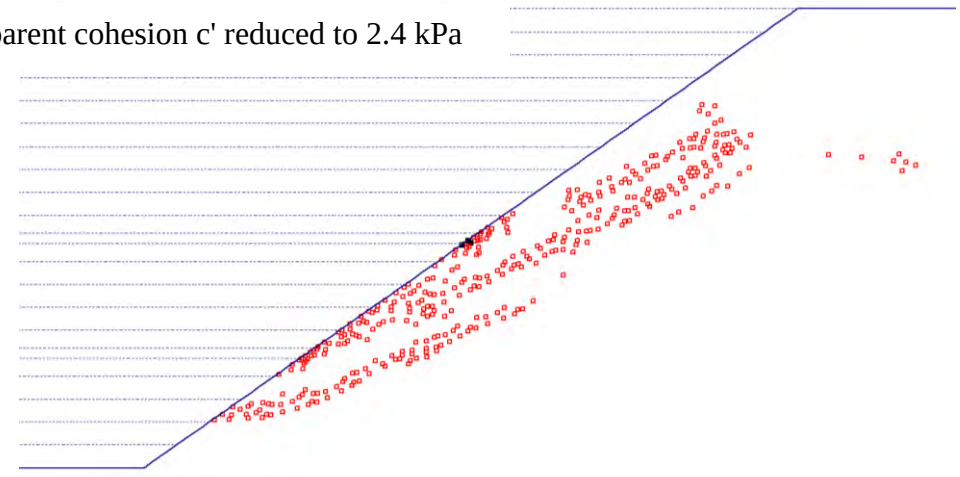

Legend:

■ Plastic zone ■ Tension cut-off zone

Figure B25 - Development of Plastic Zones - 35° Slopes; Nail Head Size = 400 mm
(Sheet 2 of 2)

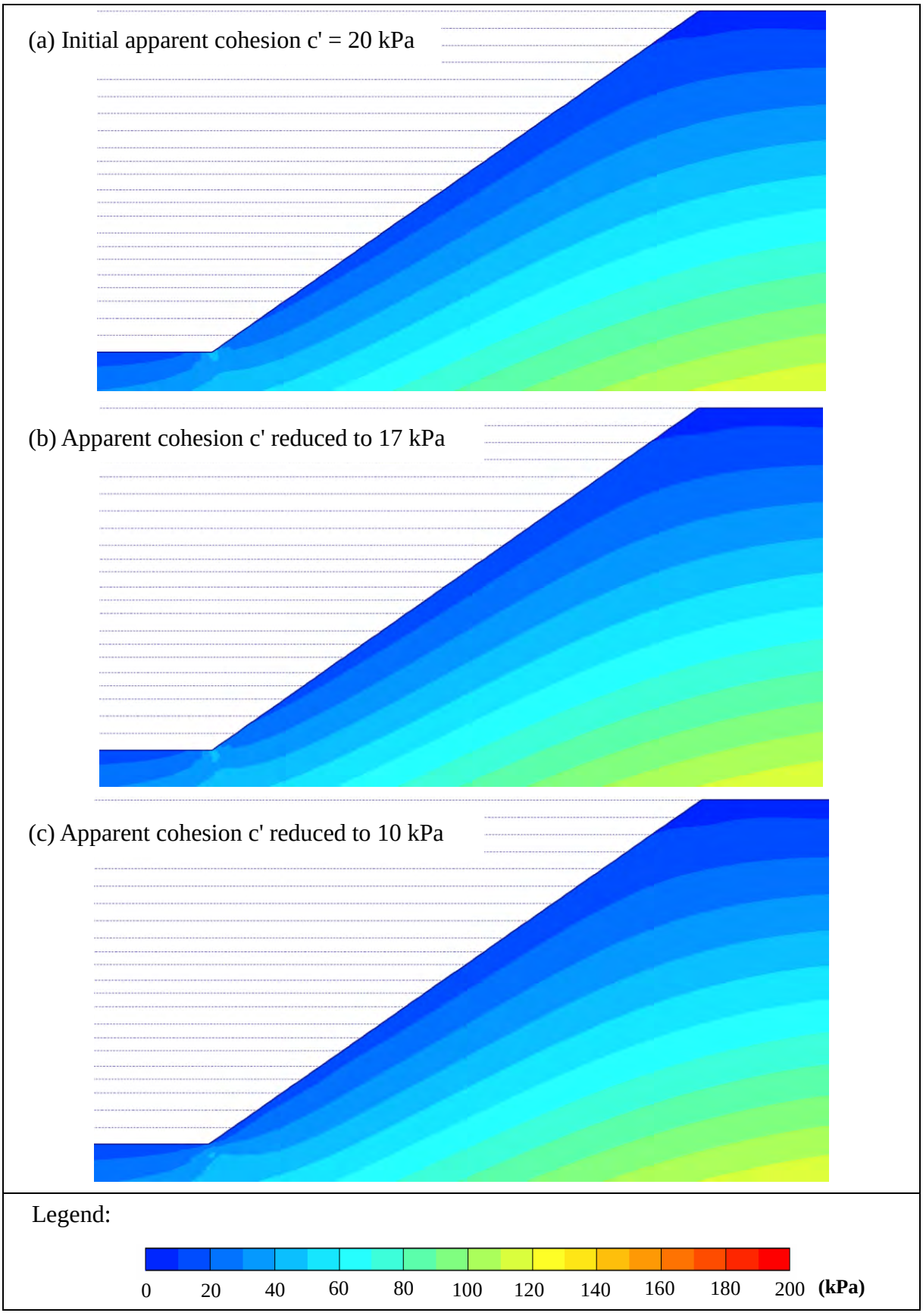

Figure B26 - Development of Mean Effective Stress - 35° Slopes; Nail Head Size = 800 mm (Sheet 1 of 2)

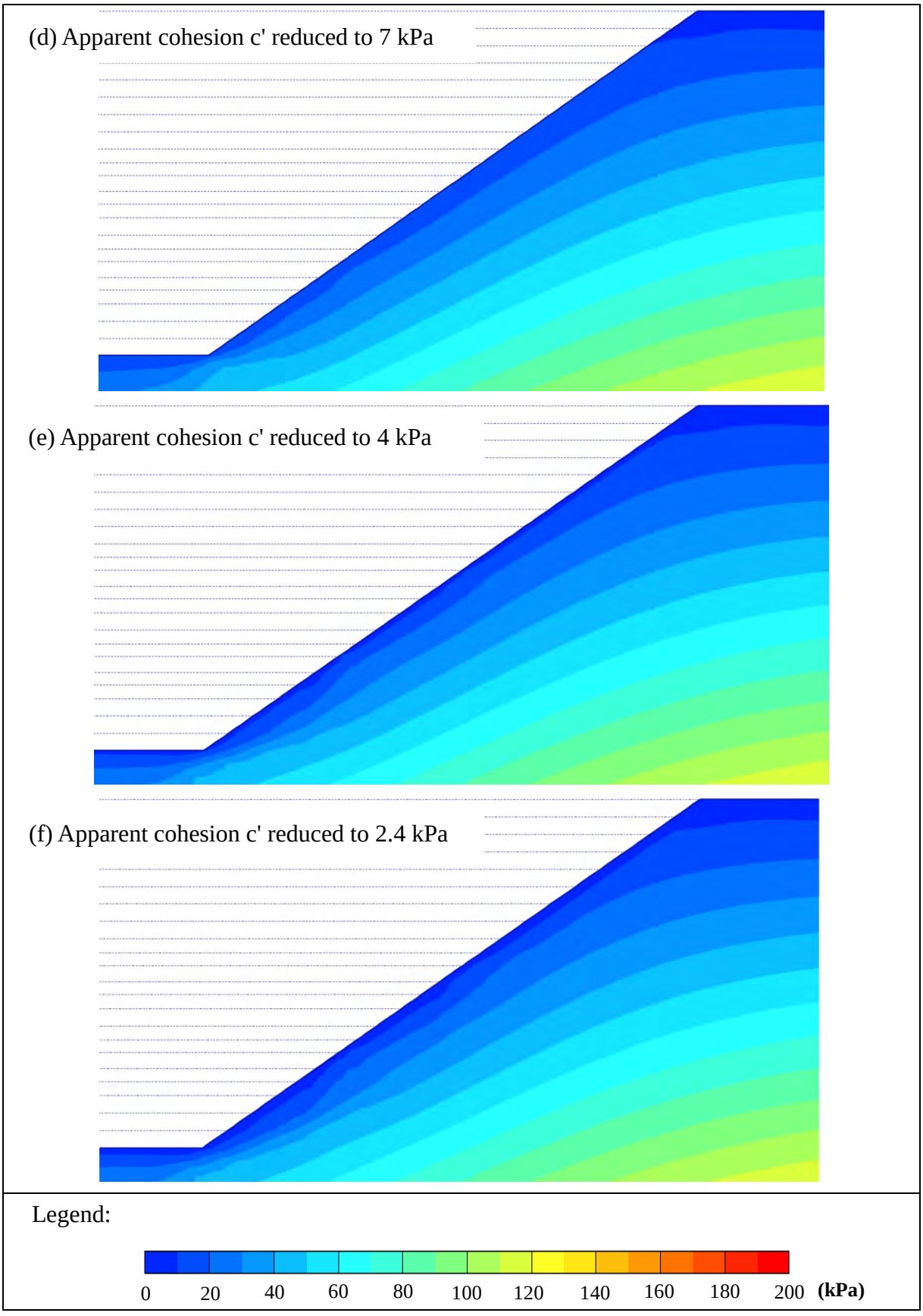

Figure B26 - Development of Mean Effective Stress - 35° Slopes; Nail Head Size = 800 mm (Sheet 2 of 2)

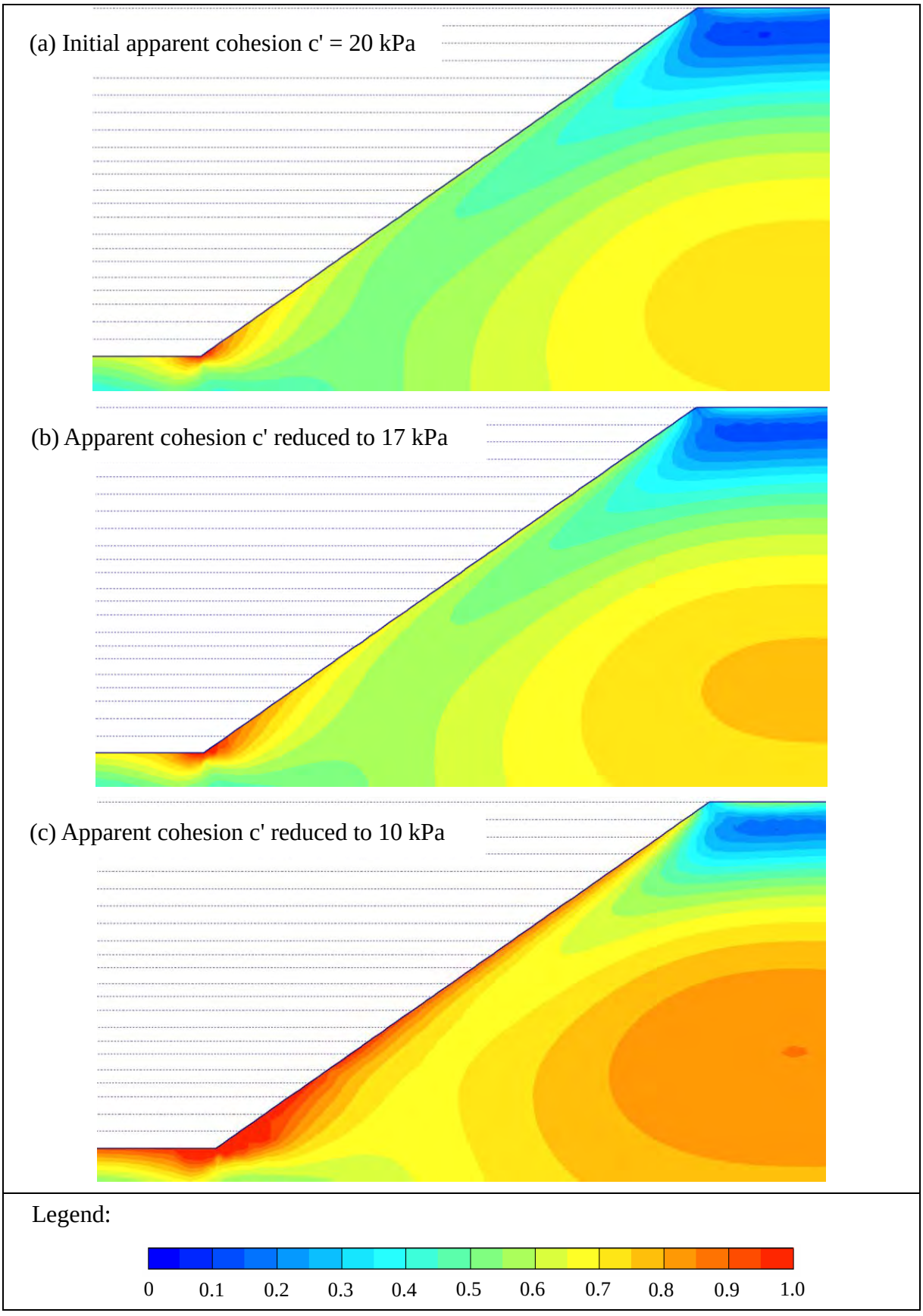

Figure B27 - Development of Relative Shear Stress - 35° Slopes; Nail Head Size = 800 mm (Sheet 1 of 2)

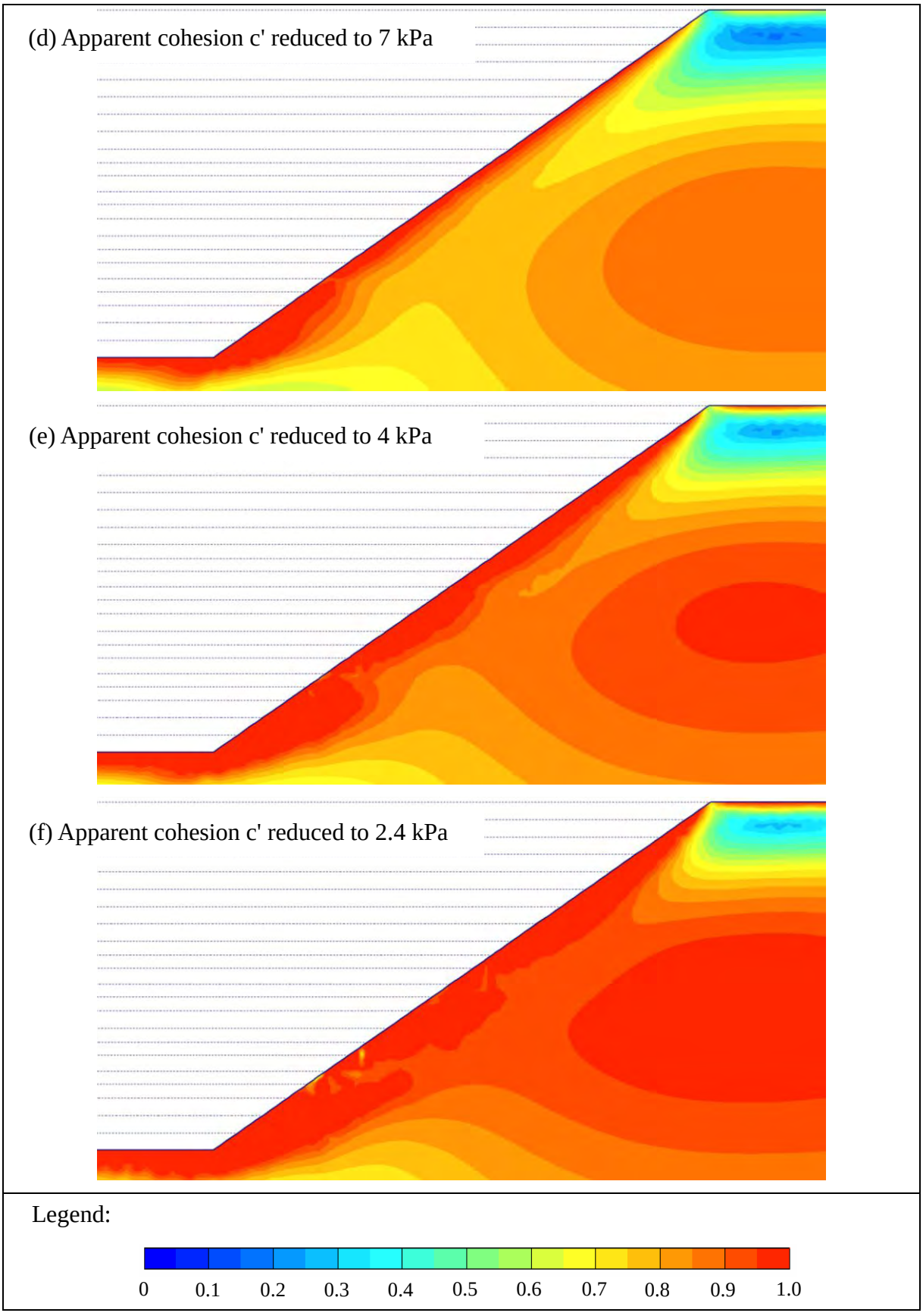

Figure B27 - Development of Relative Shear Stress - 35° Slopes; Nail Head Size = 800 mm
(Sheet 2 of 2)

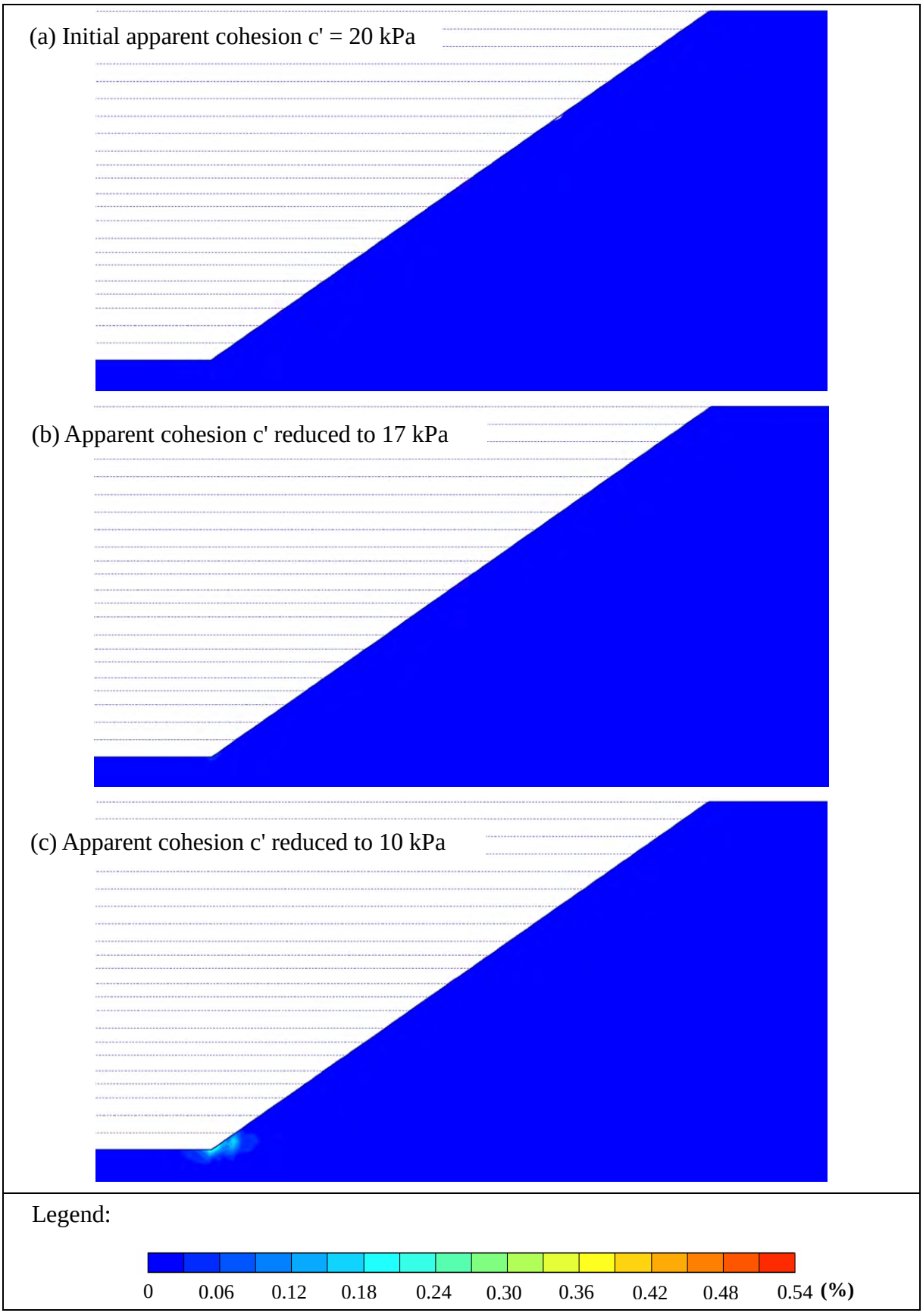

Figure B28 - Development of Shear Strain - 35° Slopes; Nail Head Size = 800 mm
(Sheet 1 of 2)

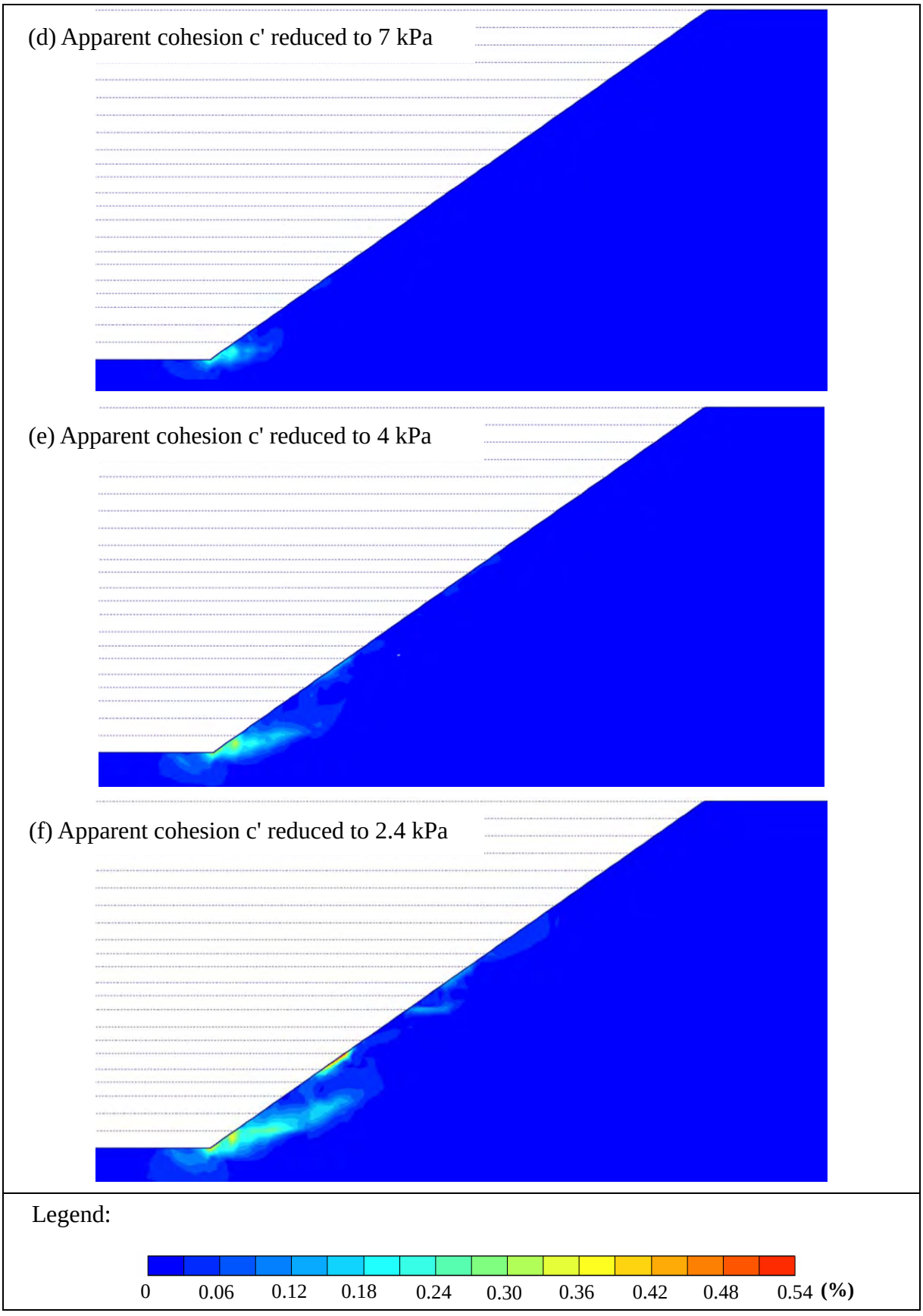

Figure B28 - Development of Shear Strain - 35° Slopes; Nail Head Size = 800 mm
(Sheet 2 of 2)

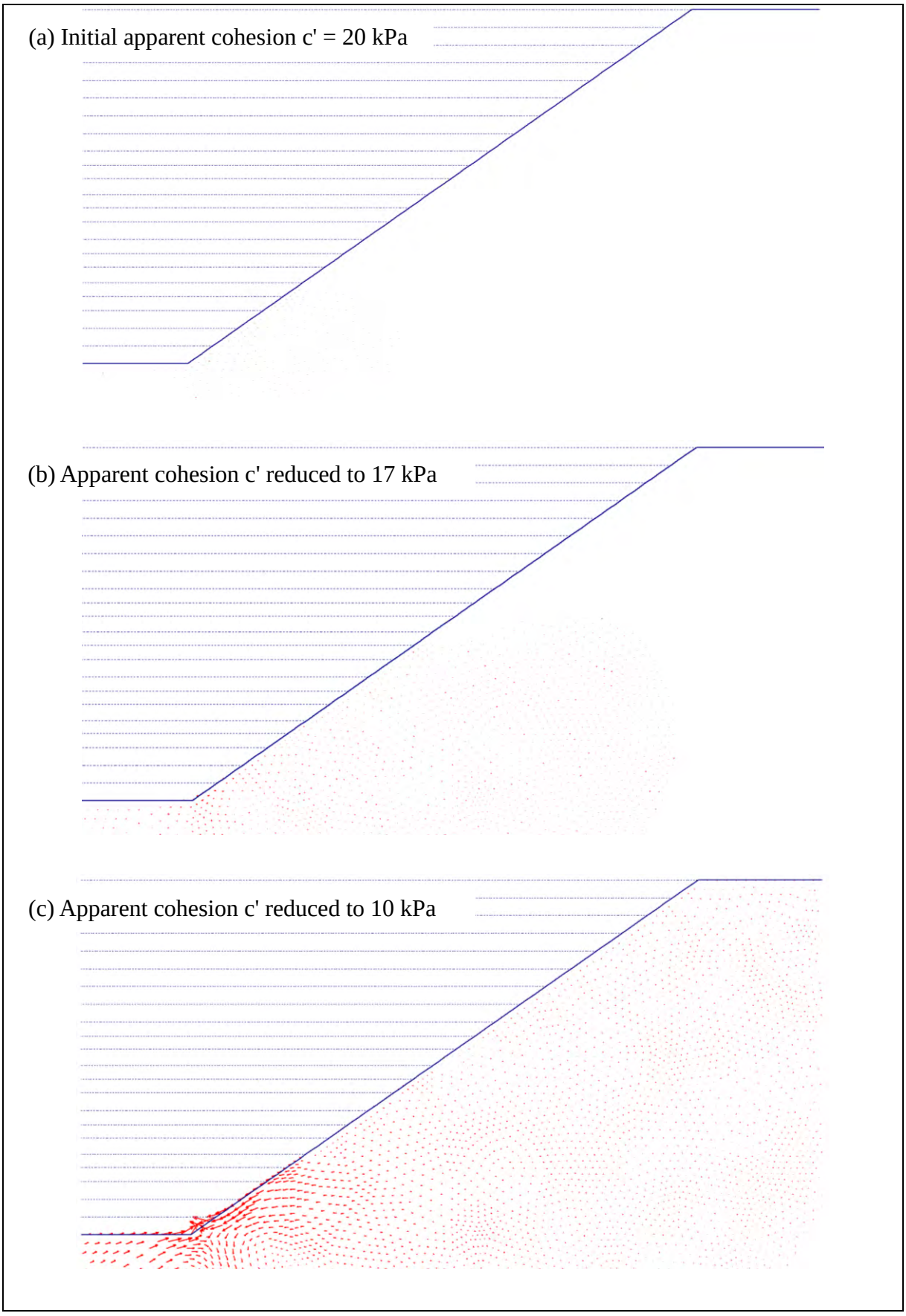

Figure B29 - Displacement Vectors - 35° Slopes; Nail Head Size = 800 mm (Sheet 1 of 2)

(d) Apparent cohesion c' reduced to 7 kPa

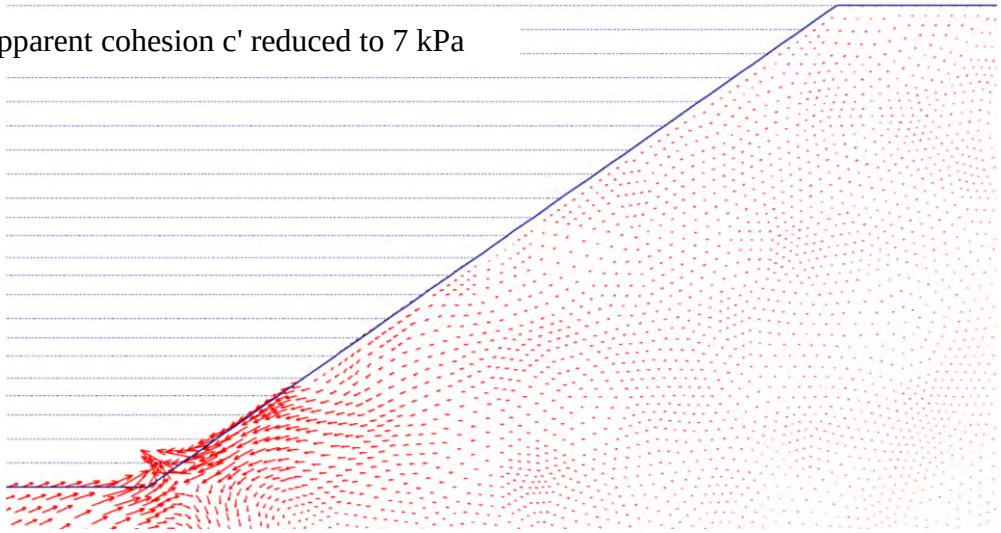

(e) Apparent cohesion c' reduced to 4 kPa

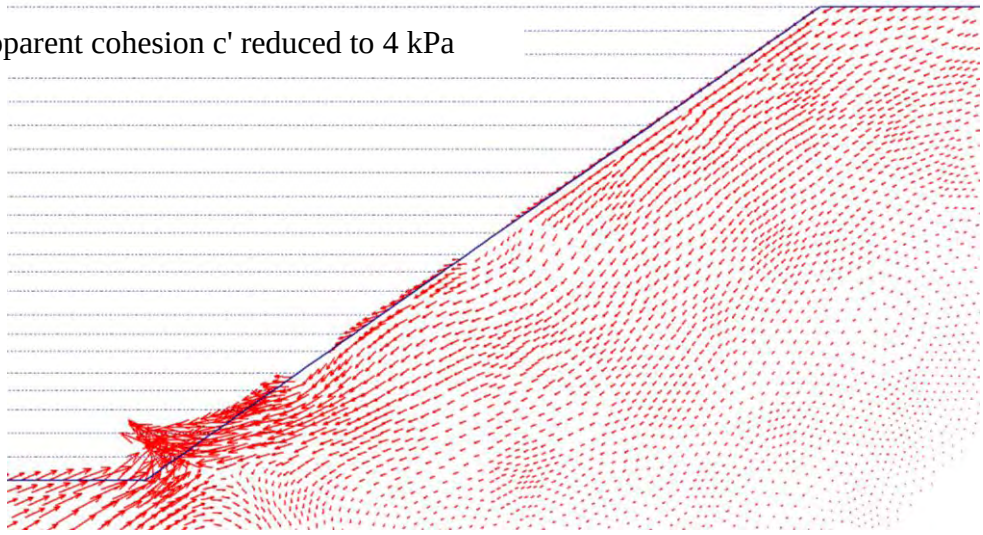

(f) Apparent cohesion c' reduced to 2.4 kPa

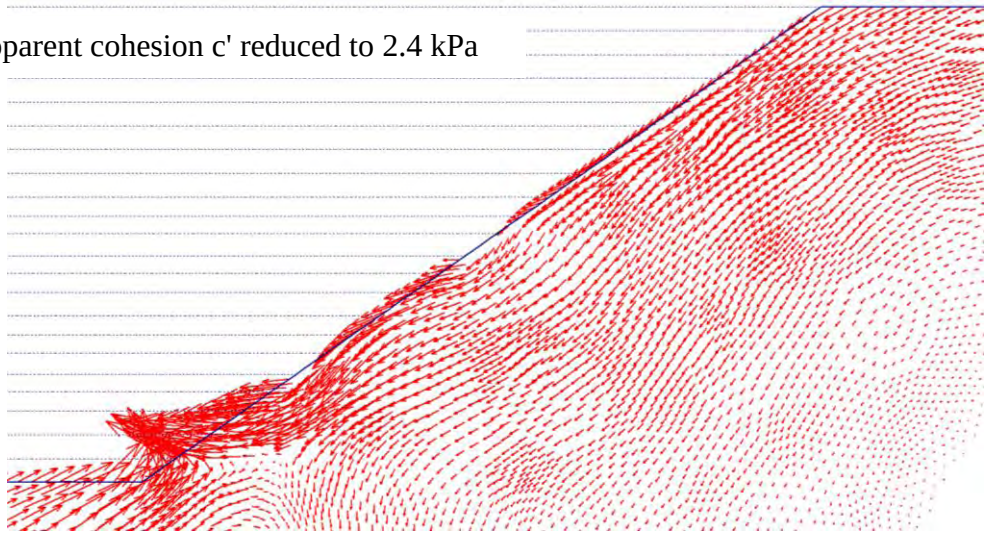

Figure B29 - Displacement Vectors - 35° Slopes; Nail Head Size = 800 mm (Sheet 2 of 2)

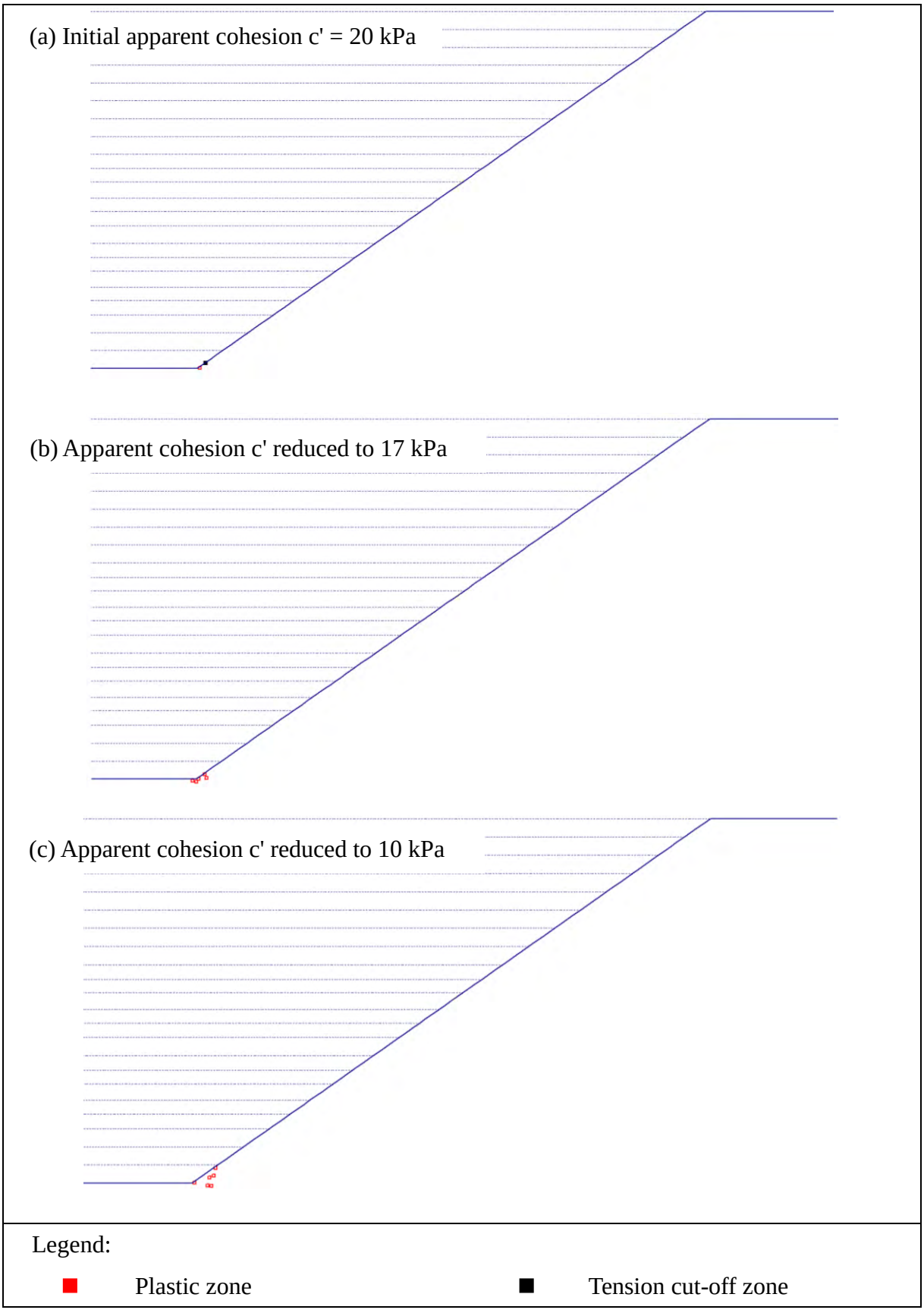

Figure B30 - Development of Plastic Zones - 35° Slopes; Nail Head Size = 800 mm
(Sheet 1 of 2)

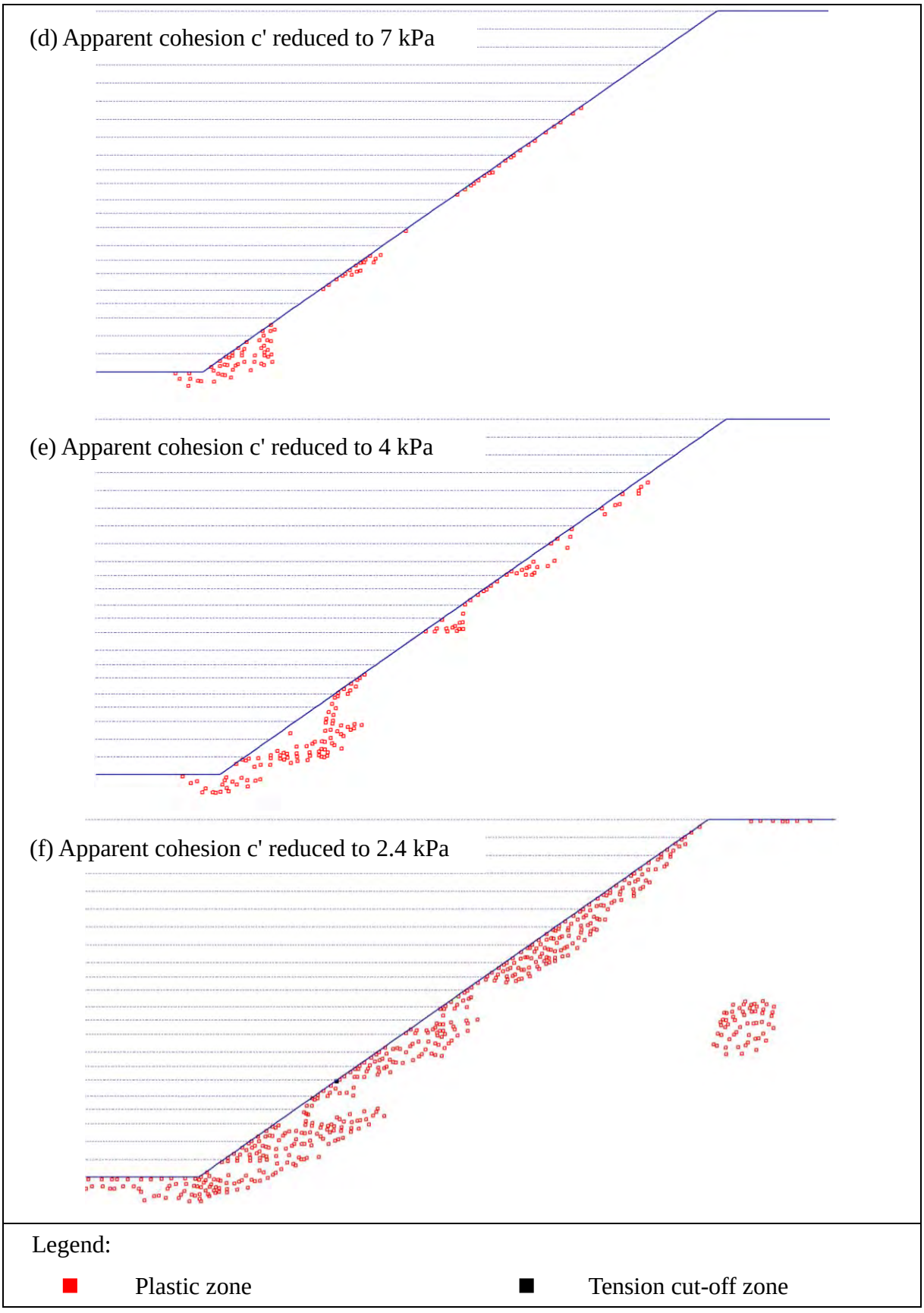

Figure B30 - Development of Plastic Zones - 35° Slopes; Nail Head Size = 800 mm
(Sheet 2 of 2)

Table of Contents
Table of Contents
Table of Contents

APPENDIX C

OUTPUT FROM NUMERICAL MODELLING FOR REINFORCED SLOPES WITH THREE ROWS OF SOIL NAILS

LIST OF FIGURES

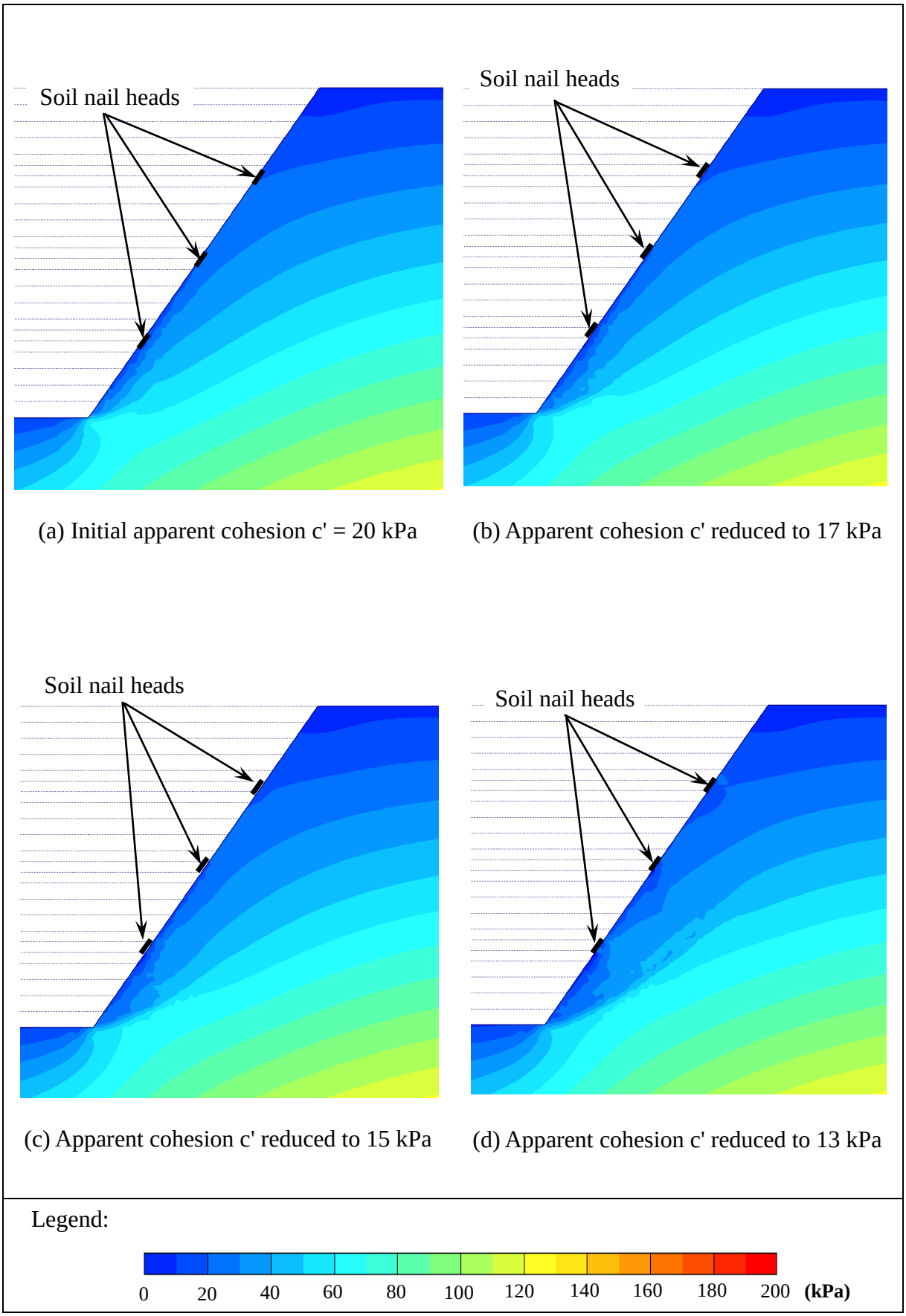

Figure C1 - Development of Mean Effective Stress - Nail Head Size = 400 mm (Sheet 1 of 2)

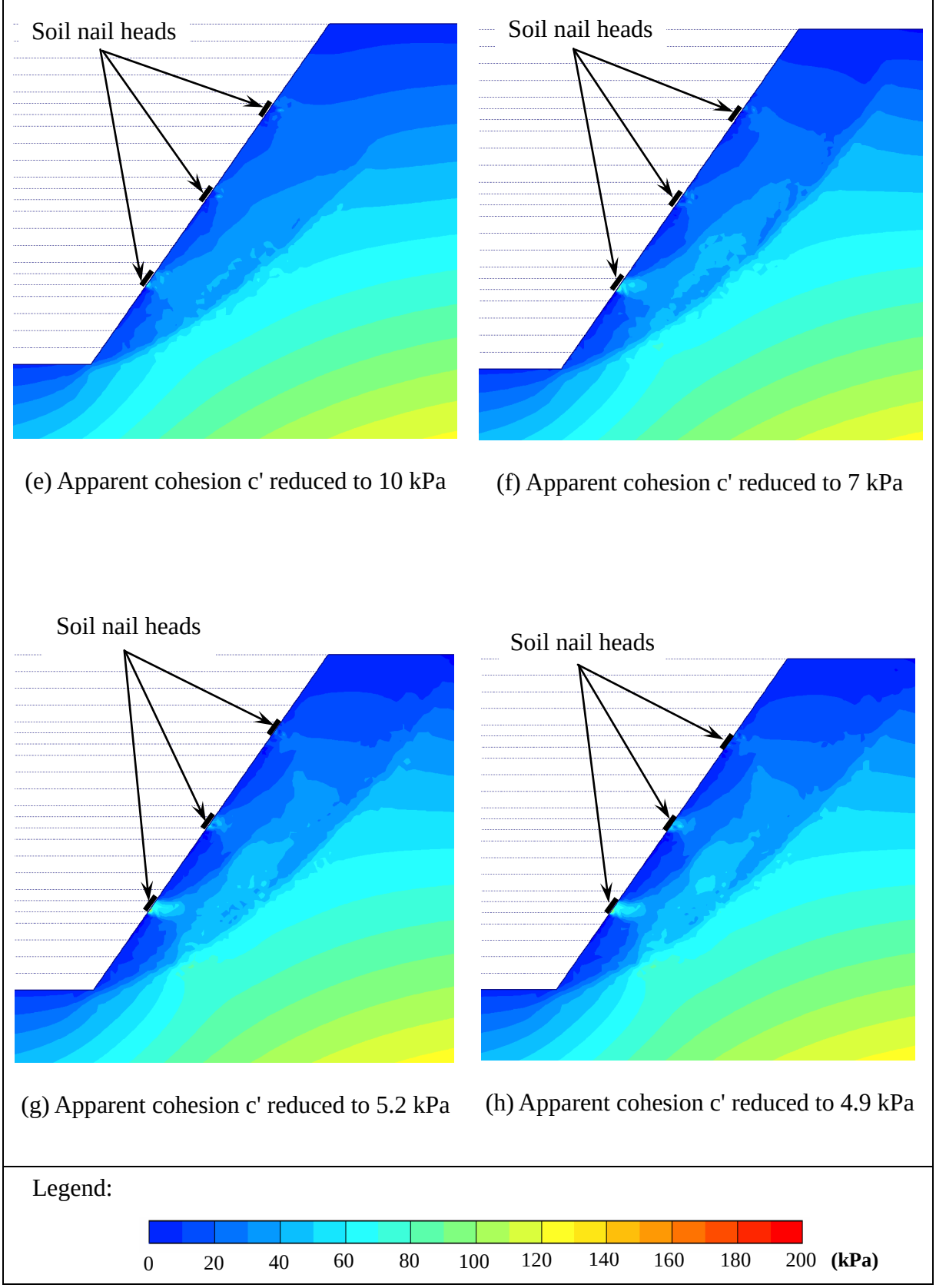

(e) Apparent cohesion c' reduced to 10 kPa

(f) Apparent cohesion c' reduced to 7 kPa

(g) Apparent cohesion c' reduced to 5.2 kPa

(h) Apparent cohesion c' reduced to 4.9 kPa

Figure C1 - Development of Mean Effective Stress - Nail Head Size = 400 mm (Sheet 2 of 2)

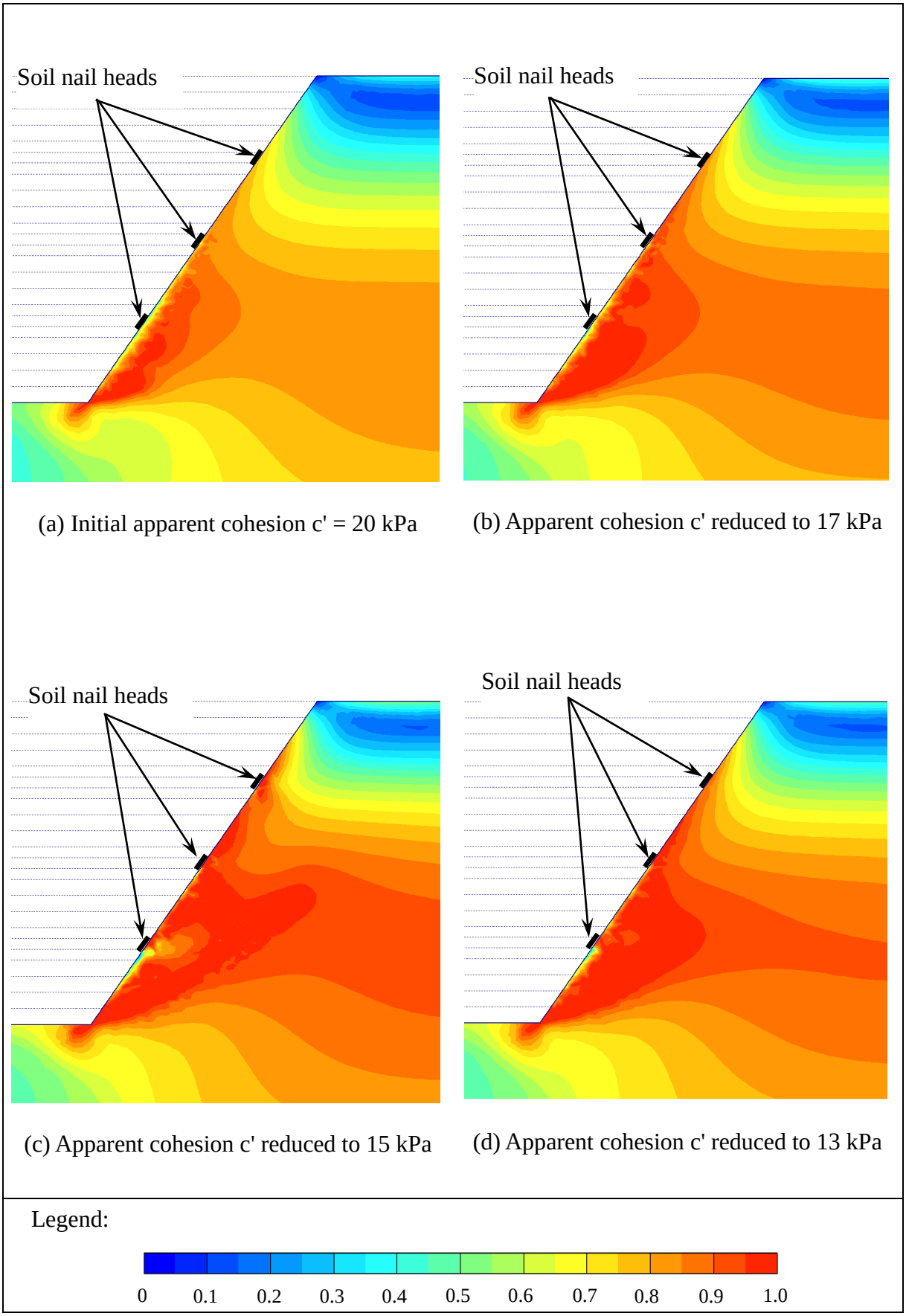

Figure C2 - Development of Relative Shear Stress - Nail Head Size = 400 mm (Sheet 1 of 2)

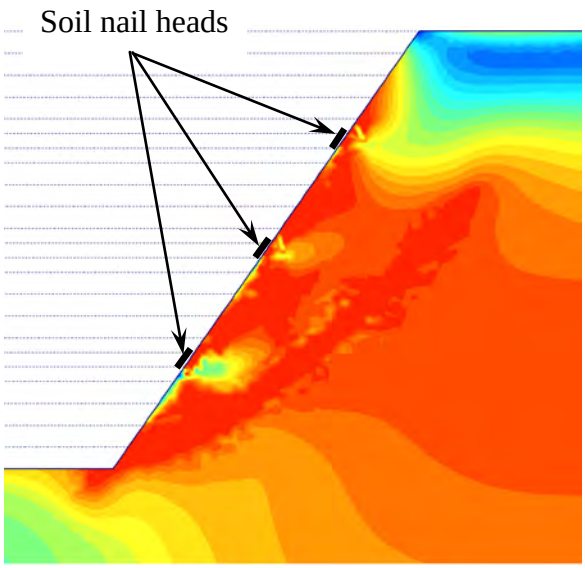

(e) Apparent cohesion c' reduced to 10 kPa

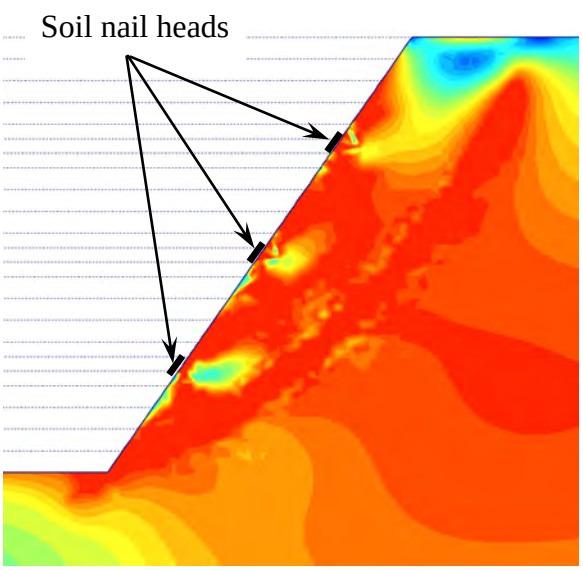

(f) Apparent cohesion c' reduced to 7 kPa

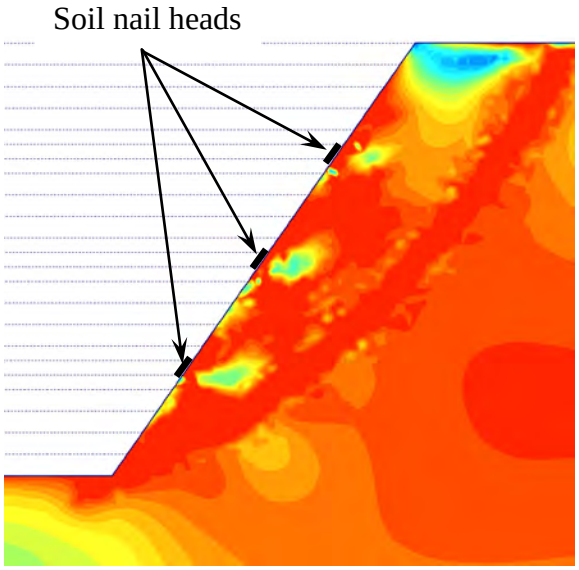

(g) Apparent cohesion c' reduced to 5.2 kPa

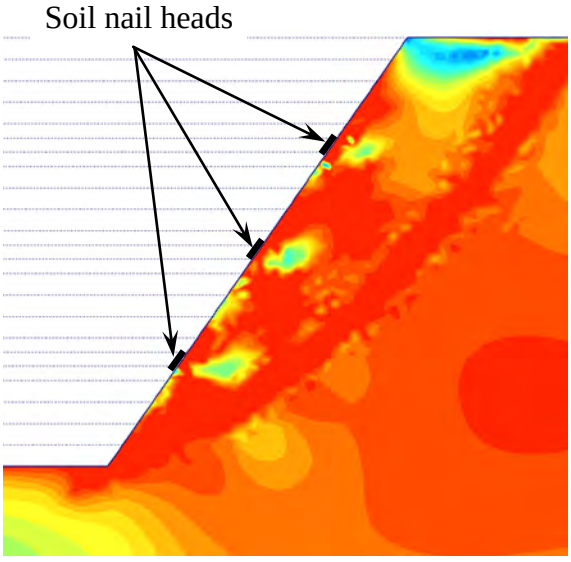

(h) Apparent cohesion c' reduced to 4.9 kPa

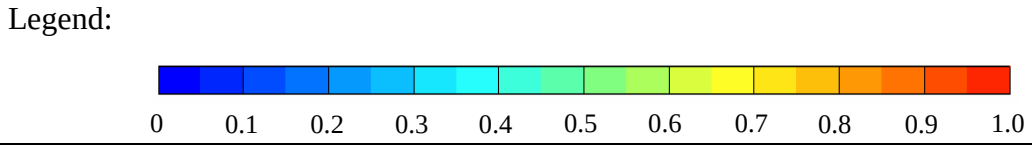

Figure C2 - Development of Relative Shear Stress - Nail Head Size = 400 mm (Sheet 2 of 2)

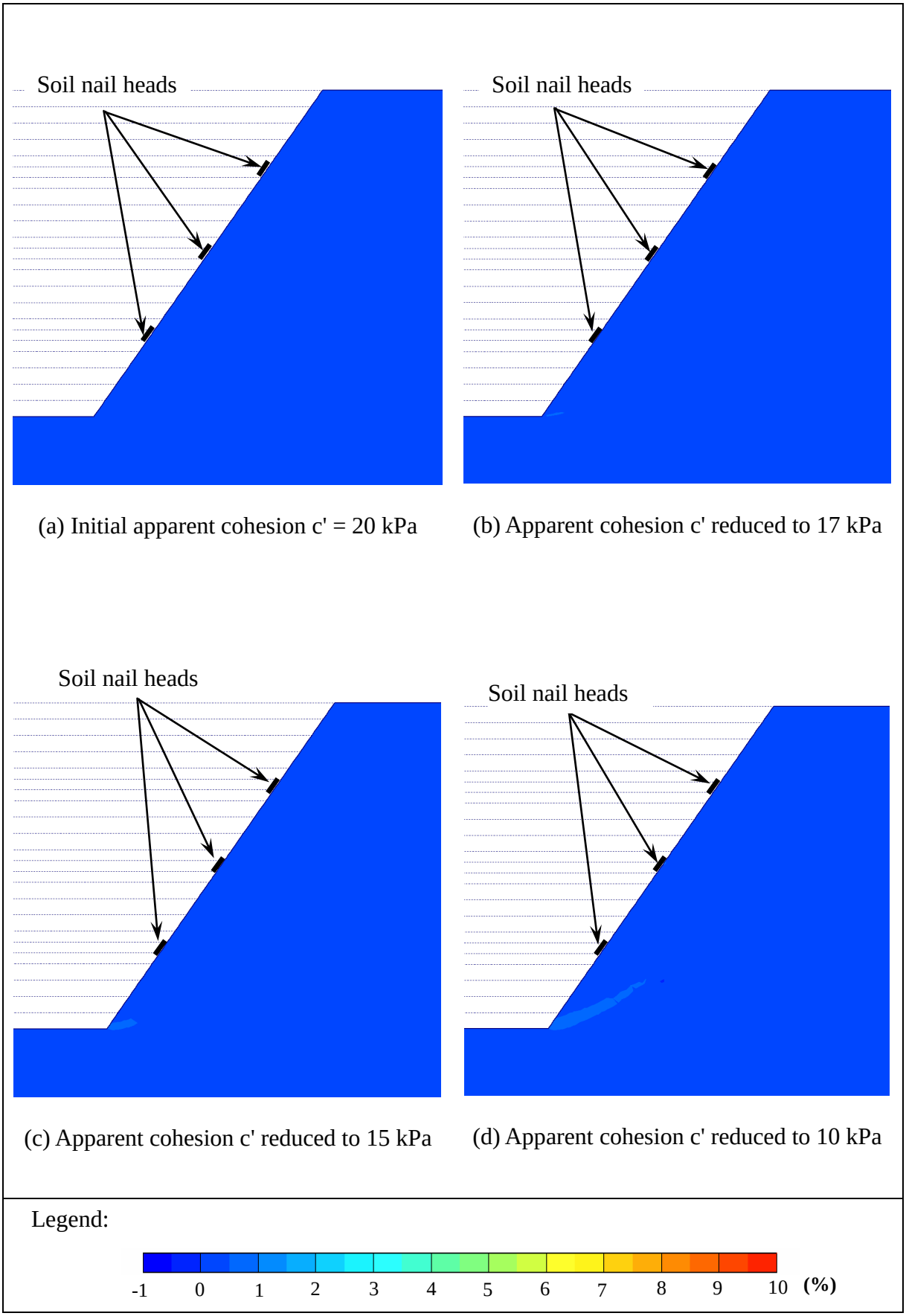

Figure C3 - Development of Shear Strain - Nail Head Size = 400 mm (Sheet 1 of 2)

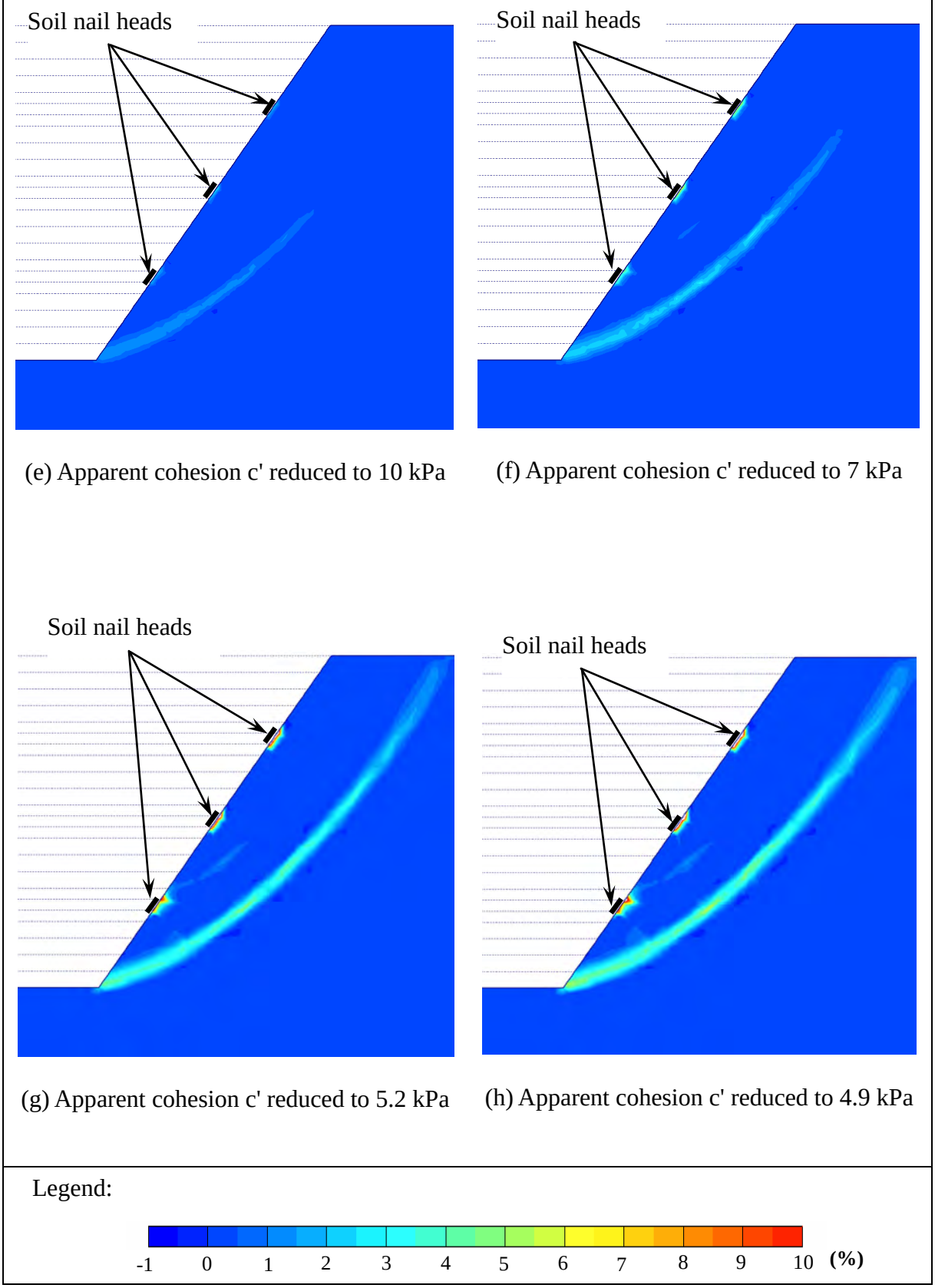

(e) Apparent cohesion c' reduced to 10 kPa

(f) Apparent cohesion c' reduced to 7 kPa

(g) Apparent cohesion c' reduced to 5.2 kPa

(h) Apparent cohesion c' reduced to 4.9 kPa

Figure C3 - Development of Shear Strain - Nail Head Size = 400 mm (Sheet 2 of 2)

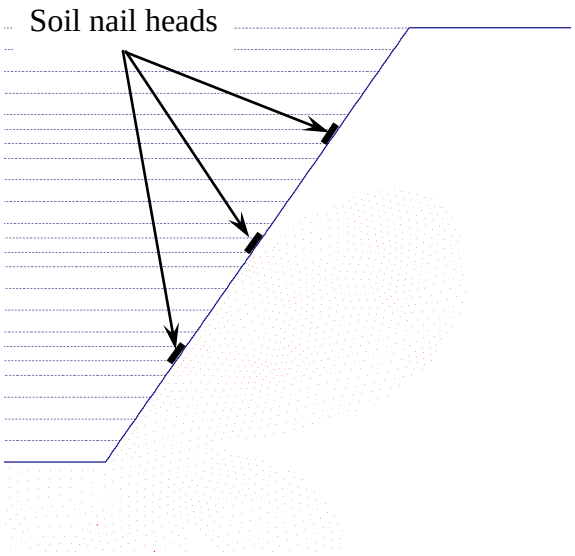

(a) Initial apparent cohesion c' = 20 kPa

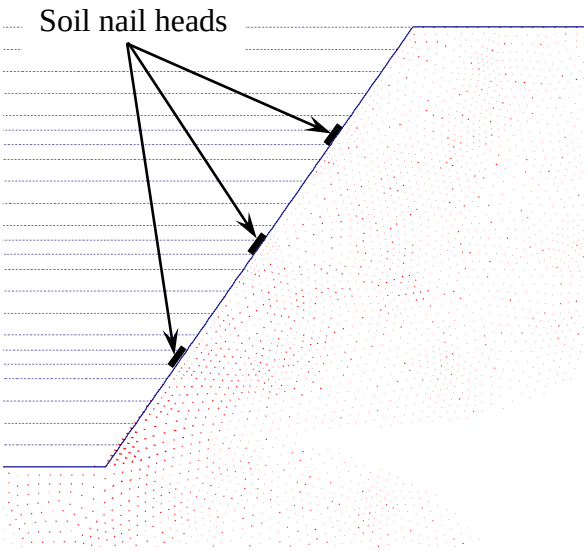

(b) Apparent cohesion c' reduced to 17 kPa

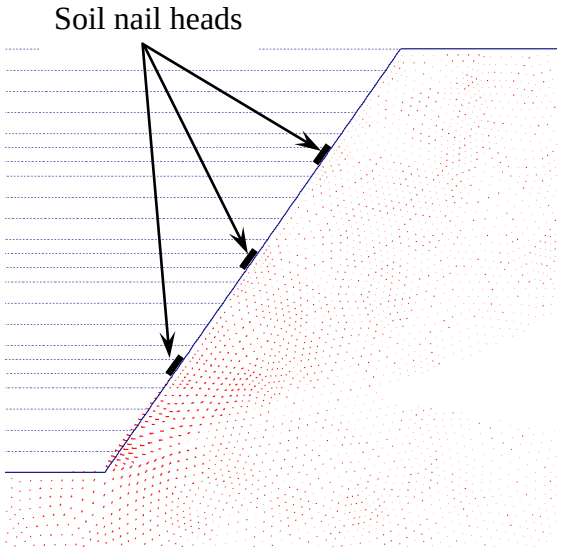

(c) Apparent cohesion c' reduced to 15 kPa

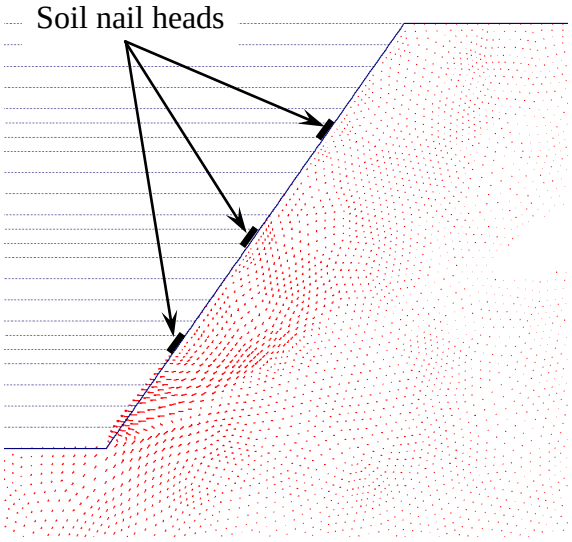

(d) Apparent cohesion c' reduced to 13 kPa

Figure C4 - Displacement Vectors - Nail Head Size = 400 mm (Sheet 1 of 2)

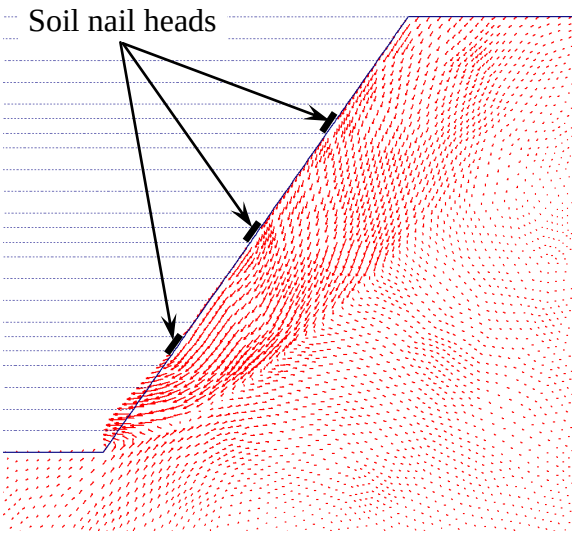

(e) Apparent cohesion c' reduced to 10 kPa

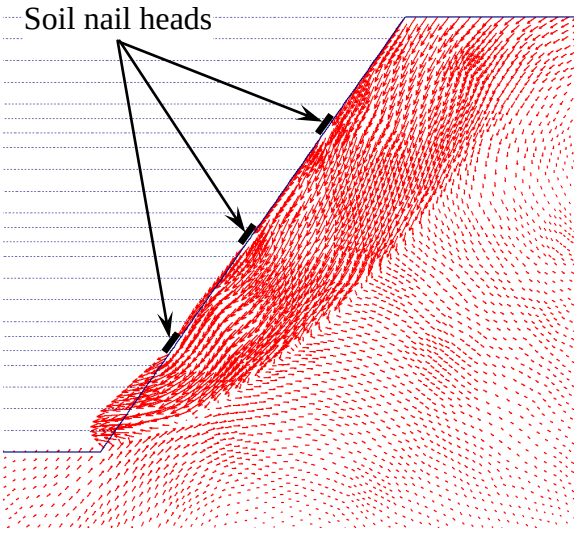

(f) Apparent cohesion c' reduced to 7 kPa

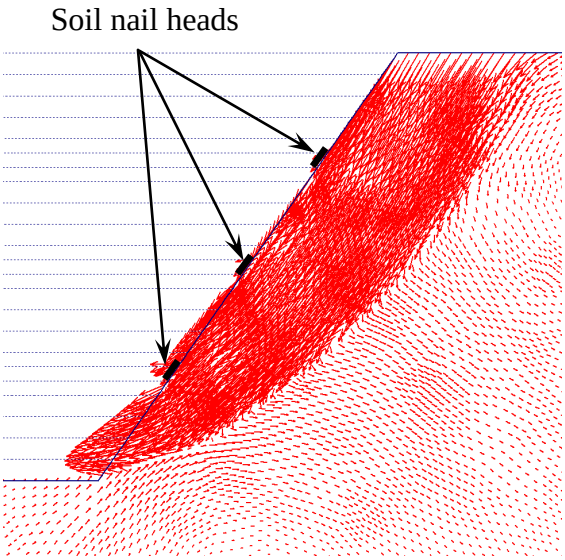

(g) Apparent cohesion c' reduced to 5.2 kPa

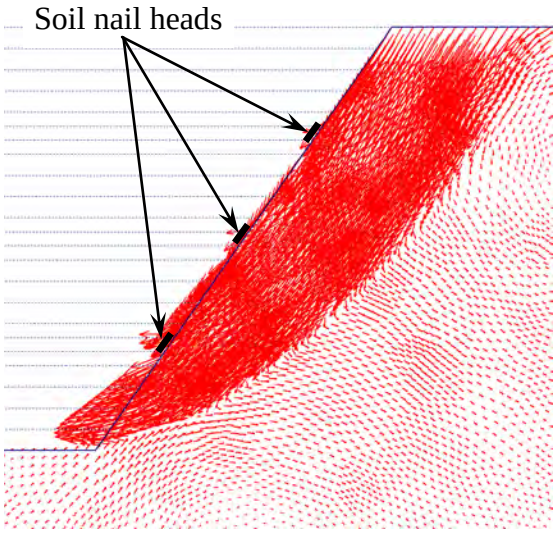

(h) Apparent cohesion c' reduced to 4.9 kPa

Figure C4 - Displacement Vectors - Nail Head Size = 400 mm (Sheet 2 of 2)

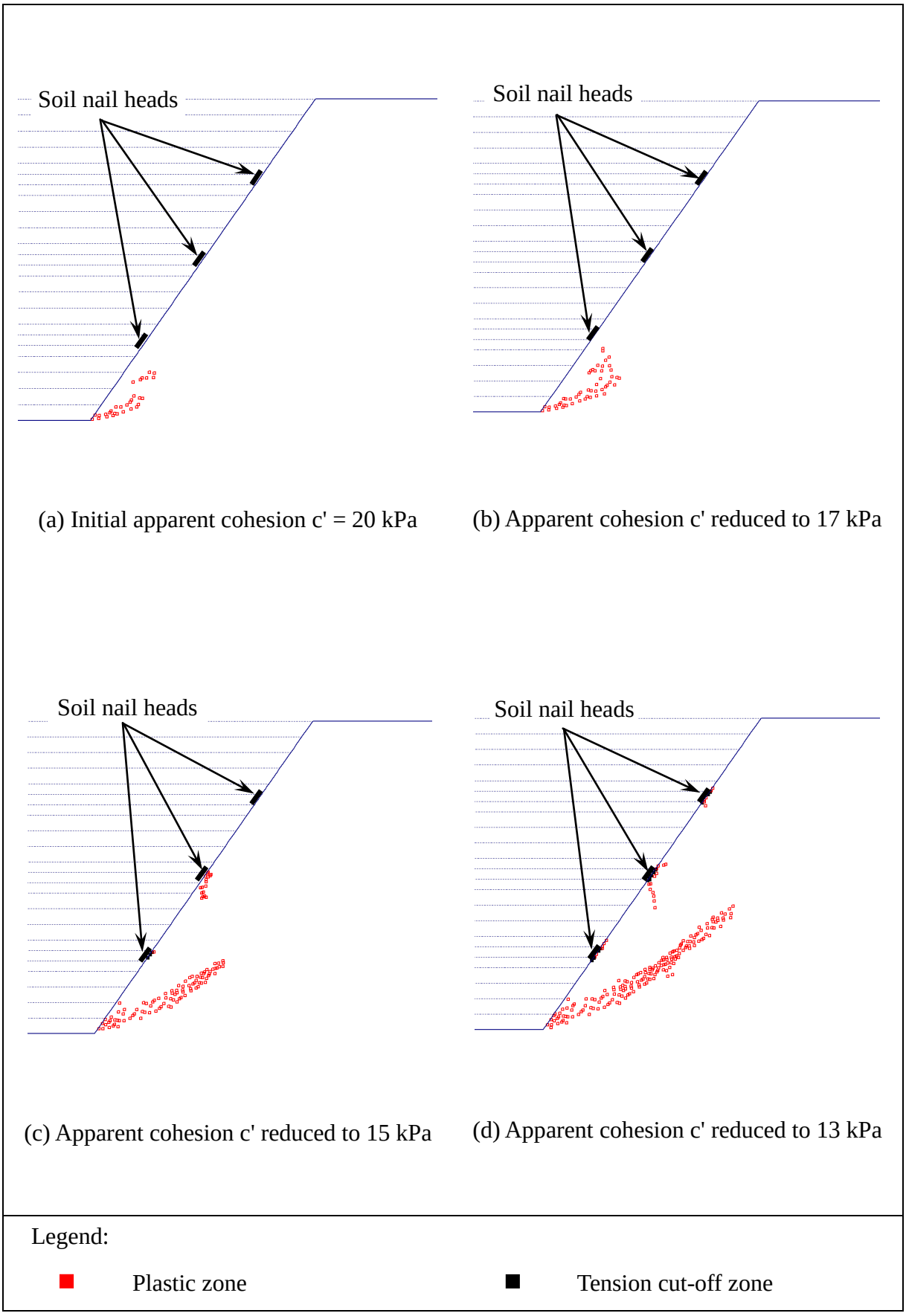

Figure C5 - Development of Plastic Zones - Nail Head Size = 400 mm (Sheet 1 of 2)

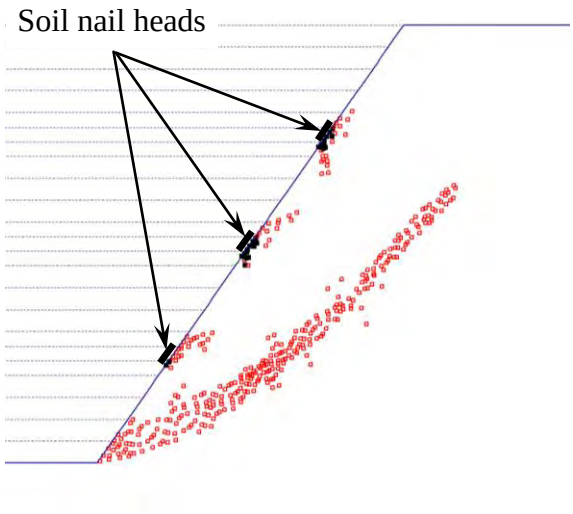

(e) Apparent cohesion c' reduced to 10 kPa

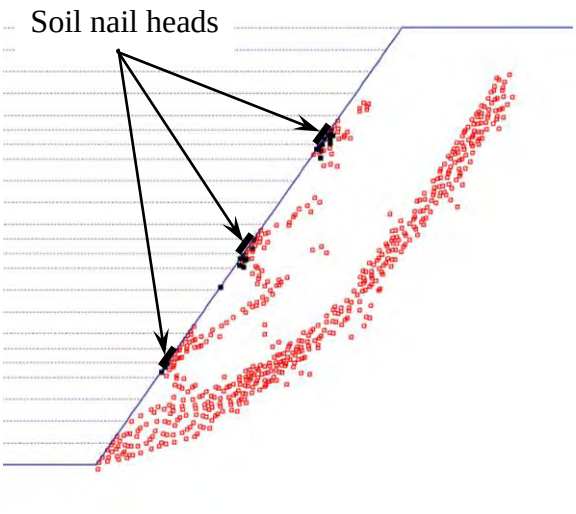

(f) Apparent cohesion c' reduced to 7 kPa

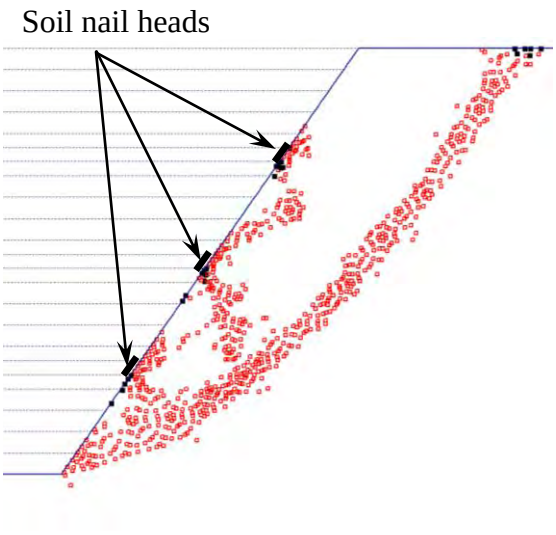

(c) Apparent cohesion c' reduced to 5.2 kPa

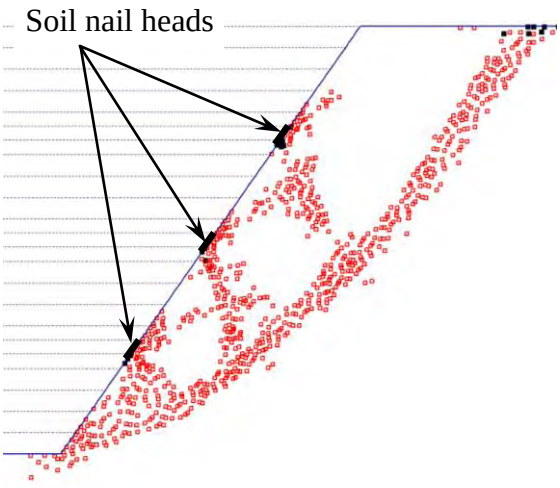

(h) Apparent cohesion c' reduced to 4.9 kPa

Legend:

■ Plastic zone ■ Tension cut-off zone

Figure C5 - Development of Plastic Zones - Nail Head Size = 400 mm (Sheet 2 of 2)

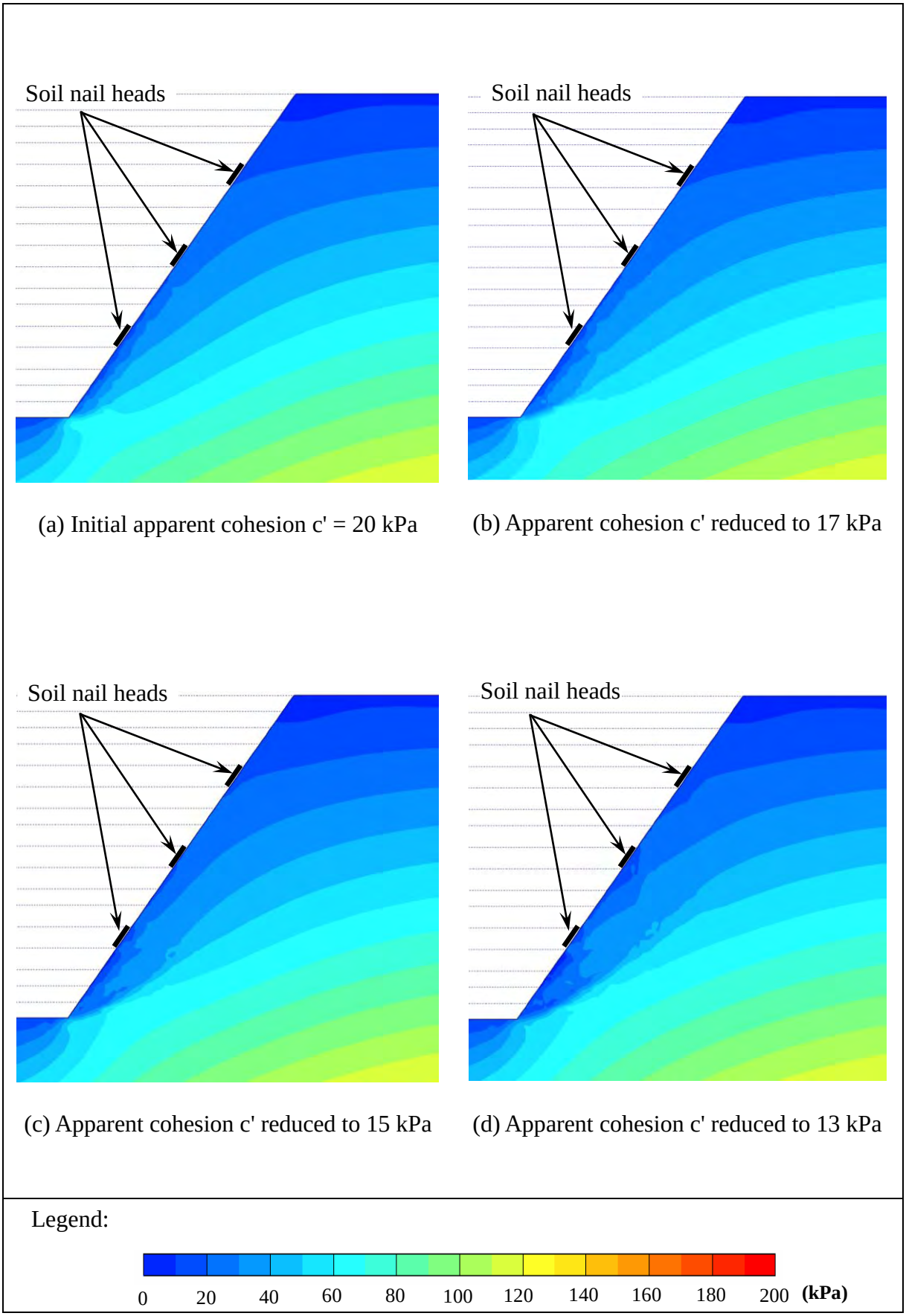

Figure C6 - Development of Mean Effective Stress - Nail Head Size = 800 mm (Sheet 1 of 2)

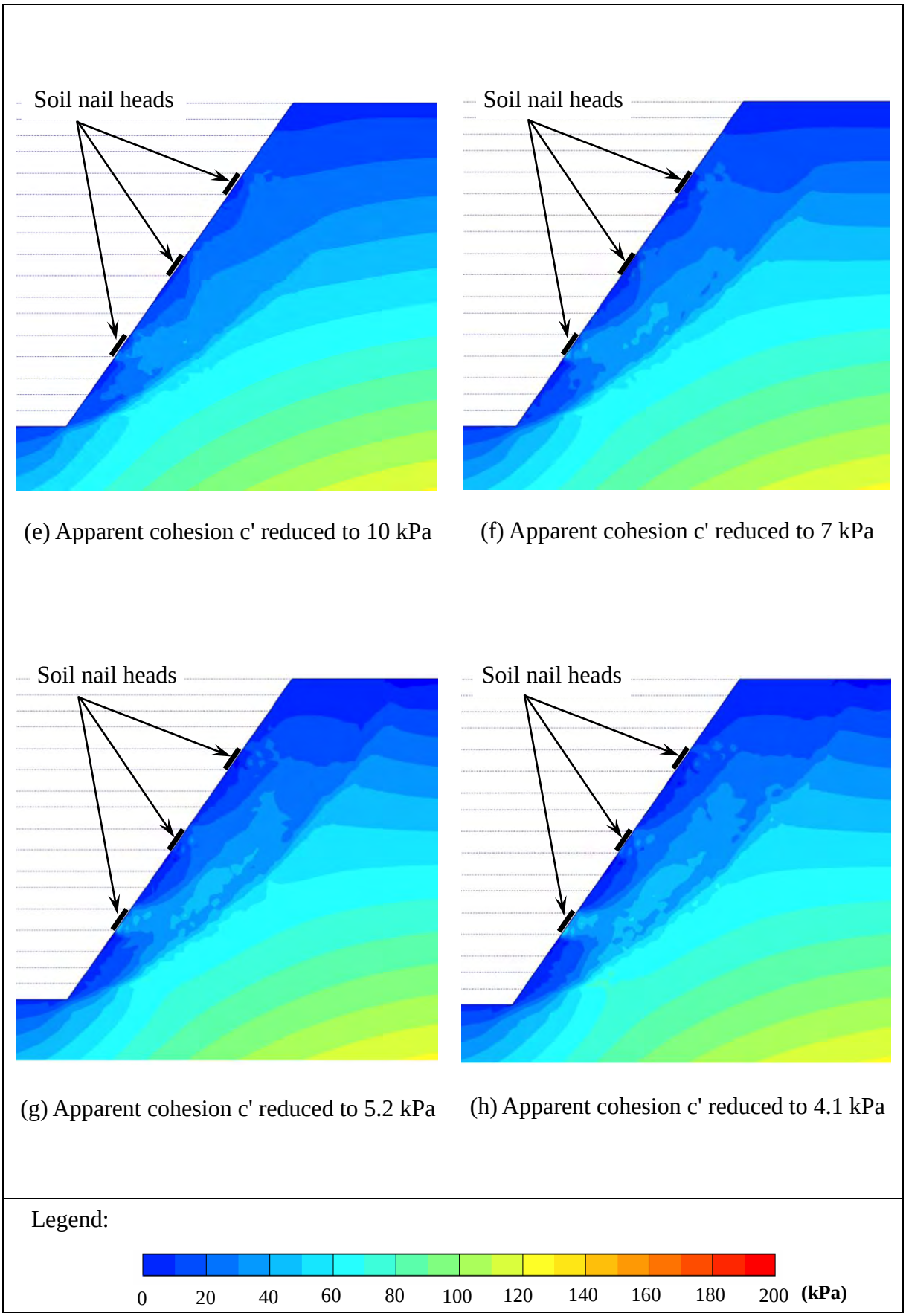

(e) Apparent cohesion c' reduced to 10 kPa

(f) Apparent cohesion c' reduced to 7 kPa

(g) Apparent cohesion c' reduced to 5.2 kPa

(h) Apparent cohesion c' reduced to 4.1 kPa

Figure C6 - Development of Mean Effective Stress - Nail Head Size = 800 mm (Sheet 2 of 2)

Table of Contents
Table of Contents
Table of Contents
Table of Contents

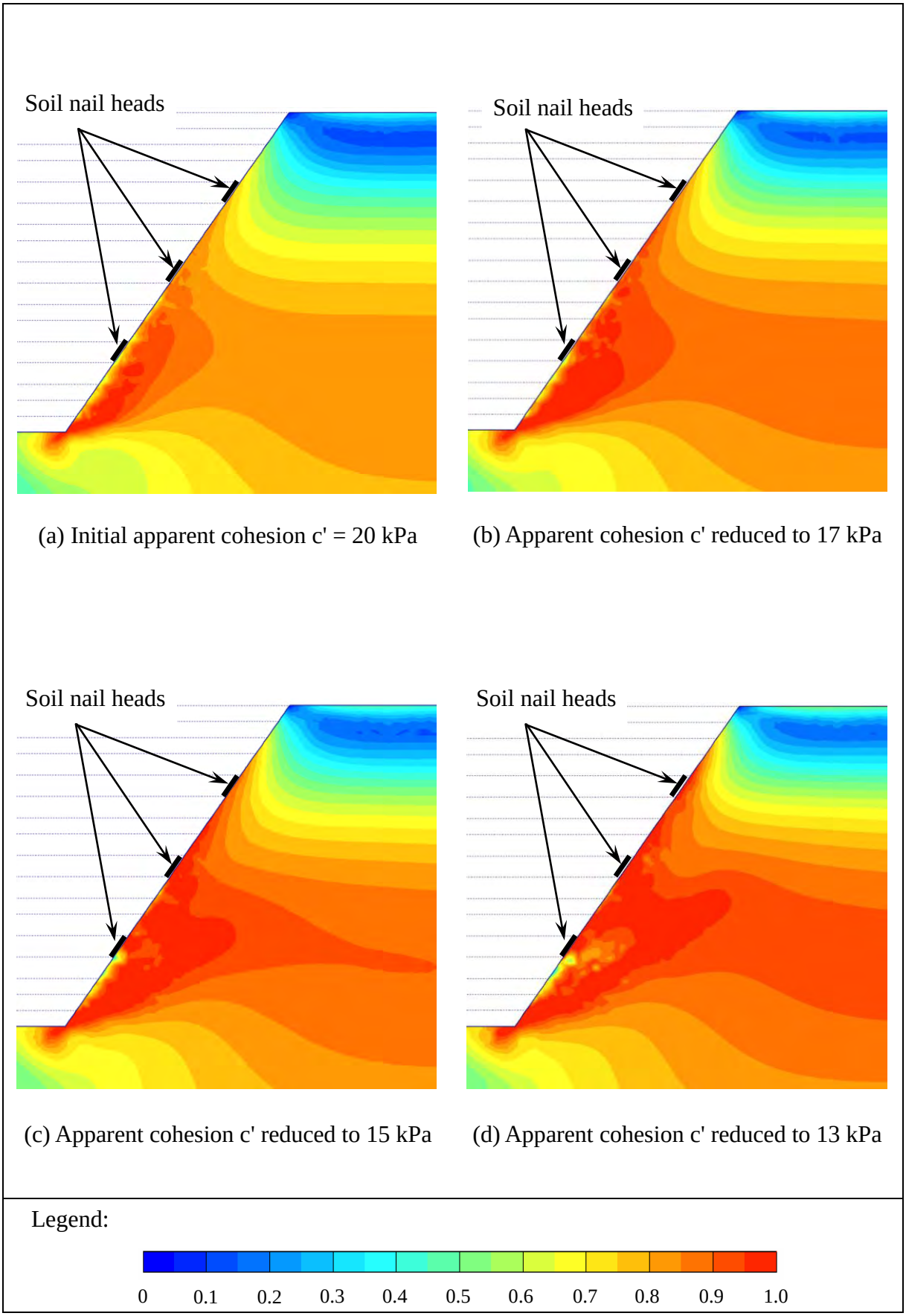

Figure C7 - Development of Relative Shear Stress - Nail Head Size = 800 mm (Sheet 1 of 2)

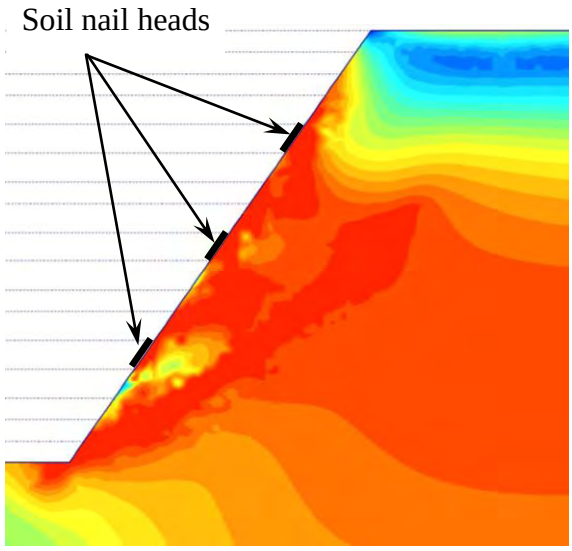

(e) Apparent cohesion c' reduced to 10 kPa

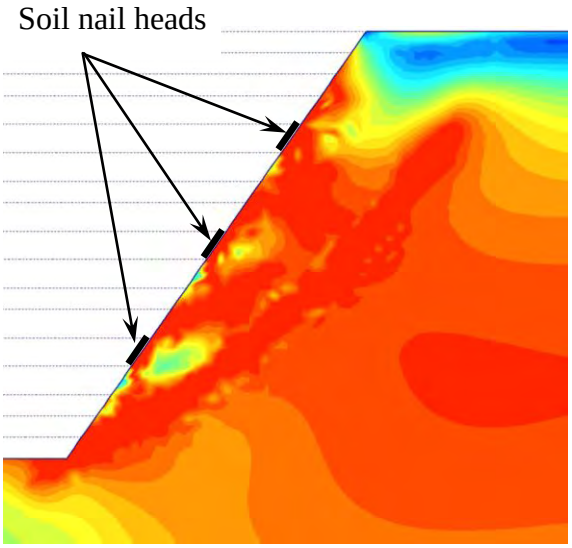

(f) Apparent cohesion c' reduced to 7 kPa

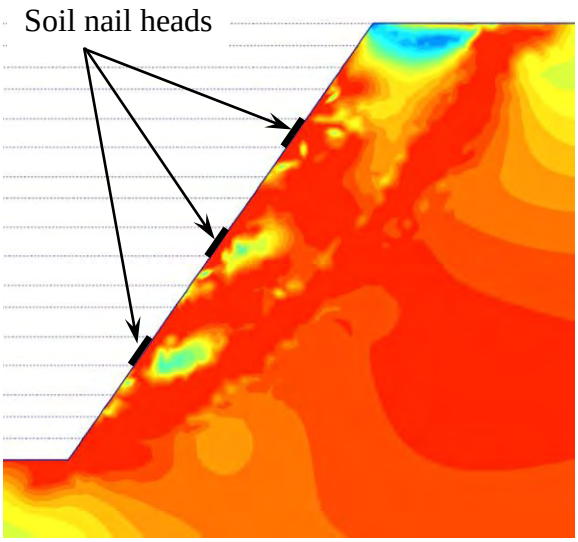

(g) Apparent cohesion c' reduced to 5.2 kPa

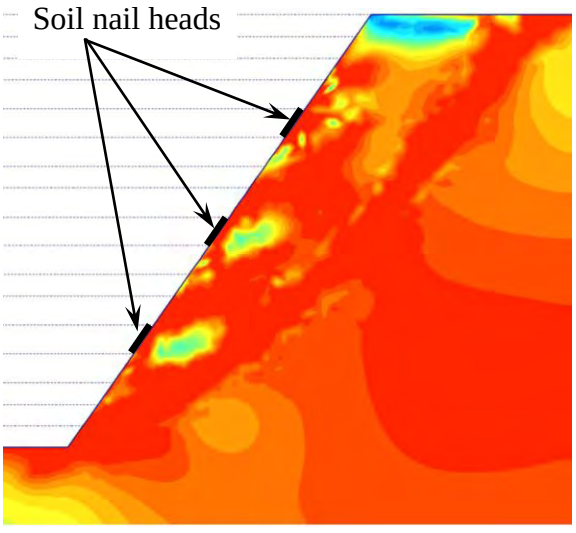

(h) Apparent cohesion c' reduced to 4.1 kPa

Legend:

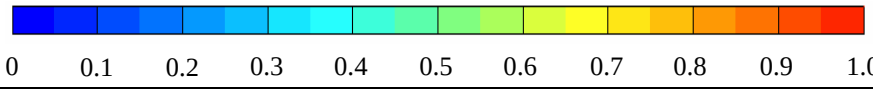

Figure C7 - Development of Relative Shear Stress - Nail Head Size = 800 mm (Sheet 2 of 2)

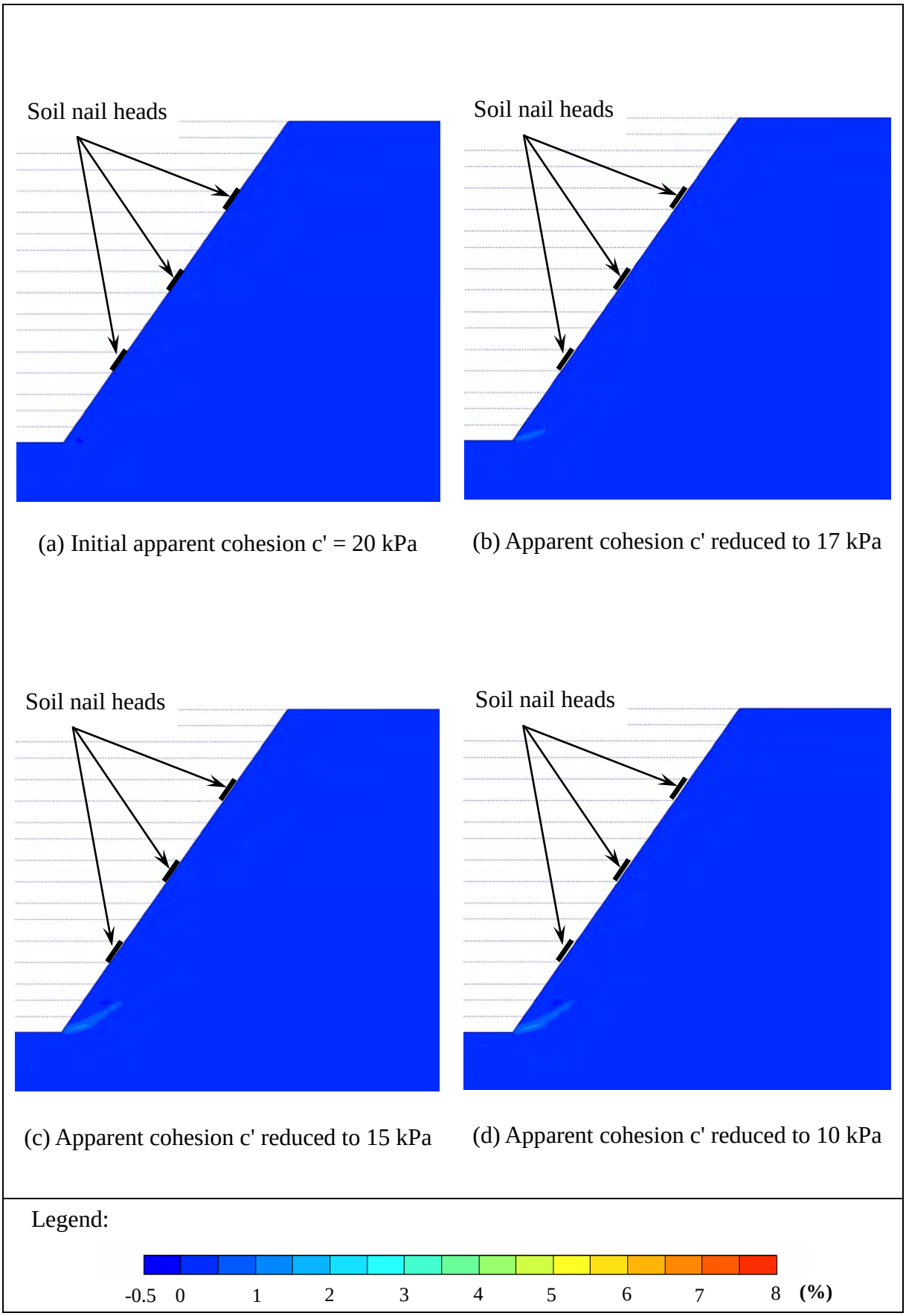

Figure C8 - Development of Shear Strain - Nail Head Size = 800 mm (Sheet 1 of 2)

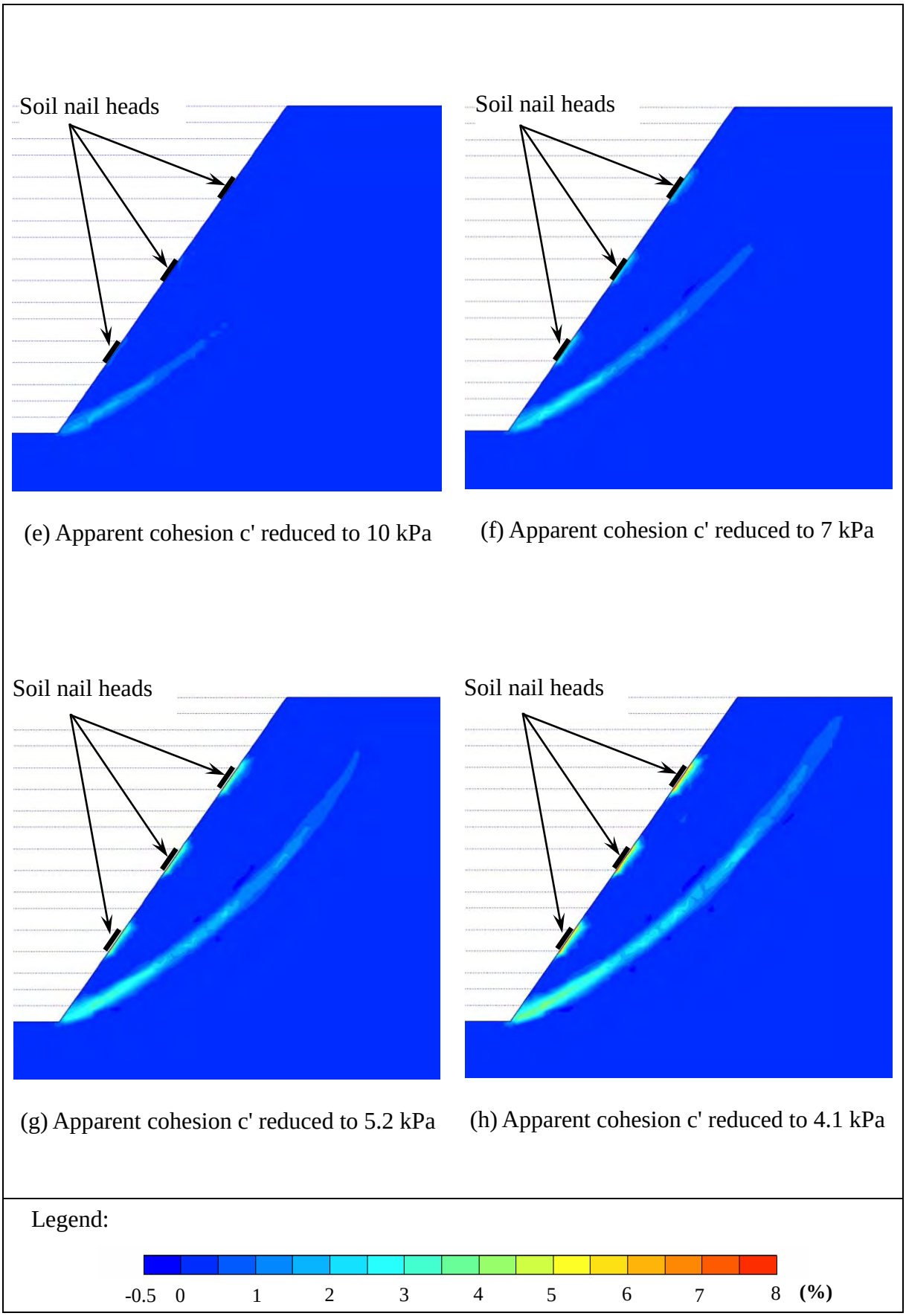

Figure C8 - Development of Shear Strain - Nail Head Size = 800 mm (Sheet 2 of 2)

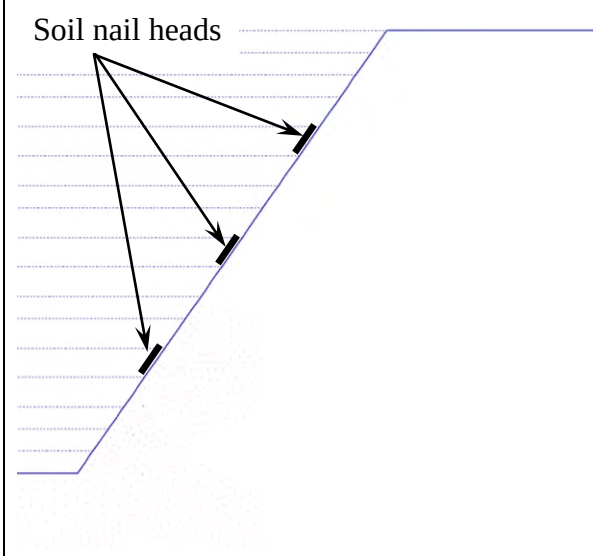

(a) Initial apparent cohesion c' = 20 kPa

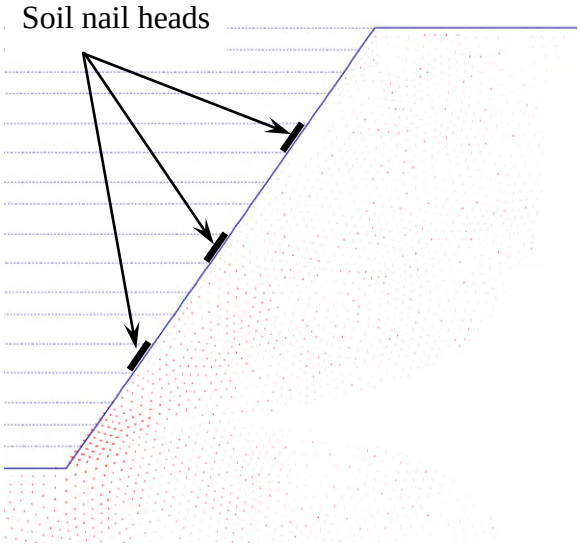

(b) Apparent cohesion c' reduced to 17 kPa

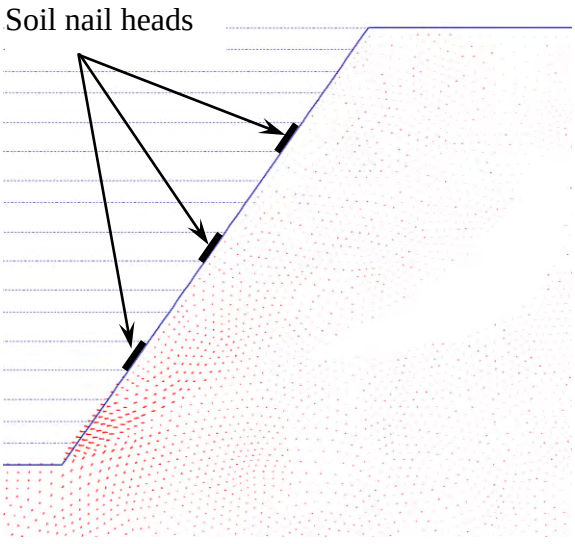

(c) Apparent cohesion c' reduced to 15 kPa

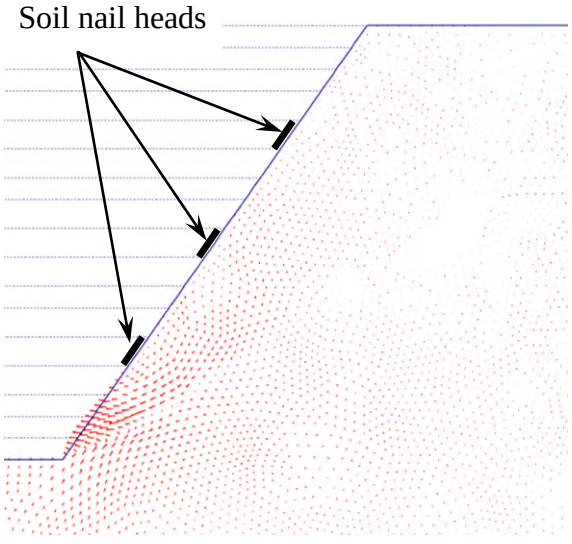

(d) Apparent cohesion c' reduced to 13 kPa

Figure C9 - Displacement Vectors - Nail Head Size = 800 mm (Sheet 1 of 2)

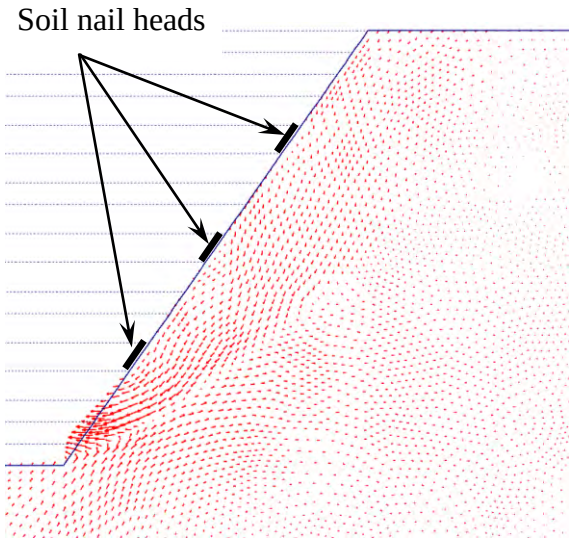

(e) Apparent cohesion c' reduced to 10 kPa

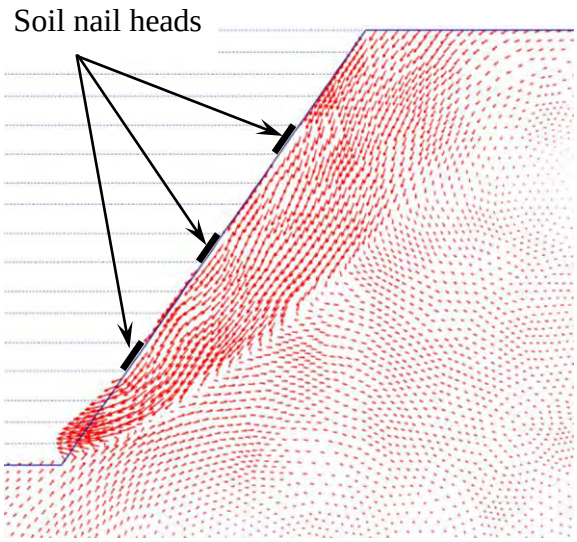

(f) Apparent cohesion c' reduced to 7 kPa

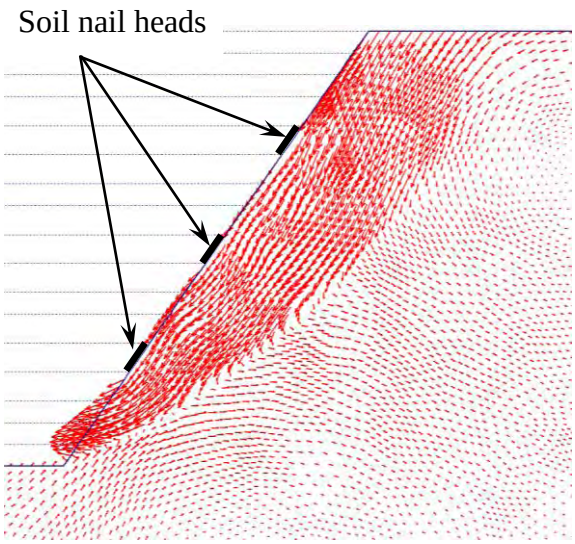

(g) Apparent cohesion c' reduced to 5.2 kPa

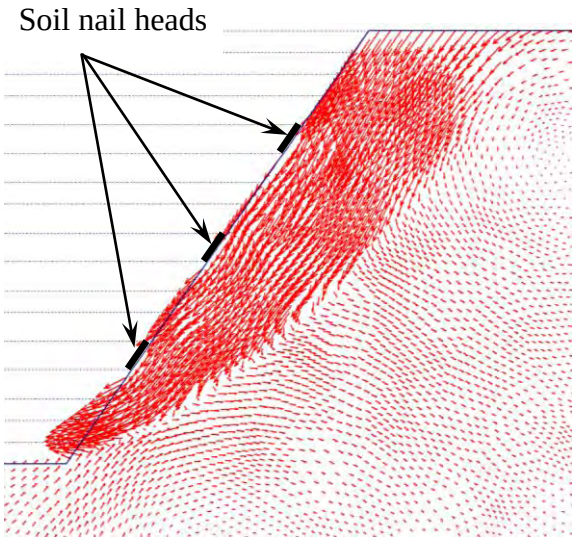

(h) Apparent cohesion c' reduced to 4.1 kPa

Figure C9 - Displacement Vectors - Nail Head Size = 800 mm (Sheet 2 of 2)

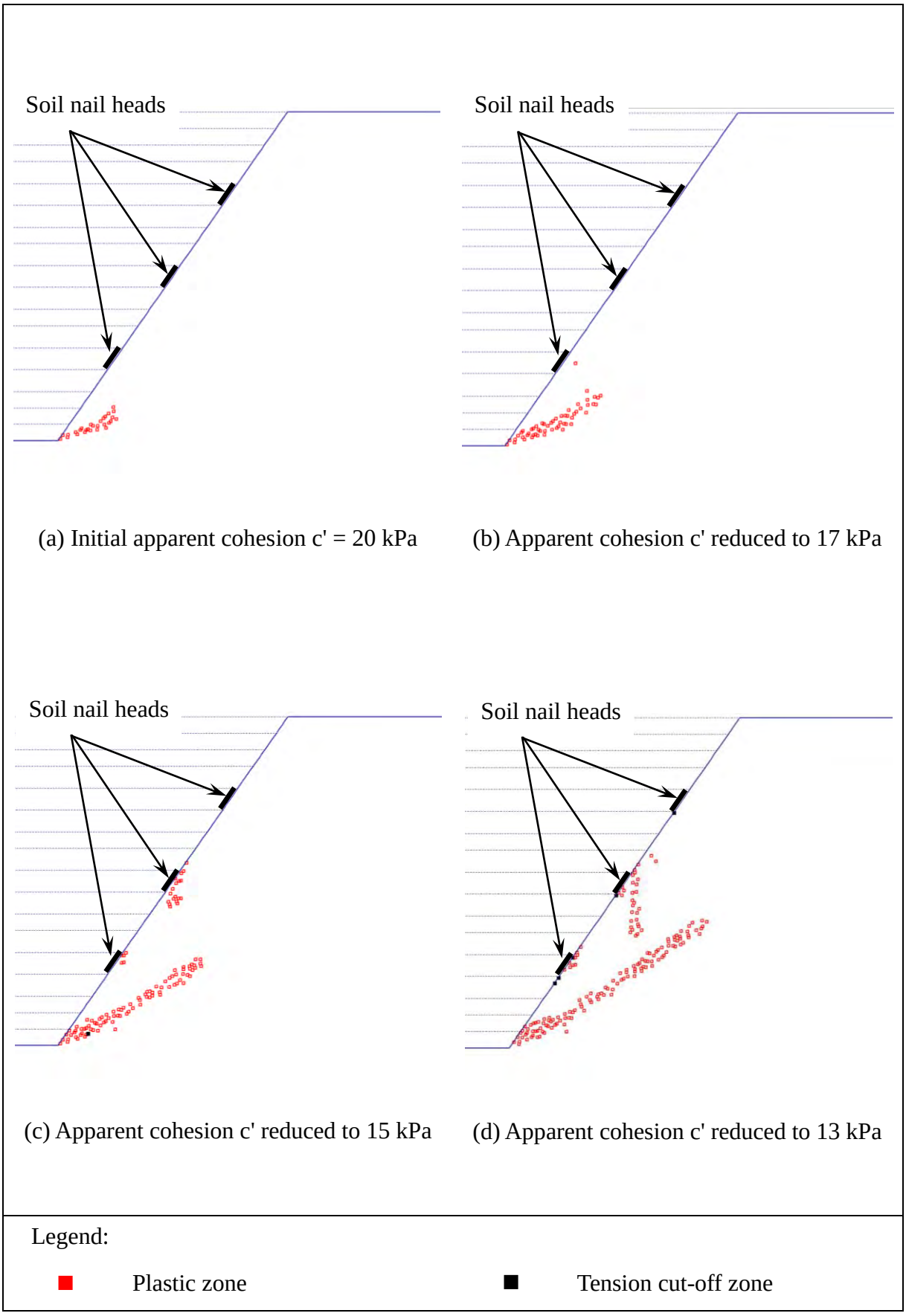

Figure C10 - Development of Plastic Zones - Nail Head Size = 800 mm (Sheet 1 of 2)

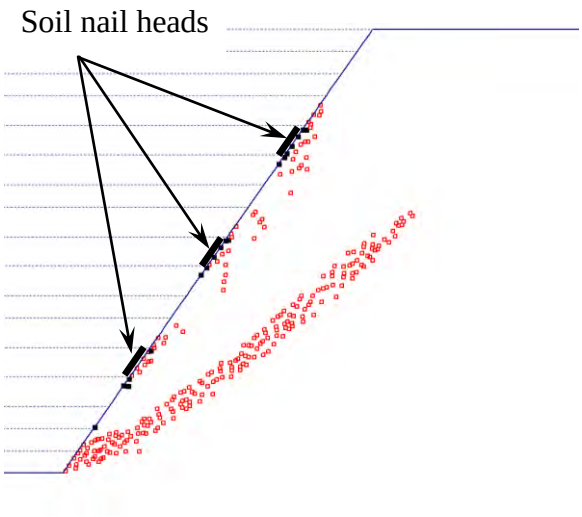

(e) Apparent cohesion c' reduced to 10 kPa

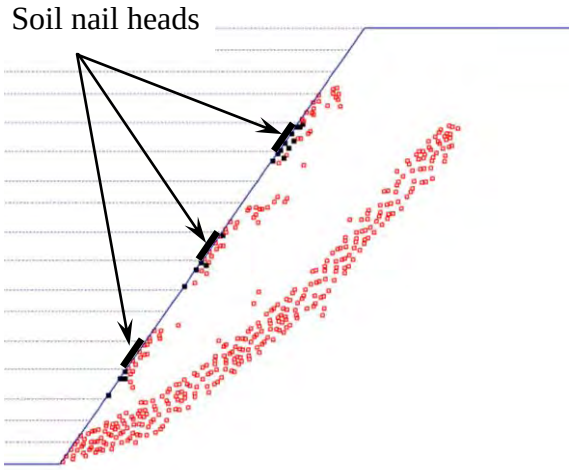

(f) Apparent cohesion c' reduced to 7 kPa

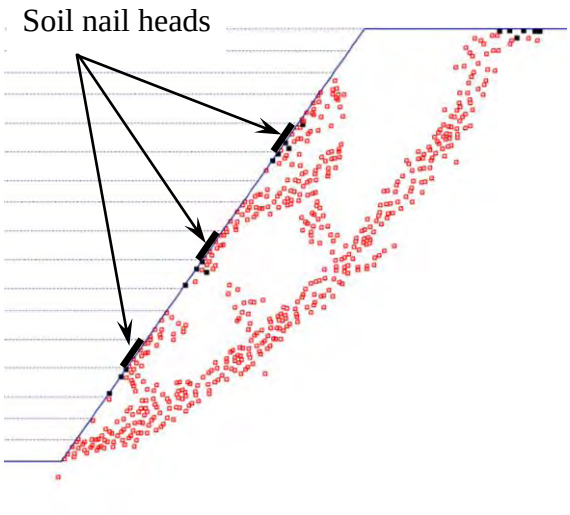

(g) Apparent cohesion c' reduced to 5.2 kPa

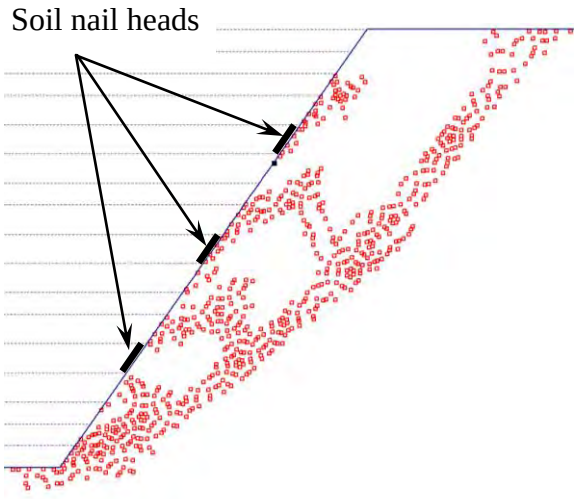

(h) Apparent cohesion c' reduced to 4.1 kPa

Legend:

Plastic zone

Tension cut-off zone

Figure C10 - Development of Plastic Zones - Nail Head Size = 800 mm (Sheet 2 of 2)

GEO PUBLICATIONS AND ORDERING INFORMATION
土力工程處刊物及訂購資料

A selected list of major GEO publications is given in the next page. An up-to-date full list of GEO publications can be found at the CEDD Website http://www.cedd.gov.hk on the Internet under "Publications". Abstracts for the documents can also be found at the same website. Technical Guidance Notes are published on the CEDD Website from time to time to provide updates to GEO publications prior to their next revision.

部份土力工程處的主要刊物目錄刊載於下頁。而詳盡及最新的土力工程處刊物目錄，則登載於土木工程拓展署的互聯網網頁 http://www.cedd.gov.hk 的"刊物"版面之內。刊物的摘要及更新刊物內容的工程技術指引，亦可在這個網址找到。

Copies of GEO publications (except geological maps and other publications which are free of charge) can be purchased either by:

Writing to
Publications Sales Section,
Information Services Department,
Room 402, 4th Floor, Murray Building,
Garden Road, Central, Hong Kong.
Fax: (852) 2598 7482

or
- Calling the Publications Sales Section of Information Services Department (ISD) at (852) 2537 1910
- Visiting the online Government Bookstore at http:// www.bookstore.gov.hk
- Downloading the order form from the ISD website at http://www.isd.gov.hk and submitting the order online or by fax to (852) 2523 7195
- Placing order with ISD by e-mail at puborder@isd.gov.hk

讀者可採用以下方法購買土力工程處刊物(地質圖及免費刊物除外):

書面訂購
香港中環花園道
美利大廈4樓402室
政府新聞處
刊物銷售組
傳真: (852) 2598 7482

或
- 致電政府新聞處刊物銷售小組訂購 (電話：(852) 2537 1910)
- 進入網上「政府書店」選購，網址爲 http://www.bookstore.gov.hk
- 透過政府新聞處的網站 (http://www.isd.gov.hk) 於網上遞交訂購表格，或將表格傳真至刊物銷售小組 (傳真：(852) 2523 7195)
- 以電郵方式訂購 (電郵地址：puborder@isd.gov.hk)

1:100 000, 1:20 000 and 1:5 000 geological maps can be purchased from:

Map Publications Centre/HK,
Survey & Mapping Office, Lands Department,
23th Floor, North Point Government Offices,
333 Java Road, North Point, Hong Kong.
Tel: (852) 2231 3187
Fax: (852) 2116 0774

讀者可於下列地點購買1:100 000、1:20 000及1:5 000地質圖：

香港北角渣華道333號
北角政府合署23樓
地政總署測繪處
電話: (852) 2231 3187
傳真: (852) 2116 0774

Requests for copies of Geological Survey Sheet Reports and other publications which are free of charge should be directed to:

For Geological Survey Sheet Reports which are free of charge:
Chief Geotechnical Engineer/Planning,
(Attn: Hong Kong Geological Survey Section)
Geotechnical Engineering Office,
Civil Engineering and Development Department,
Civil Engineering and Development Building,
101 Princess Margaret Road,
Homantin, Kowloon, Hong Kong.
Tel: (852) 2762 5380
Fax: (852) 2714 0247
E-mail: jsewell@cedd.gov.hk

For other publications which are free of charge:
Chief Geotechnical Engineer/Standards and Testing,
Geotechnical Engineering Office,
Civil Engineering and Development Department,
Civil Engineering and Development Building,
101 Princess Margaret Road,
Homantin, Kowloon, Hong Kong.
Tel: (852) 2762 5346
Fax: (852) 2714 0275
E-mail: thomashui @cedd.gov.hk

如欲索取地質調查報告及其他免費刊物，請致函：

免費地質調查報告:
香港九龍何文田公主道101號
土木工程拓展署大樓
土木工程拓展署
土力工程處
規劃部總土力工程師
(請交:香港地質調查組)
電話: (852) 2762 5380
傳真: (852) 2714 0247
電子郵件: jsewell@cedd.gov.hk

其他免費刊物:
香港九龍何文田公主道101號
土木工程拓展署大樓
土木工程拓展署
土力工程處
標準及測試部總土力工程師
電話: (852) 2762 5346
傳真: (852) 2714 0275
電子郵件: thomashui@cedd.gov.hk

Table of Contents
Table of Contents
Table of Contents

MAJOR GEOTECHNICAL ENGINEERING OFFICE PUBLICATIONS
土力工程處之主要刊物

Table of Contents

GEOTECHNICAL MANUALS

Geotechnical Manual for Slopes, 2nd Edition (1984), 300 p. (English Version), (Reprinted, 2000).

斜坡岩土工程手冊(1998)，308頁(1984年英文版的中文譯本)。

Highway Slope Manual (2000), 114 p.

GEOGUIDES

Geoguide 1	Guide to Retaining Wall Design, 2nd Edition (1993), 258 p. (Reprinted, 2007).
Geoguide 2	Guide to Site Investigation (1987), 359 p. (Reprinted, 2000).
Geoguide 3	Guide to Rock and Soil Descriptions (1988), 186 p. (Reprinted, 2000).
Geoguide 4	Guide to Cavern Engineering (1992), 148 p. (Reprinted, 1998).
Geoguide 5	Guide to Slope Maintenance, 3rd Edition (2003), 132 p. (English Version).
岩土指南第五冊	斜坡維修指南，第三版(2003)，120頁(中文版)。
Geoguide 6	Guide to Reinforced Fill Structure and Slope Design (2002), 236 p.
Geoguide 7	Guide to Soil Nail Design and Construction (2008), 97 p.

Table of Contents

GEOSPECS

Geospec 1	Model Specification for Prestressed Ground Anchors, 2nd Edition (1989), 164 p. (Reprinted, 1997).
Geospec 3	Model Specification for Soil Testing (2001), 340 p.

GEO PUBLICATIONS

GCO Publication No. 1/90	Review of Design Methods for Excavations (1990), 187 p. (Reprinted, 2002).
GEO Publication No. 1/93	Review of Granular and Geotextile Filters (1993), 141 p.
GEO Publication No. 1/2000	Technical Guidelines on Landscape Treatment and Bio-engineering for Man-made Slopes and Retaining Walls (2000), 146 p.
GEO Publication No. 1/2006	Foundation Design and Construction (2006), 376 p.
GEO Publication No. 1/2007	Engineering Geological Practice in Hong Kong (2007), 278 p.
GEO Publication No. 1/2009	Prescriptive Measures for Man-Made Slopes and Retaining Walls (2009), 76 p.

Table of Contents

GEOLOGICAL PUBLICATIONS

The Quaternary Geology of Hong Kong, by J.A. Fyfe, R. Shaw, S.D.G. Campbell, K.W. Lai & P.A. Kirk (2000), 210 p. plus 6 maps.

The Pre-Quaternary Geology of Hong Kong, by R.J. Sewell, S.D.G. Campbell, C.J.N. Fletcher, K.W. Lai & P.A. Kirk (2000), 181 p. plus 4 maps.

TECHNICAL GUIDANCE NOTES

TGN 1	Technical Guidance Documents

Table of Contents